

© 2007

Allen J Fisch

ALL RIGHTS RESERVED

**DEVELOPMENT AND TESTING OF HAPTIC  
INTERFACES USING ELECTRO-RHEOLOGICAL FLUIDS**

by

**ALLEN JOEL FISCH**

**A Dissertation submitted to the**

**Graduate School – New Brunswick**

**Rutgers, The State University of New Jersey**

**in partial fulfillment of the requirements**

**for the degree of**

**Doctor of Philosophy**

**Graduate Program in Mechanical and Aerospace Engineering**

**written under the direction of**

**Professor Constantinos Mavroidis**

**and approved by**

---

---

---

---

**New Brunswick, New Jersey**

**May 2007**

# **ABSTRACT OF THE DISSERTATION**

## **Development and Testing of Haptic Interfaces Using Electro-Rheological Fluids**

**by ALLEN JOEL (AVI) FISCH**

**Dissertation Director:**

**Professor Constantinos Mavroidis**

Research has been performed to develop haptic interface devices, utilizing advanced actuators, to transmit information and receive control signals through interaction with a user's sense of touch. *Haptic systems* convey tactile and force information through the sense of touch by applying forces to a user's hands and other similar methods.

The ability to generate force information allows systems to be designed where operators can see, hear and *feel* virtual or remote environments. In addition, using the sense of touch allows for new pathways to present information to a user, along with the standard visual and auditory interfaces.

Interface devices have been developed to improve and simplify the manner in which a person interacts with computers and other technological systems. The focus has been to develop force-feedback interface systems to be used to control various devices such as the climate control and audio systems within an automobile. These advanced computer controlled systems can be used to consolidate various controls into fewer feedback control devices to create a simpler, more efficient interface. In addition, the use of force cues allows information to be transmitted to the user and control settings to be changed by the user without requiring the user's visual attention.

Electrorheological Fluid (ERF) based actuators have been developed to provide the required feedback sensations. ERFs are fluids that change their viscosity in response to an electric field. Using the electrically controlled rheological properties of ERFs, devices have been developed that can resist operator forces in a controlled and tunable fashion.

Three ERF-based actuators have been designed and prototypes have been built. Analytical models have been developed to describe the performance of these systems, and experimental analyses performed to verify the operation of the actuators.



The actuators have been incorporated into various prototype Haptic Knob and Haptic Joystick devices. The addition of force cues allows these familiar devices to be used as advanced interface systems to provide information to and sense commands from a user.

Force information from these devices has been maximized by performing Human Factors experiments to assess whether different design variations can increase the systems' effectiveness. Factors such as hand position and handle texture have been assessed, statistical analyses performed on the results and the most effective versions have been identified.

Methods for the application to the automotive haptic devices have been developed. Demonstrations have been created to prove the ability of the systems to provide information through the use of advanced haptic interfaces. In addition, concepts for future avenues of research have been developed to allow for continued research.

## **Acknowledgements**

I have been fortunate to have the direction and guidance of Professor Constantinos Mavroidis throughout the course of this research project. From the beginning, Professor Mavroidis was receptive and enthusiastic about my working in the Rutgers University Robotics and Mechatronics Laboratory and encouraged me to continue my work when the Lab moved to Northeastern University. I will always be grateful for the opportunities for learning that he has provided.

I would like to thank Professors Haim Baruh, Zhiming Ji, and Peng Song for agreeing to take time out of their busy schedules to read and review my dissertation and to serve as members on my dissertation committee.

I am grateful to so many supportive people without whom this project would not have survived: all the past and present Robotics and Mechatronics Laboratory members, including Brian Weinberg for his efforts in developing the actuator concepts and introducing the use of Rapid Prototyping to our development efforts as well as his efforts at testing our devices; Jason Nikitzuk for his efforts in testing and programming that have allowed us to initially demonstrate the knob and joystick in real-life rather than just as words and pictures on paper; as well as all of the others for helping with the background search for haptic devices; Charles Pfeiffer for initial work on

ERFs within the Robotics Lab; Dr. Stephen Kuchnicki for his continual assistance in helping me to develop an understanding of the mathematical and scientific underpinnings of Mechanical Engineering and willingness to share his time and talents as a sounding board for technological and other non-technological questions; and the Mechanical Engineering Department staff and faculty.

Also, Jon Doughty, master of the Mechanical and Industrial Engineering Department's Machine Shop at Northeastern University, who's efforts at both explaining the use of the machine shop tools as well as his own machining efforts were instrumental in developing the physical prototype for the second generation actuators and devices.

In addition, there were many friends who offered assistance along the way, both moral and technical. Especially Dr. Evelyn Behar who provided invaluable assistance with the design of the human factors experiment as well as with the statistical analysis performed on the gathered data.

Additionally, I would like to express my appreciation to the Graduate School of New Brunswick and the Mechanical Engineering Department for awarding me a Graduate School Fellowship, as well as the National Aeronautics and Space Administration for providing financial support through a Graduate Student Researcher Fellowship (GSRP) for three years.

And finally, I am grateful for the many experiences that have come via my interactions with my brothers, parents, in-laws and the rest of my extended family; they have all very much influenced my accomplishments.

And, most importantly, I am grateful to my wife, Shirley, for her unending support and encouragement that has allowed me to pursue my studies and reach the point where I'm just a few steps away from joining her as a Doctor. In addition, her proofreading and advice giving have helped this project to reach the level that it has.

And, lastly, to my sons Orin and Eli who were born over the course of this research project. They bring such joy into our lives (as well as providing convenient distractions from our work efforts) with their boundless energy, happiness and joy of learning. I couldn't have done any of this without them.

## **Dedication**

I would like to dedicate this work to my family and friends who have been supportive of my efforts to return to the university world and to finally get that degree that I've been talking about for years.

I especially want to dedicate this to my two sons – Orin and Eli – who were both born over the course of this PhD process and who have endured Daddy's late night work sessions and days away from home with grace and maturity and who were always happy to see me when I was able to make an appearance.

And lastly, to my wife Shirley, without whom I would not have the time, wherewithal or support to complete my work. So Shirl, we're finally at the end of the road . . . what's next?

# Table of Contents

ABSTRACT OF THE DISSERTATION .....	ii
Acknowledgements.....	v
Dedication .....	viii
Table of Contents .....	ix
List of Tables .....	xiii
List of Figures .....	xiv
1 INTRODUCTION .....	1
1.1 Haptic Technologies .....	1
1.2 Research Project Goals and Plans.....	5
1.3 Important Note on Nomenclature .....	7
1.4 Research into ERF-Based Haptic Interfaces.....	8
1.5 Contributions / Acknowledgments .....	11
1.5.1 Research steps and milestones.....	12
1.5.2 Acknowledgements.....	14
1.5.3 Publications.....	15
1.6 Outline of Dissertation.....	17
2 HAPTIC SYSTEMS .....	19
2.1 Current Haptic Devices – Review.....	22
2.1.1 Exoskeletons and Stationary Devices.....	22
2.1.2 Gloves and Wearable Devices .....	25
2.1.3 Point Sources and Specific Task Devices.....	27
2.1.4 Mobility Interfaces and Full Body Force Feedback .....	29
2.1.5 Force Feedback Input Devices.....	31
2.1.6 Tactile Displays .....	33
3 HAPTIC SYSTEMS USING ELECTRO-RHEOLOGICAL FLUIDS .....	37
3.1 Electrorheological Fluids.....	37
3.2 Existing ERF-Based Haptic Devices .....	43
4 ACTUATOR CONCEPT AND MODELING – VERSION 1 .....	46
4.1 Concentric-Cylinder Actuator Concept and Modeling.....	46
4.2 Flat-Plate Actuator Concept and Modeling .....	51
4.3 Parametric Analysis of the Design of ERF Actuators .....	54
4.3.1 Preliminary Information.....	54
4.3.2 Concentric-Cylinder Actuator.....	55
4.3.3 Flat-Plate Actuator.....	59
4.4 Additional Parametric Analysis for Design Selection .....	62
4.5 Additional Design Considerations .....	66
5 TESTING - MODEL VERIFICATION .....	70
5.1 Concentric-Cylinder Actuator.....	70
5.1.1 CC Actuator Prototype and Experimental Setup .....	70
5.1.2 CC Actuator Experimental Results.....	71
5.2 Flat-Plate Actuator .....	75
5.2.1 FP Actuator Prototype and Experimental Setup.....	75
5.2.2 Flat Plate Actuator Experimental Results.....	77

6	TESTING - RESPONSE TIME.....	81
6.1	Response Time Tests - Experimental Setup .....	81
6.2	Experimental Analysis Approach .....	83
6.3	Analysis of Data.....	87
6.4	Sources of Delay .....	88
6.5	Response Time Test Conclusions .....	90
7	ERF ACTUATORS IN HAPTIC INTERFACE SYSTEMS.....	91
7.1	Haptic Knob.....	92
7.1.1	Knob Design and Prototype – v1 .....	93
7.1.2	Knob Application.....	96
7.2	Haptic Joystick.....	96
7.2.1	Joystick Design and Prototype – v1 .....	98
7.2.2	Joystick Application.....	101
8	ACTUATOR DESIGN – VERSION 2.....	103
8.1	Motivation for Redesign .....	103
8.2	Material and Component Selection.....	104
8.3	Design .....	104
8.3.1	Force Increase/Voltage Decrease.....	105
8.3.2	Reduction of Forces .....	105
8.3.3	Simplified Assembly.....	106
8.3.4	Modular Design .....	107
8.4	Development and Manufacturing .....	107
8.4.1	Fixed Electrode .....	108
8.4.2	Rotating Electrode .....	109
8.4.3	Actuator Case.....	110
8.4.4	Encoder Mount.....	112
8.5	Assembly.....	113
8.5.1	Rotating Electrode Assembly .....	113
8.5.2	Electrode Insertion.....	113
8.5.3	Cover and Additional Components.....	114
8.6	Filling the Actuator .....	117
8.6.1	Replacement ERF .....	118
8.7	Actuator v2 Design Conclusions .....	119
9	HAPTIC KNOB DESIGN AND PROTOTYPE – V2 .....	121
9.1	Development of Knob Hardware.....	121
9.1.1	Knob Hardware, Mechanical .....	121
9.1.2	Knob Hardware, Electrical.....	123
9.2	Development of Haptic Knob Interface System .....	125
9.2.1	Knob Software Interface .....	125
9.2.2	Open Loop Control .....	127
9.2.3	Hardware Interface.....	128
9.3	Haptic Knob Use.....	129
9.4	Haptic Knob v2 Design Conclusions.....	129
10	JOYSTICK DESIGN AND PROTOTYPE – V2 .....	130
10.1	Joystick Hardware.....	130
10.2	Joystick Software .....	133

10.2.1	Virtual Channels .....	133
10.3	Haptic Joystick v2 Design Conclusions.....	137
11	HUMAN INTERFACE CONSIDERATIONS IN HAPTIC KNOB DESIGN ..	138
11.1	Ergonomics – Background.....	139
11.2	Ergonomics – Knob Interface concepts .....	140
11.3	Force Profile Considerations.....	142
11.4	Human Factors Testing Motivation .....	143
11.4.1	Design Factors Being Tested .....	144
12	HUMAN FACTORS IN THE HAPTIC KNOB SYSTEM.....	145
12.1	Knob Shape Factor.....	145
12.1.1	Knob Shape Designs and Hand Motion.....	146
12.2	Knob Texture Factor .....	152
12.3	Force Profile Shaping Factor .....	153
13	HUMAN FACTORS, EXPERIMENTAL DESIGN .....	157
13.1	Hardware, Physical Layout.....	158
13.2	Software, Data Collection.....	159
13.3	Detent Test Setup.....	162
13.4	Experimental Procedure.....	164
13.5	Assembly of Data.....	165
14	HUMAN FACTORS, EXPERIMENTAL RESULTS .....	167
14.1	Introduction to Statistical Analysis.....	167
14.1.1	Variance .....	167
14.1.2	Analysis of Variance (ANOVA).....	169
14.1.3	Repeated Measures Analysis of Variance.....	172
14.2	Data Analysis .....	173
14.2.1	Data Organization .....	174
14.3	Analysis Results.....	176
14.3.1	Individual Factor – Knob Shape .....	176
14.3.2	Individual Factor – Texture .....	177
14.3.3	Individual Factor – Detent Style .....	178
14.3.4	Two Factors .....	179
14.3.5	Three Factors .....	181
14.4	Data Analysis Conclusions .....	182
14.5	Discussion of Results.....	184
15	HAPTIC INTERFACE USED WITH PHYSICAL INJURY .....	186
15.1	Motivation for Testing Physically Limited Subject.....	186
15.2	Carpal Tunnel Syndrome .....	186
15.3	Data Collection and Analysis.....	188
15.4	Physically Limited Subject Conclusions .....	190
15.5	Future Study.....	191
16	FUTURE WORK / CONCLUSIONS.....	192
16.1	Future Work.....	192
16.1.1	Open/Closed Loop Control .....	192
16.1.2	Dynamic Response Improvement and Testing .....	193
16.1.3	Haptic Interface Software Development.....	194
16.1.4	Human-Factors, Additional Factors.....	195



16.1.5	Human Factors Testing for Haptic Joystick.....	195
16.1.6	Human Trials for Users with Hand Injury .....	196
16.1.7	Simulated Active Forces .....	196
16.2	Conclusions.....	198
17	REFERENCES .....	201
18	APPENDIX.....	207
18.1	Datasheet and Wiring Diagram for Encoder Interface (4 Pages) .....	207
18.2	LabView Program – Haptic Knob .....	211
18.3	LabView Program – Haptic Joystick (2 Pages) .....	212
18.4	IRB Approval, Northeastern University .....	214
18.4.1	IRB Application (10 Pages).....	214
18.4.2	Consent Form.....	224
18.4.3	IRB Approval (3 Pages).....	225
	CURRICULUM VITA .....	228

## List of Tables

Table 1-1: Design Goal Criteria Used For Developing New Actuators. ....	5
Table 2-1: Haptic Device Categories.....	21
Table 4-1: ERF LID 3354S Parameters (*values for $E_{ref}$ and $C_s$ are for ERF LID 3354). .....	55
Table 5-1: Experimentally obtained Parameters for ERF LID 3354s versus those stated for LID 3354.....	73
Table 5-2: Concentric-Cylinder Actuator Dynamic Torque Experimental Values. ....	74
Table 5-3: Flat-Plate Actuator Dynamic Torque Average Experimental Values. ....	78
Table 6-1: Tabulated Input and Output frequencies for the 0.0 – 1.0 kV Range.....	87
Table 6-2: Tabulated Input and Output frequencies for the 0.5 – 1.5 kV Range.....	87
Table 7-1: Joystick’s FP Actuator Properties. ....	99
Table 8-1: Goals for Actuator Redesign .....	103
Table 8-2: Physical Characteristics of the CCv2 Actuator .....	119
Table 8-3: Torque Output (estimates) for CCv2, CCv1 and FP actuators.....	120
Table 9-1: Physical Characteristics of the Haptic Knob, version 2 .....	129
Table 10-1: Steps to Run the Haptic Joystick Software .....	135
Table 10-2: Physical Characteristics of the Haptic Joystick, version 2 .....	137
Table 11-1: Main Objectives for Haptic Interface Design.....	138
Table 11-2: Couplings Between Hand and Handle. [Kroemer, 2003b].....	141
Table 11-3: Factors to be Tested in Human Trials .....	144
Table 12-1: Hand-Knob Couplings to be Tested [Kroemer, 2003b] .....	145
Table 13-1: Pre-Experimental Practice Procedure.....	164
Table 13-2: Experimental Procedure .....	165
Table 14-1: F Value Table from [Urdu, 2005].....	171
Table 14-2: Data Organization within SPSS .....	174
Table 14-3: Correlation of Numerical Indicators to Actual Designs.....	175
Table 14-4: Mean Values for Knob Shape Factor .....	176
Table 14-5: Pairwise Comparisons for Knob Shape Factor.....	176
Table 14-6: Mean Values for Knob Texture Factor.....	178
Table 14-7: Pairwise Comparisons for Knob Texture Factor.....	178
Table 14-8: Mean Values for Detent Style Factor .....	178
Table 14-9: Pairwise Comparisons for Detent Style Factor .....	179
Table 14-10: Mean Values for Paired Factors, Knob Shape - Texture.....	180
Table 14-11: Mean Values for Paired Factors, Knob Shape – Detent Style.....	180
Table 14-12: Mean Values for Paired Factors, Texture – Detent Style.....	181
Table 14-13: Mean Values for Triple Factors, Knob Shape – Texture – Detent Style...	181
Table 15-1: Accuracy for Knob Shape Factor .....	189
Table 15-2: Accuracy for Knob Texture Factor .....	189
Table 15-3: Accuracy for Detent Style Factor .....	189

## List of Figures

Figure 1-1: Virtual Reality for Surgical Training.....	2
Figure 1-2: Artist rendition of a Mars Exploration Rover – <i>Spirit</i> or <i>Opportunity</i> – approaching a rock on the surface of Mars. (Courtesy NASA/JPL-Caltech) 3	3
Figure 1-3: (Left) Person reading a traditional Braille-based book by touch (Right) Pin-based display system from NIST, displaying a sine wave. ....	4
Figure 1-4: ERF-based braking systems can be more compact because they don't require transmission elements. ....	6
Figure 1-5: Multi-function haptic interface concept for vehicular instrument control. ....	8
Figure 2-1: Example of Tele-Presence control of Robonaut. ....	20
Figure 2-2: Iowa State Force Feedback Exoskeleton. ....	23
Figure 2-3: CyberForce.....	23
Figure 2-4: L-EXOS .....	23
Figure 2-5: Master Arm, Southern Methodist University.....	24
Figure 2-6: Master II, Rutgers University.....	26
Figure 2-7: Hand Held Force Display.....	26
Figure 2-8: CyberGlove .....	27
Figure 2-9: CyberGrasp Exoskeleton.....	27
Figure 2-10: CyberGlove II, Wireless System.....	27
Figure 2-11: Phantom. ....	28
Figure 2-12: VEKATS, University of Hull.....	28
Figure 2-13: Haptic Scissor (L) With Graphical Display (R), Johns Hopkins .....	29
Figure 2-14: Uniport Pedaling Interface, Sarcos, Inc. ....	30
Figure 2-15: Treadport, Sarcos Inc. ....	30
Figure 2-16: Omni-Directional Treadmill, Virtual Space Devices, Inc.....	31
Figure 2-17: Sidewinder Force Feedback Joystick, Microsoft Corp and WingMan Force Feedback Mouse, Logitech. ....	32
Figure 2-18: NIST Tactile Visual Display showing a map of the United States.....	33
Figure 2-19: Harvard BioRobotics Lab's 2-D Pin Display. ....	35
Figure 2-20: Immersion Touchscreen Tactile Display .....	35
Figure 3-1: Randomized particles rotate to form chains when electric field is applied. ..	37
Figure 3-2: Electro-Rheological Fluid at Reference (left) and Activated States (right)...	38
Figure 3-3: Behavior of Various Classes of Viscous Fluids, Including Bingham Plastics. ....	38
Figure 3-4: Programmable Surfaces based on ER Fluids. ....	43
Figure 3-5: Force Display Device using electrorheological fluids. ....	44
Figure 3-6: Haptic Joystick using ERFs. ....	44
Figure 3-7: ERF-based Tactile Pin Array.....	45
Figure 3-8: ECS Actuator - concept (Left) and prototype (Right).....	45
Figure 4-1: CC Parts –mounting cylinder, inner and outer electrode, respectively.....	47
Figure 4-2: Assembled Actuator with and without cover.....	47
Figure 4-3: Schematic of Concentric-Cylinder ERF Actuator. ....	47
Figure 4-4: The Force-Torque relationship around a cylinder (cross-section). ....	49
Figure 4-5: Assembly of Multiple Flat-Plate ERF Actuator.....	51
Figure 4-6: Flat-Plate Electrodes. ....	52
Figure 4-7: Torque vs. Voltage for Various <i>Radii</i> for the CC Actuator. ....	57

Figure 4-8: Torque vs. Voltage for Various <i>Gap Widths</i> for the CC Actuator.....	58
Figure 4-9: Torque vs. Voltage for Various <i>Radii</i> for the FP Actuator.....	60
Figure 4-10: Torque vs. Voltage for Various <i>Gap Width</i> Designs for the FP Actuator. ..	61
Figure 4-11: Torque Output for Radius and Length for CC Actuator in Static Mode.....	63
Figure 4-12: Torque Output for Radius and Length for CC Actuator in Dynamic Mode.	64
Figure 4-13: Torque Output for Radius and Length for FP Actuator in Static Mode. ....	65
Figure 4-14: Torque Output for Radius and Length for CC Actuator in Dynamic Mode.	65
Figure 4-15: Teflon O-ring Seals – Various Shaft Designs.....	67
Figure 4-16: Spring Loaded Teflon Seal on Teflon.....	67
Figure 5-1: Inner Copper Electrode.....	70
Figure 5-2: Electrode Mounted on Shaft. ....	70
Figure 5-3: CC Testbed.....	71
Figure 5-4: Close-up of top of Testbed.....	71
Figure 5-5: Static Torque vs. Voltage for CC Actuator w/ 0.50 mm Gap.....	72
Figure 5-6: Theoretical and Experimental Dynamic Torque vs. Voltage for CC Actuator with 0.50 mm Gap.....	74
Figure 5-7: FP Actuator Shafts.....	75
Figure 5-8: FP Actuator Case and Lid.....	75
Figure 5-9: Flat-Plate Actuator Assembly.....	76
Figure 5-10: Flat-Plate Actuator Test Setup.....	76
Figure 5-11: Static Torque vs. Voltage for FP Actuator w/ 0.75 mm Gap and 4 Plates. .	77
Figure 5-12: Theoretical and Experimental Dynamic Torque vs. Voltage for FP Actuator w/ 0.75 mm Gap and Four Moving Electrode Plates.....	79
Figure 6-1: New FP testbed with DC motor attached.....	82
Figure 6-2: Sample section of response-time graph with indicated features.....	83
Figure 6-3: Steps taken to clean up and isolate the input and output frequencies.....	84
Figure 6-4: Samples of Clockwise and Counterclockwise experimental runs.....	85
Figure 6-5: Processed Clockwise and Counterclockwise experimental runs.....	86
Figure 7-1: Representation of the strength of a physical sensation.....	92
Figure 7-2: Example interpretations of physical sensations.....	92
Figure 7-3: Haptic Knob Device Using an FP Actuator.....	93
Figure 7-4: Knob Attached to top of actuator testbed.....	94
Figure 7-5: Demonstrated and Potential Knob Profiles.....	95
Figure 7-6: One Knob Can Simulate Different Types of Knobs.....	96
Figure 7-7: Haptic Joystick. Handle May Have a Button Attached.....	97
Figure 7-8: Representations of the <i>Channels</i> (left) and <i>Zones</i> (right) available when using a 2-D Interface.....	97
Figure 7-9: Calculated Performance Curves for the Joystick's FP Actuator.....	99
Figure 7-10: Joystick Joint Assembly.....	100
Figure 7-11: Assembled Joystick with Joint and Two Actuators.....	101
Figure 7-12: Representation of a method to use Haptic sensations to control a radio using the Haptic Joystick. The Channels guide the user to different options.....	102
Figure 8-1: Previous sealing methods - Teflon Seal on FP shaft (L), Seal inside actuator cover (R).....	105
Figure 8-2: Reorientation of Actuator to Address Leakage.....	106

Figure 8-3: Multiple connection points for FP actuator, can result in loose components .....	106
Figure 8-4: CCv2 Fixed Electrode.....	108
Figure 8-5: Rotating electrode, with attached output shaft.....	109
Figure 8-6: Bottom of electrode with attachment lip.....	109
Figure 8-7: Cover to close bottom of electrode .....	110
Figure 8-8: Illustration of SLA Rapid Prototyping process (simplified).....	110
Figure 8-9: Body of the case, in CAD and Production Versions.....	111
Figure 8-10: Cover of case.....	111
Figure 8-11: Cover's-cover, and electrode barrier.....	112
Figure 8-12: Encoder Mount.....	112
Figure 8-13: Assembly of Rotating Electrode Components .....	113
Figure 8-14: Assembly of Rotating Electrode to Case .....	114
Figure 8-15: Threaded Attachment Point Assembled to Fixed Electrode .....	114
Figure 8-16: Cover assembled to Electrode (L) Electrode Inserted into Case (R) .....	115
Figure 8-17: Electrical Attachment to Electrode (L) and Electrode Shield (R) .....	115
Figure 8-18: Teflon Washer and Seal Insertion (L) and Cover's Cover assembly (R). ..	116
Figure 8-19: Bearing Guides and Provides Electrical Contact for Rotating Electrode ..	116
Figure 8-20: Encoder Mounted to Case and Shaft.....	117
Figure 8-21: ERF Fill Holes in Cover.....	117
Figure 8-22: Completed CCv2 Actuator.....	118
Figure 8-23: Torque Output for CCv2 actuator using the HP2 ERF .....	119
Figure 9-1: Haptic Knob Base Prototype.....	121
Figure 9-2: Actuator Inserted Into Bearing (L) Shaft Collar Holds Actuator in Place (R) .....	122
Figure 9-3: Load cell and attachment to actuator. ....	122
Figure 9-4: Complete Knob, Version 2.....	123
Figure 9-5: DAQCard-6062E, BNC-2120 connector block, and Encoder Circuit (L to R) .....	124
Figure 9-6: Labview Front Panel .....	125
Figure 9-7: Representation of the Four General Knob Profiles:.....	126
Figure 9-8: Connection of Knob to DAQ Interface and Power Supply.....	128
Figure 10-1: Joystick Housing Base (L) with Actuators (R) .....	130
Figure 10-2: Universal Joint Components (L) and Assembled Joint (R) .....	131
Figure 10-3: Miter Gear Assembly, Attaches Joint to Actuators.....	132
Figure 10-4: Haptic Joystick, Version 2 .....	132
Figure 10-5: The Haptic Joystick's Zones.....	133
Figure 10-6: The Haptic Joystick's Virtual Channels.....	134
Figure 10-7: Front Panel Interface to Joystick Program.....	135
Figure 10-8: Virtual Channels with In-Channel Force Profiles: Varying Force Profile( <i>Top</i> ) Selections( <i>Middle</i> ) Detents ( <i>Bottom</i> ) .....	136
Figure 11-1: Ergonomically Defined Preferred (crosshatched) and Regular Manipulation Space for the Hands of a Seated Human [Kroemer, 2003a] .....	140
Figure 11-2: Impulsive Square Wave Detent Style. ....	143
Figure 11-3: Forces Ramp Up and Down for a Shaped Detent Style.....	143
Figure 12-1: Enclosed Disk Grip Concept.....	146

Figure 12-2: Extended Shaft with Flattened Edges (L) Attachment to Knob Base (R) .	147
Figure 12-3: Disk Knob .....	148
Figure 12-4: Grasping the Disk Knob and Resulting Hand Motion .....	148
Figure 12-5: Ball Grip Knob.....	149
Figure 12-6: Grasping the Ball Knob and Resulting Wrist Motion.....	149
Figure 12-7: Enclosed Disk Knob.....	150
Figure 12-8: Grasping the Enclosed Disk Knob and Resulting Finger/Wrist Motion....	150
Figure 12-9: Hand Wheel Knob.....	151
Figure 12-10: Grasping the Hand Wheel Knob and Resulting Arm Motion.....	151
Figure 12-11: Knobs 5 to 8, Knob Shapes with Smooth Texture.....	152
Figure 12-12: Example of a Knurled Surface to Increase Grip .....	153
Figure 12-13: Knobs 5 to 8, Knob Shapes with Knurled Texture .....	153
Figure 12-14: <i>Square Detents</i> Force Profile .....	154
Figure 12-15: <i>Sine Detents</i> Force Profile.....	155
Figure 12-16: <i>Triangle Detents</i> Force Profile.....	155
Figure 12-17: <i>Sine Wave</i> Force Profile.....	156
Figure 13-1: Knob Test Order Grid. ....	158
Figure 13-2: Human Factors Experiment Setup .....	159
Figure 13-4: Latin Squares Defining Experimental Order .....	160
Figure 13-5: Data Collection Sheet.....	161
Figure 13-6: Non-Experimental Knob Used for Preliminary Practice .....	163
Figure 13-7: Collated Data from Experiment .....	166
Figure 15-1: Location of Carpal Tunnel (Image from[carpal-tunnel-syndrome.net])....	187
Figure 15-2: Closeup of Affected Nerves and Tendons (Image from [American Society for Surgery of the Hand]).....	187
Figure 15-3: Location of Sensation Loss or Alteration (Image from [American Society for Surgery of the Hand]).....	187
Figure 16-1: Closed-Loop Control Scheme for ERF actuator Torque output. ....	193
Figure 16-2: Possible Method to Generate Pseudo-Active Sensations with ERF Actuator .....	197

# 1 INTRODUCTION

## 1.1 Haptic Technologies

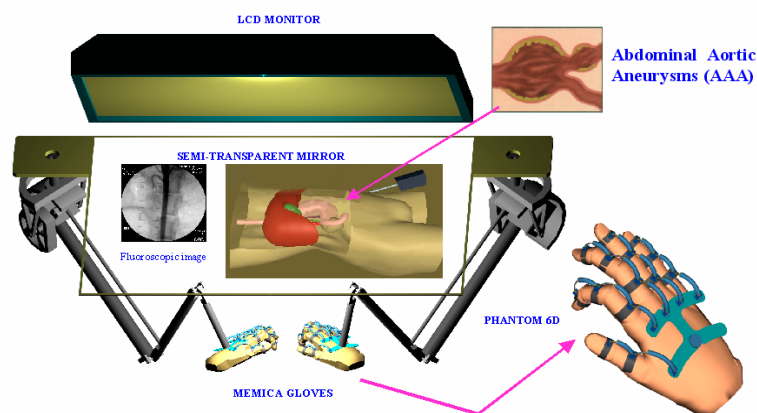
Researchers in the field of robotics have been advancing the capabilities of their robots by designing biomimetic robotic systems. Biomimetic systems attempt to copy the form or behavior of biological systems to create efficient machines and processes. Since nature has had millions upon millions of years to perfect these systems it is logical to learn from them when designing machines and processes. Another way to use the tools that nature has built is to design machines that specifically incorporate a human into the system. These biologically-incorporated systems extend the capabilities of machines by adding a human component or extend the abilities of humans with the assistance of man-made devices.

The interfaces that are used when connecting these human-machine systems together are the human senses. These interface systems can truly be called bio-mimetic systems in that they are designed to respond to, or “mimic”, the reactions and sensations of a biological system, namely the human operator. An in depth discussion of biomimetics can be found at [Bar-Cohen, 2003]

Various systems exist that provide information to the human senses of sight and hearing. Audio and video systems have been perfected over many decades so that it is now possible for a user to wear small devices, such as goggles and earphones, which allow a user to see and hear various forms of information. Systems exist and are being developed to interface with a third human sense -- the sense of touch. These systems are called *Haptic Systems* or simply *Haptics*. The inclusion of haptic systems, such as the ones presented in the following sections, allows for the creation of systems that provide a

user with three major inputs of visual, auditory and haptic stimuli, making it possible to generate almost any sensation that is desired in a believable and immersive manner. These systems can be used for virtual reality, telepresence and other applications.

*Virtual Reality* systems (or *VR*) present a computer-generated visual and auditory experience that allows a user to be immersed within a computer generated “world” for various purposes. For example, VR can be used, in conjunction with traditional computer input systems, as a powerful design tool allowing a user to see objects that he or she is designing. The application to entertainment or training simulation systems is equally useful as it allows for the creation of an infinite number of immersive environments to suit any need. The addition of haptic systems to virtual reality will greatly increase its effectiveness at simulating real-world situations. One example can potentially include a medical training system using a simulator and virtual reality where a haptic system provides doctors with the “feel” of virtual patients. Figure 1-1 shows the concept of such a medical simulation system, the visual display and the haptic gloves are combined to simulate, in this example, an abdominal aortic aneurysm surgery.



**Figure 1-1:** Virtual Reality for Surgical Training.



*Tele-presence* is a form of remote control for robotic systems, by which an operator interfaces with a robot, via visual, auditory and force feedback “as if he was there” at the remote site in place of the robot. Since the data processing and decision making power that a human is capable of far surpasses even the most advanced computer system, a human operator can control a robot in unknown or difficult situations more effectively than any computer program. The Mars Exploration Rover mission from 2004, shown in Figure 1-2, employed a simple form of telepresence. The Spirit and Opportunity rovers sent visual and other sensor data to operators on Earth who, in turn, sent instructions for the rovers to follow. The time-lag inherent in Earth to Mars communications required the rovers to act semi-independently, but it can be imagined that if the rovers were in near-instantaneous communications range they would directly act out the human-operator’s instructions.

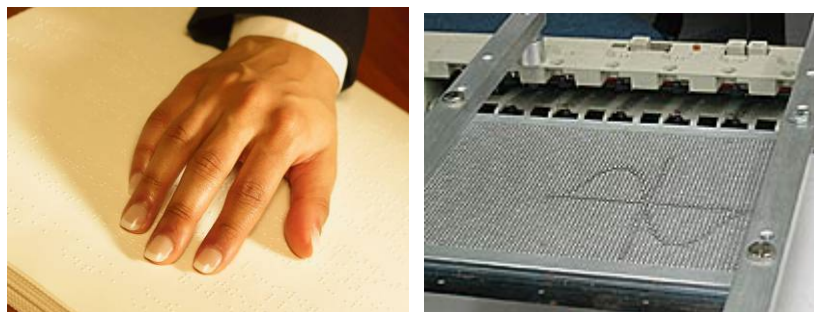


**Figure 1-2:** Artist rendition of a Mars Exploration Rover – *Spirit* or *Opportunity* – approaching a rock on the surface of Mars. (Courtesy NASA/JPL-Caltech)

*Human-Assistive* devices use the force feedback component of haptic systems to generate forces for applications such as rehabilitation and muscle enhancement. Devices such as the exoskeletons presented in the following sections can be programmed to

provide resistive forces to targeted body parts for use in rehabilitation. It can be easily imagined that a haptic glove can be used to support an injured hand while providing the means for targeted exercises to the injured body parts. Assistive systems using similar exoskeleton devices can extend a person's muscle capabilities by following the user's movement and producing external forces proportional to the forces applied by the user.

*Haptic Interfaces*, the final category of haptic devices, uses the sense of touch as a conduit to provide information to a user. A static form of haptic display is seen in the use of the Braille alphabet system for the blind. The Braille alphabet uses raised bumps and patterns impressed into paper to represent text, as seen in Figure 1-3. This system allows blind people to receive information from printed material that would otherwise have been unavailable to them. More modern versions of such touch-based interface systems, such as the pin-based system also shown in Figure 1-3, use a tactile display and computer system to update and change the display in order to provide a blind person with text as well as other graphical information. Other information may also be conveyed through similar sense-of-touch systems. The development of such haptic interface systems are presented in the following chapters as the subject of this research project.



**Figure 1-3:** (Left) Person reading a traditional Braille-based book by touch  
(Right) Pin-based display system from NIST, displaying a sine wave.

## 1.2 Research Project Goals and Plans

Although various different researchers and companies have developed many haptic systems, newer and better technologies may be able to overcome some of the limitations of the haptic systems that already exist.

I developed the Haptic systems in the course of this research project in three distinct steps – the design of new, compact actuators, the design of the haptic interface devices that make use of those actuators and experimental testing with human subjects to refine and validate the design of the interface system.

When designing a new and novel actuation technology the goal is to design actuators that meet as many of the criteria and characteristics listed in Table 1-1 as possible. The “perfect” actuator incorporates all of these criteria. This is a worthy goal, but an actuator that can meet a fraction of these criteria can be very useful as well.

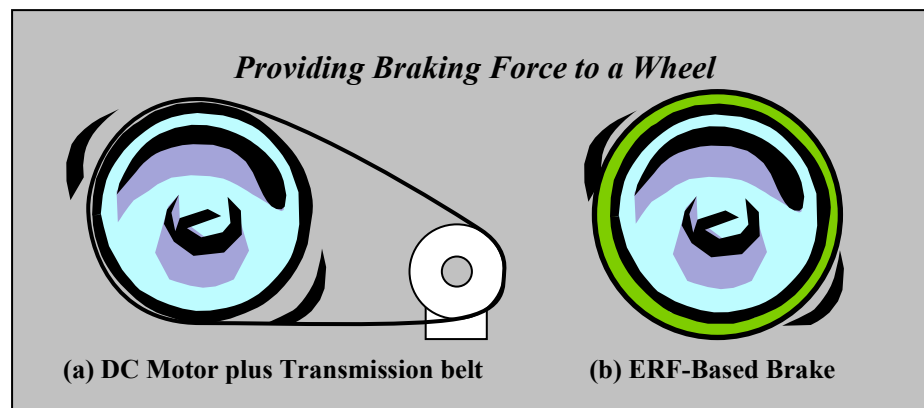
Lightweight
Compact
Large Forces
Large Displacements
High Energy Efficiency
High Energy Density
Low Cost
Quiet
High Speed

**Table 1-1:** Design Goal Criteria Used For Developing New Actuators.

This dissertation will present the explorations that I made to incorporate new actuator technologies, such as smart material technologies, into the design of haptic interfaces. The addition of new technologies is expected to increase the robustness,

flexibility and capabilities of the haptic devices, and allow for the incorporation of many of the criteria listed above.

I proposed that the class of Smart Materials known as Smart Fluids might present an opportunity to design a useful actuator for haptic systems. I examined the Smart Fluid called an Electro-Rheological Fluid or ERF. ERFs are fluids that change their viscosity when subjected to an electric field. Since building an electric field can be an almost trivial task, simply requiring two electrodes with a gap in between, it is possible to include this two-electrode system into a mechanical component and provide resistance without the need for transmission elements. Figure 1-4 illustrates how an ERF-based actuator can be more compact than a motor based actuator.



**Figure 1-4:** ERF-based braking systems can be more compact because they don't require transmission elements.

I then examined additional design improvements such as flexibility in the mechanical design and rapid prototyping techniques to develop viable actuators.

Once I developed the actuators, I added them to haptic systems – the mechanical systems that interface with the operator's sense of touch. Since many haptic systems do exist a review of current haptic systems is important to identify what type of haptic technologies will be helpful and how they can be applied in new and unique ways.

The following chapters will review some of the haptic technologies that currently exist as well as present the concept of using Smart Materials – materials that respond to stimuli from the environment in unique ways – as an actuation technology for haptic devices. I will present my design and testing of two actuators as well as the redesign of one of the actuators for a second generation system. In addition, I will present two different haptic devices and their second generation prototypes. I will also present the development of the software interface systems and lastly, the human experimental testing that I performed to validate the designs.

### **1.3 Important Note on Nomenclature**

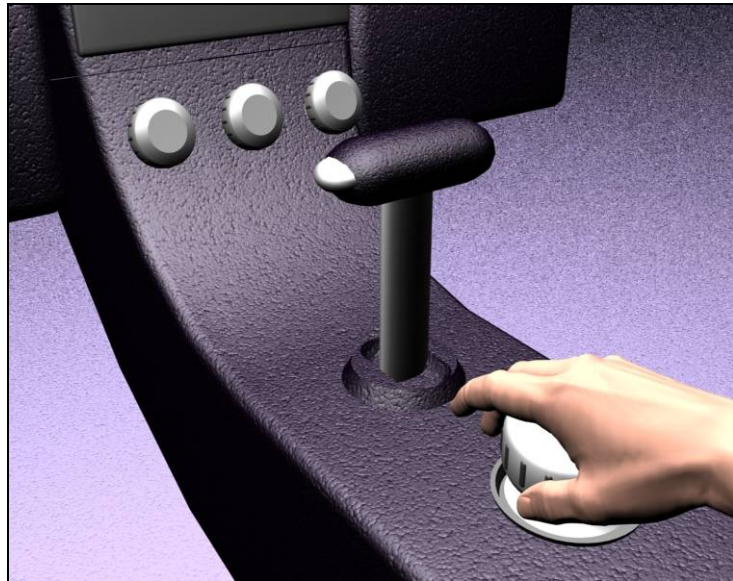
The electro-rheological fluid based actuation systems that I developed in the course of this research project can not be considered “actuators” in the strictest definition of the term. An actuator, according to accepted definition, is “a mechanical device for moving or controlling something” [Merriam-Webster’s Online Dictionary] Since ERFs generate forces by changing the viscosity of the fluid in which an object is moved, the ERF forces can only be felt when external forces are applied. The forces created within an ERF device cannot be actively generated to move an object and the device can therefore not be considered a “traditional” actuator. These non-active actuators are sometimes referred to as *passive actuators* or *semi-active brakes*.

Throughout the text of this dissertation, the actuation systems that I developed will be referred to simply as *actuators* for brevity, with the inherent understanding that they are in truth *passive* actuators, and should be considered as such.

## 1.4 Research into ERF-Based Haptic Interfaces

### *Problem Statement*

The goal of this research project was to develop a haptic interface system using advanced smart material based actuation technology. The application of that interface into the automotive industry to control the secondary systems of an automobile through the driver's sense of touch will be used as an example application. I designed the interface using new, advanced actuators to be compact, and energy efficient. Figure 1-5, below, shows conceptually how such an interface might be integrated into a vehicle's dashboard.



**Figure 1-5:** Multi-function haptic interface concept for vehicular instrument control.

The actuators that power the interface are based on electrorheological fluids (ERFs), which change their viscosity when subjected to an electric field. ERFs provide resistance to applied forces and cannot actively generate forces on their own. Design optimization and human experimental testing were necessary to maximize the amount of understandable force information generated by the ERF actuators.

### *Discussion*

I postulated that the use of haptic interfaces will increase the capabilities of many human-machine interfaces. The systems that I developed in the course of this project were designed to be flexible enough to be used in almost any appropriate system. I chose the application to an automobile interface as an example in order to provide focus to the research tasks. The discussion of the automotive application in the following sections should therefore not be seen to imply a limited application of this technology.

### *Motivation*

In many industries as well as the automotive industry, the increase in controls has created a desire to simplify and enhance the human-machine interface. By introducing the use of haptic technologies it is possible to open another pathway to provide information, in addition to visual and auditory stimuli. In the automotive example, this additional information pathway can be used by a driver to understand the operational state of his or her vehicle. The incorporation of this type of technology may allow automobile manufacturers to simplify and streamline the dashboards of their vehicles.

The use of haptic feedback interfaces can improve a driver's control of a vehicle's secondary instrumentation, such as radio and climate controls, by accessing the capabilities of the driver's sense of touch. By interacting with the sensing capabilities of the driver's hands and fingers it is possible to transmit information without requiring the driver to take his or her eyes from the road. Intuition suggests that this is a safer and more desirable method of conveying information for a vehicle's operator, although formal testing would be required to prove the point.

Using electrorheological fluid-based actuators to create haptic feedback devices results in smaller, energy-efficient, lightweight, yet powerful interfaces. By controlling the properties of ERFs, it is possible to simulate the “feel” of many existing control devices. A device that can perform multiple functions will be able to combine many different interfaces into a single device.

The use of ERFs as the actuation technology means that the device will be a passive device only. This provides a challenge to maximize the force information available through the haptic interface within the limitations of the ERF-based system. Human subject testing was necessary to identify the attributes of the system that will maximize the available force information.

The specific goals of the research project were to:

- Design Haptic devices, using electrorheological fluids, to interact with the sense of touch through force-feedback methods
  - This establishes a new user-interface method to provide information (in addition to visual and auditory information)
- Design Haptic interface systems:
  - Present information to a user in an intuitive form using force-feedback cues
  - As an example., seek to reduce clutter on the dashboard by replacing many interfaces with a single reconfigurable interface

#### *Uniqueness of Approach to Solve Problem*

In order to develop new and novel haptic devices, the research conducted over the course of this project - and presented within this dissertation - used electrorheological fluids to develop resistive forces within compact and controllable actuators. I then



incorporated these passive actuators – sometimes referred to as *semi-active brakes* - into haptic interface systems that I used to provide a variety of information to a user through the sense of touch and force feedback sensations.

While ERF-based devices have previously been used in Haptic systems, as presented in the sections below, many of those systems use ERFs as a simple braking mechanism. For an example, see the force-feedback joystick presented below in section 3.2 which provides simple resistance by placing ERF within the space inside a ball-and-socket joint. While this is a viable method for providing braking forces to a joystick, it does not allow for more complex and multiple-degree-of-freedom sensations.

The approach taken within the course of this research has been to develop multi-degree of freedom systems using novel ERF-based actuators to convey a variety of haptic sensations. I developed software to generate these haptic sensations and have presented demonstrations to show the efficacy of ERF-based Haptic Devices. I developed numerous variant forms of the interface device's prototype and used various software methods to present the force feedback cues. I performed human factor testing to isolate the device and software methods that would be most effective at presenting the force information to the users.

## **1.5 Contributions / Acknowledgments**

I recognize and appreciate the contributions that were made to the research performed in the course of this project and acknowledge the assistance provided by the members of the Robotics and Mechatronics Lab in addition to other people. This section presents the steps taken in the course of the project as well as acknowledges the people

that have contributed and the publications that have been made through the course of this research project.

### 1.5.1 Research steps and milestones

The research that my colleagues and I performed in the course of this project can be classified into the areas of ERF actuator development, haptic device development, and haptic simulation and application and haptic testing. Many steps were made along the way in each of these areas including the main points listed below:

#### *ERF actuator Development*

- Electrorheological fluid based Concentric Cylinder (CC) Actuator.
  - Concept and Design of CC actuator concept
  - Mathematical model derivation to predict performance
  - Parametric Analysis to select specific prototype design
  - Development and building of CC prototype
  - Experimental testing to confirm mathematical model
  - Update of parametric analysis for future design choices
- Electrorheological fluid based Flat-Plate (FP) Actuator.
  - Concept and Design of FP actuator concept
  - Mathematical model derivation to predict torque output performance
  - Parametric Analysis to select specific prototype design
  - Development and building of FP prototype
  - Experimental testing to confirm mathematical model
  - Update of parametric analysis for future design choices
  - Response-time experiments to classify the FP actuator's bandwidth
- Electrorheological fluid based Concentric Cylinder version 2 (CCv2) Actuator.
  - Concept and Design of CC actuator concept
  - Development and building of CC prototype

#### *Haptic Device Development*

- Haptic Knob development, version 1 and version 2
  - Concept and Design of ERF-based Haptic Knob interface
  - Prototype design and development
  - Design and building of Haptic knob test bed

- Version 2, Update and prototype revised device
- Haptic Joystick development, version 1 and version 2
  - Concept and Design of Multi-Degree-of-Freedom ERF-based haptic interface
  - Prototype design and development for Haptic Joystick
  - Design and building of Haptic Joystick test bed
  - Version2, Update and prototype revised device

### *Haptic Simulation and Application*

- Haptic Knob simulation, version 1 and version 2
  - Concept and Design of Haptic Knob demonstrations
  - Development of control software to simulate detents
  - Development of control software to simulate hard stops
- Haptic Knob application
  - Development of concepts for using Haptic Knob for automotive application
- Haptic Joystick simulation, version 1 and version 2
  - Concept and Design of Haptic Joystick demonstrations
  - Development of control software to simulate virtual channels on 2D surface
  - Development of control software to simulate detents, and other simulations-within-channel
- Haptic Joystick application
  - Development of concepts for using Haptic Joystick for automotive application

### *Haptic Testing*

- Haptic Knob Human Factors experiment
  - Develop control software to allow for the presentation of different force profiles using the Haptic Knob
  - Design detent counting experiment using Haptic Knob to explore the efficacy of the following design options:
    - Knob Shape
    - Knob Texture
    - Detent Style
  - Perform experiment, collate data and analyze results
  - Identify most effective design for the Haptic Knob, to be used for future devices and ongoing research

### 1.5.2 Acknowledgements

Much of the work done for this project and, indeed, for most of the work performed in the Rutgers Robotics and Mechatronics Laboratory as well as the Northeastern University Robotics and Mechatronics Lab owes its success to the help provided by all of the members of the Lab both past and present.

Much preliminary work done using electrorheological fluids with the Lab was performed by various graduate and undergraduate researchers throughout the years. Specific contributions to the work presented within this thesis were made by the following people.

Brian Weinberg (undergraduate research assistant) put forth much effort to build the initial actuator prototypes, and haptic devices. In addition, he made indispensable input into the development of the Flat-Plate actuator, presented in section 4.2 below, as well as generating a large number of the CAD drawing. A large percentage of the Rapid Prototyped parts used in the construction of the version 1 ERF actuators and the haptic devices were built by Brian in the Rutgers Mechanical and Aerospace Engineering Department's Rapid Prototyping Laboratory. In addition, while many of the experimental tests were developed and supervised by the author, Brian performed much of the testing for the first pair of actuators presented here.

The Flat-Plate actuator was developed along with Jason Nikitzuk (graduate student) in a collaborative effort. He is working on a different but related project using ERF actuators for orthotic devices. Jason performed a number of the actuator experiments presented within this thesis. In addition Jason performed much of the

programming used for the version 1 actuators and devices including that used to demonstrate haptic sensations using the version 1 Haptic Knob and Joystick.

Azadeh Khanicheh (graduate student) who is working on a related ERF device project for use in MRI tests provided invaluable insight into the development of the haptic systems as well as allowing herself to be used to test experimental protocols before bringing in actual test subjects.

Juan Melli-Huber (undergraduate research assistant) assisted with the development of the initial actuator mathematical models as well as some of the design concepts.

Kirti Mansukhani (graduate student) assisted with the background search for haptic devices.

Evelyn Behar (postdoctoral fellow, Boston University) who provided invaluable assistance with the design of the human factors experiment as well as with the statistical analysis performed on the gathered experimental data,

### **1.5.3 Publications**

Much of the work presented within this paper has been reported in various journals, books and other forums. A list of publications that have been made due to results obtained within the course of this research project is presented here:

#### *PAPERS PRESENTED AT CONFERENCES BY THE AUTHOR*

- Fisch A., Nikitzuk J., Weinberg B., Melli-Huber J., Mavroidis C., Wampler C.,  
“Development of an Electro-Rheological Fluidic Actuator and Haptic Systems for Vehicular

Instrument Control” 2003 ASME International Mechanical Engineering Congress and Exposition, November 15 - 21, 2003 – Washington, D.C.

- Melli-Huber J., Weinberg B., Fisch A., Nikitzuk J., Mavroidis C., Wampler C., " Electro-Rheological Fluidic Actuators for Haptic Vehicular Instrument Controls", *Eleventh Symposium on Haptic Interfaces for Virtual Environment and Teleoperator Systems*, March 22 and 23, 2003, Los Angeles, CA.

#### PUBLICATIONS

- Fisch A., Nikitzuk J., Weinberg B., Melli-Huber J., Mavroidis C., Wampler C., “Development of an Electro-Rheological Fluidic Actuator and Haptic Systems for Vehicular Instrument Control” *Proceedings of IMECE2003 2003 ASME International Mechanical Engineering Congress and Exposition*, November 15 - 21, 2003 – Washington, D.C.
- Fisch A., Mavroidis C., Melli-Huber J. and Bar-Cohen Y., "Chapter 4: Haptic Devices for Virtual Reality, Telepresence, and Human-Assistive Robotics" Invited Chapter in *Biologically-Inspired Intelligent Robots*, Editors: Yoseph Bar-Cohen and Cynthia Breazeal, SPIE Press, 2003.
- Melli-Huber J., Weinberg B., Fisch A., Nikitzuk J., Mavroidis C., Wampler C., " Electro-Rheological Fluidic Actuators for Haptic Vehicular Instrument Controls", *Proceedings of the Eleventh Symposium on Haptic Interfaces for Virtual Environment and Teleoperator Systems*, March 22 and 23, 2003, Los Angeles, CA. Also submitted for publication in the IEEE / ASME Transaction

## **1.6 Outline of Dissertation**

Over the course of this paper, I will present my design of three ERF-based actuators and four haptic devices using those actuators. The dissertation is structured in the following manner. Chapter 2 presents an overview of current haptic systems. Chapter 3 presents information about electrorheological fluids as well as providing examples of how ERFs have previously been used in haptic systems. Chapter 4 introduces the two initial ERF-based actuators I developed for this project, the design concepts used in creating these actuators, the analytical models generated to predict their performance, the parametric analyses performed to facilitate choosing the actuator parameters, as well as an examination of additional design considerations. Chapters 5 and 6 present the experiments and the results obtained for the two actuators. The incorporation of the actuators into haptic devices is presented in Chapter 7 as well as concepts of how those systems can be used to provide information to a driver. Chapter 8 presents a second generation version of one of the actuators, including design, manufacturing and assembly. Chapters 9 and 10 present the incorporation of the second generation actuator into two new haptic devices and the software I designed to control those devices to present haptic information. Chapter 11 explores the ergonomic considerations surrounding the use of a knob system to present force information. Chapters 12, 13 and 14 present the design options I explored with Human Factor experiments, the experiments that sought to maximize the designs based on those options, and the results obtained from those experiments. Chapter 15 explores whether specific testing needs to be done to maximize the haptic interfaces for people who suffer from

hand injuries, by testing one test subject who suffered from Carpal Tunnel Syndrome.

Finally, Chapter 16 draws some conclusions and presents plans for future work



## 2 HAPTIC SYSTEMS

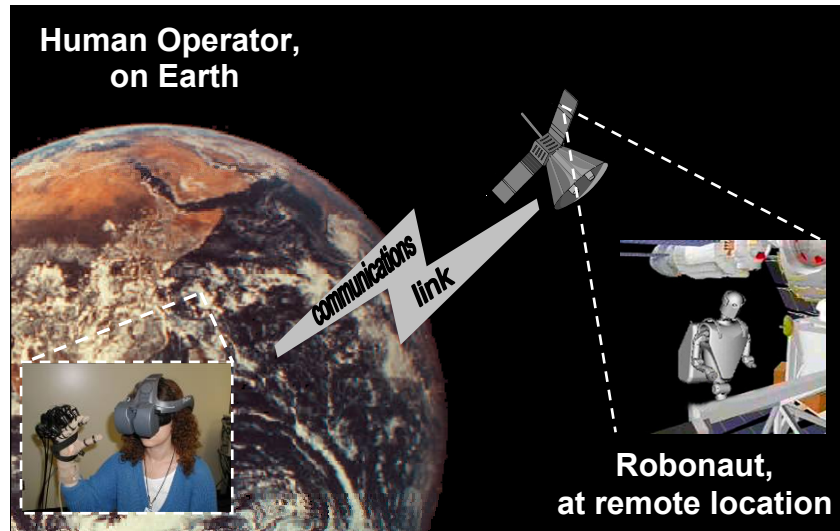
Haptic devices interact with the sense of touch by stimulating the sensory capabilities within our hands and other body parts. The increase in computer capability and the desire for better ways to connect to computer-generated environments has driven the development of practical devices for haptic interaction. Various haptic systems exist as research demonstrations. However, while research is still continuing, consumer-level haptic systems have been introduced. For example, force feedback gaming devices, such as joysticks and computer mice, are now available. In the medical field, telesurgery or surgeon-directed robotic surgery has been gaining recognition and could be even more effective if haptic sensations can be added to those systems.

The development of even more capable devices that can accurately reproduce a large range of haptic information is an important component for the technologies of virtual reality and telepresence. In medical applications, for example, it is vital for a surgeon to “feel” the difference between hard and soft tissues. For telepresence applications it is equally important for an operator to feel what the remote robot is touching to allow the operator to run the robot in a more natural and responsive manner.

Telepresence systems and, even more simply, virtual reality systems, that incorporate a successful force-feedback component can be extremely useful for a wide variety of applications. For example:

- Space operations can benefit from robust control of robots. If Robonaut, NASA’s robotic astronaut that is now in development [NASA-JSC Website], can be used with a telepresence system, it could be deployed in difficult or hazardous situations, in the place of an astronaut, with its operator, safely housed on a nearby spaceship or even

on the ground, controlling its actions in a fluid, intuitive fashion. Figure 2-1 demonstrates the concept of remotely controlling Robonaut's operations.



**Figure 2-1:** Example of Tele-Presence control of Robonaut.

- A force-feedback system could be used for rehabilitation purposes in space applications, as it can simulate gravitational forces, thus preventing the bone and muscle loss that are the result of extended operations in space.
- A virtual reality system that produces realistic sensations can be used for training, for simulations or for entertainment by allowing users to fully interact with virtual world.
- Medical students or field-medics could train with virtual surgery to allow for better training options. Surgeons could perform microsurgery by mirroring forces from the surgeon to the microsurgical tool. In addition, doctors could perform surgical operations remotely in places where there are no surgeons, as with the case of the doctor at the South Pole research facility who was diagnosed with breast cancer but could not be evacuated from the site for a few months.

The successful creation of a completely immersive interface system that can accurately convey information to the senses of sight, hearing and touch is vital to the development of these and other systems.

Haptic technology is difficult to achieve convincingly because the human sense of touch is far more sensitive than the senses of sight or sound. In visual systems a picture

needs to be refreshed at only 30 frames per second to trick the eye into thinking it is seeing continuous motion. However, the sense of touch requires that a sensation be updated 320 times per second to feel like a continuous force and up to 5,000 to 10,000 times per second to be convincingly sensed as a vibration [Burdea, 1996].

There are two main areas of application and research that are currently being developed by researchers in the haptics field - Virtual Reality/Telerobotic systems and Force Feedback/Tactile Display systems. Although both types of systems seek to simulate force information, there are differences in the types of forces being simulated. Virtual reality and Telerobotic researchers seek to develop technologies that can simulate or mirror virtual or remote forces by conveying large-scale shape and force information. Researchers in the field of Force Feedback and Tactile displays seek to develop methods of conveying information between humans and machines, using the sense of touch.

Using the criteria of large- and small-scale force generation, haptic devices can broadly be categorized as follows:

<b>Virtual Reality/Telerobotics:</b>	a) Exoskeletons and Stationary Devices;
	b) Gloves and Wearable devices;
	c) Point-sources and Specific Task Devices;
	d) Mobility Interfaces.
<b>Feedback Input devices:</b>	a) Force feedback / input devices;
	b) Tactile displays.

**Table 2-1:** Haptic Device Categories

The following sections present some of the current devices being developed from the categories listed above.

## **2.1 Current Haptic Devices – Review**

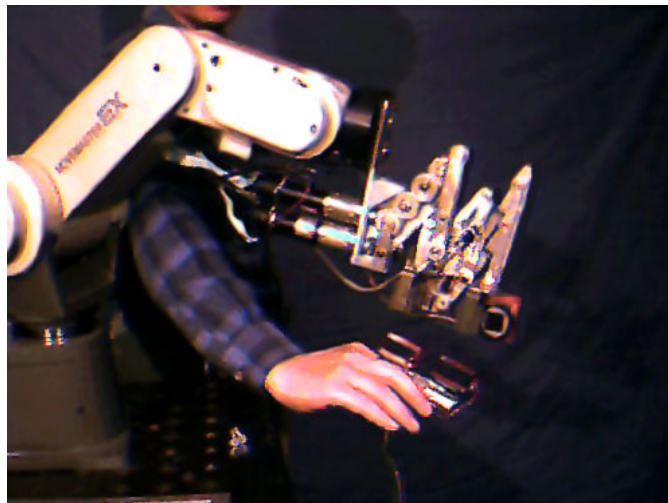
Much research is being performed to create a viable human-machine interface to use in Virtual Reality or Telerobotic systems. Various approaches have been taken to add touch information to these systems. The following section will present the categories of haptic devices that are in development - Exoskeletons and Stationary Devices, Gloves and Wearable devices, Point-sources and Specific Task Devices, Locomotive Interfaces, Force feedback / input devices and Tactile displays.

Each category will be presented with a description of the basic concept behind the devices in the category followed by various example devices from that category. Although the devices presented are all examples of the fine work being done in the field of haptic technology, the overview presented here should not be taken as a comprehensive list. Rather, the devices presented were chosen as representations of the different approaches that are available to achieve various forms of haptic information.

### **2.1.1 Exoskeletons and Stationary Devices**

The first category of systems that are being developed for Virtual Reality and Telerobotic applications are the exoskeleton and stationary devices. The term exoskeleton in biology refers to the hard outer shell that exists on many insects and other creatures. In a technical sense the word refers to a system that covers the user or that the user has to wear. Most current haptic devices that are classified as exoskeletons are large and immobile systems that the user must attach to him- or herself. The benefit of exoskeleton devices is that their large size and immobile nature allow for the generation of large and varied force information without strict size or weight constraints. Various different approaches have been taken to provide force information in this manner.

Many of the exoskeleton devices that have been developed provide force information along the whole arm or a similar area, using a variety of actuation methods. One example of this type of device is the Iowa State's Force Feedback Exoskeleton, shown in Figure 2-2, which uses magnetic fields to transfer force information to the user [Luecke and Chai, 1997, and VRAC Website].



**Figure 2-2:** Iowa State Force Feedback Exoskeleton.

Other systems exist which provide haptic information to the arm, such as the CyberForce system from Virtual Technologies, Inc. shown in Figure 2-3.



**Figure 2-3:** CyberForce

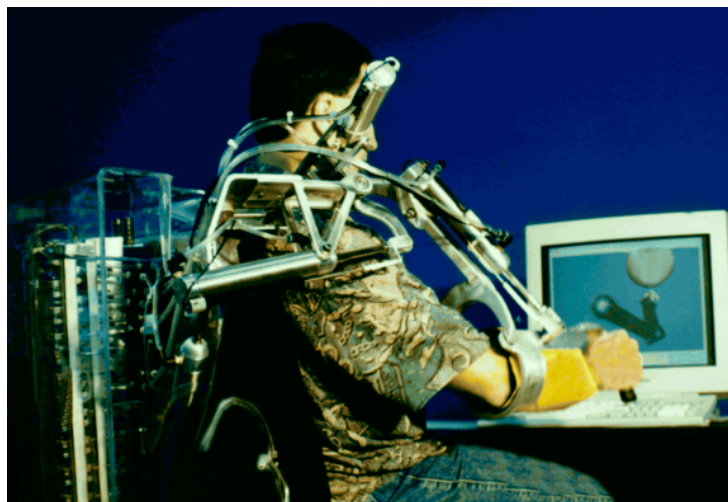


**Figure 2-4:** L-EXOS

This system attaches a haptic glove device to a force-feedback armature to provide hand and wrist force information [Immersion Corporation, Cyberforce, Website]. Forces are generated at the fingers by the use of a system of tendon-like cables.

Figure 2-4 shows L-EXOS, from PERCRO, the Simultaneous Presence Telepresence and Virtual Presence group at Scuola Superiore Sant'Anna in Italy [PERCRO website]. The L-EXOS is a wearable 5 DOF robotic haptic interface that exerts controlled force at the center of the user's right palm, with arbitrary direction in space. The device is suitable for applications where both motion tracking and force feedback are required as it incorporates actuation and sensing into the armature's joints. DC motors are located in the fixed frame and carry the generated torque to the corresponding joint by means of steel cables and reduction gears integrated within the joint axes.

Researchers at the Systems Lab at Southern Methodist University have developed an exoskeleton device called the Master Arm, shown in Figure 2-5, that operates with pneumatic actuators [Hurmuzlu, et al, and Systems Laboratory Website].



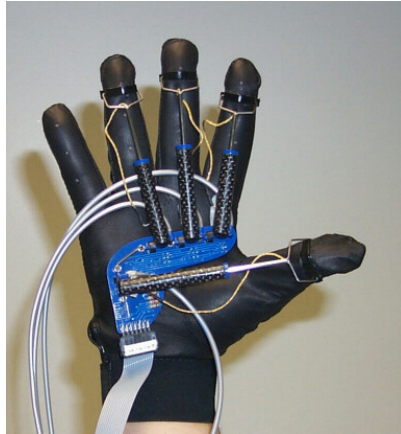
**Figure 2-5:** Master Arm, Southern Methodist University.

The device consists of an aluminum manipulator with four revolute joints. The manipulator is fixed at one end to a chair while the other end of the manipulator has a handle that is grasped by the operator. The device is strapped to the arm of the operator by using a set of inflatable cushions. Various length adjustments are used to accommodate different operators. It tracks the shoulder and elbow motions of the right arm of the operator using linear position transducers and applies forces to those joints using pneumatic cylinders.

### **2.1.2 Gloves and Wearable Devices**

The next area of research is in the development of wearable devices that are less encumbered than the exoskeleton systems described above. These devices are smaller exoskeleton-like devices that often, but not always, take the form of a glove. One major benefit of a wearable system is that the user can move more naturally without being weighed down by a large exoskeleton or other immobile device. Since the goal of building a haptic system is to be able to immerse a user in the virtual or remote environment it is important to provide as small a reminder of the user's actual environment as possible. The drawback of the wearable systems is that since weight and size of the devices are a concern, the systems will have a more limited set of capabilities. Many systems are in development such as the Rutgers Master II from the Human-Machine Interface Laboratory at Rutgers, The State University of New Jersey [Bouzit, et al, 2002, and Human Machine Interface Laboratory Website], shown in Figure 2-6, which is a glove that uses a pneumatic system to provide force information. The designers used only four actuators, leaving off an actuator for the smallest finger, in order to reduce the system's complexity. Other types of wearable devices exist that do not take the form of a

glove, such as the WearableMaster, Figure 2-7, by the VR Lab at the University of Tsukuba, Japan [Virtual Reality Laboratory, website]. It is a 3 degree of freedom, motor-driven joystick that is mounted on a user's arm.



**Figure 2-6:** Master II, Rutgers University **Figure 2-7:** Hand Held Force Display.

Another force-feedback glove is the CyberGrasp system, developed by Virtual Technologies Inc., which is commercially available from Immersion Corporation [Immersion Corporation, CyberGrasp website]. The CyberGrasp system consists of two parts: the CyberGlove [Immersion Corporation, CyberGlove] and the CyberGrasp exoskeleton, seen in Figures 2-8 and 2-9 respectively. The CyberGlove is a lightweight glove with flexible sensors that measure the position and movement of the fingers and wrist. The 22 sensor version of the CyberGlove features two bend sensors on each finger, a sensor to measure the flexion of the distal joints on the four fingers, four abduction sensors, plus sensors measuring thumb crossover, palm arch, wrist flexion and wrist abduction. The CyberGlove II, Figure 2-10, adds a Bluetooth wireless connection to attach the Cyberglove to the computer system allowing for even freer motion. The active forces for the CyberGrasp system are provided by a lightweight exoskeleton system consisting of cable driven actuators that are worn over the CyberGlove. The CyberGrasp provides 12N of continuous force per finger.





**Figure 2-8:** CyberGlove



**Figure 2-9:** CyberGrasp Exoskeleton



**Figure 2-10:** CyberGlove II, Wireless System

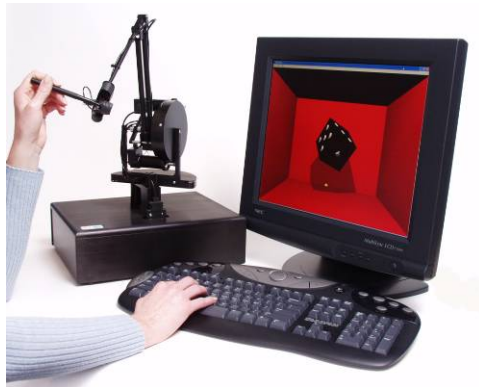
### 2.1.3 Point Sources and Specific Task Devices

The next category of Telerobotic and Virtual Reality systems is made up of Point-Source and Specific-Task devices. These devices are highly specialized in either their technology or their application. Devices that provide any type of force information that may be required can be complicated and even extremely difficult to develop. Designing a device to perform a single type of task restricts the application of that device to a much smaller number of functions. However, it allows the designer to focus the device to perform its task extremely well.

These types of devices have two general forms - single point of interface devices and specific task devices. An example of a single point of interface device is the Phantom, Figure 2-11 from Sensable Technologies [Sensable Technologies, *Phantom*].

The Phantom has a handle or a fingertip interface with an armature that provides up to six degrees of freedom to a single point.

Specific task devices seek to create more realistic simulations by providing force feedback for a single type of simulation. An example of such a specific task device is the VEKATS, the Virtual Environments Knee Arthroscopy Training System from The University of Hull Computer Science Department shown in Figure 2-12 [Sherman, et al, 2001, and Simulation and Visualization Research Group website].



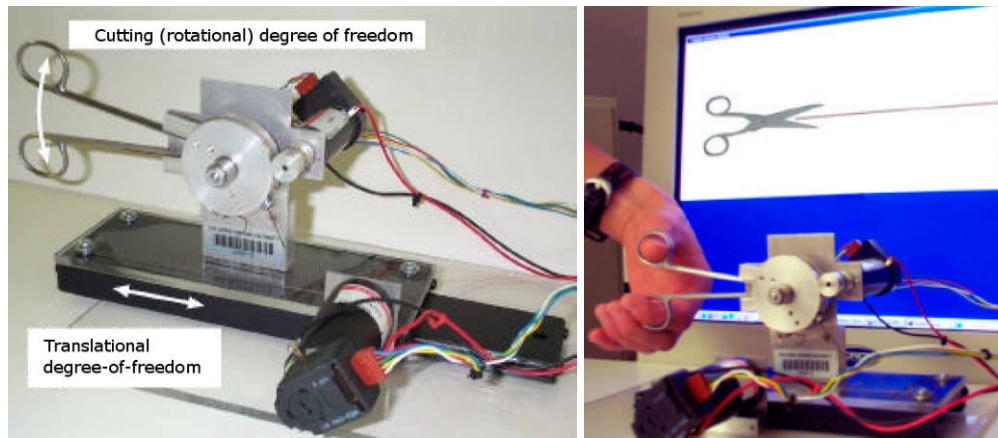
**Figure 2-11:** Phantom.



**Figure 2-12:** VEKATS, University of Hull.

The VEKATS system provides training for Knee Arthroscopy by simulating the sensation of such a procedure and reproducing the force sensation through realistic tools that are handled by the user. By focusing on the Knee Arthroscopic simulation exclusively, the researchers have been able to convincingly simulate the procedure.

Another specific task device is the Haptic Scissor device developed for medical training by the Mechanical Engineering Department at Johns Hopkins University. The Haptic Scissor can be seen in Figure 2-13.[Mahvash, 2005 and JHU Haptic Lab]



**Figure 2-13:** Haptic Scissor (L) With Graphical Display (R), Johns Hopkins

The scissor is a two degree of freedom system, controlled by motors that provide forces for the opening and closing of the scissor as well as forward and backward motion. The simulation shown in the figure illustrates how the haptic scissor is used to simulate scissor motions and forces associated with medical scissors. The goal of the research is to develop realistic simulations for surgical students to practice cutting tasks. Research into modeling the dynamics of cutting as well as the presentation of haptic forces based on those models is being performed.

#### **2.1.4 Mobility Interfaces and Full Body Force Feedback**

Another application of haptic feedback is in the form of full body force feedback called a Mobility Interface. Mobility interfaces are devices that, in a confined space, simulate unrestrained human mobility such as walking and running for virtual reality. Mobility interfaces overcome limitations of using joysticks or other similar interfaces for maneuvering, in which the user is seated and does not expend energy and therefore cannot experience a fully realistic environment. Other room-sized display-based interfaces are restricted in that their range of motion is limited to single-room environments, where only short distances can be traversed. The use of a haptic mobility

interface allows for the creation of environments with the ability for realistic navigation and engagement in modeled worlds as well as an enhanced sense of spatial layout.

One type of mobility interface is a pedaling interface such as the Uniport from Sarcos, Inc. [Sarcos website], seen in Figure 2-14. The pedaling interface is coupled with a Virtual Reality simulation, to allow for traveling within the virtual simulation.



**Figure 2-14:** Uniport Pedaling Interface, Sarcos, Inc.

The device shown in Figure 2-15 is the Treadport - a locomotion interface also created by Sarcos Inc. [Sarcos website]. The Treadport uses a treadmill, a mechanical tether, and a CAVE visual display. The Treadport is being applied towards research in perceptual and control issues involving locomotion interfaces.



**Figure 2-15:** Treadport, Sarcos Inc.

Additional mobility interfaces use multidirectional treadmills, such as the Omni-Directional Treadmill from Virtual Space Device, Inc. [Virtual Space Devices], shown in Figure 2-16, to increase the capabilities of the locomotion simulations. The treadmill moves smoothly in two dimensions to maintain the operator's position within the center of the device.



**Figure 2-16:** Omni-Directional Treadmill, Virtual Space Devices, Inc.

### **2.1.5 Force Feedback Input Devices**

Force feedback input devices are usually, but not exclusively, connected to computer systems and are designed to apply forces to simulate the sensation of weight or resistance in order to provide information to the user. As such, the feedback hardware represents a more sophisticated form of input/output device that complement other such interfaces as keyboards, mice, or trackers. Input from the user is in the form of hand – or other body segment – position, motion, or exerted force, whereas feedback from the computer or other device is in the form of force or position.

These devices translate digital information into physical sensations. For example, when a user pushes a mouse or joystick the device pushes back using, for instance, magnetic actuators and sensors built into the device. Resistance is only one of the

sensations that can be delivered. Springs, liquids, textures, vibrations, and more can be simulated as long as their mathematical equations can be translated into physical sensations through an actuation system. Various types of simple effects can be used individually or together to create a large range of sensations.

Force feedback joysticks, mice, driving wheels, and other devices, some of which are shown in Figure 2-17, have been developed [Microsoft Corp. website]. This method of conveying force information allows programmers and designers an additional way to interact with and send information to a user.



**Figure 2-17:** Sidewinder Force Feedback Joystick, Microsoft Corp and WingMan Force Feedback Mouse, Logitech.

The Logitech WingMan Force Feedback Mouse gives users a tactile, physical response when using a computer mouse input device [Logitech website]. Force feedback software has been added to a variety of popular games. It can also be used as an aid in navigating around the Internet and the computer's operating system. One can feel individual items on the menus as the pointer rolls over them as rounded speed bumps. When one grabs a small window by the corner and stretches it to fill the screen, it feels like a rubber band, pulling harder as you stretch the box. As the pointer rolls into a scroll bar or input field, one has the sensation of rolling up the lip of a trench, then down into it,



and that trench helps to hold the pointer along the bar's narrow track. In order to convey different type of information, some objects feel magnetic while others feel repulsive.

### 2.1.6 Tactile Displays

Simulation tasks involving exploration or delicate manipulation of a virtual environment require the addition of feedback data that presents an object's surface geometry or texture. Such feedback is provided by tactile feedback systems or *tactile displays*. Tactile systems differ from haptic systems in the scale of the generated forces. While haptic interfaces present the shape, weight or compliance of an object, tactile interfaces present the surface properties of an object such as the object's surface texture.

Tactile feedback applies sensations to the skin, typically in response to contact or other actions in a virtual environment. Tactile feedback can be used to produce symbols, like Braille, or simply a sensation that indicates some condition or concept. For example, the National Institute of Standards and Technology's (NIST) pin-based Tactile Visual Display, Figure 2-18 can display various forms of surface information in a tactile graphical interface [NIST Tactile Visual Display]. For haptic systems, tactile feedback interfaces can function as stand-alone systems, or they can be integrated with force feedback systems to enhance the sensation of immersion in simulated environments.



**Figure 2-18:** NIST Tactile Visual Display showing a map of the United States.

Tactile display devices stimulate the skin to generate the sensations of contact. The skin responds to several types of physical sensations such as vibration, temperature, and small-scale shape or pressure distribution. Systems are being developed that generate many of these sensations. The ability to create these types of surface sensations can be applied in various ways. Some issues related to these types of sensations are:

- **Vibration:** Information can be relayed about phenomena like surface texture, slippage, impact, and puncture. In many situations, the human sense of touch can only experience vibrations as diffuse and non-localized sensations, so a single vibrator for each finger or region of skin may be adequate.
- **Small-scale shape or pressure distribution:** This type of force will convey information about the shape and surface texture of an object. One design approach is an array of closely-spaced pins that can be individually raised and lowered against the finger tip to approximate the desired shape. For some applications, the display must be small and light enough to mount on a force-reflecting interface. To convey a range of spatial scales across a fingertip a number of fast actuators in a small area may be required.
- **Thermal display:** Since human fingers are often warmer than the "room temperature" objects in the environment, thermal perceptions are based on a combination of thermal conductivity, thermal capacity, and temperature. This allows people to infer material composition as well as temperature difference. A few thermal display devices have been reported, usually based on Peltier thermoelectric coolers.
- **Other tactile display sensations** have been created using a number of different technologies, including electrorheological devices for conveying compliance, electrocutaneous stimulators, ultrasonic friction displays, and rotating disks for creating slip sensations.

One pin-based Tactile Display device is the Shape Display device by the Harvard BioRobotics Lab, seen in Figure 2-19, consists of a 6x6 matrix of individually actuated

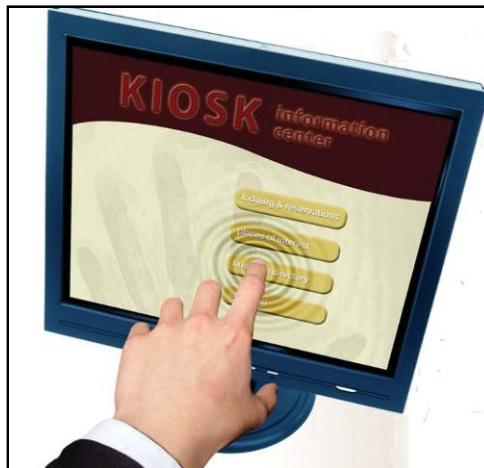


pins that are raised against the fingerpad using RC servomotors [Wagner, 2004, and Biorobotics Laboratory website]. The display can present small force and displacement information to provide surface sensations.



**Figure 2-19:** Harvard BioRobotics Lab's 2-D Pin Display.

A Tactile Display developed by Immersion Technology incorporates vibration actuators into a visual display. Figure 2-20 shows this display.



**Figure 2-20:** Immersion Touchscreen Tactile Display

When the user touches the display in the appropriate location, vibrators beneath their finger send force sensations to convey information, such as menu selections, or surface texture information. The goal is to use this technology to create more intuitive

kiosk and other similar systems, by simulating the feel of button presses on the touchscreen surface. This button press sensation conveys the message to the user that he or she has successfully pressed the button, while users of non-haptic touch screens have no such feedback to indicate the correct usage of the system.

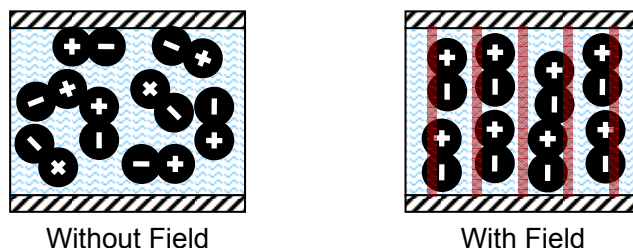
The following chapter will introduce the class of Smart Materials known as Electrorheological Fluids. These fluids were used to develop the haptic devices for this research project. The review of current haptic devices will then continue with an exploration of current haptic devices using Electrorheological Fluids.

### 3 HAPTIC SYSTEMS USING ELECTRO-RHEOLOGICAL FLUIDS

The information presented within this chapter was collected over a number of years through the efforts of various graduate and undergraduate researchers in the Robotics Laboratory. Although this information has been presented in various forms, including the papers listed in section 1.4.3, it is presented here for completeness.

#### 3.1 Electrorheological Fluids

Electrorheological fluids, or ERFs, are fluids that experience dramatic changes in fluid properties, such as viscosity – essentially its resistance to motion – in the presence of an electric field. ERFs are, in general, comprised of a base fluid with a suspension of fine particles having electric dipoles. In the presence of an electric field the particles line up along the field lines, indicated by the red lines in Figure 3-1, altering the fluid's resistance to motion and changing its viscosity. The stronger the electric field, the stronger the particles are held in the lines, and the more viscous the fluid becomes.

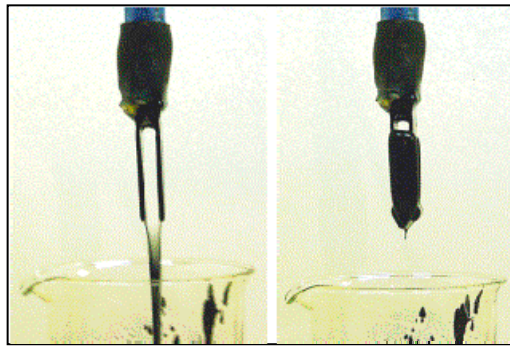


**Figure 3-1:** Randomized particles rotate to form chains when electric field is applied.

The electro-rheological effect, sometimes called the *Winslow effect*, was named after Willis M. Winslow who first explained the effect in the 1940's using oil dispersions of fine powders [Winslow, 1949].

The suspended particles are usually one tenth to one hundredth microns in size with a particle volume fraction of 20% to 60%. In an electric field the particles, due to an induced dipole moment, form chains along the field lines. These chains alter the ERF's

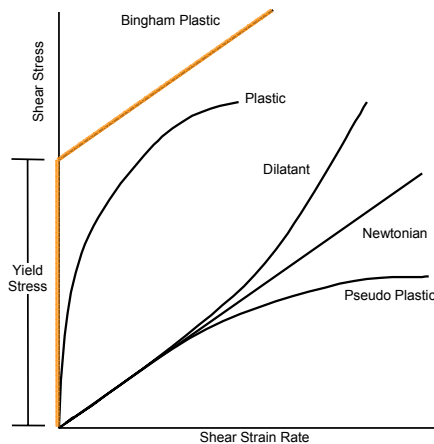
viscosity and yield stress, changing its consistency from a liquid to something solid-like, such as a gel. The response time to changes in the field is on the order of milliseconds. Figure 3-2 shows the fluid state of an ERF without an applied electric field and the solid-like state that is induced when an electric field is applied.



**Figure 3-2:** Electro-Rheological Fluid at Reference (left) and Activated States (right).

Further reviews of the ERF phenomenon and the theoretical basis for ERF behavior can be found in [Block and Kelly, 1988; Gast and Zukowski, 1989; Weiss, et al, 1994; Conrad, 1998].

Under an electric field, the ERF alters its state from a Newtonian oil to a non-Newtonian Bingham plastic. As an ideal Bingham plastic, highlighted in Figure 3-3, the ERF exhibits a linear relationship between stress and strain rate, like a Newtonian fluid, only after a minimum yield stress is exceeded. Before that point, it behaves as a solid.



**Figure 3-3:** Behavior of Various Classes of Viscous Fluids, Including Bingham Plastics.

At stresses higher than this minimum yield stress, the fluid will flow, and the shear stress will continue to increase proportionally with the shear strain rate (see the Bingham Plastic line in Figure 3-3), so that:

$$\tau = \tau_y + \mu \dot{\gamma} \quad (1)$$

where  $\tau$  is the shear stress,  $\tau_y$  is the yield stress,  $\mu$  is the dynamic viscosity and  $\gamma$  is the shear strain. The  $\dot{\gamma}$  term indicates the shear strain's time derivative, the shear strain rate.

The yield stress  $\tau_y$  and the dynamic viscosity  $\mu$  are two of the most important parameters that affect the design of ERF-based devices. The dynamic viscosity  $\mu$  is mostly determined by the base fluid and the electric field. The field-induced yield stress  $\tau_y$  depends on the electric field strength. Some theoretical models have been derived but none is yet able to reflect these relations properly. In general, one can assume that the yield stress increases quadratically with the electric field strength [Lampe, 1997].

The two important values for the yield stress are: the static yield stress  $\tau_{y,s}$  and the dynamic yield stress  $\tau_{y,d}$ . The static yield stress is defined as the amount of stress needed to initiate flow, i.e., the stress needed to change from solid to liquid. The dynamic yield stress is the amount of stress needed in zero strain rate conditions to go from a solid to liquid. Usually, the static yield stress is noticeably higher than the dynamic yield stress although the exact proportions vary from fluid to fluid. This phenomenon, called "stiction", is highly dependent on the particle size and shape [Weiss, 1994].

The current density  $J$ , defined as the current per unit electrode area is used to estimate the electric power consumption of ERF-based devices. The measurable electric current through ERFs is believed to be possible due to charge leakage between particles.

ERF properties can change with temperature, which can tremendously affect the performance of ERF-based devices. "Good" ERFs should show constant properties over a large range of temperatures. There is no unified model describing the temperature dependence of the parameters of ERFs. This temperature dependence varies from fluid to fluid. The largest temperature related problem for ERFs results from the huge increase of current density with increasing temperatures. This increases power consumption but also increases safety concerns for human operators of ERF devices.

A database of commercially available ERFs, including property comparison tables, can be found in [Lampe, 1997]. A review of the material compositions for ERF patents can be found in [Weiss, et al, 1994].

The work presented in this research project mostly employed the electrorheological fluid LID 3354S, manufactured by Smart Technology Ltd. [Smart Technology Ltd, 2001]. LID 3354S is an ERF made of 35%, by volume, polymer particles in a silicone/fluorolube base oil. It is designed for use as a general-purpose ER fluid with a balance of properties such as the strength of the ERF effect and a low no-field viscosity.

The equations describing the field dependencies for this particular ERF, as supplied by the fluid's manufacturer, are given by the following:

$$\tau_{y,s} = C_s (E - E_{ref}) \quad (2)$$

$$\tau_{y,d} = C_d E^2 \quad (3)$$

$$\mu = \mu_o - C_v E^2 \quad (4)$$

Equation (2) describes the yield stress in static mode, Equation (3) describes the yield stress in dynamic mode and Equation (4) describes the viscosity of the fluid. These equations are all functions of the material properties of the given fluid and the applied electric field. The zero field viscosity is given by  $\mu_o$ , while  $C_s$ ,  $C_d$ ,  $C_v$  and  $E_{ref}$  are constants supplied by the manufacturer. The subscripts  $s$  and  $d$  correspond to the static and dynamic yield stresses while  $v$  denotes the constant associated with the fluid's viscosity calculations. The formula for static yield stress is only valid for fields greater than  $E_{ref}$ , the reference electric field strength.

Control over a fluid's rheological properties creates many possibilities for engineers to develop novel ways to actuate and control mechanical motion. For example, devices that rely on hydraulics can benefit from ERF's quick response times and reduction in device complexity. The fluid's solid-like properties in the presence of a field can be used to transmit forces over a large distance and have found various applications.

A description of the engineering applications of ERFs can be found in [Duclos, et al, 1992; & Coulter, et al, 1994]. Devices designed to use ERFs include engine mounts [Sproston, et al, 1994], active dampers and vibration suppression [Choi, 1999], clutches [Bullough, et al, 1993], brakes [Seed, et al, 1986] and valves [Coulter, et al, 1994]. Reviews of the use of ERFs for vibration control can be found in [Stanway, et al, 1996].

Until now, the application of ERFs in robotics has been limited. They have mainly been used as active dampers for vibration suppression [Ghandi, et al, 1987; and Furusho, et al, 1997]. An ERF-based safety-oriented mechanism has been proposed for human-robot cooperative systems [Arai, et al, 1998].

ERF-based devices have many potential applications in the field of Haptics. Since ERFs are actuated by the application of electric fields, which can easily be generated by situating two conducting plates facing each other with a gap in between, they can be incorporated into very small devices. This property along with their high yield stress, allows for the possibility of small haptic devices that can fit inside the human palm without creating obstructions to motion.

In addition, ERFs do not require any transmission elements to produce high forces, so direct drive systems can be produced with less weight and inertia. The ability to easily change the fluid's rheological properties gives designers of ERF-based haptic systems the possibility of controlling a system's compliance, and hence, the ability to accurately mirror remote or virtual compliance.

Finally, ERFs respond almost instantly, in milliseconds, allowing for very high bandwidth control, which is important when mirroring fast motions.

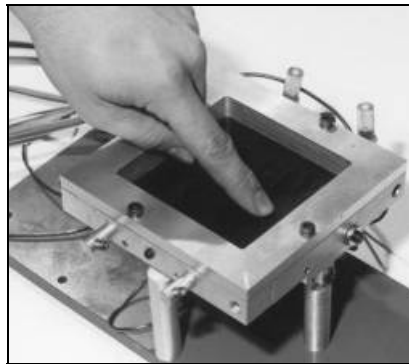
One potential concern in developing ERF-based haptic devices is the need to generate high voltages to develop the forces and compliance required. This has two consequences: a) it increases the complexity of the electronic system needed to develop the high voltage and b) it raises safety concerns for the human operator. Both issues can be solved with modern electronic circuit design techniques. Today, low power and small size circuits can be used to generate the required high voltage using a very low current on the order of micro-amps. Consequently, the required power becomes extremely low, on the order of mWatts, posing no hazard for human operators.



### 3.2 Existing ERF-Based Haptic Devices

A number of ERF-based haptic devices have been developed by various research teams over the past few years. Some of these devices are presented in this section.

Kenaley and Cutkosky proposed the use of ERFs for tactile sensing in robotic fingers [Kenaley and Cutkosky, 1989]. Other researchers have proposed the use of ERFs in tactile arrays to interact with virtual environments [Wood, 1998]. Monkman [1992] proposed devices for Braille reading systems for the blind. Figure 3-4 shows the ERF based programmable surface developed at the University of Newcastle upon Tyne, UK, [Taylor et al 1996a; Taylor et al 1996b; and Intelligent Mechanical and Manufacturing Systems Research website].



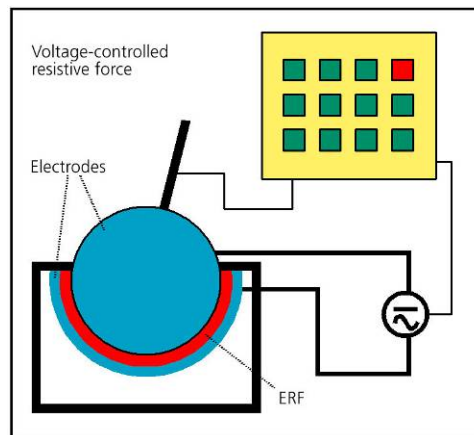
**Figure 3-4:** Programmable Surfaces based on ER Fluids.

Researchers at Osaka University in Japan developed a 3-Degree of Freedom Upper Limb Rehabilitation system using ERF-brakes to provide force-feedback information. Called the EMUL, the device is shown in Figure 3-5 [Sakaguchi & Furusho 1998a; Furusho 2001, Human-Machine Interaction Subarea website]. The system can be use as a motion guide robot or a force display device.



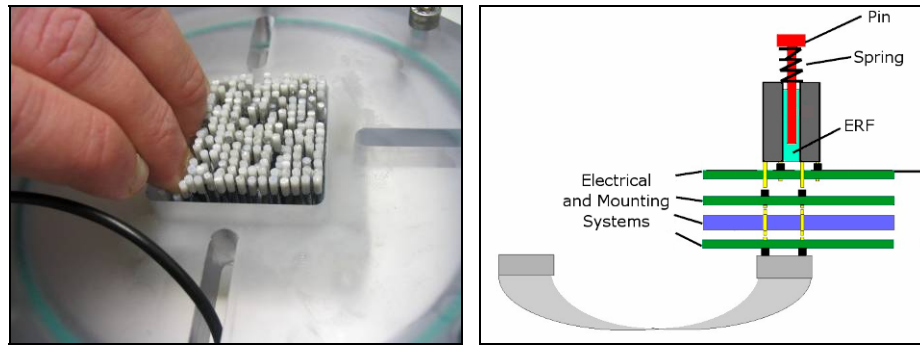
**Figure 3-5:** Force Display Device using electrorheological fluids.

An ERF-based force-feedback joystick has been developed in Fraunhofer-Institut in Germany. The joystick consists of a ball and socket joint with ERF placed in the space between the ball and the socket, illustrated in Figure 3-6. The operator feels a resistive force to motion resulting from the controlled viscosity of the ERF [Böse, et al, 2000].



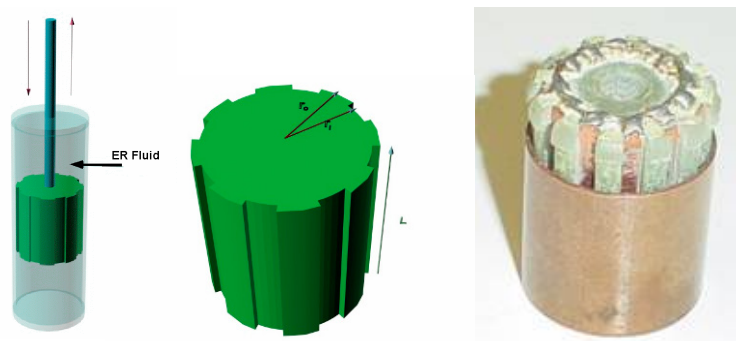
**Figure 3-6:** Haptic Joystick using ERFs.

In addition, the Fraunhofer Institut, in conjunction with the Institut für Mikrotechnik Mainz, also in Germany has developed a tactile pin array of 32 x 32 elements whose forces are generated by ERF elements [Institut für Mikrotechnik Mainz]. The images in Figure 3-7 show the pin array as well as a drawing of the actuator elements.



**Figure 3-7:** ERF-based Tactile Pin Array.

Finally, researchers at Rutgers University and NASA's Jet Propulsion Laboratory developed a family of ERF-based force-feedback devices called MEMICA (MEchanical Mirroring using Controlled stiffness and Actuators). Charles Pfeiffer, a researcher in the Rutgers Robotics Lab developed the ECS actuator shown in Figure 3-8. The MEMICA concept and the ECS actuator were presented in [Bar-Cohen et al, 2000a.; Bar-Cohen, et al, 2000b; Bar-Cohen, et al. 2000c; Bar-Cohen, et al 2000d; Mavroidis, et al, 2000a; Mavroidis, et al, 2000b; Mavroidis, et al, 2000c; and Mavroidis, et al, 2001].



**Figure 3-8:** ECS Actuator - concept (Left) and prototype (Right).

The ECS or Electronically Controlled Stiffness actuator is a linear actuator that develops an electric field within the channels cut into the piston head between the copper strip in the base of the channels and a copper cylinder that is attached to the outer edge of the piston head. Some experimental testing demonstrated that the actuator was able to resist linear forces applied along the piston's shaft.

## **4 ACTUATOR CONCEPT AND MODELING – VERSION 1**

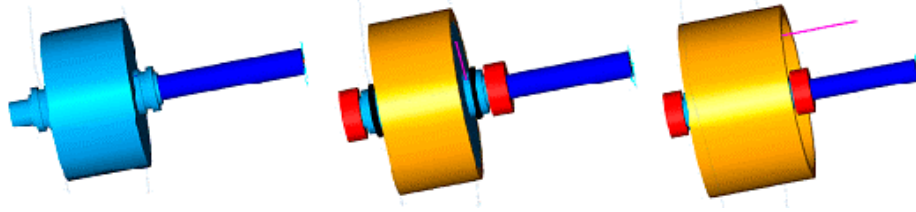
I proposed that haptic feedback devices could address the need to simplify and enhance the human-vehicle interface. These devices use passive ERF-based actuators to induce resistive forces. The design considerations include overall dimensions, power consumption, reaction torque and safety. My designs of two actuators, referred to as the Concentric-Cylinder (CC) and Flat-Plate (FP) actuators are discussed in this chapter.

While I developed the CC actuator concept, the FP actuator design and derivations shown in this chapter have been developed in collaboration with other members of the Robotics and Mechatronics Laboratory. Therefore, these designs and equations also appear in almost identical fashion in one of the members of our group, Jason Nikitzuk's, Master's thesis [Nikitzuk, 2004]. They are included for completeness.

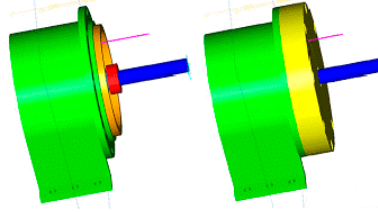
In addition, for the sake of brevity the manufacturing and assembly of the actuators in the following sections will be presented in an abbreviated form. I developed a second generation actuator, to be presented in a later chapter, to perform experiments related to the PhD research. The development of that newer actuator will be presented in depth.

### **4.1 Concentric-Cylinder Actuator Concept and Modeling**

The CC actuator consists of inner and outer cylindrical copper electrodes separated by a gap. The inner electrode is mounted on a cylinder that rotates on bearings mounted to the base. An encoder measures angular displacement. Figures 4-1 and 4-2 show the assembly of the actuator.

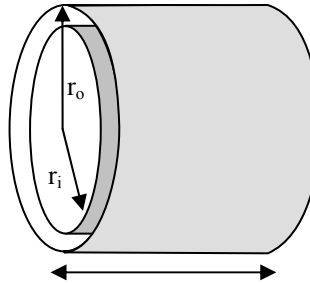


**Figure 4-1:** CC Parts –mounting cylinder, inner and outer electrode, respectively.



**Figure 4-2:** Assembled Actuator with and without cover.

The two concentric cylinders, drawn schematically in Figure 4-3, act as electrodes with the gap between them filled with electrorheological fluid. Applying an electric field across the gap causes the properties of the fluid, including the yield stress and viscosity, to change, thereby changing the resistive torque generated by the actuator.



**Figure 4-3:** Schematic of Concentric-Cylinder ERF Actuator.

To understand and predict the capabilities of the actuator, it is necessary to derive a mathematical model to describe the actuator's performance. These equations will calculate the torque that will be felt when operating a device with this actuator. The reaction torque felt by the operator is a function of the actuator's geometry (inner radius, outer radius, and length), the applied voltage and characteristics of the ERF.

The first steps to model the behavior of the actuator are shown here in Equation 5.

$$\oint \vec{E} \cdot d\vec{A} = \frac{q}{\epsilon_o} \rightarrow EA = E(2\pi rl) = \frac{q}{\epsilon_o} \rightarrow E(r) = \frac{q}{2\pi\epsilon_o rl} \rightarrow \vec{E}(r) = \frac{q}{2\pi\epsilon_o rl} \hat{r} \quad (5)$$

The electrical field,  $E$ , is provided by an applied voltage,  $V$ , to be defined in the next step. Gauss' law is used to define the electric field. A charge of  $q$  is assigned to the charged core with  $\epsilon_o$  as the electrical permittivity of free space. The field is known to be in the radial direction, so that the dot product becomes the scalar product. Then a Gaussian surface  $A$  of radius  $r$  and length  $l$  between the inner  $r_i$ , and outer  $r_o$  radii (see Figure 4-3) is defined. The right-most equation then gives the Electric field as a function of radius, with  $\hat{r}$  being a unit vector in the radial direction.

The expression for the voltage,  $V$ , which defines the electric field, can be found from the difference in electrical potential computed between the inner and outer walls,

$$V = -\int_{r_o}^{r_i} E(r) dr = -\int_{r_o}^{r_i} \frac{q}{2\pi\epsilon_o rl} dr = -\frac{q}{2\pi\epsilon_o l} \int_{r_o}^{r_i} \frac{dr}{r} = \frac{q}{2\pi\epsilon_o l} \ln\left(\frac{r_o}{r_i}\right) \rightarrow \left(\frac{q}{2\pi\epsilon_o l}\right) = \frac{V}{\ln\left(\frac{r_o}{r_i}\right)} \quad (6)$$

Equations (5) and (6) are combined, in scalar format, to relate the electric field directly to the applied voltage and geometry:

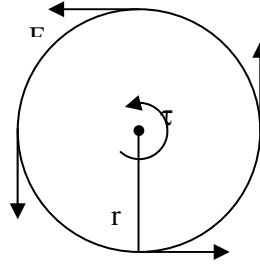
$$E = \left(\frac{q}{2\pi\epsilon_o l}\right) \frac{1}{r} = \left(\frac{V}{\ln\left(\frac{r_o}{r_i}\right)}\right) \frac{1}{r} \quad (7)$$

Since the rotational inertia of the actuator is negligible, the torque applied by the operator,  $T_{app}$ , is equal to the reaction torque  $T_R$  exerted on the rotating, inner cylinder by the ERF. The reaction torque is the sum of two torques - a shear torque  $T_\tau$  and a friction

torque  $T_f$ . Significant effort has been made to minimize the friction in the system so that the friction torque will be considered as negligible. The reaction torque is defined as:

$$T_R = T_{app} = T_\tau + T_f \approx T_\tau \quad (8)$$

The total torque felt by rotating the actuator against the resistance generated by the ERF is due to the linear force generated at the surface of the cylinder multiplied by the radius. Figure 4-4 shows a schematic of the force – torque relationship.



**Figure 4-4:** The Force-Torque relationship around a cylinder (cross-section).

Equation (9) derives an expression for the torque. The torque is defined as a force,  $F$ , acting at a distance,  $r$ . That force acts perpendicular to the moment arm and is given as a product of the shear stress,  $\tau$ , and the surface area,  $A$ . The total torque due to shear forces,  $T_\tau$ , is calculated by considering the entire surface area in contact with the ERF, specifically the outer area of the inner electrode given by  $A = 2\pi r_i l$ .

$$T = F \times r_i = F r_i = \tau A r_i = \tau 2\pi r_i^2 l \quad (9)$$

Since there are different values for the reaction torque depending on whether the system is in motion, designated as *dynamic torque*, or not in motion, designated *static torque*, the analysis will yield two different equations for the two modes of operation.

### *Static Torque – CC actuator*

The first case to consider is the actuator operating in static mode. Since the system is static, the shear rate indicated in Equation (1) ( $\tau = \tau_y + \mu\dot{\gamma}$ ) is zero. Therefore, combining Equations (1), (2), (7), and (9) and rearranging terms, the following expression is found for the reaction torque of the CC actuator in static mode.

$$T_s = 2\pi r_i l C_s \left( \frac{V}{\ln\left(\frac{r_o}{r_i}\right)} - E_{ref} r_i \right) \quad (10)$$

### *Dynamic Torque – CC actuator*

To calculate the reaction torque felt when the actuator is moving (i.e. dynamic case), the analysis starts with Equation (1), with a non-zero value for the shear strain rate,  $\dot{\gamma}$  which is given, by definition, as  $\frac{v}{\Delta r}$ , with the velocity of the ERF equal to the velocity of the inner electrode cylinder, and  $\Delta r$  the gap distance between the electrodes. The linear velocity,  $v$ , is given by  $v = \dot{\theta} r_i$ , with  $\dot{\theta}$  being angular velocity. Combining Equations (1), (3), (4), (7) and (9) and rearranging terms yields the equation for reaction torque in dynamic mode:

$$T_d = 2\pi l \left[ \left( C_d - \frac{C_v \dot{\theta} r_i}{r_o - r_i} \right) \frac{V^2}{\left( \ln\left(\frac{r_o}{r_i}\right) \right)^2} + \frac{\mu_o \dot{\theta}^2 r_i^2}{r_o - r_i} \right] \quad (11)$$

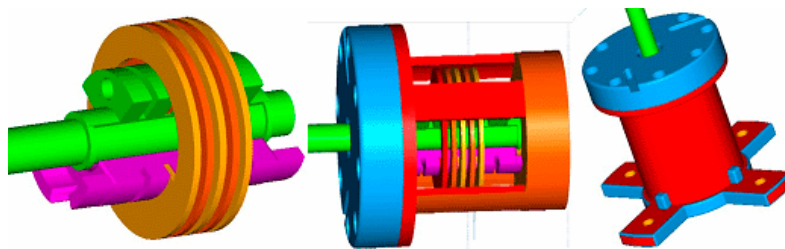


## 4.2 Flat-Plate Actuator Concept and Modeling

Building on the experience gained with the CC actuator, we designed a second actuator to exceed the CC's capabilities. The parameter that could be manipulated to increase the output torque was the available surface area. As shown in Equation (9) above, the torque depends on the shear stress and the area upon which that shear stress works. By increasing the surface area the output torque increases as well.

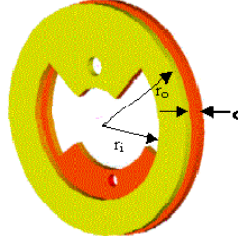
A new actuator consisting of multiple parallel rotating electrode plates was designed to increase the surface area of the actuator. The Flat-Plate or FP actuator uses multiple flat-plates attached to rotating and fixed shafts to create a multiple-plate multiple-gap system to multiply the torque that is generated by a single-gap system.

As shown in the left-most picture in Figure 4-5, several circular copper plates, in light orange, are situated parallel to each other on a fixed axis, while on a parallel, concentric axis, another set of copper plates, dark orange, are assembled in between the fixed plates. The latter set of plates can rotate relative to the fixed plates. The gaps between the plates are then filled with ERF. By applying an electric field across the gaps the fluid viscosity changes, resulting in output torque. Figure 4-5 shows the components of the Flat-Plate ERF actuator, the plates inserted into the case (with cut-away sides for clarity) and the completed assembly of the actuator.



**Figure 4-5:** Assembly of Multiple Flat-Plate ERF Actuator.

The copper electrode plates have an inner and outer radius,  $r_i$  and  $r_o$ , respectively and a gap of  $d$  between plates, as shown in Figure 4-6.



**Figure 4-6:** Flat-Plate Electrodes.

The basic equations are similar to those for the CC actuator. The shear stress, yield stress and viscosity equations are the same, however the electric field equation differs. Since the configuration is a flat plate system, the electric field is given by:

$$E = \frac{V}{d} \quad (12)$$

where  $V$  is the voltage and  $d$  is the gap distance between plates. The reaction torque is given here, first for a single-plate system and then for the multiple-plate actuator:

$$T = Fr = (\tau A)r_i \rightarrow T = \int_{r_i}^{r_o} r\tau(r)dA(r) \rightarrow T = 2N \int_{r_i}^{r_o} r\tau dA \quad (13)$$

where  $N$  is the number of rotating plates, with two sides to each plate, and  $dA = 2\pi r dr$ . The integral accounts for the change in “viewable surface area” that is seen as the radius increases from the inner to outer radii.

#### *Static Torque – FP actuator*

To determine the reaction torque for the actuator in static mode Equations (1), (2), (12) and (13) are combined to get:

$$T_s = \frac{4}{3} N \pi C_s \left( \frac{V}{d} - E_{ref} \right) (r_o^3 - r_i^3) \quad (14)$$

### *Dynamic Torque – FP actuator*

In order to develop the dynamic equation, the definition for the shear strain rate must be found. Starting with  $\dot{\gamma} = v/d$ , with  $v$  being the linear velocity and  $d$ , the gap distance. While the angular velocity of the circular plate,  $\dot{\theta}$ , stays constant, the linear velocity,  $v$ , is given by  $v = \dot{\theta}r$  which will vary as the distance to the axis of rotation changes. Then, beginning with a restatement of Equation (13):

$$T = 2N \int_{r_i}^{r_o} r \tau(r) dA$$

Where  $\tau$  is defined using Equations (1), (3) and (4) for stress in dynamic mode.

Using  $dA = 2\pi r dr$ , the torque then becomes:

$$T = 4\pi N \int_{r_i}^{r_o} r^2 \left( \tau_y + \mu \frac{\dot{\theta}r}{d} \right) dr \quad (15)$$

Then, combining Equations (1), (3), (4), (12), (13) and (15) gives the reaction torque in dynamic mode as:

$$T_d = 4\pi N \left[ C_d \left( \frac{r_o^3 - r_i^3}{3} \right) - \frac{C_v \dot{\theta}}{d} \left( \frac{r_o^4 - r_i^4}{4} \right) \right] \frac{V^2}{d^2} + \pi N \frac{\mu_0 \dot{\theta}}{d} (r_o^4 - r_i^4) \quad (16)$$

The equations developed in the past sections are useful in understanding the abilities of the CC and FP actuators. In addition, when writing software to control the actuators, these models will become the basis for implementing any open-loop or closed-loop control schemes. The first application for the mathematical models is to use them as

guidelines to develop physical prototypes of the actuators for testing and system design purposes. The next section discusses the parametric analysis performed to determine the physical parameters of the actuator to meet specific torque output requirements.

### **4.3 Parametric Analysis of the Design of ERF Actuators**

Equations (10), (11), (14) and (16) predict the reaction torque that the two ERF actuators – the CC and FP actuators – are capable of producing as a function of the applied voltage in static and dynamic modes. Other parameters, chosen in the design phase, affect the capabilities of the actuator by defining its physical characteristics.

Several of these factors affect the amount of reaction torque that the actuator is capable of producing, including ERF properties, actuator geometry, applied voltage and speed of actuation. In order to understand how the different parameters affect the capabilities of the actuator, I performed an analysis that varied individual parameters while holding the rest fixed. I used this information as a guideline to choose the parameters used to build the prototypes of the actuators. This section presents the parametric analyses performed for the two actuator systems.

#### **4.3.1 Preliminary Information**

Human studies have shown that the controllable maximum force that a human finger can exert is between 40 and 50 Newtons [Burdea, 1996]. However, maximum exertion forces create discomfort and fatigue to the human operator. Comfortable values of exertion forces are between 15 and 25% of the controllable maximum force exerted by a human finger. Thus, I selected a force output of 10 N as a design goal.

Since I performed the analysis assuming the specific properties of the ERF LID 3354S, the ERF characteristics cannot be changed for this parametric analysis. The ERF parameters, determined from the manufacturer's specifications, are summarized in Table 4-1 [Smart Technology Ltd., 2001]. As stated above, the data for the static performance of this fluid is not available; therefore the  $C_s$  and  $E_{ref}$  values for ERF LID 3354, a similar but older fluid, are used in the analysis of the static mode performance. These values should over predict the performance of the actuators in static mode.

$E_{ref}$	1090*	V/mm
$C_s$	2.77*	Pa mm/V
$C_d$	0.00019	Pa mm <sup>2</sup> /V <sup>2</sup>
$C_v$	0.904 E-5	Pa s mm <sup>2</sup> /V <sup>2</sup>
$\mu_0$	0.110	

**Table 4-1:** ERF LID 3354S Parameters  
(\*values for  $E_{ref}$  and  $C_s$  are for ERF LID 3354).

The actuators developed for this research project are used in haptic devices, which are low-speed devices. A study of the torque output equations revealed that for slower speeds, between 1 and 1000 mm/s, the reaction torque is almost independent of the velocity imposed by the user. This is due to the fact that the velocity contribution in the reaction torque is much smaller than the voltage related term. Thus for this analysis, an arbitrary velocity value of 10 mm/s was used for the dynamic torque calculations.

#### 4.3.2 Concentric-Cylinder Actuator

Applied voltage and geometric properties ( $r_o$ ,  $r_i$ ,  $l$  and  $d$ ) are the principle parameters affecting the performance of the actuator. For safety as well as power considerations, it was critical to minimize the applied voltage, which drove some of the design decisions for the CC actuator prototype. In addition, since one intended

application is within an automobile console, size constraints limited the outer dimensions of the actuators. Thus, finding a combination of an appropriately sized actuator that would accommodate the torque requirements at lower voltages was especially important.

For the CC actuator, increasing the actuator surface area or decreasing the gap width between electrodes improves the response torque performance. Figure 4-7 shows the performance of the actuator in dynamic and static modes. The length (32mm) and gap width (0.75mm) are fixed. Torque is plotted versus applied voltage for five different outer radius values: 12, 15, 18, 21 and 24 mm.

Similarly, the performance curves for various gap widths in dynamic and static modes are shown in Figure 4-8. The outer radius (15.75mm) and length (32mm) of the actuator are fixed and the gap width is varied from 0.25 to 1.25 mm.

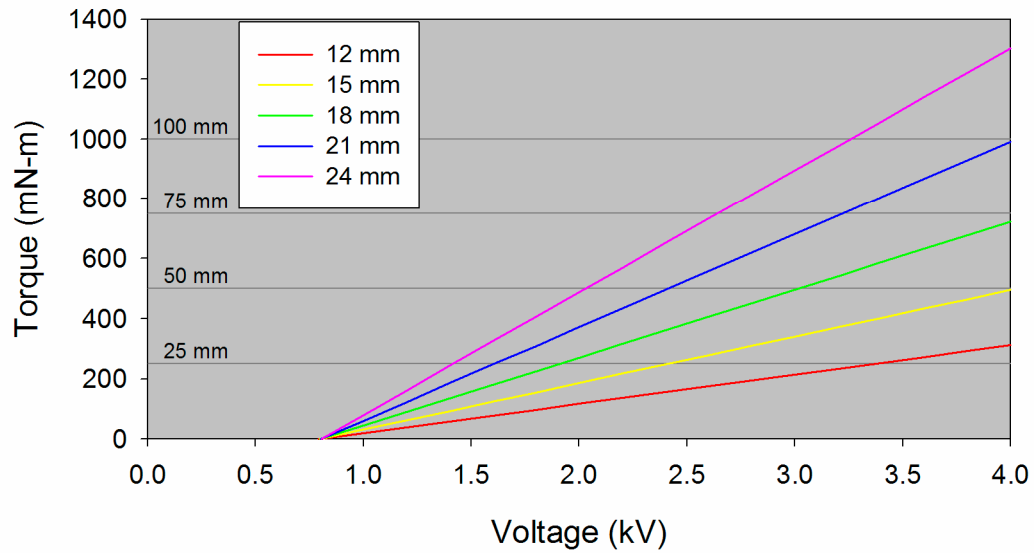
The horizontal lines in the graphs represent the torque needed to produce 10N and 3N of force in static and dynamic modes, respectively, for various moment arm lengths. These lines serve as a guide to estimate which actuator designs will be able to perform at the levels required by the 10N force requirement discussed above.

The 3N requirement in dynamic mode serves as a general indication of the lower capabilities of the dynamic mode operation of the actuators, rather than as a design goal. The 10N requirement for static mode will drive the overall parameter selection.

### CC Actuator Outer Radius Parametric Curves - Static Mode

Outer Radius - 12, 15, 18, 21, 24 mm

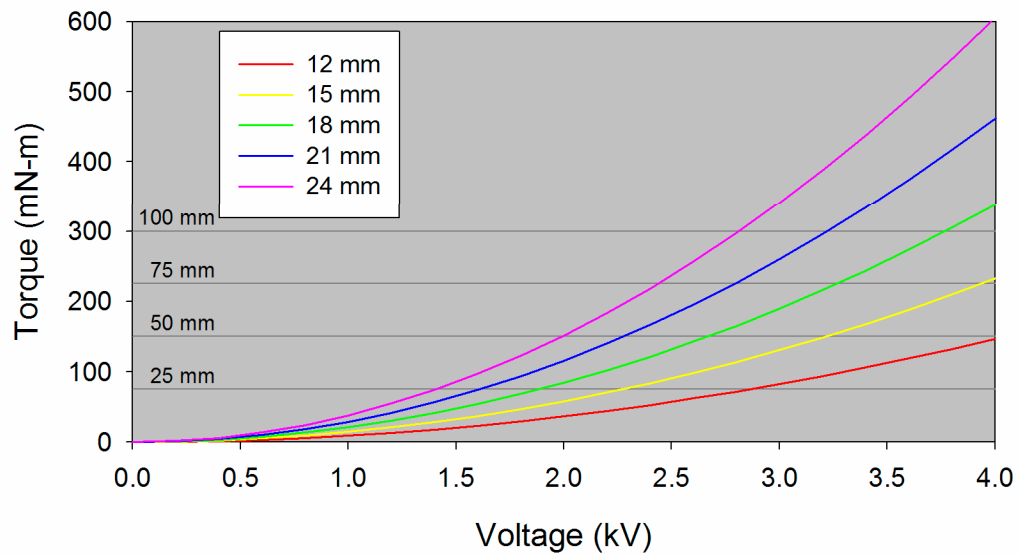
(Gap - 0.75 mm; Length - 32 mm)



### CC Actuator Outer Radius Parametric Curves - Dynamic Mode

Outer Radius - 12, 15, 18, 21, 24 mm

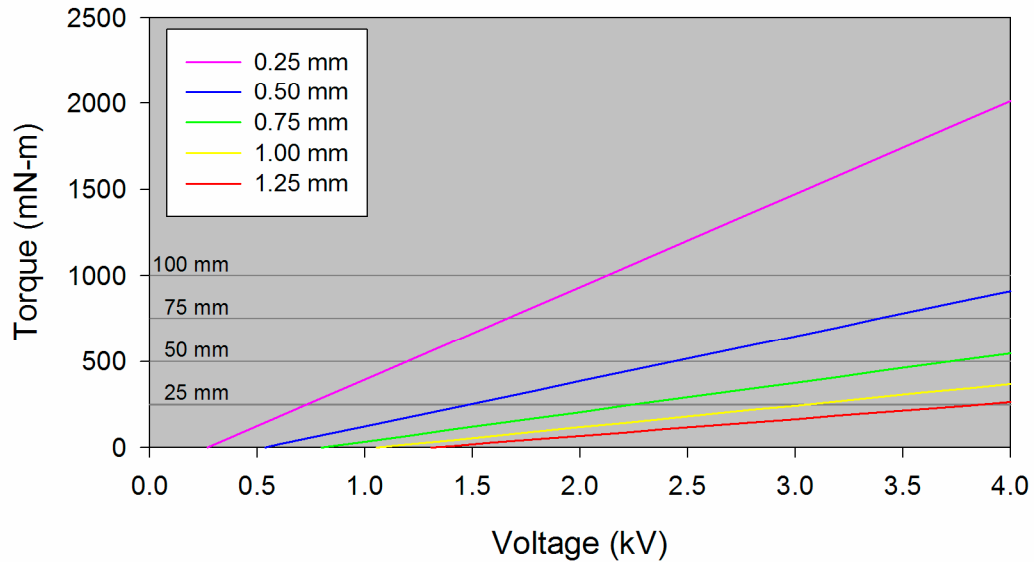
(Gap - 0.75 mm; Length - 32 mm)



**Figure 4-7:** Torque vs. Voltage for Various *Radii* for the CC Actuator.

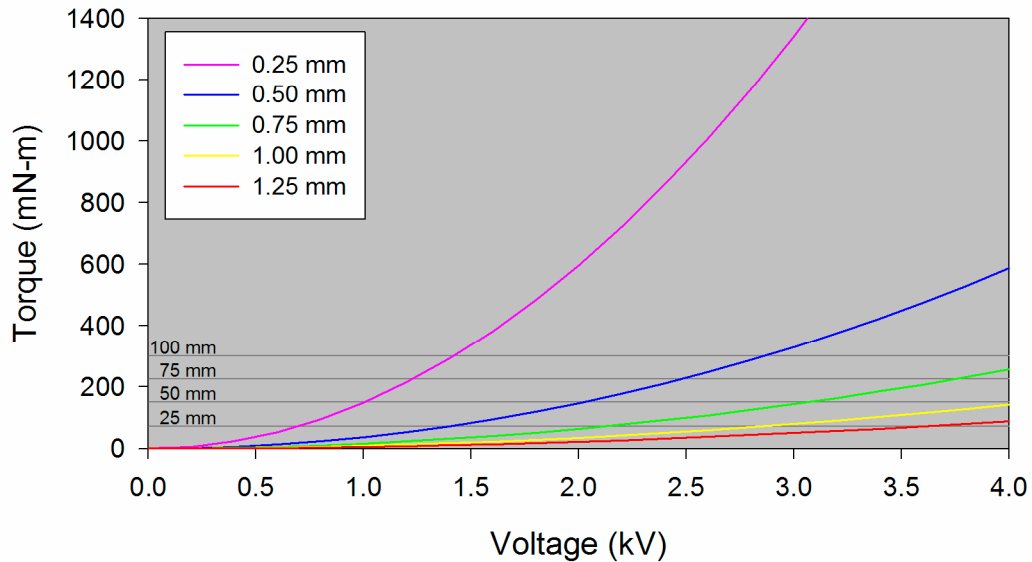
### CC Actuator Gap Size Parametric Curves - Static Mode

Gaps - 0.25, 0.50, 0.75, 1.00, 1.25 mm  
(Length - 32 mm; Outer Radius - 15.75 mm)



### CC Actuator Gap Size Parametric Curves - Dynamic Mode

Gaps - 0.25, 0.50, 0.75, 1.00, 1.25 mm  
(Length - 32 mm; Outer Radius - 15.75 mm)



**Figure 4-8:** Torque vs. Voltage for Various *Gap Widths* for the CC Actuator.



Figures 4-7 and 4-8 imply that a very small gap width is extremely instrumental in both reducing the overall size of the device and lowering the activation voltage required. Smaller gap sizes, however, are more difficult to manufacture, can lead to arcing and result in a higher no-field drag. Increasing the radius improves the performance, but results in larger outer dimensions. These considerations needed to be taken into account when designing the physical prototype.

### 4.3.3 Flat-Plate Actuator

For the Flat-Plate actuator, the inner radius ( $r_i$ ), outer radius ( $r_o$ ), gap distance between plates ( $d$ ) and number of plates ( $N$ ) are all modifiable design parameters. The larger the plate surface area is, the higher the resultant torque will be. Since the inner radius cannot be made smaller than the shaft radius, it is set as a fixed value.

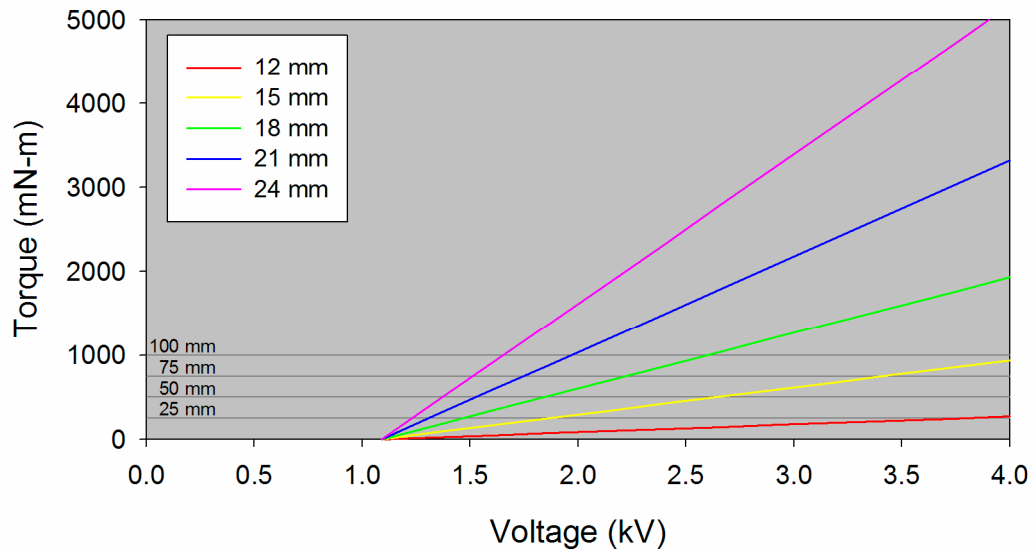
Figure 4-9 shows the performance curves in dynamic and static mode for this actuator with various outer radii: 12, 15, 18, 21 and 24 mm. The inner radius (10.2mm), gap between the plates (1mm) and number of moving plates (4) are fixed.

The performance curves for the various gap distances in dynamic and static modes are shown in Figure 4-10. The inner radius (10.2mm), outer radius (15mm) and number of plates (4) are fixed. The horizontal lines again represent the torque needed to produce 10N and 3N of force in static and dynamic modes, respectively, for various moment arm lengths.

## FP Actuator Outer Radius Parametric Curves - Static Mode

Outer Radius - 12, 15, 18, 21, 24 mm

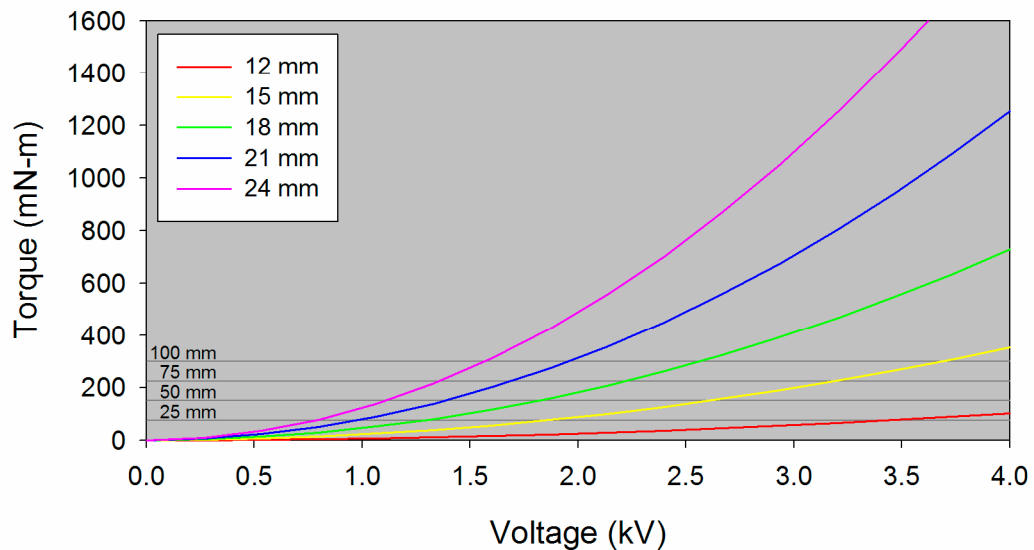
(Inner Radius - 10.2 mm; Gap - 1.0 mm; Rotating Plates - 4)



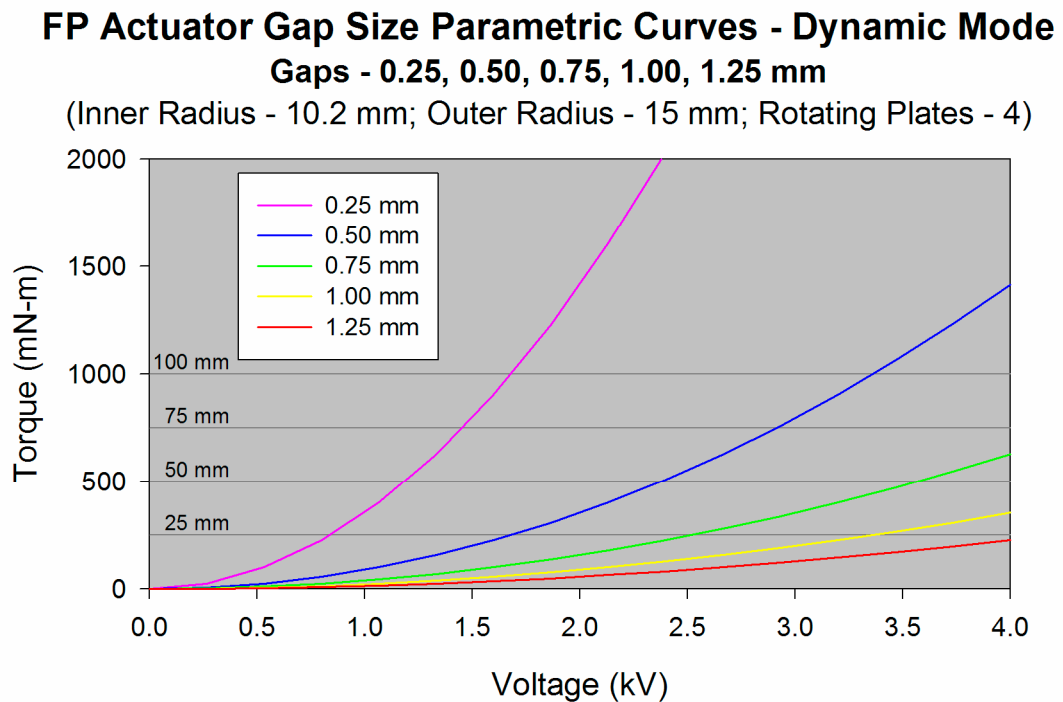
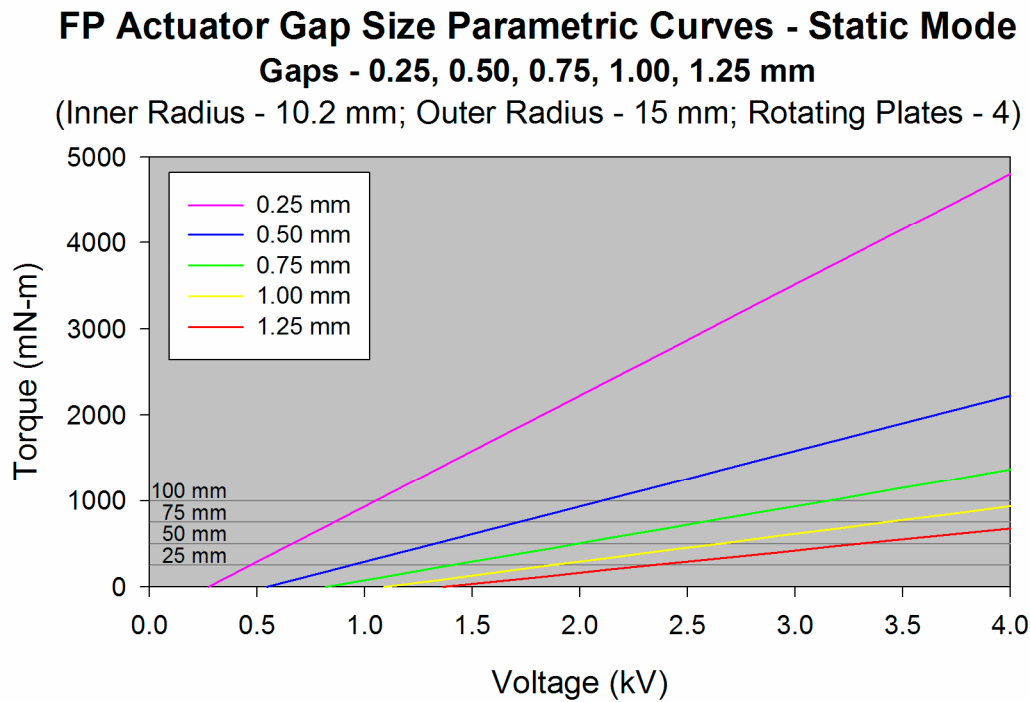
## FP Actuator Outer Radius Parametric Curves - Dynamic Mode

Outer Radius - 12, 15, 18, 21, 24 mm

(Inner Radius - 10.2 mm; Gap - 1.0 mm; Rotating Plates - 4)



**Figure 4-9:** Torque vs. Voltage for Various *Radii* for the FP Actuator.



**Figure 4-10:** Torque vs. Voltage for Various *Gap Width* Designs for the FP Actuator.

#### **4.4 Additional Parametric Analysis for Design Selection**

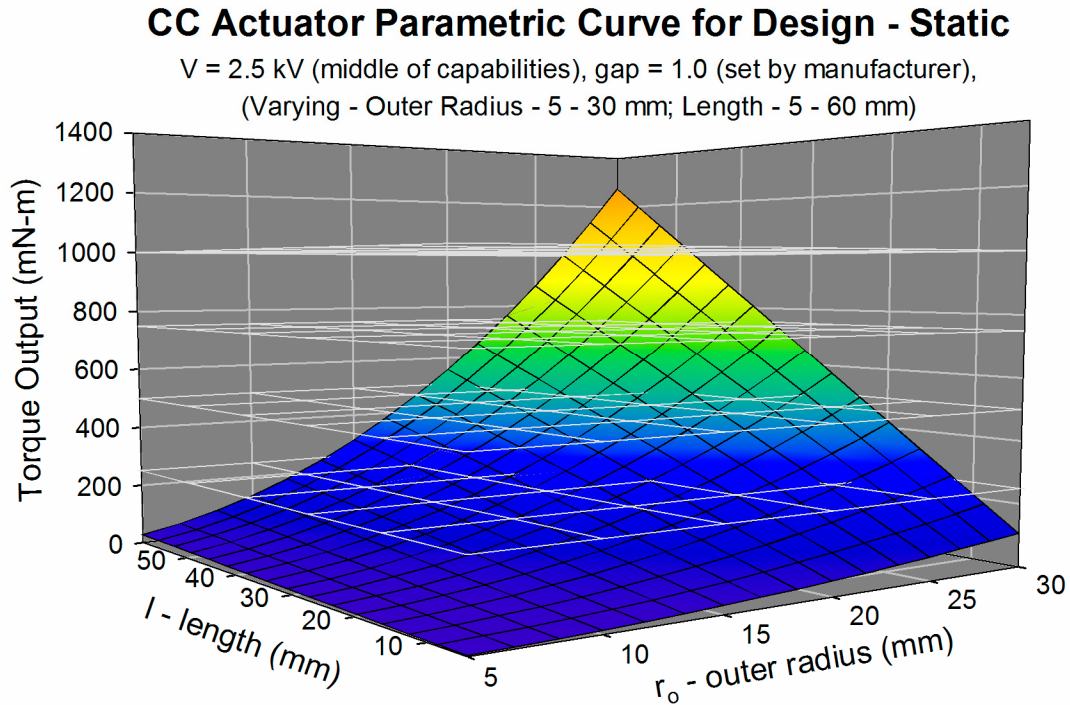
I conducted additional analyses of the effect of the design parameters on the total torque output of the ERF actuators subsequent to the analysis performed in the previous section. I incorporated new information, supplied by the manufacturer of the ERF fluid into the analysis to provide a basis for selecting variations to the actuator to meet specific design criteria.

Previous analyses focused on varying the gap-width in order to increase the actuators' torque output. This is an intuitive choice since a smaller gap-width affects the strength of the generated electric field as well as affecting the overall dimensions of the actuator. Unfortunately, I discovered through experience with the original prototypes and subsequently confirmed from the ER fluid's manufacturer - Smart Technologies Inc. - that the ERF's characteristics can become unpredictable when it is operated in an environment with a gap-width below 1mm. In addition, the manufacturing of very small but consistent gap widths was difficult to achieve.

With this limitation in mind, future design variations used a gap-width of 1 mm. Since gaps larger than 1 mm decrease the effectiveness of the actuator, as seen in the analyses presented above, as well as increasing the overall size of the device, it was no longer necessary to consider the gap-width as a design variable.

The parametric analyses serve as a basis to choose the physical design of the actuator to suit particular torque output criteria. Since the gap-width was no longer a variable parameter, additional analysis was required to determine the physical parameters of the actuators that would be able to meet a specific torque output requirement.

The design parameters for the CC actuator that could be varied are the outer cylinder (inner-wall) radius and the length of the cylinders. The inner cylinder (outer-wall) radius is a function of the outer cylinder radius and the gap-width, with the gap-width set at 1 mm. The torque-output surface, shown in Figure 4-11, is generated by varying the outer radius and the length of the cylinders for the CC actuator in static mode.

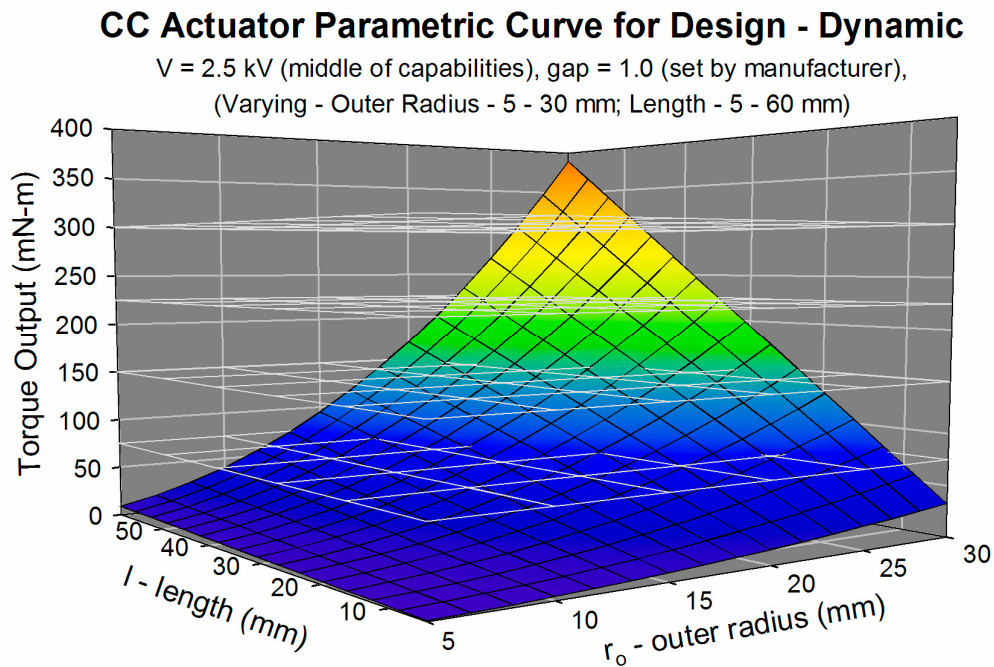


**Figure 4-11:** Torque Output for Radius and Length for CC Actuator in Static Mode.

The parameter defined to generate this curve is the applied voltage which was set at 2.5 kV. Since this curve was to be used to determine a physical design based on a desired torque output, I chose this voltage value to be at the center of the operating range of the high voltage power supplies used in the Rutgers Robotics Laboratory. If the designed actuator was capable of reaching the desired output at less than the maximum power supply capability, that would leave additional power resources available in case they were required to reach the desired torque output in non-optimal conditions.

The wire frame planes that are shown in the figures represent some possible torque-output criteria. Where the planes intersect the graph, the range of designs represented by that intersection curve, as well as all of the designs represented on the surface above that curve, would be capable of meeting the torque requirements.

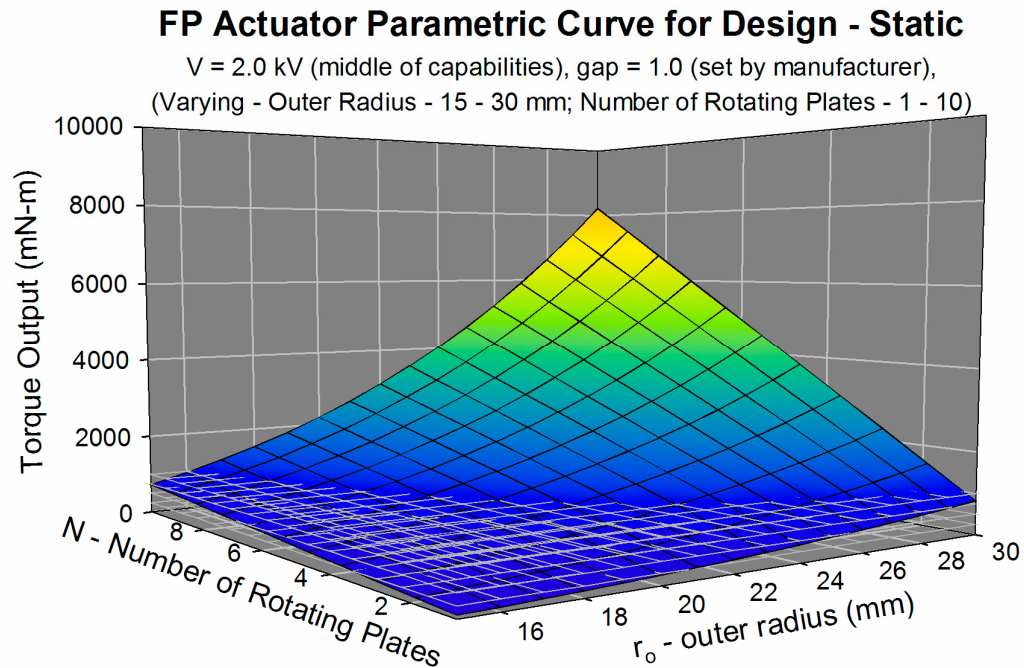
Figure 4-12 shows the comparable curve for the CC actuator acting in Dynamic mode. The speed of rotation was set at 10 mm/s, as an average value, in order to generate this curve. Since the application being considered for this research is a haptic system that will interact with the capabilities of the human hand, it was not necessary to take into account high-speed variations in the torque output. Other applications may, however, require this analysis to be performed.



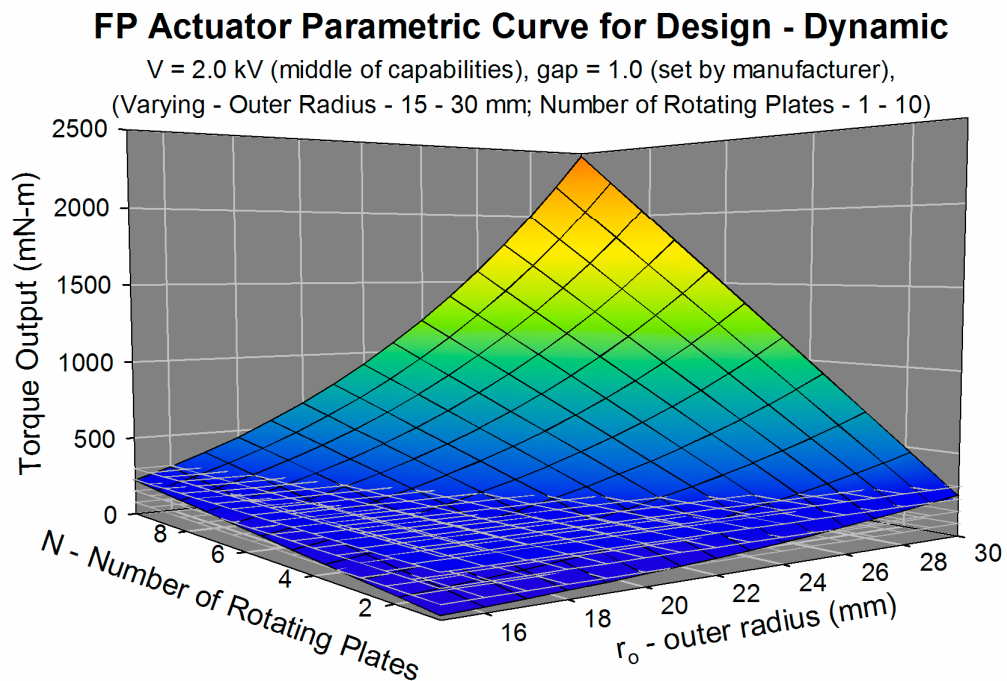
**Figure 4-12:** Torque Output for Radius and Length for CC Actuator in Dynamic Mode.

I performed comparable analysis for the Flat-Plate actuator as well. The defined parameters for the analysis of the FP design are the gap-width – 1 mm, velocity – 10

mm/s and the applied voltage – 2.0 kV. Figures 4-13 and 4-14 show the curves for the FP actuator in static and dynamic modes respectively.



**Figure 4-13:** Torque Output for Radius and Length for FP Actuator in Static Mode.



**Figure 4-14:** Torque Output for Radius and Length for CC Actuator in Dynamic Mode.

The wire-frame planes in these figure represent the desired torque outputs as defined in the previous section for the Static and Dynamic modes. When the number of plates and the outer radius of the plates were varied, the designs would easily meet the stated criteria. Although the designs may have been numerically possible the represented physical design may have been impractical. An analysis of the physical parameters and the assembly process had to be incorporated when using these curves to determine a viable design.

The following section presents some additional design considerations that had to be addressed when designing and building these actuators.

#### **4.5 Additional Design Considerations**

While the prototypes of the actuators will be presented in subsequent sections, some additional considerations relating to the design of the physical prototypes themselves are presented here.

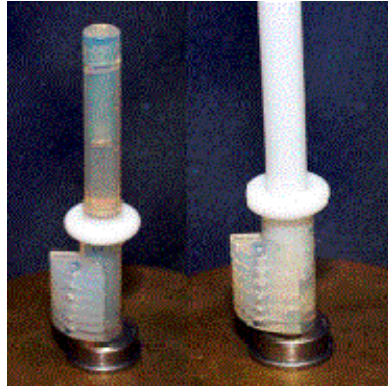
##### *Sealing*

One of the concerns with ERF-based actuators is effectively sealing the fluid from leakage while still minimizing the zero-field resistance associated with the device. Since the actuators are to be used for a haptic application, it is critical that the friction of the seal be reduced.

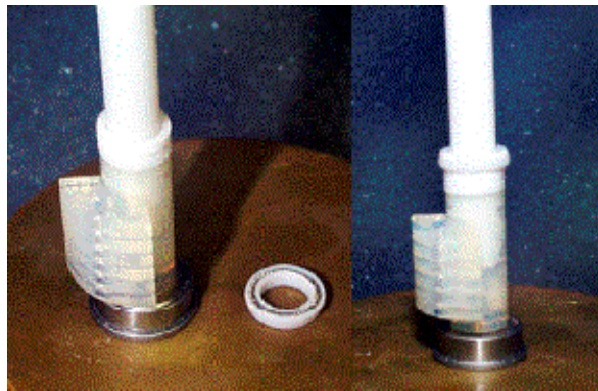
Initially, a simple Teflon<sup>®</sup> O-ring was fit between the rapid-prototyped shaft and the lid to prevent leakage. This resulted in a relatively large amount of static friction. Modifying the design such that the portion of the shaft in contact with the O-ring was made of Teflon (Figure 4-15, left), further reduced the friction. Another design replaced



the entire shaft with a Teflon shaft (Figure 4-15, right). Finally, a spring-loaded Teflon seal (Figure 4-16) was inserted to replace the O-ring.



**Figure 4-15:** Teflon O-ring Seals – Various Shaft Designs.



**Figure 4-16:** Spring Loaded Teflon Seal on Teflon.

In order to check the efficacy of the seal, a test was set up that subjected the shaft and seal to repetitive rotations using a DC motor and a belt attached to the actuator shaft. After running the device for several hours there was a minimal amount of leakage. To test the static torque needed to rotate the sealed device after this procedure, The following test was performed: a wheel was attached to the shaft, a wire was wrapped around the wheel and a weight was hung. Different weights to determine the minimum torque

needed to rotate the shaft. It was determined that the torque needed to rotate the actuator from a stopped position, with no electric field applied, measured about 1 mN-m.

Thus the use of a Teflon-on-Teflon seal or a similar pairing of low-friction materials seems to be an effective method to prevent leakage of the fluid while reducing the amount of mechanical friction inherent in any type of sealing method.

### *Safety*

When designing a high-voltage application for use within an automobile console, safety is a top concern. Since the operator will be in direct contact with the mechanism, it is imperative to make the device safe for use by any untrained person. Based on the current designs and power capabilities of the prototype equipment, the device will operate with an estimated maximum of 4000 volts DC at 1 mA of current. This is a relatively low amount of electrical power which should be well within safety ranges.

As a safety guideline, these devices should be designed to be no more dangerous than many currently existing consumer products. Television sets and computer monitors which rely on cathode ray tubes to display an image operate at voltages as high as 10,000 to 35,000 volts DC. However the current needed is relatively low [Health Physics Society, 2001a]. Microwave ovens on the other hand, operate at voltages up to 4000 volts DC at 300 mA [Health Physics Society, 2001b]. This is a much more dangerous combination than the actuators being designed.

To make these devices safe, the components are enclosed within grounded metal enclosures to prevent accidental contact. Additionally, all high voltage wiring, switches, and metal parts have sufficient insulation and are designed to be inaccessible to the operator. Warning labels indicating the hazards of high voltages are located on the

outside of the device. Similar steps can easily be taken to address the safety of the CC and FP actuators.

## 5 TESTING - MODEL VERIFICATION

To prove the accuracy of the torque modeling equations given above experimental testbeds were built. The testbeds (Figures 5-3 and 5-10, below) are equipped with sensors to read force, torque, linear and angular displacement. Although the proposed applications only required rotation from the actuators, the CC actuator test bed was designed to perform linear as well as rotational tests, to allow for future development options. Since the FP actuator only runs in rotation, its testbed acts in rotation only.

The following sections present the experiments that were performed to verify the mathematical models derived for the CC and FP actuators. Descriptions of the test beds, the prototypes and the experiments performed are given as well.

### 5.1 Concentric-Cylinder Actuator

#### 5.1.1 CC Actuator Prototype and Experimental Setup

The prototype of the CC actuator is made of a hollow outer copper cylinder resting inside of a one-inch internal diameter Pyrex<sup>®</sup> piping sleeve six inches in length, and filled with ERF (seen in Figure 5-3). A smaller inner copper electrode (Figure 5-1), mounted to a hollow steel shaft (Figure 5-2) using a rapid-prototyped insert, fits inside the outer electrode. The distance between the copper electrodes can be varied, by changing the diameter of the inner electrode, in order to test different gap sizes.

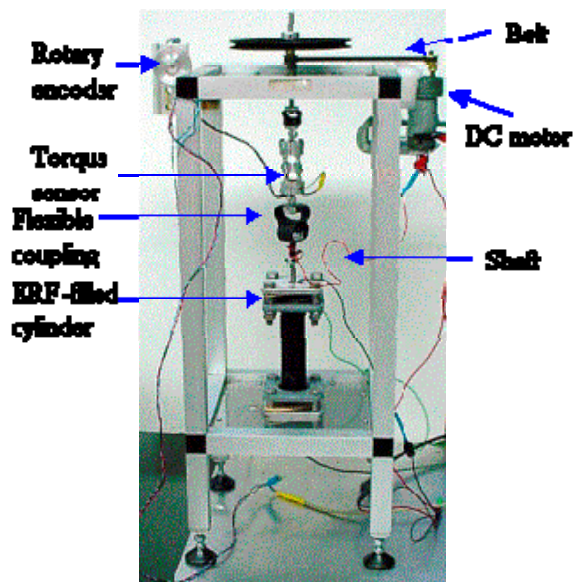


**Figure 5-1:** Inner Copper Electrode.

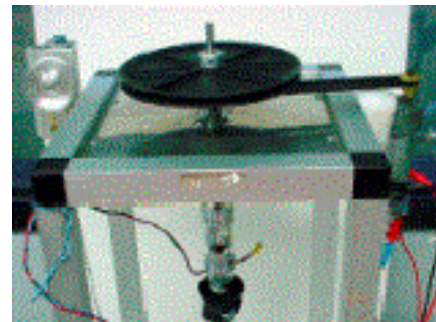


**Figure 5-2:** Electrode Mounted on Shaft.

The shaft attached to the inner electrode runs vertically to a 70 mm radius pulley wheel. An optical encoder is used to measure the angular displacement. Alternatively, a belt can be attached around the shaft so that a DC motor can drive the setup. A torque sensor is included to determine the resulting reaction torques. To apply voltage to the fluid, a supply wire is run down through the hollow shaft and into the inner electrode, making an electrical connection. A second wire runs to the outer electrode. The pulley wheel has a cable that runs over a second pulley wheel, which is attached to an optical encoder. Weights can be hung from the cable to apply torques to the system. The test bed is shown in Figures 5-3 and 5-4.



**Figure 5-3:** CC Testbed.



**Figure 5-4:** Close-up of top of Testbed.

### 5.1.2 CC Actuator Experimental Results

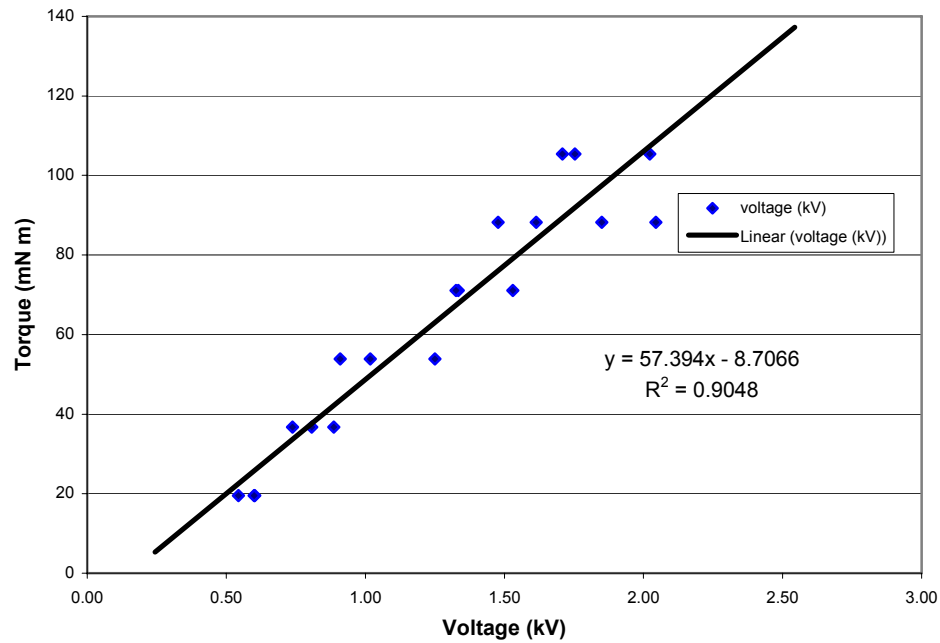
Static and Dynamic tests were conducted to verify the accuracy of the predictive models. These experiments are presented in the following sections.

#### *Static Mode test*

The static torque is defined as the amount of torque being resisted by the actuator at the moment when the actuator switches from being stationary to moving.

The physical dimensions of the prototype actuator used for these tests contributed to the capabilities of the actuator and the amount of resistive torque that was observed. The actuator has cylinder lengths of 25.4 mm, with the inner cylinder radius of 10.5 mm and the outer cylinder radius of 11.0 mm. The gap between the electrodes is 0.5 mm.

In this experiment a mass was hung from the pulley to apply torque. Voltage was applied to the actuator and then decreased until the mass began to move. That voltage was recorded. This process was repeated for several masses. As can be seen in the static test results shown in Figure 5-5, the torque-voltage relationship is approximately linear.



**Figure 5-5:** Static Torque vs. Voltage for CC Actuator w/ 0.50 mm Gap.

Unfortunately, the accuracy of the results cannot be validated relative to the mathematical model, since the manufacturer of the ERF LID 3354S does not have information regarding the static response of the fluid.

Nonetheless, the experimental data in Figure 5-5 shows, approximately, the linear relation between the applied voltage and the output torque, as predicted by Equation 10.

This result can be considered to validate the form of the mathematical model if not its specific numerical values.

Using the data graphed here and the mathematical model, the experimental values for  $C_s$  and  $E_{ref}$  were determined.  $C_s$  equals 1.218 Pa mm/V and  $E_{ref}$  equals 1210 V/mm. These values are summarized in Table 5-1 and compared to the values supplied by the ERF manufacturer for their older fluid LID 3354.

Model Parameters	LID 3354 S (Experimental)	LID 3354 (Manufacturer)	Percentage Difference
$C_s$	1.218 Pa mm/V	2.77	~56 %
$E_{ref}$	1210 V/mm	1090	~10 %

**Table 5-1:** Experimentally obtained Parameters for ERF LID 3354s versus those stated for LID 3354.

### *Dynamic Mode*

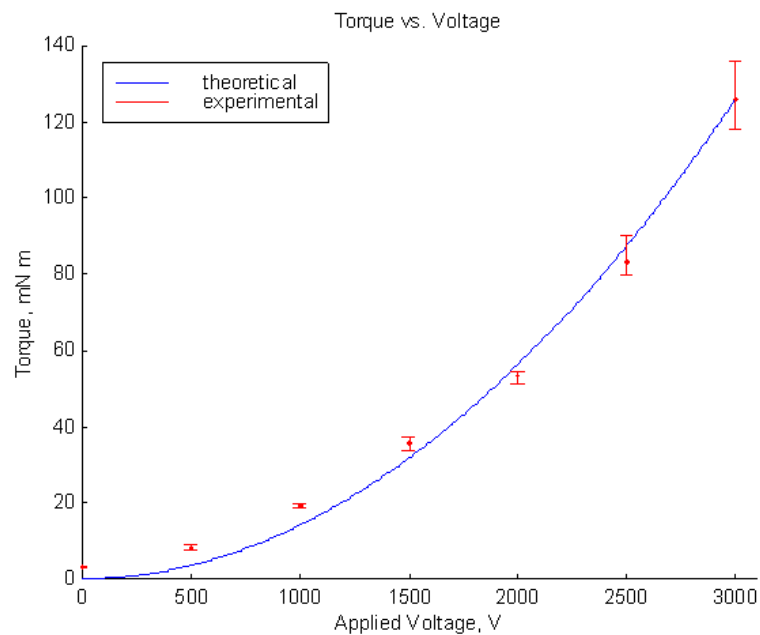
Experiments were also performed to validate the predicted system response for the actuator in dynamic mode, which is defined as any time the system is in motion. The resistive torque felt in the dynamic mode is usually lower than that felt in static mode.

Using the experimental setup for the CC actuator described above, tests were performed to measure the reaction torque produced for a given voltage when the system is in motion. A DC motor was run at a fixed voltage, and a belt was used to connect the motor shaft to the actuator shaft. The motor was run for approximately 10 seconds, and a voltage was applied to the actuator. Voltages between 0.0 and 3.0 kV were applied in increments of 0.5 kV. The average recorded torque for each run was calculated. The test was run three times at each voltage level, and the average for the three runs was then calculated. Table 5-2 shows the results of these tests.

Voltage (kV)	Torque (mN m)
0.0	3.2
0.5	8.4
1.0	19.3
1.5	35.6
2.0	53.2
2.5	83.3
3.0	126.0

**Table 5-2:** Concentric-Cylinder Actuator Dynamic Torque Experimental Values.

Figure 5-6 is a plot of both the theoretical curve predicted from equation 11 and the experimental data from Table 5-2.



**Figure 5-6:** Theoretical and Experimental Dynamic Torque vs. Voltage for CC Actuator with 0.50 mm Gap.

The graph shows that the experimental data points match the theoretical curve convincingly well. Therefore, the equation developed for the CC actuator in dynamic mode can be considered to be accurate. Further testing would then be needed to



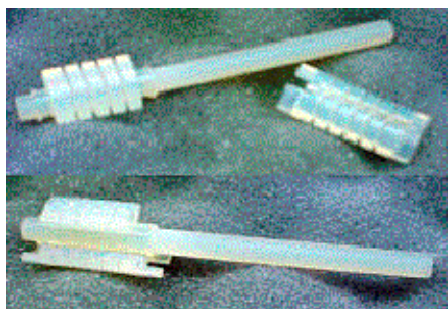
determine if this equation would be accurate enough to control the actuator in an open-loop scheme or if an even more refined model will be required.

## **5.2 Flat-Plate Actuator**

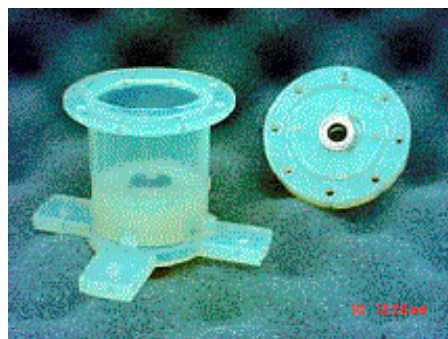
### **5.2.1 FP Actuator Prototype and Experimental Setup**

An experimental set-up has been built to validate the predicted performance of the FP actuator. Tests were designed to determine the relationship between the applied voltage and the reaction torque as predicted by Equations (14) and (16). The prototype actuator was built with the following configuration. The actuator has four rotating electrode plates with an inner radius of 10.2 mm and outer radius of 15.0 mm. There is a gap of 0.75 mm between electrodes.

Some of the components of the FP actuator, specifically the fixed and rotating shafts, are shown in figure 5-7, separately and in the assembled configuration. The fixed shaft is mounted to an enclosure (Figure 5-8), which contains bearings to hold the rotating shaft and a seal to prevent leakage of the ER fluid. Effort was made to reduce the friction caused by the seal as explained above.

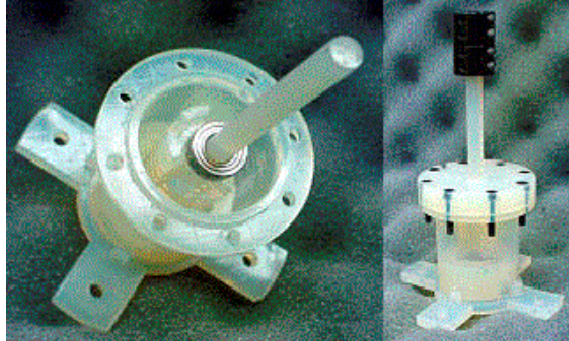


**Figure 5-7:** FP Actuator Shafts.



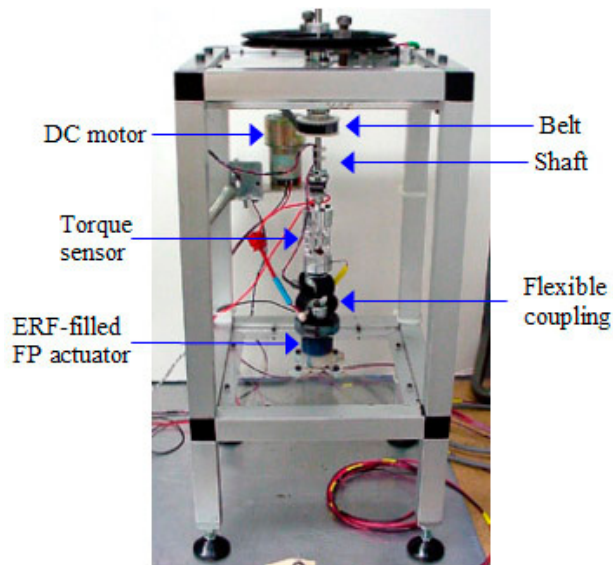
**Figure 5-8:** FP Actuator Case and Lid.

Figure 5-9, below, shows the assembled actuator, without the copper plates, with and without the lid attached. The shafts, enclosure and lid were built using rapid prototyping methods.



**Figure 5-9:** Flat-Plate Actuator Assembly.

The experimental setup for the flat plate actuator system, shown in Figure 5-10, is similar to the CC system described above. The actuator's shaft is attached to a flexible coupling to ensure proper alignment. This coupling is then attached to a torque sensor. The shaft which extends from the torque sensor has a pulley wheel that is connected to a DC motor through a belt. This motor drives the setup during the dynamic tests. An optical encoder attached to the shaft is used to measure the angular displacement.



**Figure 5-10:** Flat-Plate Actuator Test Setup.

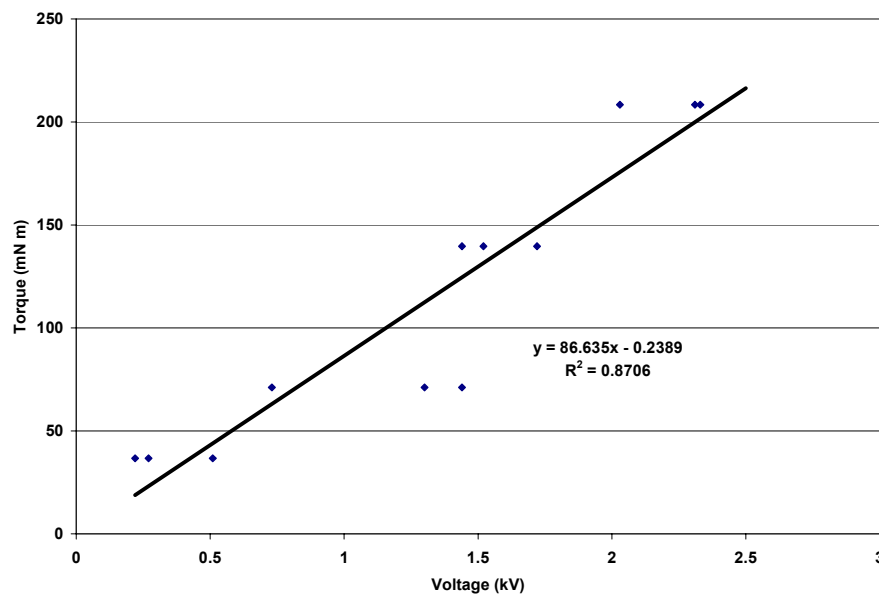
## 5.2.2 Flat Plate Actuator Experimental Results

Tests were performed to verify the accuracy of the mathematical models that predict the reactive torque due to applied voltage for the Flat-Plate actuator. Static as well as dynamic experiments were conducted to verify the different equations.

### *Static Mode*

In this experiment, a mass was hanged from the pulley to generate torque. A high voltage was applied and then slowly decreased until the mass started to move, the voltage was then recorded. This process was repeated for several runs with various masses.

The results of static tests are shown in Figure 5-11. As with the CC actuator, the relationship between torque and voltage was found to be approximately linear, although the accuracy of the numerical results cannot be validated since the manufacturer of the ERF does not supply information regarding the static response of the fluid.



**Figure 5-11:** Static Torque vs. Voltage for FP Actuator w/ 0.75 mm Gap and 4 Plates.

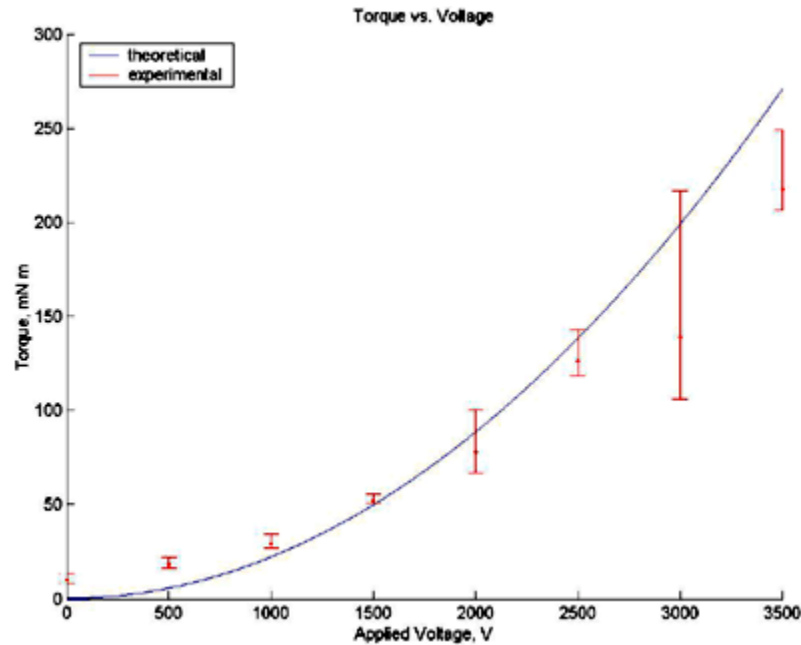
### *Dynamic Mode*

Using the experimental setup for the FP actuator, tests were performed to measure the reaction torque produced in dynamic mode to validate the accuracy of the dynamic torque response model. A DC motor was run at a fixed voltage, and a belt was connected to turn the actuator shaft. The motor was turned on, a voltage was applied to the actuator, and the reactive torque was recorded. Voltages between 0.0 and 3.5 kV were applied, in increments of 0.5 kV. The test was run six times at each voltage level. The average recorded torque was calculated for each run, and the six values for each run were then averaged together. Table 5-3 shows the results of the experimental tests.

<b>Voltage (kV)</b>	<b>Torque (mN m)</b>
0	11.8
0.5	20.3
1.0	31.9
1.5	53.8
2.0	89.0
2.5	134.3
3.0	171.9
3.5	228.2

**Table 5-3:** Flat-Plate Actuator Dynamic Torque Average Experimental Values.

Figure 5-12 is a plot of both the theoretical curve (predicted from Equation 11) and the experimental data from Table 5-3. The results in Figure 5-12 show a good correlation between the theoretical and experimental torque values for low and medium voltages. At higher voltages, the correlation is not as good and there is higher error in the experimental results.



**Figure 5-12:** Theoretical and Experimental Dynamic Torque vs. Voltage for FP Actuator w/ 0.75 mm Gap and Four Moving Electrode Plates.

The difference between the theoretical and experimental curves is presumed to be due to errors in the physical construction of the actuator rather than errors in the concept or the mathematical model. The dimension with the greatest uncertainty is the gap size between the electrode plates. Since there is a strong relationship between gap size and torque, as can be seen from the parametric studies above, a small error in gap size, possibly due to the inherent inaccuracies of the rapid prototyping process, can account for the difference in the comparison between the experimental results and the theoretical model.

Also, at higher voltages and subsequently higher torques, the stresses occurring within the actuator may be strong enough to shift the position of the electrode plates, thus changing the gap width. Even a slight change in this dimension will introduce variability in the torque measurement.

Because of this effect, it was important to alleviate some of these problems when designing the next prototype of the FP actuator. Attention was then paid to the strength of the attachment points for the plates and shafts, and the accuracy of the parts, so that the gap width would remain more accurately uniform, allowing the torque output to be more accurately predicted.

## **6 TESTING - RESPONSE TIME**

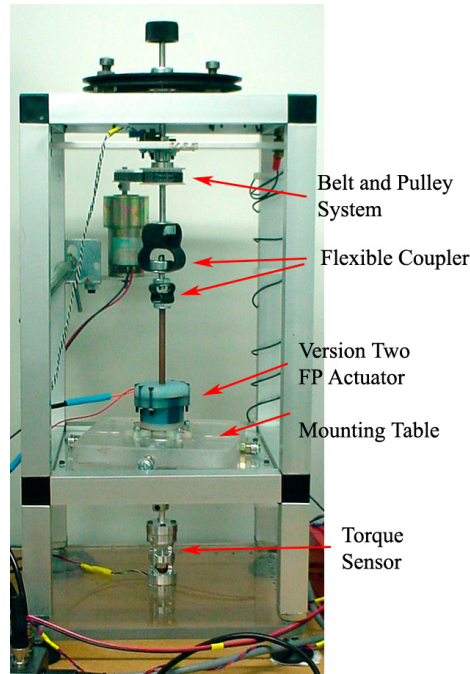
The actuators and devices designed for this project were used to create practical haptic interfaces that interact with a user's sense of touch, by applying forces to the person's hand. For these sensations to be believable they must be able to update and refresh themselves at a rate that will be transparent and convincing to the user. Thus, the speed at which the actuators operate is important to understand how they can be incorporated into a haptic device.

The actuators presented in the previous sections are based on the use of ER fluids to generate resistive forces. The body of literature for ERFs suggests that the ERF effect occurs over a 1-2 ms timeframe. It was important to perform experiments to see if it is possible to generate this level of response. The experiments that I performed to classify the FP actuator's response time will be presented in this section.

### **6.1 Response Time Tests - Experimental Setup**

The goal of these experiments was to determine how fast the ERF-based FP actuator could respond to a signal to change its viscosity. I designed an experiment to test the ability of the actuator to respond to a periodic activation signal. The periodic signal was increased in frequency to test the limits of the response capabilities of the actuator.

An updated testbed was built for the FP actuator in order to provide more accurate results by eliminating many of the sources of friction inherent in the original testbed. Figure 6-1 shows this new testbed and indicates some of the changes that were made compared to the testbed presented above in section 5.2.



**Figure 6-1:** New FP testbed with DC motor attached.

Some of the sources of error and friction in the original testbed were a result of misaligned shafts. To address that issue, flexible couplers were installed to alleviate some of the torque that was placed on the shafts. The actuator was mounted to a table that rotates about a single point, as indicated in the figure. The torque sensor was mounted to the rotation point in order to directly read the actuator's resistive torque. The DC motor was attached with a belt system in order to impart a rotation to the actuator.

I conducted the experiment using the testbed, the DC motor and a computer data acquisition system. The response time tests were conducted in the following way:

1. A DC motor was attached to the rotating wheel of the FP testbed, and set in motion so that the resistance generated by the actuator could be measured.
2. The data acquisition computer generated a control voltage using a sine-wave function, with variable frequency. This control voltage was recorded.
3. The Torque sensor recorded the output torque generated by the FP actuator based on the control voltage.
4. The frequency of the sine-wave function was increased and the experiment repeated multiple times.

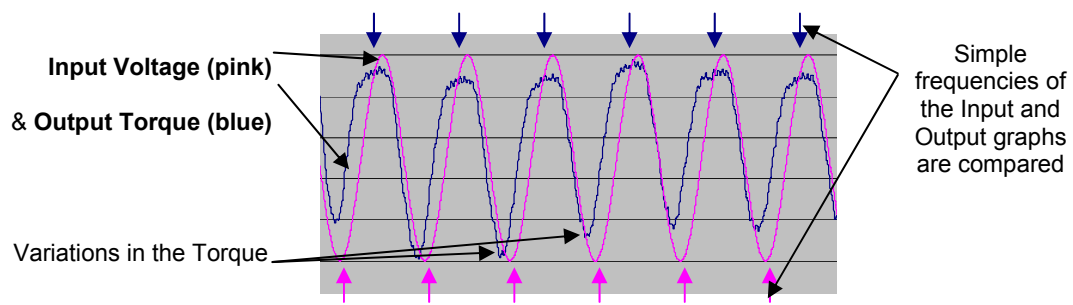


## 6.2 Experimental Analysis Approach

The goal of this experiment was to determine the maximum frequency at which the actuator system can generate a requested amount of torque. By using a sine wave input it is possible to generate a rising and falling amount of requested torque at a fixed frequency. In addition it is simple to increase the frequency of the sine wave function in order to observe the response of the actuator system to a faster input.

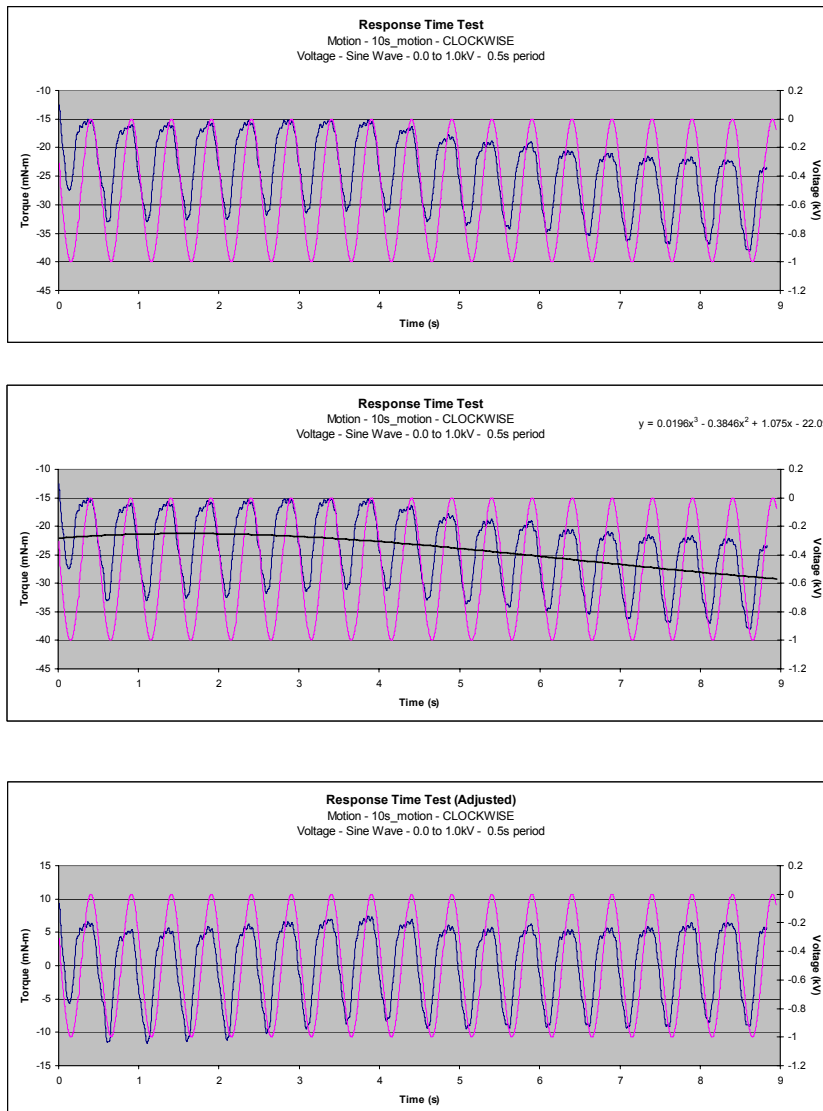
Many inaccuracies are possible in the readings that are recorded by the data acquisition system. In addition, errors in the forces that are generated and inaccuracies in those sensed within the actuator system itself may compound the errors in the torque output readings. It is expected that a closed-loop control scheme will be able to accurately follow the requested torque levels. This experiment, however, was designed to show the *speed* at which the actuator system responds to approximately the desired torque.

Therefore the approach for this experiment was to observe the frequency of the torque output curves without taking into account the quality or accuracy of the actual torque reading. Figure 6-2 shows an excerpt of one of the generated graphs in order to indicate the types of data that were collected and how the data was used in the response-time analysis.



**Figure 6-2:** Sample section of response-time graph with indicated features.

The sequence through which the response time graphs were generated is indicated in the following figure, Figure 6-3. The steps indicated were taken to isolate and identify the frequency of the torque output.



Voltage and Torque are plotted vs. time on separate y-axes

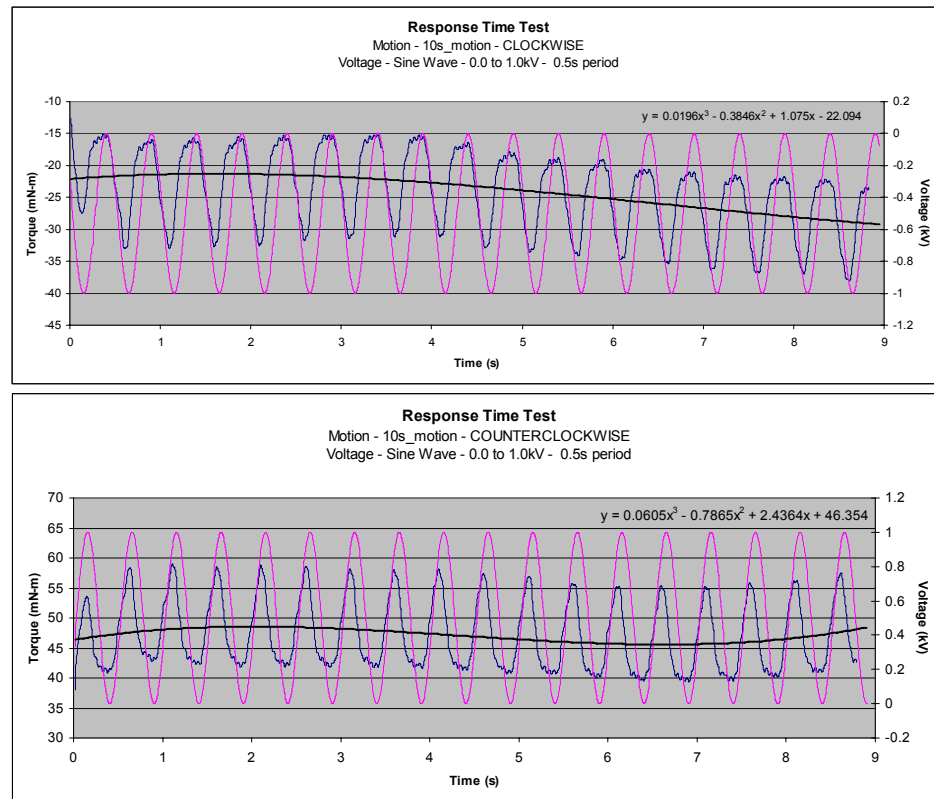
A trendline is fit to the Torque output data, to indicate the variable offset of the data.

The Torque output is regraphed, minus the offset, and resized to “match” the voltage input

**Figure 6-3:** Steps taken to clean up and isolate the input and output frequencies.

I conducted the experimental runs in two different groups. First the sine wave voltage input was set to vary from 0 to 1.0 kV. Experimental runs were then made with the actuator turning in clockwise motion and again in counterclockwise motion. The

change in direction was made to test the system's response to different directions of motion. As indicated in Figure 6-4, the clockwise experimental runs read the torques as negative values and the counter-clockwise runs as positive values.

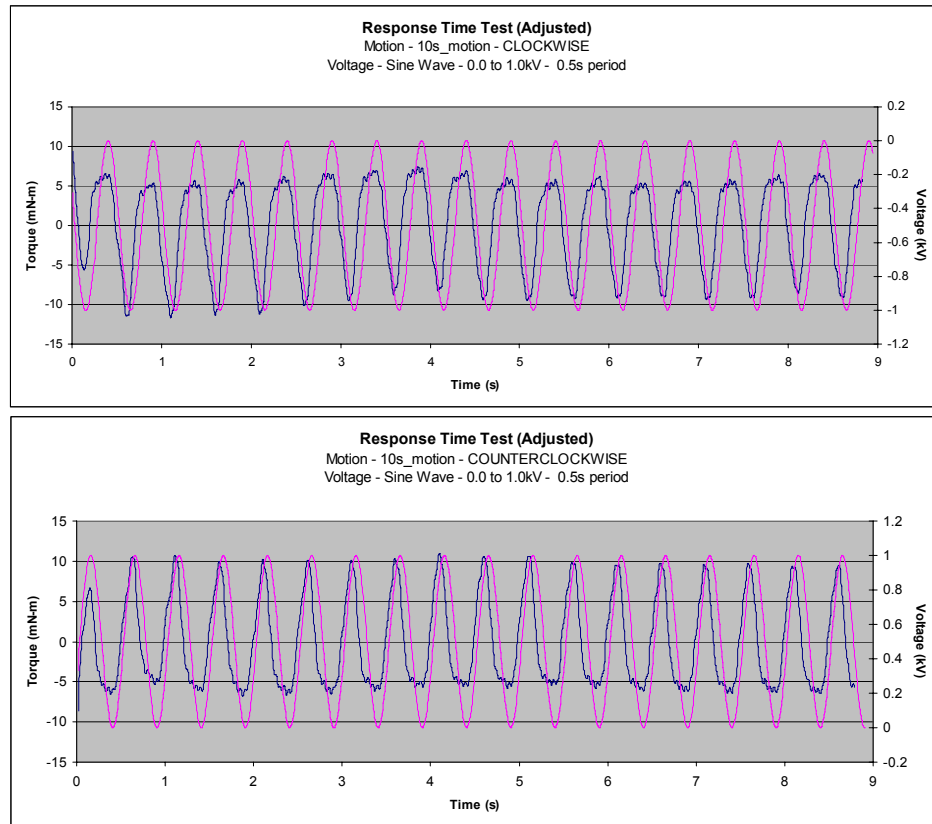


**Figure 6-4:** Samples of Clockwise and Counterclockwise experimental runs.

Due to limitations of the power supply systems used, only positive voltage could be generated. In order to maintain the clarity of the graphs, the voltages in the clockwise direction were artificially made negative when they were graphed in order to maintain the sine wave inputs and outputs with the same structure.

However, after the offset is calculated and deleted from the torque output curves, as shown in Figure 6-5, the two directions maintain the same quality of frequency response, although one is inverted relative to the other due to the sign of the recorded

torque value. Therefore the subsequent analysis does not address the direction of motion, only the frequency calculated.



**Figure 6-5:** Processed Clockwise and Counterclockwise experimental runs.

I collected data in this way for various frequencies of the input voltage waves, and repeated the tests multiple times in order to collect as accurate data as possible.

In addition, I repeated the tests for an input voltage range of 0.5 – 1.5kV in order to determine if limitations in the power supply’s ability to completely dissipate its voltage would affect the outcome. In the following section I collect the data, analyze it and draw some conclusions about the frequency response of the actuator system.

### 6.3 Analysis of Data

As indicated above I conducted the analysis to determine the input voltage wave's frequency versus the output torque wave's frequency. I took the steps shown above in Figure 6-3 for each of the experimental runs. These runs were conducted in two stages. First the sine wave function was generated using a 0 – 1.0 kV range. A separate set of experimental runs used a range of 0.5 – 1.5 kV.

Although the torque output wave is offset from the input wave, as can be seen throughout the figures presented above, the input and output frequencies can still be examined. Table 6-1 below shows the collected input and output frequencies determined from the experiments for the 0 – 1.0kV range. Table 6-2 shows the results for the 0.5 – 1.5 kV range. Once I found the results for the first set of tests, the second round of tests, tabulated in Table 6-2, were limited to the faster frequency tests only in order to simplify the experimental process.

<b>Voltage Input Peak-to-peak Period</b>	<b>Measured Torque Output Period</b>
<b>1.0 s</b>	<b>1.0 s</b>
<b>0.5 s</b>	<b>0.5 s</b>
<b>0.25 s</b>	<b>0.25 s</b>
<b>0.1 s</b>	<b>0.1 s</b>
<b>0.05 s</b>	<b>0.05 s</b>
<b>0.01 s</b>	<b>0.05 s</b>

**Table 6-1:** Tabulated Input and Output frequencies for the 0.0 – 1.0 kV Range.

<b>Voltage Input Peak-to-peak Period</b>	<b>Measured Torque Output Period</b>
<b>0.25 s</b>	<b>0.25 s</b>
<b>0.1 s</b>	<b>0.1 s</b>
<b>0.05 s</b>	<b>0.05 s</b>
<b>0.01 s</b>	<b>0.05 s</b>

**Table 6-2:** Tabulated Input and Output frequencies for the 0.5 – 1.5 kV Range.

Each of the experiments was conducted three times, so that the above values could be verified. The input and output frequencies are the same through the 0.05s period test. After that, the input voltage period decreases but the output torque period remains at 0.05s. Thus, the minimum period that the FP actuator system - including the power and the computer systems - can generate is 0.05s or a frequency of 20 Hz.

## 6.4 Sources of Delay

The response frequency determined in the above section is valid only for the specific actuator system that was tested. The components of the experimental system, including the actuator, computer, power supplies, and other components, all contribute to the frequency response that was seen. Many sources of delay may have contributed to the overall system response. Some of these sources of delay are discussed here.

### *Computer and I/O Boards*

The actuator system uses a Personal Computer system to: generate command signals based on a computer program; interface with the Input/Output cards to allow communication with the external components of the system; generate the control voltage that will be sent to the power supply; communicate through the I/O ports to the power supply; as well as, processing the incoming signals from the sensors. All of these steps take a finite amount of computer processing time and power. The computer system should be able to handle each of these steps individually at a high rate of speed.

However, since the computer system being used is run by a Microsoft Windows operating system, it has a lot of overhead - other activities that it must engage in, in order to keep the system operating. For example, the graphical interface system and the low level systems that interact with the computer hardware all must be running along side the

actuator program and Input/Output processes. All of these processes running simultaneously could be sources of delay for the overall actuator system being tested.

Since the computer system used was not designed to be a high speed system, it is not surprising that delays would be evident in its operation. Other systems are available that are designed to run Real-Time programs and, I believe, one of these systems may be able to solve the delays caused by the computer and its Input/Output systems.

### *Power Supply*

The power supplies that I used to generate the activation voltage sent to the actuator use a capacitor system to store and release electrical energy. Capacitors require finite amounts of time to charge and discharge. In addition the charging and discharging profiles are rarely linear, so that discharging the final amount of voltage to reach the 0 kV goal that was used in some of the trials may require a longer amount of time than would be desirable.

In addition, the voltage signal that was recorded and plotted was the control voltage sent from the computer to the power supply, not the actual voltage sent by the power supply to the actuator. This control voltage had to be recognized by the power supply, processed by the supply's on-board electronics to determine the actual voltage requested, and then the capacitors charged and released to provide the desired voltage. All of these steps may have inherent delays which could contribute to the frequency response that was seen for the system.

High speed power supplies do exist, and specialized electrical circuits can be designed that may be able to alleviate some of the delays caused by the power supply system.

## **6.5 Response Time Test Conclusions**

The 20 Hz response that I observed in the course of this experiment, although not as high a response as would be needed for very intricate and high resolution applications, might be enough to design a haptic interface to be used to convey information. Future work could be done to alleviate some of the delays seen in the system, as presented above. In addition, the incorporation of more specialized hardware and software might be needed to increase the frequency and resolution capable in the system.

I believe, although it is not as easy to prove, that the delays themselves were caused mostly by the hardware and software, rather than the actuator itself. Revisions to the system and the actuator would allow the system to run at much higher frequencies than those seen in these tests.



## **7 ERF ACTUATORS IN HAPTIC INTERFACE SYSTEMS**

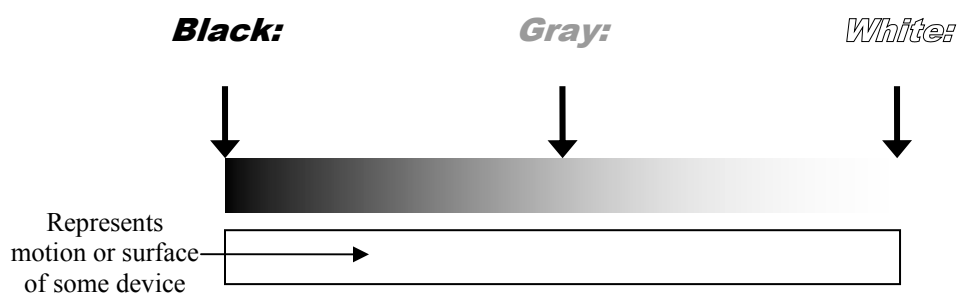
The goal of this research project has been to design and implement Haptic Interface systems that will allow for the transmission of information and control signals by interacting with an operator's sense of touch. The specific application that was examined was to develop such a force-feedback interface system to be used to control the secondary systems on an automobile's dashboard.

Since the dashboard contains a large number of control knobs and switches, there is a desire in the automotive industry to explore methods to simplify the dashboard's interface systems while maintaining the density of information that a driver wants and needs to have access to. The use Haptic Interface systems allows for the incorporation of force-feedback cues, as a complement or replacement of existing visual and auditory feedback methods, to create additional pathways to provide information to a user about the vehicle's status. The use of ERF-based actuators in building these haptic interfaces allows for the development of compact and highly capable devices that can mimic the methods that currently provide information to a driver as well as create new and innovative methods of providing information.

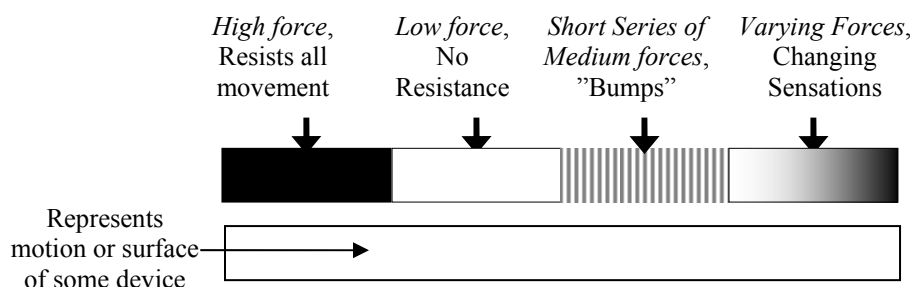
The following sections will present the two devices developed as force-feedback interface systems using the ERF-based actuators presented above. These devices are a Haptic Knob and a Haptic Joystick.

Since the haptic devices will be used to generate forces and torque that will be felt by a user, it is necessary to describe the sensations visually so that the designs and development plans can be easily understood. In the following sections the physical sensations will be represented visually by gray bands of varying intensity floating near or

on top of a drawing of a device. Figures 7-1 and 7-2 illustrate how this method will be used in the following descriptions of the Haptic Knob and Joystick.



**Figure 7-1:** Representation of the strength of a physical sensation.



**Figure 7-2:** Example interpretations of physical sensations.

This chapter will provide the ideas and design concepts for how the Haptic Knob and Joystick may be used to generate haptic sensation to control and simplify the secondary systems of a car.

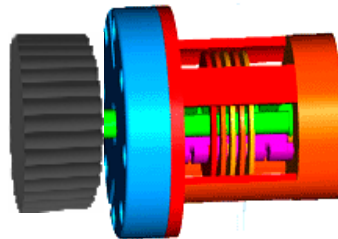
## 7.1 Haptic Knob

The first haptic system developed for use in a vehicle is a single degree-of-freedom haptic knob. The use of a knob as an interface is simple and easily understood by any operator. Knobs are used as control interfaces for an uncountable number of devices and are already an extremely common interface in automobiles. Therefore, any learning curve for the use of a Haptic Knob can be expected to be steep.

The use of a knob that can be changed “on-the-fly” to have the characteristics of any type of common knob can be useful in reducing the clutter on a vehicle’s dashboard by using a single knob to replace various different knobs. In addition, new types of knob “profiles” can be developed to provide different information, such as varying the force as the knob is turned to convey information to the driver about the control being used.

### 7.1.1 Knob Design and Prototype – v1

The Haptic Knob is assembled by attaching a knob to the end of a rotary actuator. Either ERF-based actuator presented above will work well in this application; however, I chose the CC actuator for the prototype of the Haptic Knob, as its minimum number of components allows for a low no-field friction. Figure 7-3 shows an early conceptual drawing for the Haptic Knob (using an existing FP actuator image).



**Figure 7-3:** Haptic Knob Device Using an FP Actuator.

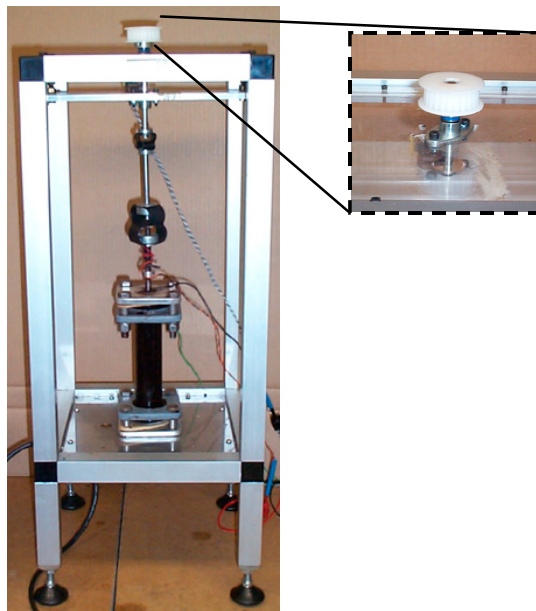
Sensors incorporated into the Knob design are used to read the position and applied torques and generate a torque response to those inputs in order to generate informative sensations. The use of an ERF-based actuator allows for the generation of simple force characteristics such as the feeling of detents and hard stops, but also allows for more complicated feelings that are available due to computerized control software and the viscous nature of the ERF.

The CC actuator's design is flexible enough to meet the space requirements of a given application. By increasing the radii and shortening the length of the copper cylinders a desired force output can be maintained while changing the actuator's volume. If a thinner but longer actuator is desired, longer and narrower cylinders can be used.

If the FP actuator were chosen to be the basis of the Knob, it is physically flexible as well. The volume that the FP actuator occupies can be changed by increasing the size and reducing the number of plates or by choosing a larger number of smaller plates. In this way the system can maintain a specified force output while varying its physical dimensions.

The physical flexibility of the actuator component allows the Haptic Knob to be easily incorporated into almost any physical space required, including the dashboard of a car that already has a large number of components.

The Haptic Knob's experimental testbed, shown in Figure 7-4, was developed by attaching a knob, for a user to grasp, to the top of the CC actuator's experimental set-up.

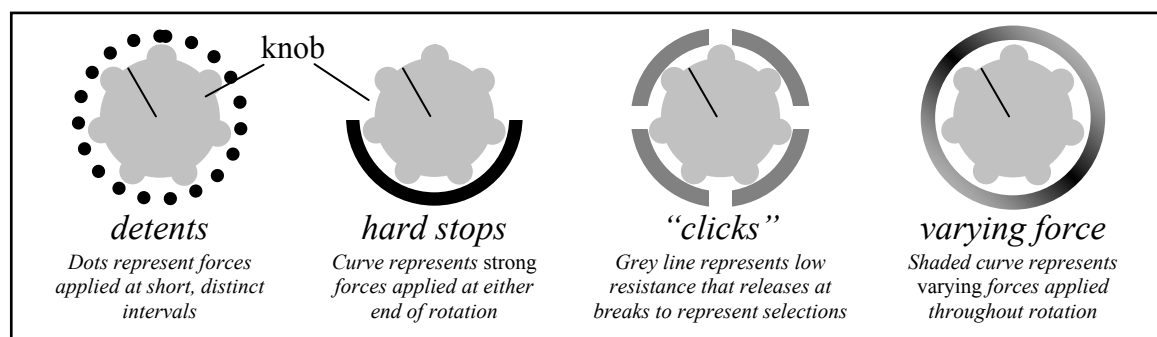


**Figure 7-4:** Knob Attached to top of actuator testbed.

While future versions of the Haptic Knob can be made very compact, by correctly sizing the actuator to meet the force output requirements, the experimental version of the knob is somewhat larger. This setup was used to demonstrate the Haptic Knob's abilities. In addition, the setup was used as a development platform to design the control and interface software.

The prototype of the Haptic Knob was used to prove the concept of using an ERF-based actuator for controlling a haptic interface. Software was written to provide resistive torque for a particular angular rotation along the knob's range of motion.

The first two figures in Figure 7-5 show the types of demonstrations that my colleagues and I in the lab had performed – detents and hard stops. Detents are a common force profile felt in knobs such as the volume knob on a radio. Hard stops define a range of motion that is acceptable. The use of multiple hard-stops can simulate distinct “clicks” as in a selection knob such as the control for fan speed.

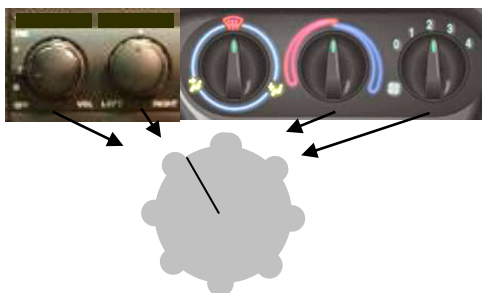


**Figure 7-5:** Demonstrated and Potential Knob Profiles.

For preliminary testing purposes we used simple force characteristics, such as impulsive or square-wave types of forces. Later testing would then include the use of more intricate force profiles, as illustrated in the right-hand images in Figure 7-5, and could also use the viscous forces inherent in ERFs to provide even more interesting force profiles.

### 7.1.2 Knob Application

The Haptic Knob can be used to reduce the clutter on the dashboard of an automobile by replacing various knobs that perform separate functions with a single knob that can change the functions that it performs, as illustrated in Figure 7-6.

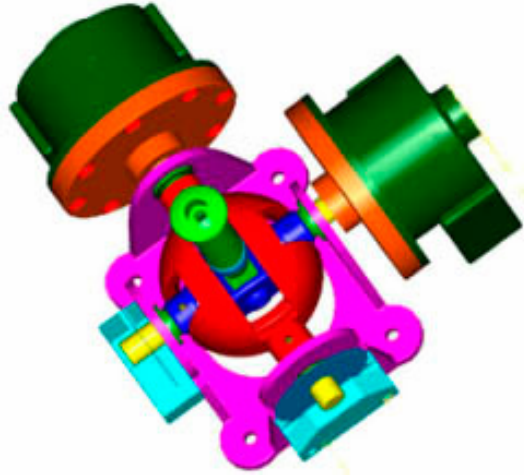


**Figure 7-6:** One Knob Can Simulate Different Types of Knobs.

Since the Haptic Knob is designed to work as an interface for the average person, it would be necessary to perform human subject testing to determine the ability of people to use the knob as an interface. Future studies of ergonomic factors and human interface factors will also determine if a visual display or other additional forms of feedback are necessary.

## 7.2 Haptic Joystick

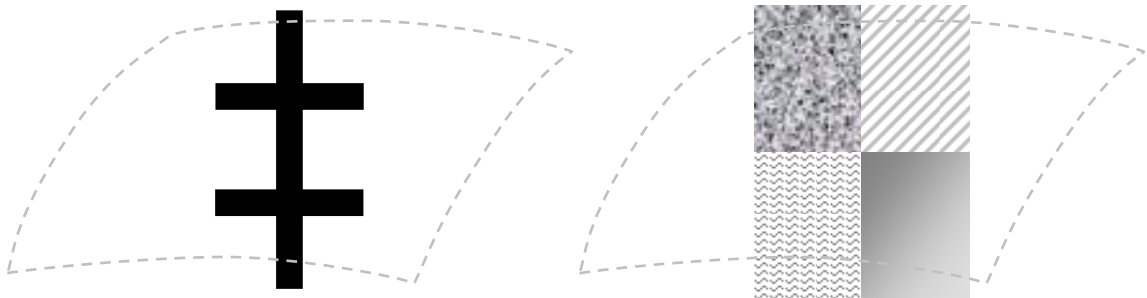
While the Haptic Knob is useful for simple applications, devices with a larger number of degrees of freedom will be required to make a significant leap into replacing the controls and information displays for the vehicle. The use of a joystick, with two rotational degrees of freedom, and possibly with a knob or button at the top of the handle, allows for more pathways for a useful human-machine interface to be designed. The CAD drawing for the Haptic Joystick is shown in Figure 7-7:



**Figure 7-7:** Haptic Joystick. Handle May Have a Button Attached.

Two rotational actuators, in this case FP actuators, are connected to a universal joint. The actuators can provide resistance to motion in the two rotational degrees of freedom inherent in the joint. Using the force profiles generated for the Haptic Knob as a basis, complex 2-Dimensional sensations can be achieved.

The addition of a second degree of freedom to the Haptic Interface system allows for the development of two new categories of sensations – Channels and Zones. Figure 7-8 illustrates these two categories of sensations.



**Figure 7-8:** Representations of the *Channels* (left) and *Zones* (right) available when using a 2-D Interface.

The use of “Channels”, illustrated in the Figure, is a method to define specific locations where motion may occur. An example of such defined channels in a non-haptic system is the manual stick-shift in an automobile, in which specific motions are allowed along a defined pathway in order to select between gears.

The use of “Zones” represents a method for defining sections of the available surface which have different types of sensations in order to present information. For example, sensors may read position, velocity, forces, etc. and generate a surface sensation accordingly. The different sensations in the different quadrants of the surface, as presented in the figure, may represent specific information for a user.

Although the universal joint of the Joystick actually moves along a 3-Dimensional curved surface, represented by the dashed curves in the background of the figure, the forces will be generated using the two rotational degrees of freedom offered by the two FP actuators. For simplicity, the sensations will be illustrated by simple rectangles, with the understanding that in actuality they represent a 3-D curved surface.

### **7.2.1 Joystick Design and Prototype – v1**

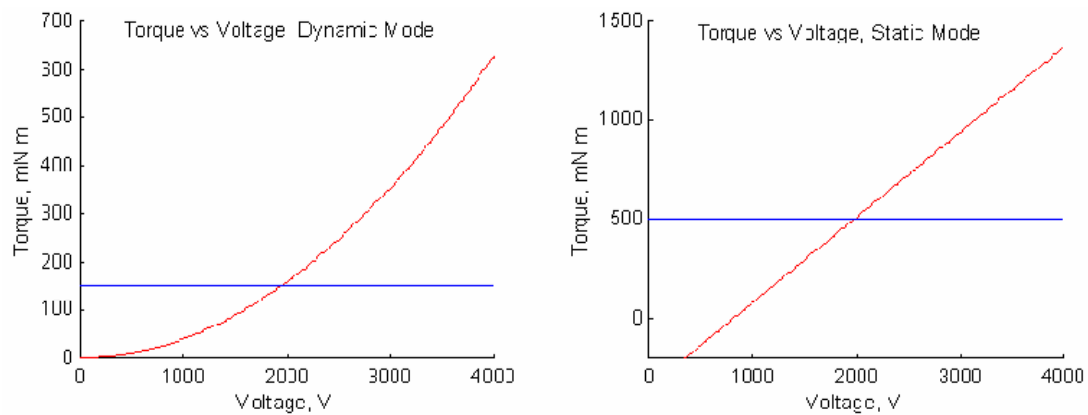
As stated previously, the proposed haptic feedback device must provide 10N of reaction force in static mode. To keep the overall dimensions of the device small, a moment arm of 50 mm was selected. A larger moment arm would require a larger actuator because higher torque levels would then be needed. It is also important that the voltage required to actuate the device be kept to a minimum for user safety and power consumption. Although voltages as high as 4 kV are possible, a 2 kV limit was set as the maximum to reduce the power requirement as well and to allow for a temporary increase in voltage if the control software requires it to maintain a certain force output level.

A design requirement for the Haptic Joystick system is that it should fit into approximately a 4-inch by 4-inch footprint, in order to allow for incorporation into a vehicle’s dashboard or center panel. The design of the FP actuator prototype’s physical dimensions was chosen to allow the Joystick to fit into this space requirement



The FP actuator was designed with a gap of 0.75 mm. The inner radius (10.2 mm) is fixed, since it must accommodate the diameter of the rotating shaft. The outer radius of 15.0 mm was selected to meet the specified force requirements. Four positive moving electrode plates and five negative stationary electrode plates are needed for this configuration. Adding plates will increase the performance without significantly increasing the volume. Each plate is only about 1 mm thick.

Figure 7-9 shows the performance curves for the FP actuator with the chosen parameters. The horizontal blue lines represent the required torque levels. Table 7-1 summarizes the actuator's properties



**Figure 7-9:** Calculated Performance Curves for the Joystick's FP Actuator.

	<b>FP actuator</b>
<b>Inner radius</b>	10.2 mm
<b>Outer radius</b>	15.0 mm
<b>Gap width</b>	0.75 mm
<b>Static Torque at 2 kV</b>	507.9 mN m
<b>Static Torque at 4 kV</b>	1367.0 mN m
<b>Dynamic Torque at 2 kV</b>	157.2 mN m
<b>Dynamic Torque at 4 kV</b>	628.3 mN m
<b>Range of motion</b>	150°

**Table 7-1:** Joystick's FP Actuator Properties.

The proposed Haptic Joystick is made of a joint with two rotational degrees of freedom, with one actuator required to control each of these degrees of freedom. Sensors are attached to each of the rotational axes to read the position and force at any point along the range of motion of the joint. Figure 7-7, above, shows the two degree-of-freedom joint (red and blue in the picture). The overall size of the joystick due to the chosen actuator parameters does fit into the required 4in x 4in design goal.

A prototype of the Joystick has been built for experiments and simulations. The two-degree of freedom joint was built using rapid-prototyped parts, with the exception of the bearings and bolts which were purchased. The parts and completed joint are shown in Figure 7-10.

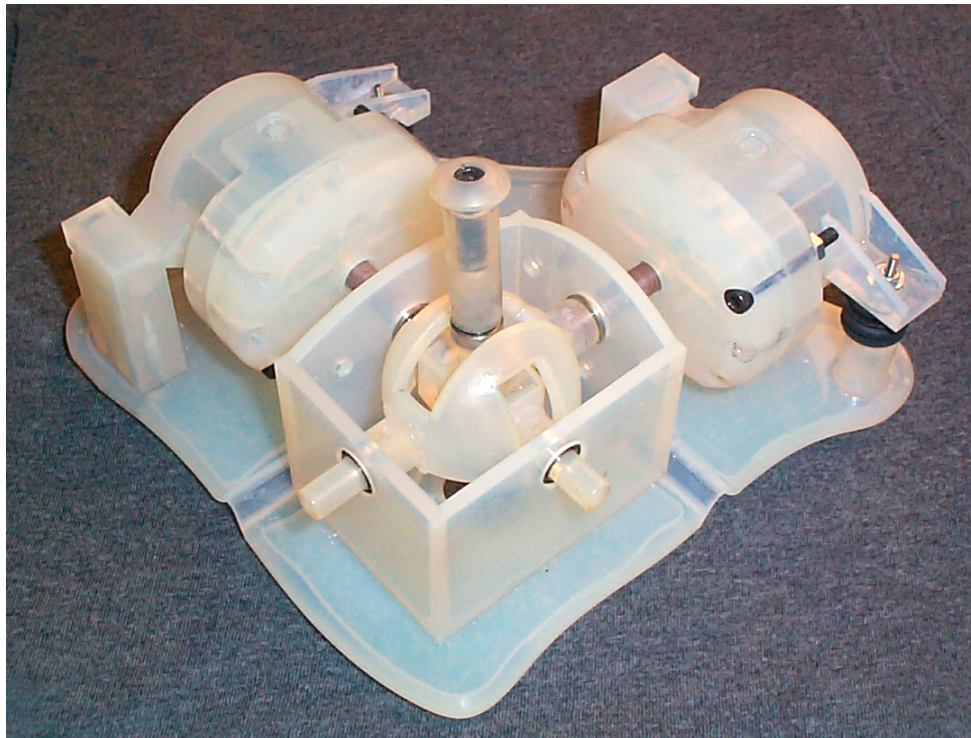


**Figure 7-10: Joystick Joint Assembly.**

The shafts from the actuators extend towards the shafts of the joint where they are coupled together. The joint itself is mounted with four bearings, to reduce bending

moment on the shafts. A low-profile rotary encoder is attached to each shaft to measure angular displacement. The external dimensions of the FP actuator joystick assembly are about 4.32 in. by 3.77 in. This size is calculated from the CAD drawings and the known component sizes.

The complete joystick assembly is shown in Figure 7-11. The optical encoders and the actuators' copper plates have been left out of the picture for clarity.



**Figure 7-11:** Assembled Joystick with Joint and Two Actuators.

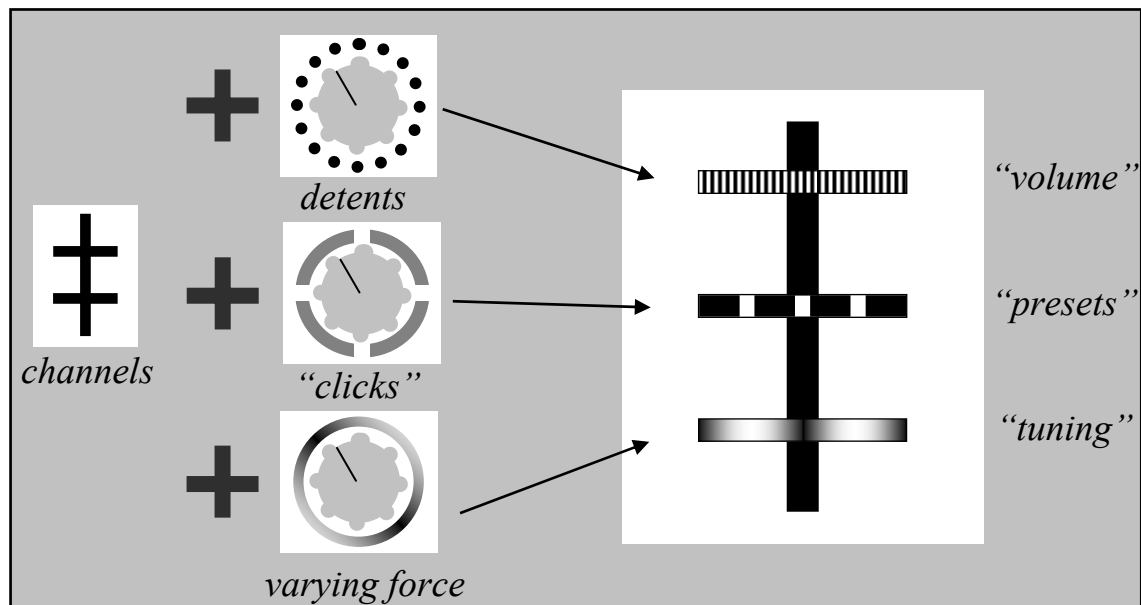
### 7.2.2 Joystick Application

As stated, the Haptic Joystick can be used to reduce the clutter on the dashboard of the car by controlling the secondary systems in the vehicle, such as the radio and the climate control by presenting information to the driver through the sense of touch.

The joystick is designed with sensors that read the position, motion and force input at any point within its range of motion. The actuators can react to these sensor

inputs and apply forces at any point within the range of motion. Various different feelings can be produced with the two rotational degrees of freedom, including the Channels and Zones described above .

Figure 7-12 shows, conceptually, a method to control the radio of the car. The vertical channel guides the user's motion up to the horizontal channels, which use sensations developed for the haptic knob such as detents, clicks, etc. to provide information about different functions of the car radio.



**Figure 7-12:** Representation of a method to use Haptic sensations to control a radio using the Haptic Joystick. The Channels guide the user to different options.

It will be necessary to develop methods for using the Haptic Joystick as a control interface. Since using a joystick in this manner is a unique application, it will be necessary to address ergonomic and human factors issues to design the interface. Human subject tests will need to be performed to determine the validity of using a Joystick in this manner. Future studies will also be needed to determine if additional feedback, such as auditory or visual, will be necessary to make this a viable interface.

## 8 ACTUATOR DESIGN – VERSION 2

After the actuators in the above chapters were developed and tested I determined that it would be useful to develop a new version of one of the actuators, in order to overcome some inherent limitations and add other capabilities. I then used this new actuator in developing the next version of the haptic interfaces that I employed for additional haptic testing. The following sections describe the development of this actuator, and subsequent chapters will describe the incorporation of that actuator into the haptic interface devices.

### 8.1 Motivation for Redesign

Although the CC and FP actuators presented in the previous chapters do perform as anticipated, I made a decision to develop a second generation version of one of the actuators in order to address some of the design issues that were encountered while developing the CC and FP prototypes. In addition it provided a chance to increase the capabilities of the actuator so that it could be used in more demanding applications. Some of the issues that are addressed with a redesign of the actuator are:

1.	Increasing the force generating capability
2.	Decreasing the voltage requirements
3.	Reduction of non controllable forces, such as the friction that is inherent in the device when no electric field applied
4.	Simplifying the assembly of the device
5.	Design the actuator to be more modular so it can be used more flexibly in various devices

**Table 8-1:** Goals for Actuator Redesign

In addition, I decided to focus the following design efforts on a generalized haptic display rather than the automotive-specific display as described for the previous actuators. To that end the remaining design and testing efforts do not specifically address

the automotive application. However, the designs and experimental results obtained can be applied to the automotive interface as well.

## 8.2 Material and Component Selection

It was desirable to develop the actuator and subsequent haptic devices using as many of the materials and components already existing in the Robotics Lab as possible. In addition, since two actuators would be required to develop the haptic joystick the existing material would need to suffice for both actuators. The material and components that existed in the Robotics Lab that were used to develop the second generation actuator were:

- 3 ½” diameter (approx) aluminum rod, left over from other projects
- Optical Encoders from Version 1 actuators
- Rapid Prototyped parts using the Robotics Lab’s Stereo Lithography system
- Various nuts, bolts, screws and other items from the Lab’s supplies
- ERF stored in the Lab from current and past projects

Additional components and materials were acquired as needed.

## 8.3 Design

After the developing the version 1 CC and FP actuators I determined that although the FP actuator, as discussed above, allows for generation of greater forces due to the larger surface area available with the multi-plate system, the CC actuator was simpler to build, assemble and predict its performance. Due to these considerations I decided to develop a version 2 of the CC actuator – referred to here as *CCv2 or CC2*.

The remainder of this section discusses the design decisions that I made to address the redesign goals as set out in Table 8-1 above.

### 8.3.1 Force Increase/Voltage Decrease

In order to make use of the existing components, specifically the existing aluminum rod, I decided to relax the initial design directive to develop a small actuator and instead maximize the force output of the system by developing as large an actuator as possible given the existing material. Therefore I designed the CC2 actuator to have a 3” diameter and a length of 2”. By increasing the size of the actuator it allowed for a larger surface area in contact with the ERF thus increasing the force output of the system. In addition, since the actuator would be stronger it would require less voltage to reach the same force output as the previous actuator. This design decision allows for addressing two of the redesigning goals – force increase and voltage decrease.

### 8.3.2 Reduction of Forces

One of the main design elements that contributed to the amount of no-field or friction forces inherent in the original CC actuator was the seal that was required to contain the ERF fluid while the actuator was in a horizontal attitude, as seen in the joystick prototype presented in chapter 7. Figure 8-1 shows some of the seals that were used in previous prototypes.

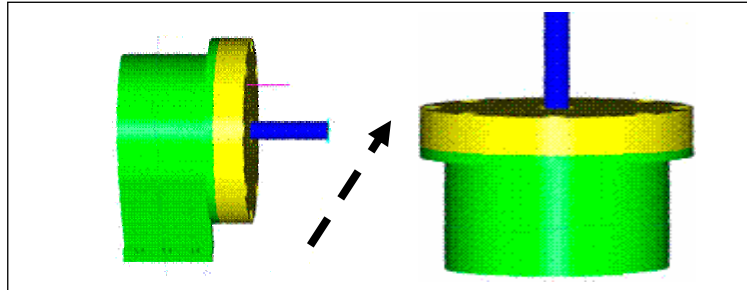


**Figure 8-1:** Previous sealing methods - Teflon Seal on FP shaft (L), Seal inside actuator cover (R).

For the seals to contain the ER fluid while the shaft rotates they must be held tightly against the shaft as well as tightly against the cover (Figure 8-1). This inherently introduces friction forces to the system than cannot be controlled with the ERF system.



The reorientation of the CCv2 to a vertical configuration – allowing gravity to hold the fluid in place – as seen in Figure 8-2 would address that issue by reducing the need for a tight seal around the shaft opening and therefore reducing the friction forces.

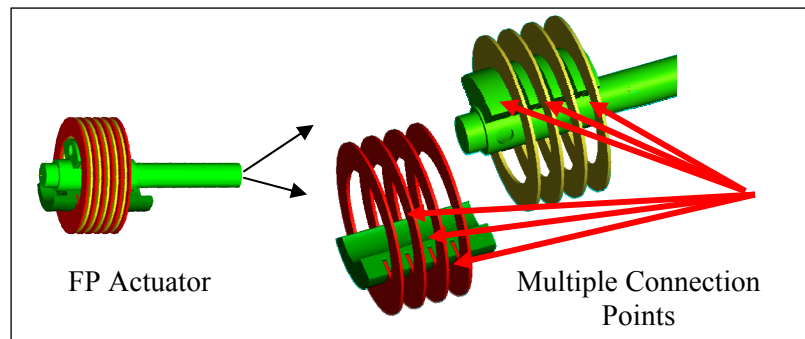


**Figure 8-2:** Reorientation of Actuator to Address Leakage

By reorienting the opening in the cover into a vertical orientation, the fluid will be held inside the actuator by gravity while a looser seal can be used to prevent splashing and spillage. These changes would allow for a reduction in non-field forces and would allow for a more controllable force profile than was possible with the version1 actuators.

### 8.3.3 Simplified Assembly

The main reason for choosing the CC actuator for revision was that the CC actuator was much simpler to build and assemble than the FP actuator. The FP actuator, using the multi-plate system, required numerous parts to be assembled. The deviation in the production of those parts (as discussed in section 5.2.2) resulted in components that can wobble (see Figure 8-3) and therefore create unpredictable results.



**Figure 8-3:** Multiple connection points for FP actuator, can result in loose components



The CC actuator by comparison has a single moving part – the rotating cylinder – which can be built as a single component. This allows for a tighter mechanical system as well as a simpler manufacturing process.

### **8.3.4 Modular Design**

One of the goals of this redesign was to allow the actuator to be used “as-is” in various different systems. I have designed the actuator case to allow just that type of flexibility. The following sections will describe how the actuator was designed to allow it to be applied in this manner. Additionally, other sections will describe how that single actuator design will be applied to new versions of the Haptic Knob and Haptic Joystick.

## **8.4 Development and Manufacturing**

The hardware components for the CCv2 actuator, as stated above, were obtained, as much as possible, from existing material and components available in the Robotics Lab. The mechanical components that I produced were made either using the SLA Rapid Prototyping system that is in the Robotics Lab or were machined from blocks of aluminum using the tools in the Machine Shop.

The four main components that were manufactured for the CCv2 actuator were:

- Fixed Electrode
- Rotating Electrode
- Case
- Encoder Mount

The two electrodes were manufactured using tools in the machine shop while I manufactured the case using rapid prototyping tools.

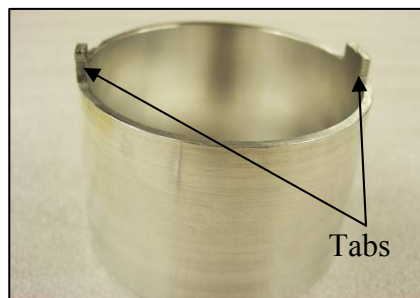
All of the metal forming work was performed in the Northeastern University Mechanical and Industrial Engineering’s Machine Shop under the auspices of the Shop’s

supervisor, Jon Doughty using the various available mills, lathes, and computer controlled machinery. I performed the Rapid Prototyping in the Robotics Lab, under the auspices of Professor Dinos Mavroidis, using a 3D Systems Stereolithography system.

I performed all of the manufacturing tasks, with the assistance of the above mentioned individuals, as well as various individuals within the Robotics and Mechatronics Lab and the Machine Shop.

#### **8.4.1 Fixed Electrode**

As with the first CC actuator, the two electrodes that are used to generate the electric field to activate the ERF are simply cylindrical aluminum forms that are held in a concentric configuration. The fixed electrode, shown in Figure 8-4 is simply a cylindrical shape with two tabs sticking up at the top that will allow it to be attached to the actuator's case allowing it to act as the fixed, unmoving, electrode.



**Figure 8-4:** CCv2 Fixed Electrode

The electrode was manufactured to be approximately 3.02" (3" plus 2 mm, to allow for 1 mm gap between the two electrodes) in diameter with a length of 2". I chose these dimensions to maximize the strength of the actuator given the size of the existing aluminum material that was available within the Lab. The manufacturing process was done mostly with a Computer Controlled Lathe (CNC Lathe), while the tabs were formed using a manually controlled milling machine.

### 8.4.2 Rotating Electrode

I manufactured the Rotating Electrode which is what spins within the viscous fluid to generate resistive forces, with an attached shaft which would stick outside of the actuator and attach to whichever device it is being used for. It can be seen in Figure 8-5.



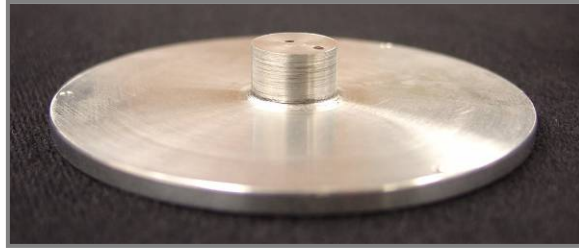
**Figure 8-5:** Rotating electrode, with attached output shaft

The electrode was manufactured from a single piece of aluminum using the CNC Lathe. In addition, the inside of the body of the electrode was hollowed out, to reduce the weight and reduce the amount of uncontrolled inertia that that weight would generate. A lip was created in the bottom of the electrode that will be used in sealing this opening. Figure 8-6 shows the bottom of the electrode and the attachment lip.



**Figure 8-6:** Bottom of electrode with attachment lip

The opening of the electrode was closed using a cover, Figure 8-7, which was permanently attached to the bottom of the electrode using spring pins and adhesive sealant. There would be no significant forces applied to this connection once the actuator was assembled, so this two-part assembly of the rotating electrode would not create the instability seen within the FP actuator due to its multiple component assemblies.



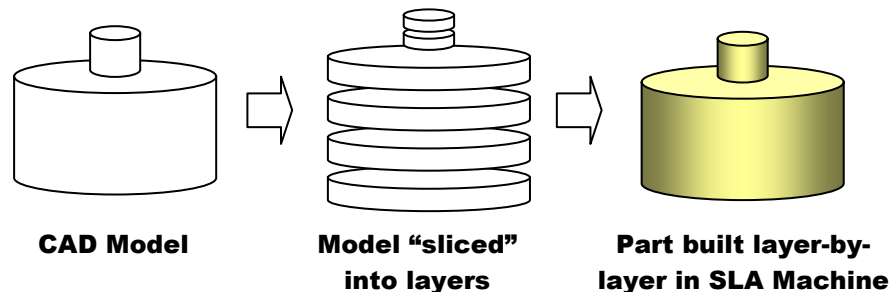
**Figure 8-7:** Cover to close bottom of electrode

The pin protruding from this cover is sized to fit into a ball bearing that attaches to the case in order to guide the rotation of the electrode and hold it in proper alignment.

### 8.4.3 Actuator Case

I manufactured the actuator case using a stereolithography (SLA) process, which creates three dimensional parts from a plastic resin, using a laser to draw out and solidify the parts layer-by-layer. The resolution between the layers is 0.002” or 0.004”, while the resolution within each layer can be even higher than that.

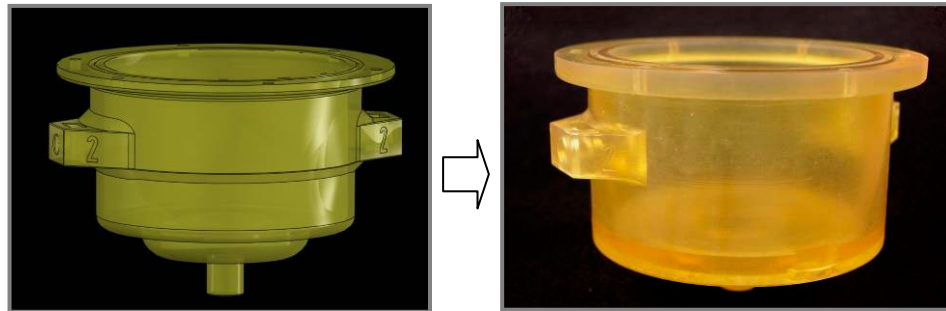
I produced the actuator case by drawing the case with a 3D CAD software such as Solidworks or ProEngineer, then sending the 3D file to a software processor that “sliced” the 3D part into layers and generated the code to guide the SLA system. That instruction set was then sent to the SLA computer which guided the laser to draw the part, one layer at a time, within the photosensitive resin. Figure 8-8 illustrates the process.



**Figure 8-8:** Illustration of SLA Rapid Prototyping process (simplified).

I designed the body of the actuator case within Solidworks, and then built, cleaned and cured, the part using the SLA system. I designed the part with certain

sections thinned out, in order to reduce the amount of material required. Figure 8-9 shows the case in CAD form as well as a (slightly different) produced version.

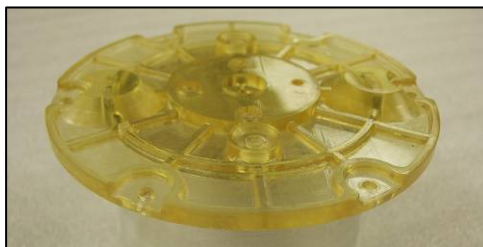


**Figure 8-9:** Body of the case, in CAD and Production Versions

The pin sticking out of the bottom of the case is used to attach, align and guide the actuator when it is assembled into a system such as the Haptic Knob or Joystick. This addresses the modularity issue presented above and allows for this actuator to be used in various different devices.

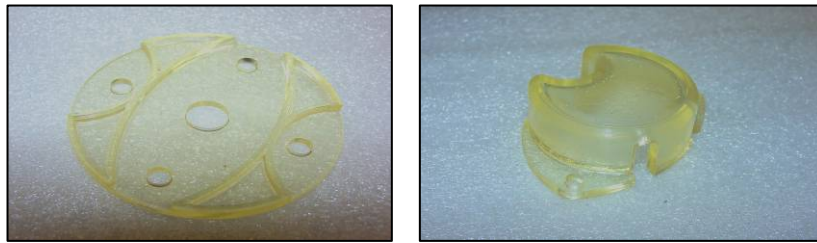
In addition, the square blocks along the side of the case are used to attach and fix the case to the frame of a device, as well as to provide an attachment point for a force sensor, when needed.. The specific assembly of the case to the Haptic Knob and Joystick will be presented in Chapters 9 and 10.

The cover of the case was generated using the same SLA process. In addition various sections of the cover were cutout or thinned in order to reduce the amount of material in use. Figure 8-10 shows this cover.



**Figure 8-10:** Cover of case

Additional components that I generated to complete the actuator case were the Cover's-cover which closes the opening in the central portion of the cover to contain the components mounted there, as well as a shield that mounts over the electrical connection point for the fixed electrode. Both components can be seen in figure 8-11.



**Figure 8-11:** Cover's-cover, and electrode barrier

#### **8.4.4 Encoder Mount**

For some applications, such as the Haptic Knob system, an encoder would be mounted to the case of the actuator, to allow for the sensing of shaft rotation. I manufactured this mount using the SLA process. It was sized to fit over the central portion of the case's cover as well as the electrode barrier. Figure 8-12 shows this encoder mount. A depression in the shape of encoder was created to help align the encoder as well as holes in the mount to allow for the encoder to be attached to the mount with screws.



**Figure 8-12:** Encoder Mount

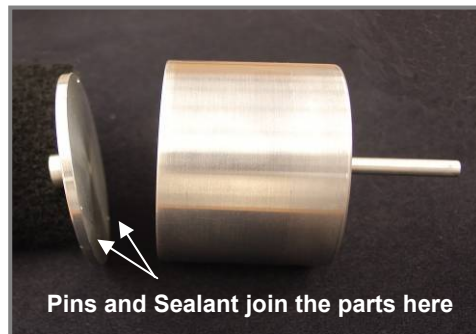
The following section will show how these components were assembled to form the completed CCv2 actuator.

## 8.5 Assembly

The CCv2 actuator was assembled in three stages. First the rotating electrode was assembled, the electrodes were mounted into the actuator case, and then the cover and its additional components were attached to seal the system.

### 8.5.1 Rotating Electrode Assembly

The two components of the rotating electrode are the body of the electrode and the electrode cap. The components are assembled using spring pins pushed through holes in the cap and inserted into corresponding holes in a depression in the bottom of the electrode. Figure 8-13 shows the assembly of the electrode cap to the electrode itself. Aquarium sealant was used to seal the electrode from accumulating the ER Fluid.

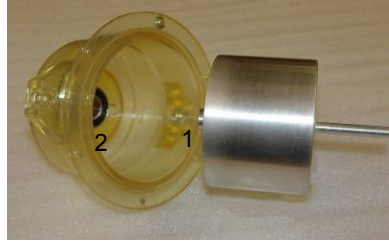


**Figure 8-13:** Assembly of Rotating Electrode Components

### 8.5.2 Electrode Insertion

The two electrodes are then inserted into the case. First a ball bearing is inserted into the bottom of the case. The bearing used is in a double-sealed type, which has a rubber gasket for sealing contaminants out of the components of the bearing in addition to utilizing a solid lubricant which cannot leak out into the ERF and contaminate the system. The pin in the bottom of the rotating electrode is then inserted into that bearing in order to align the bearing in relation to the fixed electrode and provide a smooth platform for the electrode to rotate upon. Figure 8-14 shows these assembly steps.

**Electrode  
Pin (1)  
Inserts  
into  
Bearing (2)**



**Figure 8-14:** Assembly of Rotating Electrode to Case

The Fixed electrode is then inserted with its two tabs facing upward. The case and electrode are sized so that the electrode is held in approximately the correct location to insure that the gap between the two electrodes will be the required 1mm distance. A Threaded Rod is then attached to a hole in the top of one of the pins. This rod will provide the attachment point for the electrical connections to be attached to the electrode. Figure 8-15 shows the attachment of the threaded rod.



**Figure 8-15:** Threaded Attachment Point Assembled to Fixed Electrode

### 8.5.3 Cover and Additional Components

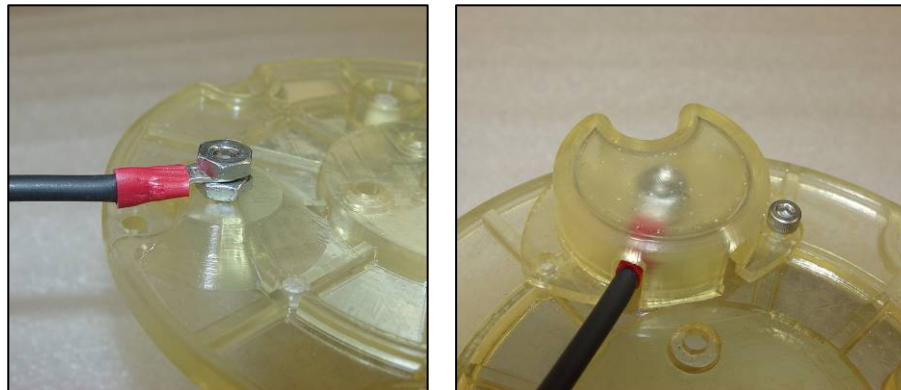
The cover of the case is then attached to system, so that the pins at the top of the fixed electrode attach to locations in the cover. In addition, the threaded rod to be used for electrical contact is aligned through a hole in the cover. Screws are inserted through the underside of the cover to allow for attachment points that later components will connect to. The screws used for this step are self-sealing screws that have a rubber washer attached to the screw head to prevent leakage through these screw openings. Figure 8-16 shows these assembly steps.





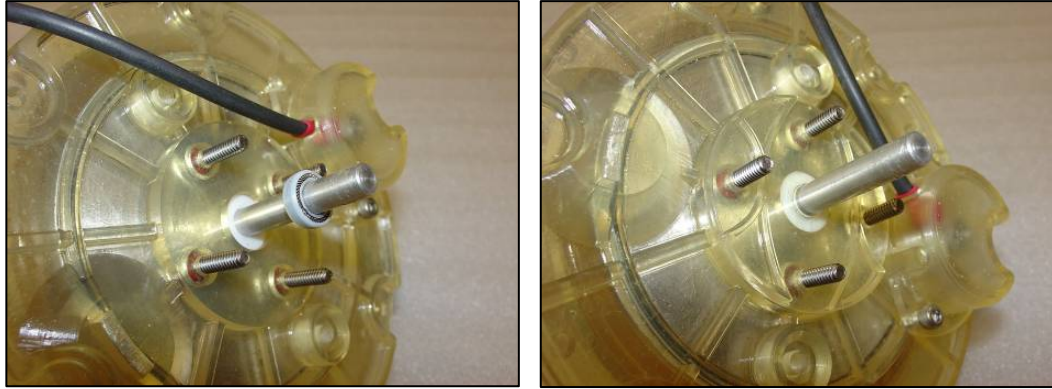
**Figure 8-16:** Cover assembled to Electrode (L) Electrode Inserted into Case (R)

The electrical connection is then made to the threaded rod and the electrode shield is attached to cover it to prevent accidental contact. This step can be seen in Figure 8-17.



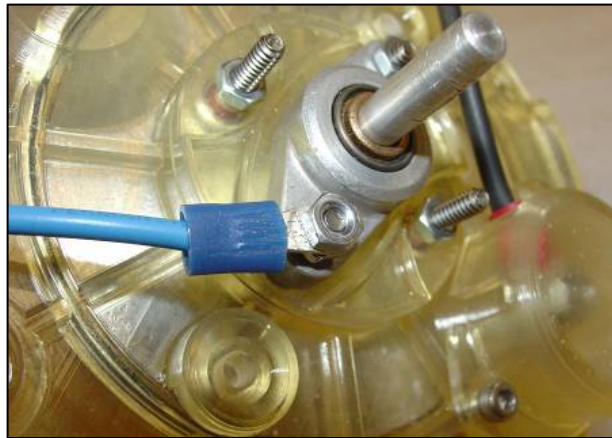
**Figure 8-17:** Electrical Attachment to Electrode (L) and Electrode Shield (R)

A teflon washer is then inserted into the central area of the cover around the output shaft. This washer is sized so that it sits snugly against the shaft, allowing free rotation, but still preventing leakage. In addition a spring seal, which has a teflon case, and a compression spring inside is attached to the shaft and pushed down against the washer. This is loose within the cover, so will not add any friction to the system. It is intended as a second layer of defense to prevent leakage from within the case, in addition to preventing lubricant applied to the shaft from leaking into the ERF and contaminating its properties. In addition, the cover's cover is then assembled to hold these components in place. Figure 8-18 shows the washer and seal, as well as the cover's cover assembly.



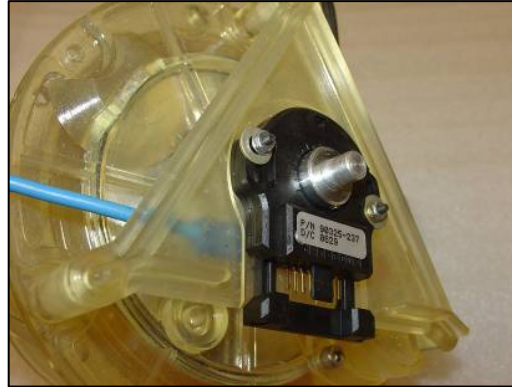
**Figure 8-18:** Teflon Washer and Seal Insertion (L) and Cover's Cover assembly (R).

A mounted sleeve bearing is then attached to the case to provide a guide for the output shaft. In addition, a conductive lubricant is applied to the bearing, so that an electrical connection can be made to the rotating shaft. The connection is made by attaching the electrical wire to one of the screws holding the sleeve bearing in place. That electrical connection goes to the ground terminal on the power supply and will not provide a shock on accidental contact. Figure 8-19 shows these steps.



**Figure 8-19:** Bearing Guides and Provides Electrical Contact for Rotating Electrode

In some applications, the encoder is then mounted to the top of the case. Figure 8-20 shows the mounted encoder

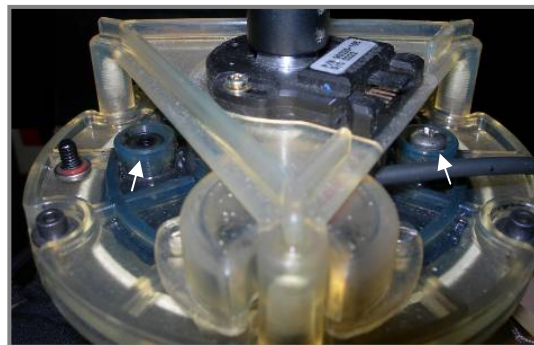


**Figure 8-20:** Encoder Mounted to Case and Shaft

## 8.6 Filling the Actuator

Once the case is assembled, the final step is to fill it with ERF. Two threaded holes were left in the top of the case. This configuration allows for the ERF to be inserted via syringe through one hole while allowing air to escape through the other hole. Once the ERF is added to the actuator it is allowed to settle for a little while to filter down to the bottom of the actuator. The ERF is then topped off to completely fill the system and self-sealing screws are used to close the two filling holes. Figure 8-21 shows the fill holes through which the actuator is filled. The picture shows one hole open and one closed with the self-sealing screw.

**Fill  
hole  
locations  
indicated  
by  
arrows**



**Figure 8-21:** ERF Fill Holes in Cover

Figure 8-22 shows the completed actuator. The connector attached to the output shaft at the top will be used for the haptic system described in later chapter.



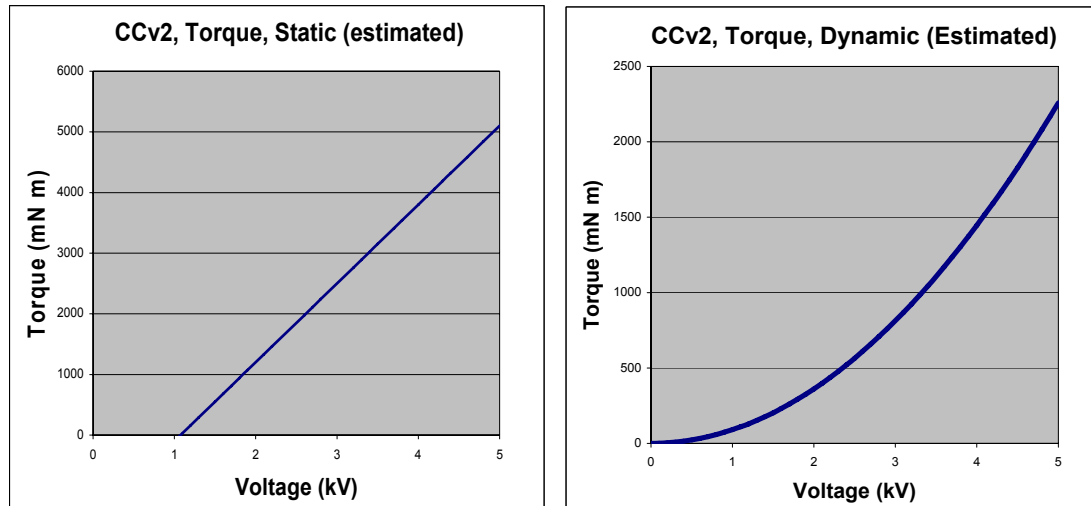
**Figure 8-22:** Completed CCv2 Actuator

### **8.6.1 Replacement ERF**

When the actuators were assembled and it was time to fill them with ERF I determined that the existing supply of LID 3354S was insufficient to fill the two actuators that had been built. It was not possible to obtain any further supplies of 3354S so a replacement ERF was required.

During the course of developing the CC and FP actuators, two different ERF supplies were obtained – the LID 3354S and Bridgestone HP2 ER Fluids. Through informal testing it was determined that both fluids behaved similarly, and the LID 3354S was chosen for use in those the original actuator systems. The HP2, an experimental ERF obtained from a researcher at Bridgestone-Firestone [Bridgestone-Firestone, website], remained unused, and therefore enough of a supply existed to fill the version 2 actuators when it was determined that the LID 3354S supply was insufficient

The following figures show the estimated Torque values for the CCv2 actuator. The data is based on the LID 3354 and 3354s constants, and as such are to be seen as an estimate of the HP2-based actuator's performance.



**Figure 8-23:** Torque Output for CCv2 actuator using the HP2 ERF

## 8.7 Actuator v2 Design Conclusions

My goal in redesigning the actuator was to develop a better, more capable actuator than the version 1 actuators. By relaxing the size restrictions imposed for the earlier actuators the redesign efforts were able to proceed. The following table, Table 8-2, gives the physical characteristics of the CCv2 actuator (without ERF). Table 8-3 compares the estimated torque outputs relative to the version 1 CC and FP actuators.

Parameter	CCv2 Actuator (Body of actuator)	CCv2 Actuator (incl. Centering Pin)	CCv2 Actuator (incl. Pin and Shaft)
Diameter	4.68"	4.68"	4.68"
Height	2.98"	4.08"	~5.1"
Weight (Total Assembly)	1.38 lb.	1.38 lb	1.38 lb

**Table 8-2:** Physical Characteristics of the CCv2 Actuator

Parameter	CCv2 Actuator	CCv1 Actuator	FP Actuator
Static Torque at 2.5 kV (mN m)	1852	130	220
Dynamic Torque at 2.5 kV (mN m)	565	85	135
Percent Increase to the CCv2 level		1425% (Static) 665% (Dynamic)	842% (Static) 419% (Dynamic)

**Table 8-3:** Torque Output (estimates) for CCv2, CCv1 and FP actuators

Comparing the CCv2 to the table of desired actuator characteristics, in Table 1-1, the new actuator has a higher force output than the older versions, but due to the size of the system, it is not as compact or lightweight than those. It has the benefits of incorporating ERF, namely the high energy efficiency and speed. Due to its rotational configuration it also has an infinite displacement. It therefore meets many of the listed criteria and can be a very useful actuator for many applications. The next sections discuss just such an application to the development of new two haptic interfaces.



## 9 HAPTIC KNOB DESIGN AND PROTOTYPE – V2

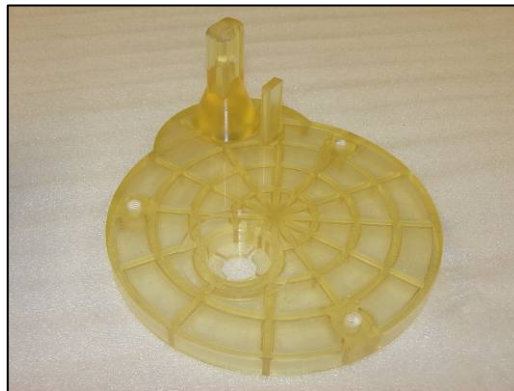
In addition to redesigning the ERF actuator, it was necessary to redesign the two haptic interfaces as well. In keeping with the desire for modularity in the design of the actuator, I designed the Haptic Knob and Haptic Joysticks to use the same interfaces.

### 9.1 Development of Knob Hardware

The second generation Haptic Knob utilizes the larger CCv2 actuator and is therefore more capable of generating forces than the version 1 Knob. While the first generation Knob was developed around the existing test platform, I designed the version 2 system to be freestanding to allow for more flexibility in its application. In addition to updating the physical hardware, I also decided to update the electronics.

#### 9.1.1 Knob Hardware, Mechanical

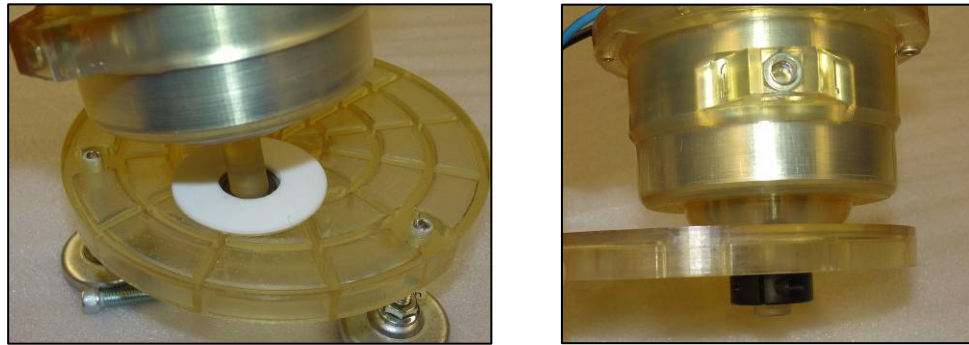
I manufactured most of the mechanical hardware used in this version of the system using an SLA Rapid Prototyping (RP) system. I designed the components in Solidworks and built them on the 3D systems Viper RP machine in the Robotics Lab. As with the RP components in the CCv2 actuator, I thinned, cutout and shaped the components of the knob in order to minimize the amount of material needed. Figure 9-1 shows the base of the knob system into which the CCv2 would be incorporated.



**Figure 9-1:** Haptic Knob Base Prototype

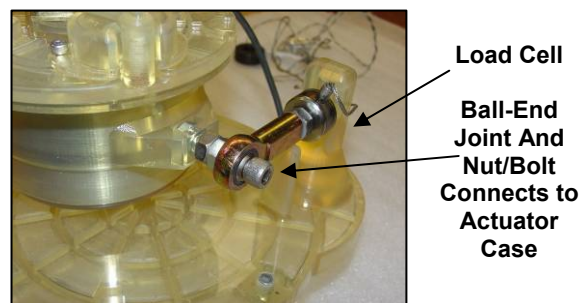
In addition, I added components such as non-skid feet to allow the knob to be freestanding, to allow for testing of the haptic systems in real world applications.

There are two attachment points where the CCv2 is incorporated into the system. First, the pin at the bottom of the CCv2 slots into a bearing at the center of the base. This bearing can be seen in Figure 9-2, where it is covered by a large Teflon washer to allow for smooth rotation of the CCv2 on top of the bearing. The actuator is held in place by a shaft collar attached to the pin sticking through the bottom of the base, also in Figure 9-2.



**Figure 9-2:** Actuator Inserted Into Bearing (L) Shaft Collar Holds Actuator in Place (R)

As stated, many of the components used in the system were taken from previous devices in order to reduce the amount of material that needed to be purchased. To that end, the load cell force sensors that were used in the version 1 joystick were incorporated here as well. The load cell was attached to a ball end joint, and secured to the column sticking up from the base of the device. A bolt was then attached between the block on the side of the actuator case and the ball end joint. These can be seen in Figure 9-3.

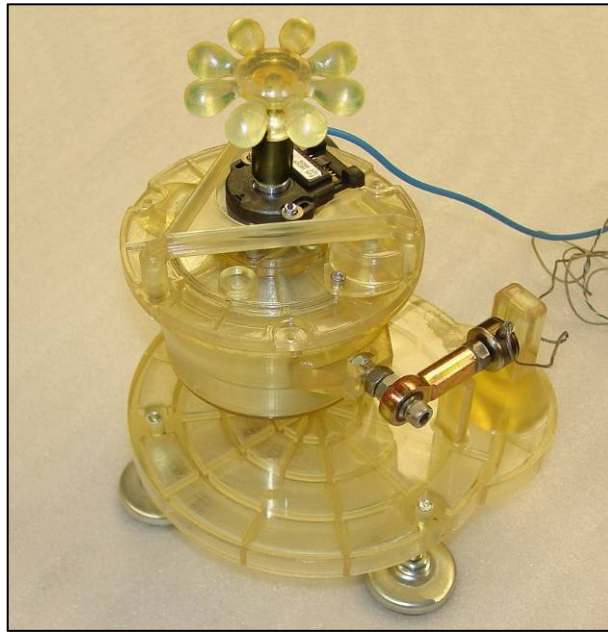


**Figure 9-3:** Load cell and attachment to actuator.



Since this distance is known, then the forces read by the load cell can easily be translated into torque values by multiplying the force by the distance from the center of rotation of the actuator. This configuration holds the actuator in place, and allows for forces generated at the output shaft to be felt by a user rotating an attached knob.

To complete the Haptic Knob device's mechanical components, a knob handle is simply attached to the output shaft at the top of the actuator. Figure 9-4 shows to completed Knob Interface.



**Figure 9-4:** Complete Knob, Version 2

### **9.1.2 Knob Hardware, Electrical**

In addition to the mechanical upgrades introduced, I upgraded the electrical system and computer interfaces as well. The first change was to incorporate a computer Data Acquisition (DAQ) card from National Instruments [National Instruments, website]. I chose a DAQ-Card 6062E card which is rated at a data acquisition rate of 500 kS/s (kilo-samples per second). This DAQ-Card is a PCMCIA device that can be used in a computer laptop's expansion slot, allowing for the prototype system to be more portable

than the previous computer desktop based systems. In addition I used a BNC-2120 terminal block to make connections to the hardware devices.

A circuit was needed to connect the actuator's encoder to the BNC-2120. I built a clock converter circuit to act as a signal conditioner for the encoder, to filter out any unwanted vibrations from sending false signals to the system. Since the device would be used specifically as a possibly unsteady hand-based haptic interface, the filter circuit was necessary. The circuit diagram and datasheets for the clock converter's components are included in the Appendix. Figure 9-5 shows the three I/O system components.



**Figure 9-5:** DAQCard-6062E, BNC-2120 connector block, and Encoder Circuit (L to R)

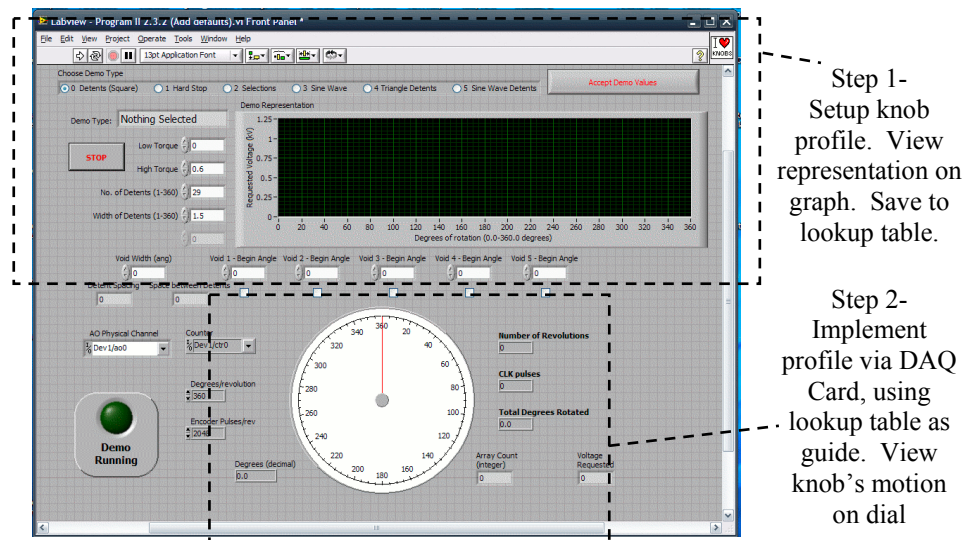
Another change made to the electrical components of the system was the addition of new high voltage power supply. The power supply that was chosen was a High Voltage D.C. Amplifier, the Trek 609C-6 [Trek, website] which converts the command voltage sent from the computer system – 0-5V – into the actuation voltage required by the ERF system – 0-5kV. As described above, the supply voltage is connected to the actuator's fixed electrode while the ground voltage is connected to the rotating electrode.

## 9.2 Development of Haptic Knob Interface System

### 9.2.1 Knob Software Interface

I chose the software development platform Labview, also from National Instruments. Labview is a graphical programming language that uses icons and wires to represent the interconnections of program blocks. I chose Labview for the ease with which it interfaces with the hardware components of the system through its DAQmx driver architecture.

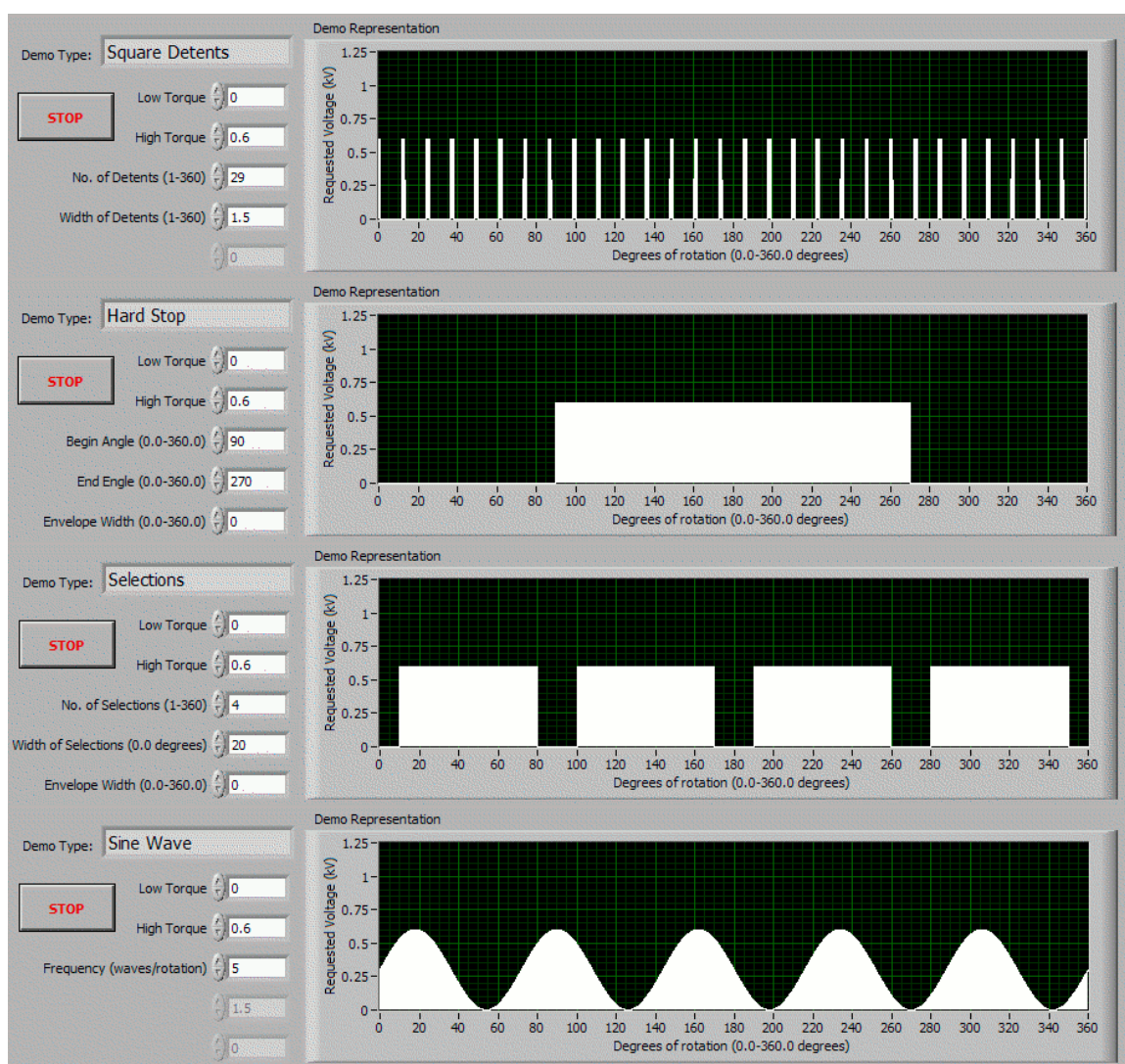
The haptic knob system is designed to present force sensation to the user based on the angular position that the knob has been turned to. The program runs in two distinct blocks in order to setup the software to present force information in this way. Figure 9-6 shows the front panel interface for the software, highlighting the two step process.



**Figure 9-6:** Labview Front Panel

In the first step, the Knob's force vs. rotation profile – in the form of a command voltage for each angular value – is setup and saved into a lookup table. The Knob profile is generated, using 4 different generalized force profiles – Detents, Sine Wave, Selections and Hard Stops. *Detents* presents short “bumps” around the full rotation of the knob.

*Sine Wave* changes forces smoothly across the rotation to represent varying information. *Selections* generates a low level force along the full rotation, except for drop offs in certain locations to represent “clicking into place” at selection points. *Hard Stop* defines a set range of motion and generates a high level of force to prevent rotation past the limits of that range. Figure 9-7 shows representations of the four different generalized profile modes. The white areas represent the force levels generated at the given angle. One full rotation is represented on the linear graph for 0-360°.



**Figure 9-7:** Representation of the Four General Knob Profiles:

Different variables can be changed to modify the four basic force profiles – e.g. defining the number and width of the selection points for the Selections profile. The generated force profile is represented visually on the graph area. (Note: Waviness in the lines in the Detent profile are due to graphical display errors, while in actuality, the forces are presented as a clear step function.) Although the forces are presented based on a reading of the knob's rotation angle, the profile is presented on a linear graph for the sake of clarity. Once the force profile is set up it is accepted by pressing the “Accept Demo” button, and the voltage versus angle array of values, representing the force profile is generated and stored in a lookup table. This array uses a matrix of 3600 elements, allowing for varying forces at a resolution of  $1/10^{\text{th}}$  of a degree of rotation.

In the second step, the DAQ system is activated to control the ERF. The DAQCard reads the angular value of the encoder and generates forces for that angle, by finding the angular value on the lookup table and commanding the corresponding voltage to the power supply. In this way a force-vs.-angle relationship is created. The rotation of the knob is presented on the dial at the bottom center of the front panel in Figure 9-6.

### **9.2.2 Open Loop Control**

I decided to use an open loop control scheme to generate the sensations commanded by the knob profiles. The encoder is read to determine the angular position of the knob and then a command voltage is sent to the ERF actuator to generate the forces. It is assumed, for the open loop scheme, that the forces will be consistent or close to consistent for the same voltage time after time. I determined that this would be acceptable for the purposes of the Knob force profiles to be used in the human factors experiments, to be presented in later chapters. Since the human subjects would need to



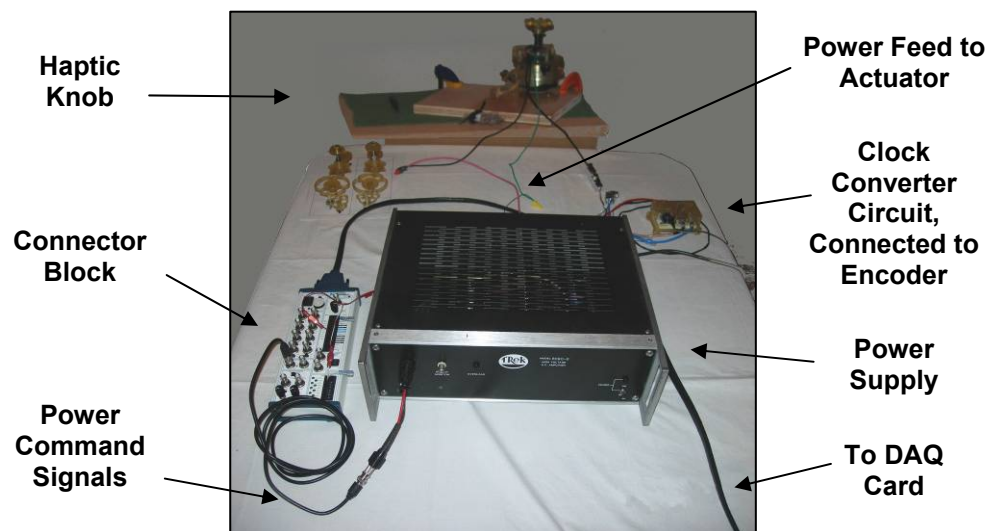
determine whether the force existed or not, exacting precision in the force value would not be necessary.

### 9.2.3 Hardware Interface

The attachment of the Knob hardware to the DAQ system is made through four connection points – the electrical connections and the electronics connections. The electrical connections, as stated above, were made between the Rotating and Fixed electrodes using wire strung between connection points on the actuator and the output terminals on the High Voltage power supply. The Power Supply was commanded by the DAQCard through a connection to the BNC-2120 connector block.

The encoder was connected first to the clock converter circuit and the circuit was connected to the BNC-2120 connector block. The load cell connection is available to be connected, through a digital display/signal conditioner, to the connector block as well.

All of these connections were made through quick-connect type of connectors to allow for ease of assembly and disassembly. Figure 9-8 shows how these connections form the complete Haptic Knob system.



**Figure 9-8:** Connection of Knob to DAQ Interface and Power Supply

### 9.3 Haptic Knob Use

The application for this Haptic Knob is to generate force information to be interpreted by a user holding the Knob handle. Later chapters are devoted to examining this knob interface in an attempt to maximize the information output that is available with this ERF based Haptic Knob system. The goal is to maximize ease of use as well as accuracy of information processing.

### 9.4 Haptic Knob v2 Design Conclusions

The goal for redesigning the Haptic Knob was to incorporate the CCv2 actuator, as well as to develop a system by which the actuator could be used as a modular component for the Knob, the Joystick and other devices. The design and assembly descriptions above have illustrated how those goals have been accomplished. Table 9-1, gives the physical characteristics of the Haptic Knob, version 2. The measurements are approximate, since the machining of the metal components, namely the rotating electrode with output shaft, has produced shafts with varying lengths. In addition, the actual knob handles were not included in the calculation, since the variability of knob shapes allows for an almost infinite number of possible measurements.

Parameter	Haptic Knob (To top of output shaft, where knob would be attached)
Width	6.87"
Depth	6.18"
Height	5.06"
Weight	1.88 lb

**Table 9-1:** Physical Characteristics of the Haptic Knob, version 2

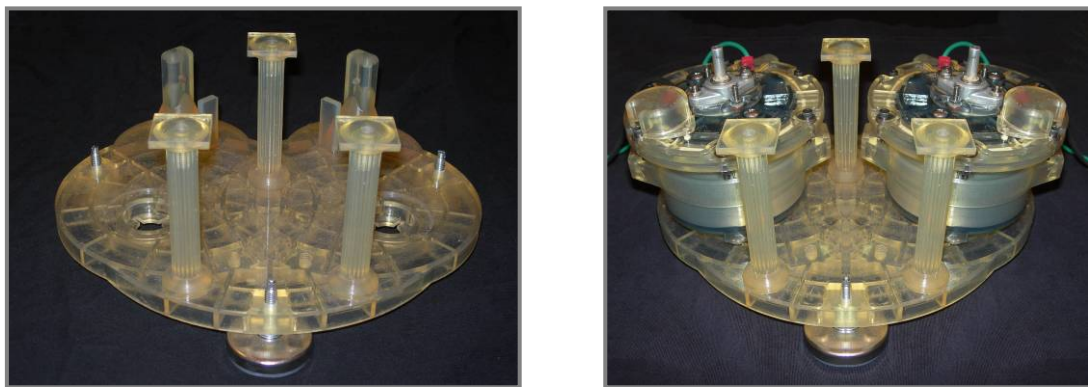
## 10 JOYSTICK DESIGN AND PROTOTYPE – V2

I updated the Haptic Joystick as well to incorporate two CCv2 actuators as the force generating elements. The actuators used were the exact same as those for the Haptic Knob, and as such the explanation of the hardware interfaces will be the same as those described in the previous chapter. The specifics for the Joystick will be presented here. Chapter 7 described the motivation for the development of the first Haptic Joystick, and this version 2 joystick is designed to extend the capabilities of that system.

### 10.1 Joystick Hardware

I built the hardware used in the Joystick system mostly using the Rapid Prototype system in the Robotics Lab. The system was designed with two main assemblies – an actuator housing component and a joystick handle component. These subassemblies are connected in a stacked two-level orientation in order to preserve the vertical orientation of the CCv2 actuators.

I configured the actuator housing assembly similarly to the Knob's base assembly, in that the pins at the bottom of the two actuators fit into bearings in the base of the housing. Figure 10-1 shows this housing component and how the actuators are attached. Non-skid feet provide stability to the platform.



**Figure 10-1:** Joystick Housing Base (L) with Actuators (R)

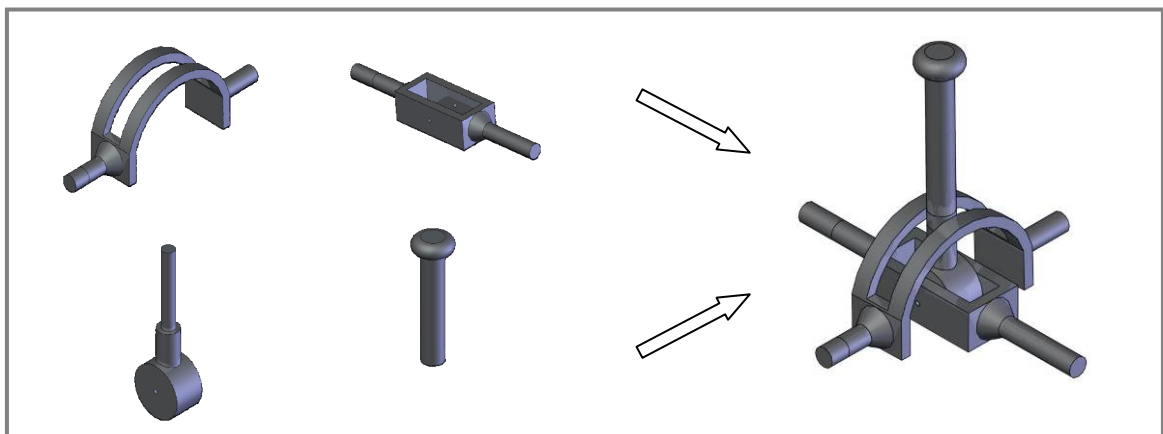


The columns seen in the figure are used to connect this assembly to the upper level assembly. The columns were designed to bear the forces associated with the upper assembly. They were shaped as Grecian columns, taking advantage of the capabilities of the RP system, for aesthetic purposes.

The physical connections, as well as the electrical connections were made in the same manner as the Knob system. However, the encoder was not connected to the output shafts of the actuators as they were added to the upper level assembly instead.

The output shafts of the actuators were inserted through bearings in the upper level assembly which was attached to the support columns to complete the actuator housing subassembly.

The upper level, joystick assembly holds the universal joint that makes up the physical interface of the Haptic Joystick. This joint was built in the Machine Shop using available aluminum material using the manual lathes as well as the manual milling machines. The components that make up this universal joint can be seen in Figure 10-2. The handle at the top of the joint is screwed on as a separate component to allow for changing of the handle for different applications.



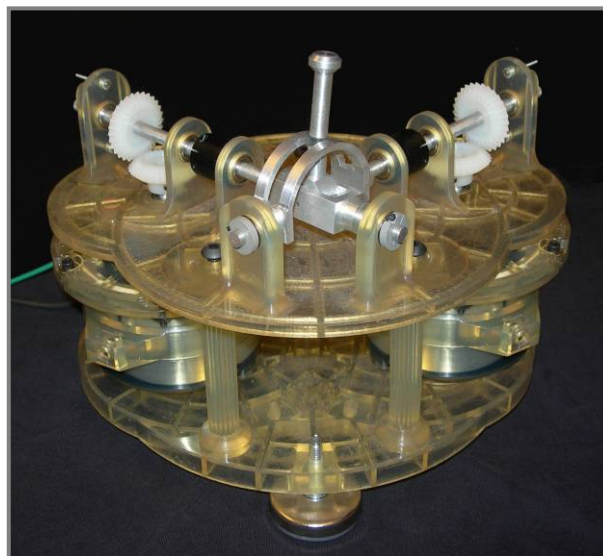
**Figure 10-2:** Universal Joint Components (L) and Assembled Joint (R)

I designed these Joint components to provide rocking motion in both forward-backward motion as well as side-to-side to allow for the two degree of freedom movement of the joystick. Sliding surfaces were incorporated so that the handle components can move smoothly against the arcing component. The output shafts of the joint are each connected to an actuator, via shaft couplers and additional shafts, through a miter gear system to allow the vertical output shaft of the actuators to attach to the horizontal shaft of the joint. Figure 10-3 shows the incorporation of these gears.



**Figure 10-3:** Miter Gear Assembly, Attaches Joint to Actuators

The encoders are connected to the rotating shafts by attaching to the bearing blocks that the shafts slot through. This allows the encoders to directly provide rotation information about the joint's motion. Figure 10-4 shows the assembled Haptic Joystick.



**Figure 10-4:** Haptic Joystick, Version 2

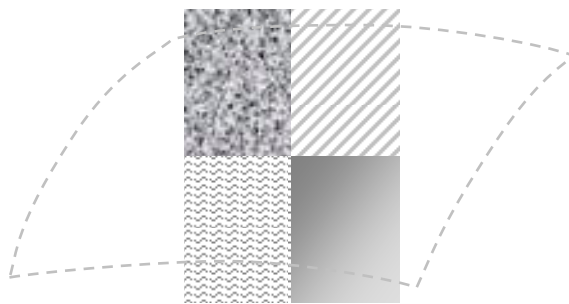
## 10.2 Joystick Software

In order to demonstrate the capabilities of the Haptic Joystick, I wrote software within the LabView programming environment to operate the joystick. The software took elements of the Haptic Knob software and extended them into the two dimensional realm available with the Haptic Joystick. In order to do this, two encoder inputs were required, to read the rotation of the two actuator shafts and their two attached encoders, and two Analog (Voltage) Outputs were required to send voltage to activate the two actuators that make up the force generating elements of the Joystick.

### 10.2.1 Virtual Channels

As discussed previously, the Joystick extends the Haptic Interface capabilities into two dimensions. The addition of the second dimension creates two additional capabilities to send force information to the user – Zones and Virtual Channels.

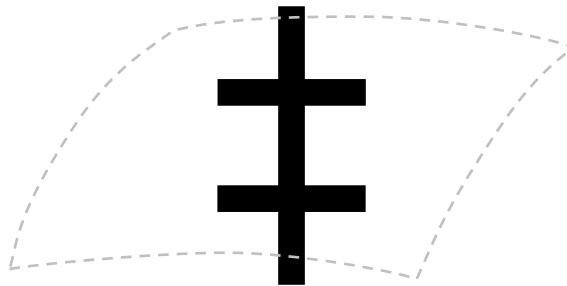
The Zones allow for the generation of different force sensations in specific regions along the surface generated by the motion of the joystick. Figure 10-5 shows one possible representation of these Zones. The different quadrants indicated in the figure represent different types of force information being presented depending on where the user has moved the joystick.



**Figure 10-5:** The Haptic Joystick's Zones

In using the Joystick to present information, the Zones allow the user to select different modes by moving the joystick into the appropriate Zone. Different force profiles representing different types of information are then activated within those Zones.

The software developed for the Haptic Joystick demonstrated the other two dimensional capability – Virtual Channels. Virtual Channels represent specific pathways that the joystick can be moved through, similar to the pathways found in a car's shift lever. However, since these channels are generated through a software interface they can be reconfigured on-the-fly, they can be changed to represent different and more useful information as needed.

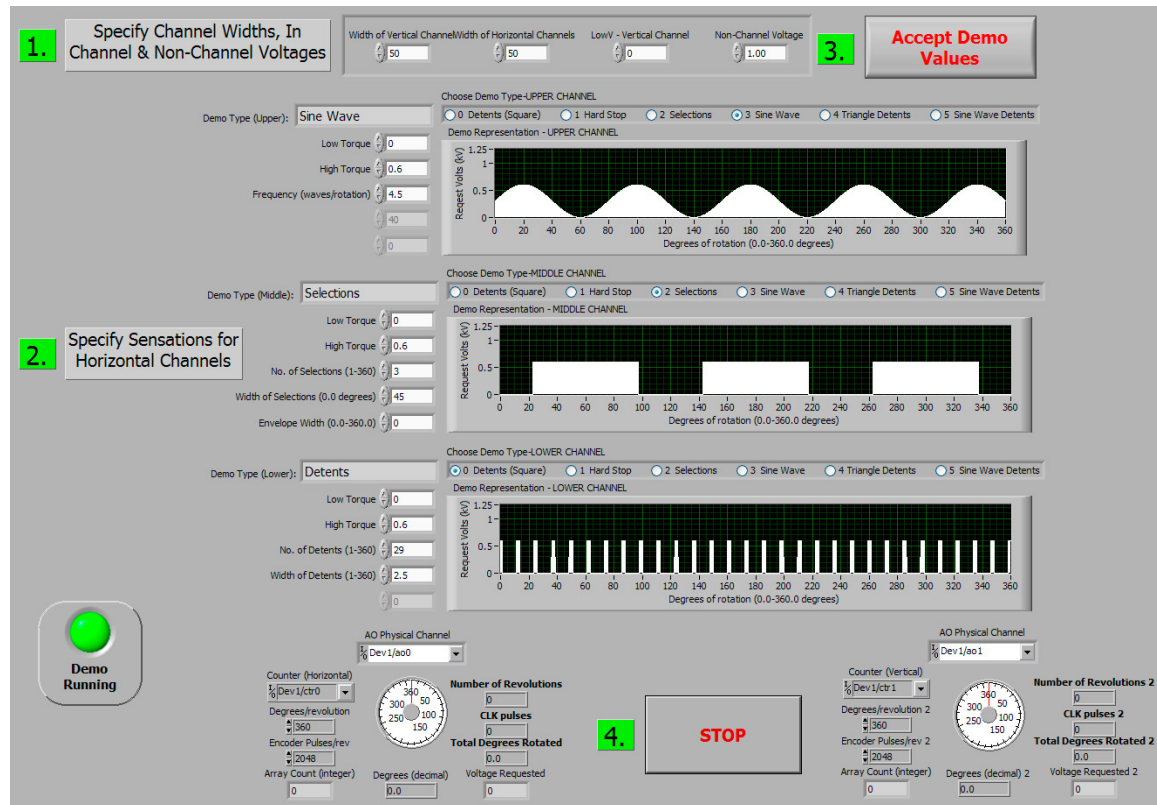


**Figure 10-6:** The Haptic Joystick's Virtual Channels.

Figure 10-6 illustrates the concept of the Virtual Channels. The black bars indicate locations in which the joystick can move, while the white indicates high force that prevents motion in those locations. The Virtual Channels allow for the selection of different modes by moving the Joystick vertically up the center channel, to the appropriate horizontal channel to choose the desired mode. Once within the horizontal channel, different force profiles, similar to the profiles used for the Haptic Knob, can present different types of information.

In order to simplify the development of the Joystick software, I limited the selections to three horizontal channels and a single vertical channel connecting them.

The horizontal channels are configured using similar force profiles to those developed for the Haptic Knob. Figure 10-7 shows the Front Panel developed to interface with the Joystick software. The full Block Diagram program is included in the appendix.



**Figure 10-7: Front Panel Interface to Joystick Program**

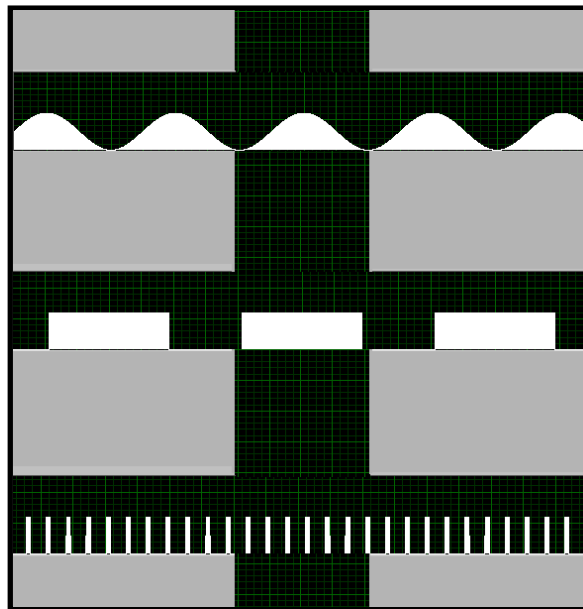
In order to clarify the operation of the program, I attached numbered labels to show the steps to take to generate force profiles. Those steps are:

Step 1	Specify the Angular Widths of the Vertical and Horizontal Channels, Specify the Low Voltage for within the Channels and the High Voltage for outside the channels in the “solid” areas.
Step 2	Individually specify the Force profiles for the three horizontal Channels
Step 3	Once satisfied, accept the demo to initiate the encoders and power supply to activate and control the actuators.
Step 4	When demo is complete, shut down the power supply and software with the Stop button.

**Table 10-1: Steps to Run the Haptic Joystick Software**

The dials at the bottom of the Front Panel track the rotation of the optical encoders. Additional status information about rotation angles and voltage levels is presented in the text boxes as well.

The Virtual Channels generated by the settings in the above Front Panel can be seen below in Figure 10-8. (Note: the angular widths of the channels in the picture are not to scale.) The black pathways indicate locations where the joystick can move, while the white shapes indicate the force levels generated within the Virtual Channels, based on side to side motion, to present information to the user. The grey locations indicate high force levels that represent locations where the Joystick cannot travel.



**Figure 10-8:** Virtual Channels with In-Channel Force Profiles:  
Varying Force Profile(*Top*) Selections(*Middle*) Detents (*Bottom*)

I developed the software that generates the Virtual Channels for the Haptic Joystick to demonstrate the capabilities of the Joystick system. Future versions of the software may allow for the user to select the number of channels to generate as well as defining the force profiles to be generated within those channels.

### 10.3 Haptic Joystick v2 Design Conclusions

The goal for redesigning the Haptic Joystick was to continue incorporating the CCv2 actuator as a modular component into the developed haptic interface systems. The design and assembly descriptions above have illustrated how those goals have been accomplished. Table 10-2, gives the physical characteristics of the Haptic Joystick, version 2. The measurements are given from the extreme top of the joystick's handle to the bottom of the actuators' centering pins. Since the handle that is grasped at the top of the joystick can be of varying designs, as well as there being varying mounting options for either stabilizing feet or other mounting surfaces, these measurements should be considered approximate. Again, the weight of the ERF has not been included.

Parameter	Haptic Joystick
Width	9.84"
Depth	9.12"
Height	8.96"
Weight	4.74 lb

**Table 10-2:** Physical Characteristics of the Haptic Joystick, version 2

## 11 HUMAN INTERFACE CONSIDERATIONS IN HAPTIC KNOB DESIGN

The goal of designing the Haptic Knob and Haptic Joystick was to develop an interface that can present information, in a meaningful manner, to a user through interacting with his or her sense of touch. The main goals in designing that type of interface were twofold:

1	Maximize the force capabilities and resolution of the actuation system
2	Maximize the understandability of that information by the human operator

**Table 11-1:** Main Objectives for Haptic Interface Design

The first objective in Table 11-1, to develop a hardware system that can present force information in a controlled and tunable fashion, has been addressed in the previous chapters in discussing the development and testing of the ERF actuators and the Haptic interfaces. The second objective, to maximize the understandability of those forces, had to be addressed in the confines of the hardware system that has been developed.

Since the Haptic Knob and Joystick have been developed around ERF-based actuators, there are a few challenges that must be addressed. The ERF actuators, as stated earlier, are inherently a passive actuation system in that the ERF effect can provide resistive forces but cannot provide active forces. Therefore, the force profiles that can be generated must take into account that limitation and seek to generate force cues that make full use of the ERF effect. The ERF effect does provide opportunities for force sensations that are not available with other actuation technologies – such as the feeling of viscosity or fluid type sensations – that can also be incorporated into the force profiles for



the haptic interfaces. This addresses the force generation challenge inherent with a passive actuation system.

In addition, the passive actuation creates a challenge to maximize the quality of the force cues that are *understood* by the user who is receiving them. The following chapters seek to examine the human factors inherent in the haptic interface system in order to attempt to leverage the capabilities of the human sensory system to maximize the user's comprehension of the force cues being provided.

My focus for the human factor testing has been the Haptic Knob. This allows for an examination of the hand-device interface. I believe that the conclusions drawn about the human factors issues inherent in the Knob system will also be applicable to maximizing the understandability of the Joystick system. To this end, the first step was to examine the hand-knob interface. Much research has been done in the field of Ergonomics to examine this interface, and as such provides a starting point in the search to maximize that interface in the context of the Haptic Knob system.

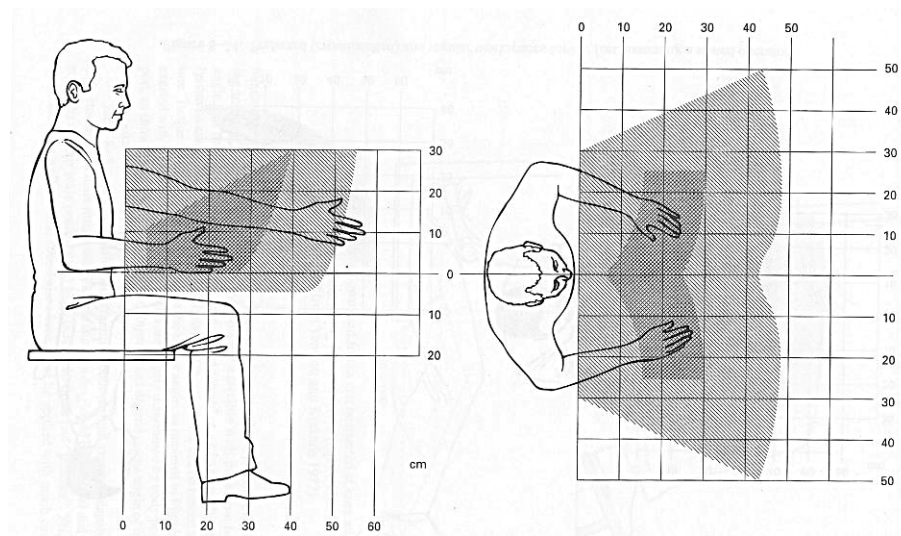
## 11.1 Ergonomics – Background

Ergonomics is defined by the Merriam-Webster online dictionary as:

*... an applied science concerned with designing and arranging things people use so that the people and things interact most efficiently and safely—called also biotechnology, human engineering, human factors*

Ergonomics seeks to maximize the comfort and efficiency of the interface between humans and technology and other objects. This science has been applied to many areas, for example, the design of automobile dashboards has been greatly influenced by ergonomic considerations and has benefited from the more effective placement of controls and displays in modern automobiles. Another example of the

application of ergonomics theory is in the placement of keyboards and computer displays in the modern office environment. Factors such as the comfortable range of motion of the human hand have been instrumental in changing the shape of desks, keyboards and displays in order to minimize the discomfort of using those technologies and minimizing injuries such as carpal-tunnel syndrome that can result from improper use of these devices. Figure 11-1 shows an example of how the workspace of a person is defined by ergonomic considerations to minimize injury and maximize efficiency of the task.


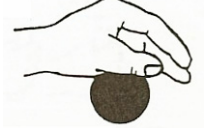


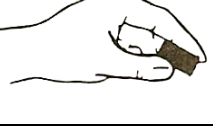
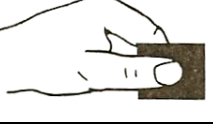


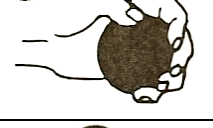



**Figure 11-1:** Ergonomically Defined Preferred (crosshatched) and Regular Manipulation Space for the Hands of a Seated Human [Kroemer, 2003a]

## 11.2 Ergonomics – Knob Interface concepts

While the science of ergonomics covers a vast array of human-device interactions, the interaction that is of most concern for the development of haptic interfaces is that between the human hand and a handle or knob interface.

Ergonomics suggests that the manner in which a user grasps a handle affects the quality of control that can be exerted by the user over that interface. Table 11-2 shows the ergonomic classifications of a hand interfacing with various styles of handles.

Coupling #1	<u>Digit Touch</u> One digit touches an object	
Coupling #2	<u>Palm Touch</u> Some part of the palm (or hand) touches the object.	
Coupling #3	<u>Finger Palmar Grip (Hook Grip)</u> One finger or several fingers hook(s) onto a ridge, or handle. This type of finger action is used where thumb counterforce is not needed.	
Coupling #4	<u>Thumb-Fingertip Grip (Tip Pinch)</u> The thumb tip opposes one fingertip.	
Coupling #5	<u>Thumb-Finger Palmer Grip (Pad Pinch, or Plier Grip)</u> Thumb pad opposes the palmar pad of one finger (or the pads of several fingers) near the tips. This grip evolves easily from coupling #4.	
Coupling #6	<u>Thumb-Forefinger Side Grip (Lateral Grip, or Side Pinch)</u> Thumb opposes the (radial) side of the forefinger.	
Coupling #7	<u>Thumb-Two Finger Grip (Writing Grip)</u> Thumb and two fingers (often forefinger and middle finger) oppose each other at or near the tips.	
Coupling #8	<u>Thumb-Fingertips Enclosure (Disk Grip)</u> Thumb pad and the pads of 3 or 4 fingers oppose each other near the tips (object grasped does not touch the palm). This grip evolves easily from coupling #7.	
Coupling #9	<u>Finger-Palm Enclosure (Collet Enclosure)</u> Most, or all, of the inner surface of the hand is in contact with the object while enclosing it. This enclosure evolves easily from coupling #8.	
Coupling #10	<u>Power Grasp</u> The total inner hand surface is grasping the (often cylindrical) handle which runs parallel to the knuckles and generally protrudes on one or both sides from the hand. This grasp evolves easily from coupling #9.	

**Table 11-2:** Couplings Between Hand and Handle. [Kroemer, 2003b]

Ergonomics looks at the comfort and efficacy of a human's manipulation of knobs and similar handles, however, to explore the interactions with haptic devices the

examination must go further in looking at how the device interacts with the human side of that equation. For the Haptic Knob it is therefore necessary to examine whether the choice of grip type will affect how well the knob relays force information to the user. Of the 10 couplings in Table 11-2, there are some that describe the type of grasp used while manipulating common type of knobs. Specifically couplings 5,6,7,8, and 9 can be seen as having real-world use in grasping a knob type of interface.

In addition, ergonomics suggests that the texture of an object's surface also plays a role in the quality of the human-object interface. In describing the considerations for developing a knob type of interface, Kroemer [Kroemer, 2003c] suggests that

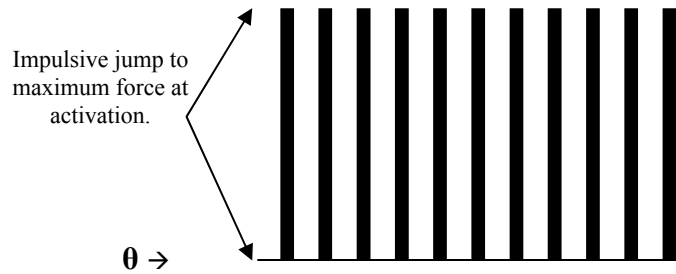
... one may want to put a slight cavity into the surface of a pushbutton so that the fingertip does not slide off, to hollow out the handle of a scalpel slightly so that the fingertips can hold on securely, and to roughen the surface of a dentist's tool and not make it round in cross section ... design details that facilitate holding onto the tool, moving it accurately and generating force or torque play important roles ...

Although the consideration of handle's texture is, again, in relation to the efficacy of the human's control of an object, it suggests the necessity to examine whether the texture of the Knob's handle will also affect the efficacy of the force feedback interface.

### **11.3 Force Profile Considerations**

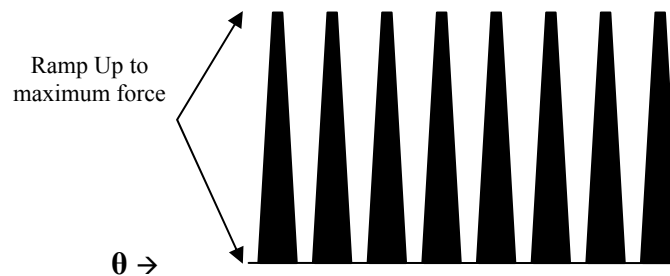
Another pathway that may reveal ways to increase the effectiveness of the Haptic Knob interface is to examine the quality of the forces being presented to the user. My initial tests with the version 1 Haptic Knob and Joystick presented force information to the user in terms of impulsive forces, as presented in Chapter 7. The user would turn the knob to a specific angle, and a force would be impulsively generated at that angle. When presenting a detent type of interface – short bumps throughout the full rotation of the

knob – this force profile suggested a square wave formation, such that the maximum force would be generated when the knob was rotated to the activation angle and would be minimum at all other points.. Figure 11-2 shows this type of detent style, in the form of a graph of the force profile.



**Figure 11-2:** Impulsive Square Wave Detent Style.

Although an effective method to present “bumps”, I considered whether “shaping” the force profile would present information in a better, more understandable format. Figure 11-3 suggests a trapezoidal profile, in which the force ramps up to the maximum amount and then ramps back down. I hypothesized that this may be less jarring to the senses and may in fact be more easily understood.



**Figure 11-3:** Forces Ramp Up and Down for a Shaped Detent Style

## 11.4 Human Factors Testing Motivation

In order to explore the suggested designs for maximizing the Haptic Knob’s efficacy, it was necessary to perform experiments that would clarify the effects of these designs on the usefulness of the haptic interface. Since these tests would need to explore the usefulness of the Haptic Knob for a human operator, the class of experiments that

need to be performed are referred to as *Human Factors* experiments. Human Factors are strongly related to Ergonomic considerations in that they explore the human component of a system, they are defined as:

... that field which is involved in conducting research regarding human psychological, social, physical, and biological characteristics, maintaining the information obtained from that research, and working to apply that information with respect to the design, operation, or use of products or systems for optimizing human performance, health, safety, and/or habitability. [Stramler, 1993]

This varies subtly from ergonomics which focuses on the physical aspects of the human-machine interaction, while human factors focuses more on the mental and perceptual aspects. Although in practice the terms often get used interchangeably.

In order to perform human factors testing, a statistically significant sample of test subjects needed be found and the variations to the design needed be developed in order to present them to the test subjects. The following chapters will present the experimental setup as well as the results obtained from the testing.

### 11.4.1 Design Factors Being Tested

The three design factors that were chosen to be tested using human trials were:

1	Knob Shape
2	Knob Texture
3	Force profile shaping

**Table 11-3:** Factors to be Tested in Human Trials

My goal was that by examining these human factors issues, I would obtain a better understanding of the human sensory capabilities when interacting with the Haptic Knob system which could lead to the development of more effective, accurate and useful haptic interfaces.





## 12 HUMAN FACTORS IN THE HAPTIC KNOB SYSTEM

In an effort to maximize the potential of the ERF based Haptic Knob and by extension, other similar haptic interfaces, I determined that the human-machine interface must be examined from the human side. I chose three design factors that affect the human experience when using the Knob to undergo Human Factors testing: Knob Shape, Knob Texture and Force Profile Shaping.

The variations that I chose to explore within the knob shape and knob texture factor will be presented. In addition, I determined that the force profile shaping should focus on a simple, yet information rich force profile for the purposes of the experiment. Thusly, I decided to focus on the Detent profile, and therefore the third factor under examination will be referred to as Detent Style. How the force profile of the detent style which was varied will also be discussed.

### 12.1 Knob Shape Factor

The first factor to be examined was the knob shape. As explained previously, various grasp types lend themselves to the use of a knob type of interface. Those that I chose to examine were taken from Table 11-2 and are:

Coupling #6	<u>Thumb-Forefinger Side Grip (Lateral Grip, or Side Pinch)</u> Thumb opposes the (radial) side of the forefinger.	
Coupling #7	<u>Thumb-Two Finger Grip (Writing Grip)</u> Thumb and two fingers (often forefinger and middle finger) oppose each other at or near the tips.	
Coupling #8	<u>Thumb-Fingertips Enclosure (Disk Grip)</u> Thumb pad and the pads of 3 or 4 fingers oppose each other near the tips (object grasped doesn't touch the palm).	
Coupling #9	<u>Finger-Palm Enclosure (Collet Enclosure)</u> Most, or all, of the inner surface of the hand is in contact with the object while enclosing it.	

**Table 12-1:** Hand-Knob Couplings to be Tested [Kroemer, 2003b]

In addition to the existing grasp types, I also examined an additional coupling referred to as an Enclosed Disk Grip (modified from Coupling #8). That coupling was similar to the described coupling, but added an additional structure to the knob, that would separate the fingers in a specific manner. Figure 12-1 shows a drawing of the knob that accommodated the enclosed disk grip.



**Figure 12-1:** Enclosed Disk Grip Concept

The goal in examining the knob shape was to explore not just the shape of the person's grasp but also the resulting motion of the hand that is created by that grasp. The question to be answered was whether the hand's position and motion affects a person's ability to understand the force cues being provided by the Haptic Knob device.

### **12.1.1 Knob Shape Designs and Hand Motion**

The Knobs were numbered 1 - 4 in order to more clearly identify them during experimental procedures. The numbers were chosen in no particular order, and the knobs are presented here in that order.

The specific knob shapes were developed, often by trial-and-error experimentation, in order to guide the users into the desired grasp types and hand/arm motions. The specific grasps and motions elicited will be described below.

All of the knobs used in these experiments were built using the Rapid Prototyping system, allowing for the development of knobs that would conform to the required specifications. All of the knobs were developed from the same basic form, and as such the following information will be applicable to every knob used.



I designed the knobs were to fasten to the output shaft of the Haptic Knob system through 3 set screws spaced evenly around the base of the knob. Figure 12-2 shows the base of the knob as well as how it attaches to the Haptic Knob device. The output shaft was extended with a shaft coupler and shaft segment that had been ground down to accommodate the 3 set screws.



**Figure 12-2:** Extended Shaft with Flattened Edges (L) Attachment to Knob Base (R)

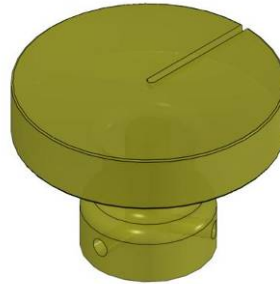
Since the knobs were built from plastic using the Rapid Prototyping system, and were attached to the output shaft which was grounded as part of the electrical circuit that forms the electrical field, the user was safely isolated from the electrical system.

In order to focus on the knob's shape as a factor in determining the effectiveness of the system, I took care to ensure that the knobs were shaped in such a way that the torque felt by the user would remain the same across all of the knob designs. To that end, the grasping point for the knob shapes were always at  $\frac{3}{4}$  inches from the center of the knob's rotation, thus the diameter of the grasping surface (not necessarily the full structure of the knob, as will be seen) was  $1\frac{1}{2}$  inches across.

### *1. Disk Knob, Finger Motion*

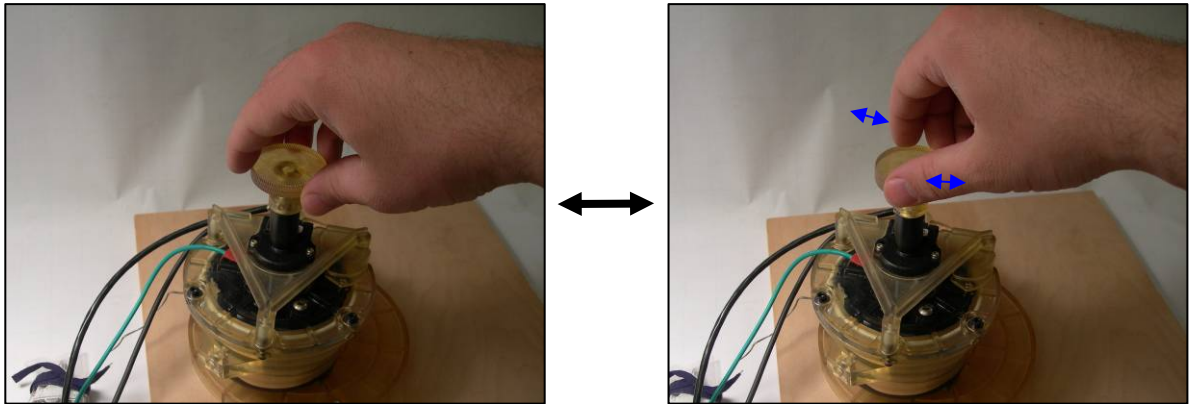
I formed the Disk Knob by adding a disk shaped component above the knob base. The simple disk design would allow for a familiar interface and a short or non-existent

learning curve for new users. Figure 12-3 shows the structure of the Disk Knob. The line etched into the top surface of the knob indicates a direction to allow the user to better gauge of the rotation of the knob.



**Figure 12-3: Disk Knob**

The Disk Knob can be grasped using either Coupling #6 – Lateral Grip – or Coupling #8 – Disk Grip. Either grasp will guide the user to rotate the knob using their fingertips and fingers. Figure 12-4 shows the expected grasp type and illustrates the anticipated motion inherent to that grip.

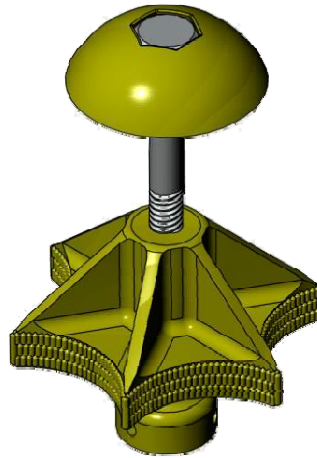


**Figure 12-4: Grasping the Disk Knob and Resulting Hand Motion**

## *2. Ball Grip Knob- Wrist Motion*

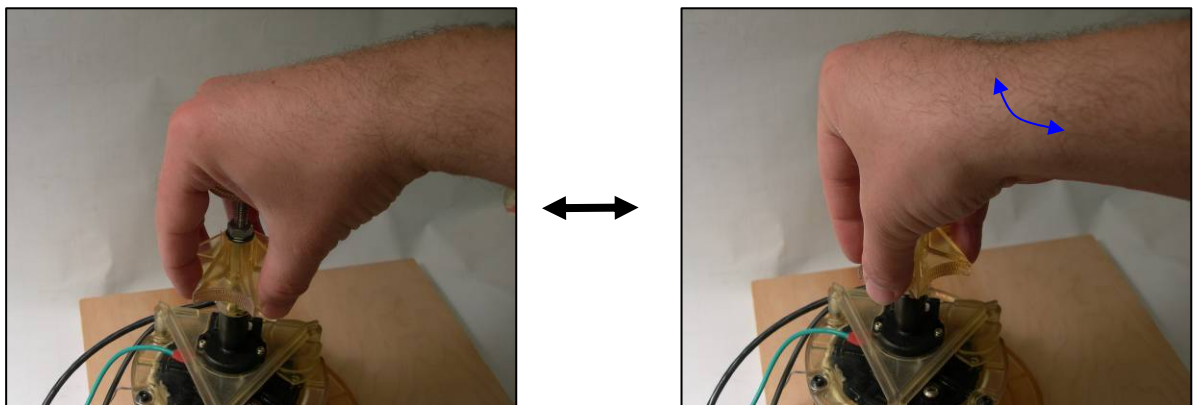
The Ball-Grip Knob employs the grasp coupling #9, in which the fingers and the surface of the palm are both in contact with the grasped object. In ergonomic term this

allows for a strong grasp on the object and a comfortable manner in which to manipulate that object with higher levels of force. Figure 12-5 shows the Ball-Grip knob.



**Figure 12-5:** Ball Grip Knob

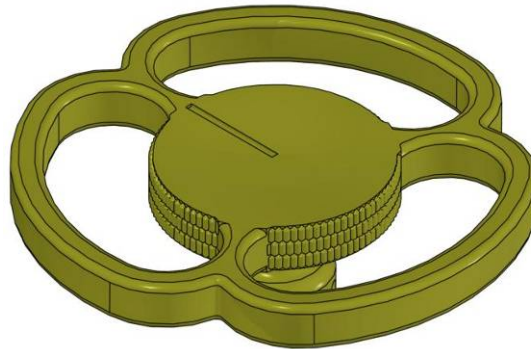
I designed the knob in two sections connected by a threaded bolt in order to allow it to be resized for different sized hands. While this configuration does not allow the knob's surface to contact the full surface of the palm, it does cause the hand to assume the correct position for a Ball Grip. This type of grip will tend to cause the user to use wrist motion to turn the knob's handle. Experimentation would determine whether this was an advantageous motion when receiving force cues from the Haptic Knob. Figure 12-6 shows the expected grip and motion of the hand for the Ball Grip Knob.



**Figure 12-6:** Grasping the Ball Knob and Resulting Wrist Motion

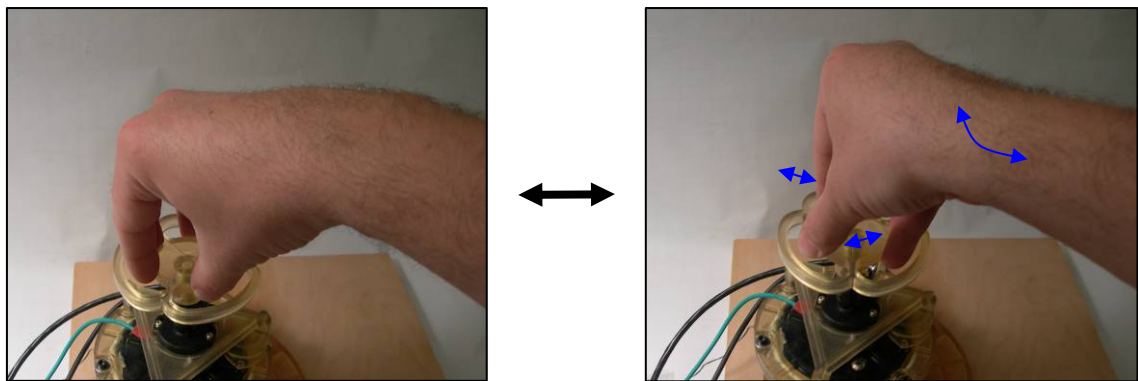
### 3. Enclosed Disk Knob, Finger/Wrist Motion

The Enclosed Disk Knob is an extension of the Disk Knob shown above. The Enclosed version of the knob adds an outer ring to the Disk in order to enclose the fingers that are gripping the disk. Figure 12-7 shows the knob.



**Figure 12-7:** Enclosed Disk Knob

The addition of the outer ring encloses the fingers that grasp the knob and, due to the supporting structure between the disk and the ring, creates three pockets around the disk into which the grasping fingers are separated. This separation and enclosure of the fingers transforms the disk knob that operated with finger motion into the enclosed disk knob that tends to operate with a combined finger and wrist motion. Again, the efficacy of this configuration was studied during the course of the Human Factors tests. Figure 12-8 shows the expected grip and hand motion associated with this knob.



**Figure 12-8:** Grasping the Enclosed Disk Knob and Resulting Finger/Wrist Motion

#### 4. Hand Wheel Knob, Arm Motion

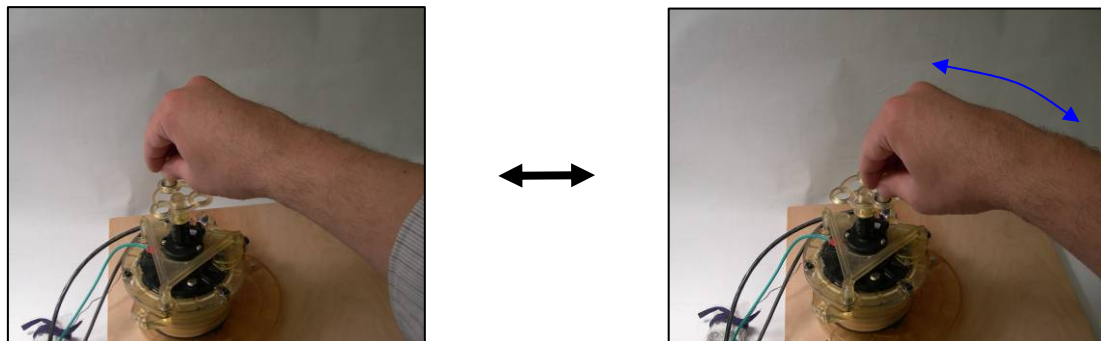
The Hand Wheel Knob differs from the previous knobs in that the grasping surface is offset from the rotating surface of the knob. Like a traditional hand wheel the knob has a central wheel with an extended, rotating, handle that is grasped in order to turn the knob. The hand wheel configuration allows for fast rotation and is used in many applications where quick opening and closing of valves is required. The handle is grasped most comfortably with coupling #7. Figure 12-9 shows the Hand Wheel Knob.



**Figure 12-9:** Hand Wheel Knob

The extended handle is attached with a bearing to allow free rotation within the wheel – and is located at the same radial distance as the previous knobs so that the torque felt while grasping the handle will be the same.

This knob configuration and grasp type require arm motion with almost no finger or wrist motion at all. Figure 12-10 shows the expected grip and motion for this knob.



**Figure 12-10:** Grasping the Hand Wheel Knob and Resulting Arm Motion

## 12.2 Knob Texture Factor

The second factor to be examined with the Human Factors experiments was the Knob Texture. This sought to explore whether the texture of the knob's handle would have an effect on the understandability of the force cues being provided. I chose two basic textures, in order to focus the analysis – smooth and knurled.

I made each of the four knob shapes presented above with both textures, resulting in a total of eight knobs that were built using the Rapid Prototyping system. The knobs were numbered 1 to 4 for the knurled versions and 5 to 8 for the smooth versions.

### *1. Smooth Texture*

The smooth texture was obtained by building each knob with smooth surfaces. Figure 12-11 shows the four knob shapes as built by the Rapid Prototype system.



**Figure 12-11:** Knobs 5 to 8, Knob Shapes with Smooth Texture

Since the knob surfaces are simple, the haptic forces generated may be presented more “cleanly” to the user, allowing for more understandability of the force cues.

### *2. Knurled Texture*

Knurls are a series of ridges or bumps on a surface that aids in gripping. Knurls are commonly seen in small metal tools such as medical, dental and other precision tools



where a firm grip is required to hold a tool steady. Figure 12-12 is an image taken from the McMaster-Carr catalogue [McMaster-Carr website] that shows a knurled surface for one of their knob products.



**Figure 12-12:** Example of a Knurled Surface to Increase Grip

The application of knurls to the haptic interface sought to explore whether the form that the knurls take – short ridges or bumps – can aid in the understanding of the haptic cues that are presented. Unlike the smooth texture, the knurls have numerous contact points that are made when the user grasps the knurled surface. This increase in distinct contact points might help increase the sensitivity of the sensing system in the finger. Figure 12-13 shows the four knobs as they were built with knurled surfaces.



**Figure 12-13:** Knobs 5 to 8, Knob Shapes with Knurled Texture

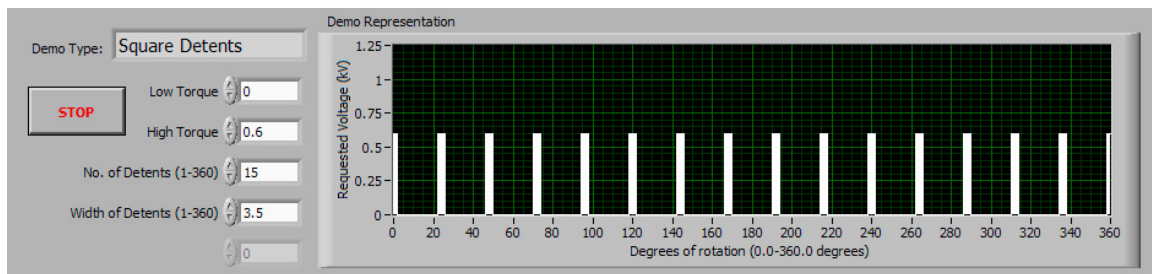
### 12.3 Force Profile Shaping Factor

The third factor to be examined was the Force Profile Shaping factor. The power supply and DAQ cards employed for the version 2 haptic interfaces operate at a sufficient

speed to allow for the varying of force information quickly enough to change the profile of the generated forces. Initially the haptic sensations were generated as an impulsive force that outputs the highest force level in one step. The faster systems allows for a more shaped force which can ramp up to the highest force in a gentler fashion. I postulated that by changing the quality of the force cues it might also increase the understandability of the haptic information being provided.

The force profile that I used for the human factor experiments was the detent profile. Detents are short bumps presented around the rotation of the knob. They are seen often on volume knobs for radios and provide haptic cues for a user to gauge the rate and the amount of rotation by interpreting the number of bumps that have gone by.

I developed four different detent profiles using the Labview software that controls the generation of force information for the Haptic Knob. The first profile created was the Square Wave Detent profile. This follows the original detent style in which an impulsive force is generated to present the highest force level in one step. Figure 12-14 illustrates this detent style.

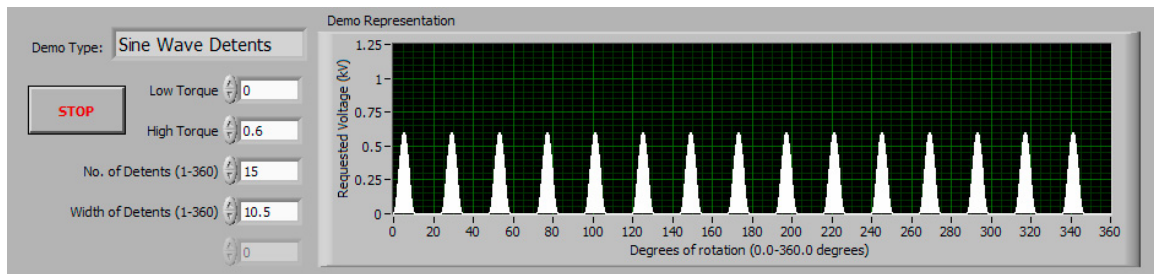


**Figure 12-14:** *Square Detents* Force Profile

The force sensation that is felt when operating this detent is that of “hitting a wall” at the point where the detent is activated. Thus, the force sensation that indicates the detent is the transition from no force to a sudden high force.

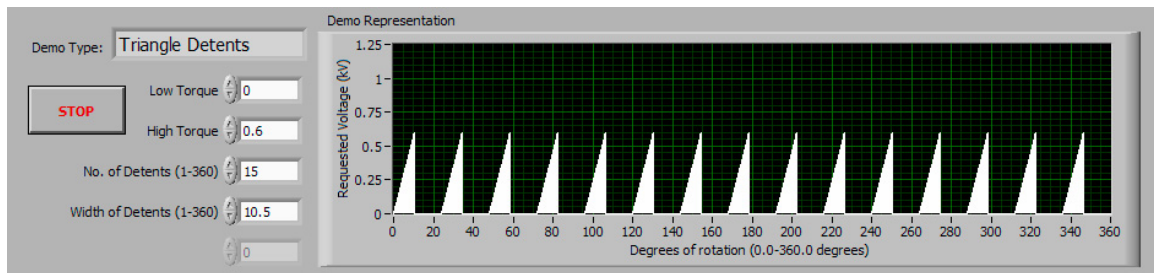


The second detent profile is the Sine Wave Detent. A force envelope in the shape of a sine curve is generated around the point where the detent is to be felt. Figure 12-15 illustrates the force sloping upward to the detent peak and then downward again. The sensation is similar to the square detent, but has a gentler feel, in that the forces do not “jump” to the highest level, but quickly ramp up to the level. The force transition that indicates the detent is the force of getting over the hump of the sine curve.



**Figure 12-15:** *Sine Detents* Force Profile

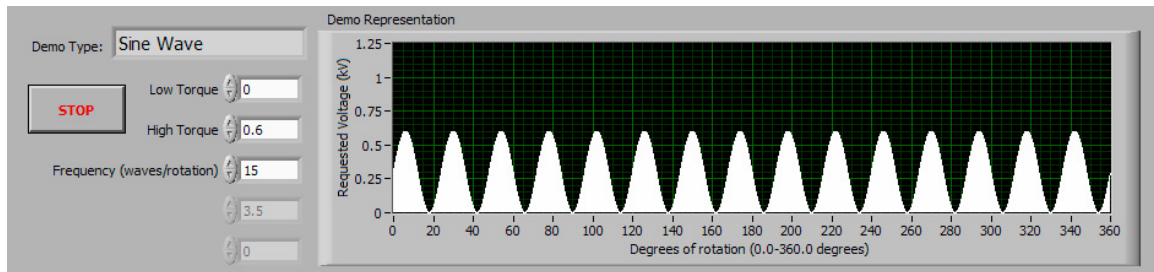
The next force profile is the Triangle Detent profile. As can be seen in Figure 12-16, the triangle detent ramps up to the high point and then drops off back to the low point. The detent sensation that is felt is at the point of drop off where there is a sudden drop in the force. This is, in a way, the opposite of the square detent sensation where the transition is the jump up to the high force not the drop down to the low.



**Figure 12-16:** *Triangle Detents* Force Profile

The final detent profile is the Sine Wave profile. A sine wave is repeated continuously across the full range of motion. When enough sine waves are generated for the rotation, the ramp up and down is sharp enough to be felt as distinct bumps. Figure

12-17 illustrates this detent style. The force sensation is similar to the Sine Wave Detent above, but has an even gentler feel. The transition that indicates the detent location is, again, the feeling of getting over the hump of the sine curve, however in this case the forces only drop to the low point momentarily and are then ramped upward again.



**Figure 12-17:** *Sine Wave* Force Profile

I explored the three Factors presented here through the Human Factors testing that will be presented in the following chapters. The goal of the experiments was to determine if the design variations in Knob Shape, Knob Texture and Force Profile would affect the understandability and usability of the Haptic Knob system and by extension other related haptic interfaces as well.

### **13 HUMAN FACTORS, EXPERIMENTAL DESIGN**

To test the capabilities of the Haptic Knob and to explore the different design parameters that could affect the Knob's understandability, experimentation needed to be performed using human subjects. This would allow the system to be used under real conditions by the people who will be using the haptic interface once it is developed.

I performed the experiment at the Robotics and Mechatronics Laboratory at Northeastern University in Boston. The test subjects were assembled from the student population on a purely volunteer basis. No test subjects were taken from the members of the Robotics Lab, in order to reduce the possibility of bias within the testing results due to familiarity with the project.

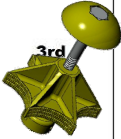
There were 6 female and 9 male subjects, all approximately 20 to 30 years of age and in apparent good health, with 11 of them being right-handed and 4 left-handed.

Since human subjects were used in the experiment, approval was obtained from Northeastern University's Division of Research Integrity and the Institutional Review Board (IRB) to perform the experiment [Division of Research Integrity, website]. The IRB reviewed the experimental plan in regard to the safety and treatment of the human subjects and gave approval for the experiment to be performed. A copy of the IRB application, the consent form and the IRB's approval form are included in the appendix.

The task that I gave to the test subjects to perform was to count the number of detents that were presented to them for a full rotation. This was a straightforward task to perform and would allow for an exploration of the accuracy that would be expected for a detailed task with haptic cues. The accuracy of the subject's detent count would be used as an objective rating of the usefulness of the knob being tested.

### 13.1 Hardware, Physical Layout

The Haptic Knob hardware that I developed for use in this experiment has been described in previous chapters. The Knob was designed so that the knob handles could be exchanged simply by loosening the set screws installed in the handles. The eight knobs being tested were laid out in the order in which they would be used, but were not hidden from the sight of the test subject. Figure 13-1 shows the layout grid that was used to organize the tested knobs, with an example knob placed on the grid.

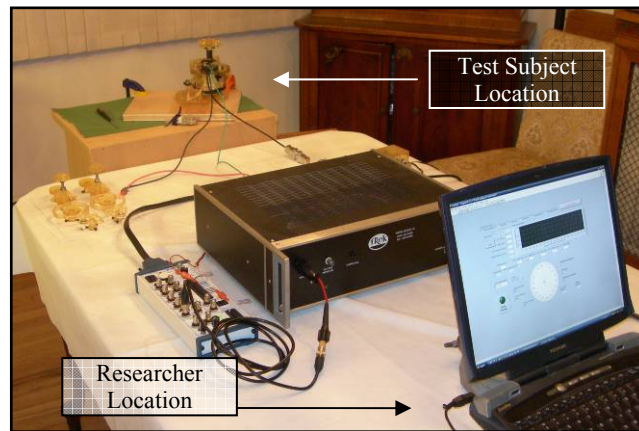
Knob Testing Order			
1st	2nd	3rd	4th
			
5th	6th	7th	8th

**Figure 13-1:** Knob Test Order Grid.

The Knob device was attached to a lab table by clamps in order to provide a stable and consistent testing environment. Subjects were instructed to only grasp the knob handle and not the housing of the device to make sure that the force sensations were only transmitted to the user through the knob and not the housing of the unit.

The test subjects were allowed to stand or sit in front of the Knob device at their discretion in which ever way was most comfortable to them. In instances when needed a stool was offered to the shorter test subjects to stand on to elevate themselves to a comfortable height. The researcher performing the experiment was situated on the opposite side of the lab table. The test computer was set up so that the monitor and

keyboard were hidden from the subject so that the test settings could be changed by the researcher without the subject seeing. Figure 13-2 shows a picture of a testing setup, similar to the one used in the Robotics Lab in that the researcher and subject are at opposite ends of the table, with the computer screen visible only to the researcher.



**Figure 13-2:** Human Factors Experiment Setup

### 13.2 Software, Data Collection

The software I used to run the experiment was Labview, using the program presented above. I had the ability to select from four different detent style tests (Square Detent, Sine Envelope Detent, Triangle Detent and Continuous Sine Wave) and was able to alter the detent parameters to tune the test to an appropriate level.

One method that is used to minimize the bias in an experiment is to randomize the order in which factors are presented to the test subjects. This helps to alleviate an artificial bias that may occur if a certain parameter is presented in the same manner for every subject. For example, if Knob #1 is always the first knob to be presented and Knob #6 is always the last, the unfamiliarity of the first test might make Knob #1 perform worse than otherwise and the experience gained by the time Knob #6 is presented last may increase the performance of that knob. To minimize this effect it is customary to

present test cases in a different order for each subject. The randomization method that I used to structure the order in which the knob shape, texture and detent style were presented was the Latin Square method. A Latin Square is a square matrix structure by which the parameters are not repeated and are never given in the same order either horizontally along the matrix or vertically. Figure 13-3 shows a 4x4 Latin Square matrix.

The four knob shapes and the two knob textures result in eight total knobs. For the Latin Square randomization, they were collected and randomized together in an 8x8 Latin Square matrix. Since the Latin Square randomization requires a square matrix, the eight knobs were randomized for eight consecutive test subjects. Figure 13-4 shows how the Latin Square matrices were used in developing the test plan.

Size - 4x4

1	2	4	3
2	3	1	4
3	4	2	1
4	1	3	2

**Figure 13-3:**  
Latin Square  
Matrices, 4x4

		Knob #										Detent Style			
Subject 1	-	1	2	8	3	7	4	6	5	1st Knob	-	A	B	D	C
Subject 2	-	2	3	1	4	8	5	7	6	2nd Knob	-	B	C	A	D
Subject 3	-	3	4	2	5	1	6	8	7	3rd Knob	-	C	D	B	A
Subject 4	-	4	5	3	6	2	7	1	8	4th Knob	-	D	A	C	B
Subject 5	-	5	6	4	7	3	8	2	1	5th Knob	-	A	B	D	C
Subject 6	-	6	7	5	8	4	1	3	2	6th Knob	-	B	C	A	D
Subject 7	-	7	8	6	1	5	2	4	3	7th Knob	-	C	D	B	A
Subject 8	-	8	1	7	2	6	3	5	4	8th Knob	-	D	A	C	B

**Figure 13-4:** Latin Squares Defining Experimental Order

The 8x8 matrix allocated the order in which the knobs were presented for each subject. The 4x4 matrix defined, for each subject, the order in which the four detent styles were presented for the 1<sup>st</sup> through 4<sup>th</sup> knobs, while the matrix was repeated for the 5<sup>th</sup> through 8<sup>th</sup>. The 8x8 matrix defined eight distinct setups for the subjects. In order to accommodate a larger number of subjects, the 8x8 matrix was repeated as necessary.

Data was logged in individual data files for each text subject using Microsoft Excel spreadsheets. Figure 13-5 shows an example of a data collection sheet. The knob

order, shown in column B was determined by the 8x8 matrix. Each data file was loaded with a different knob order. The Detent Style variations are shown in columns D, F, H and J. The detent style headings remained fixed, but the labels ‘1<sup>st</sup>’ through ‘4<sup>th</sup>’ indicate the order in which the styles were presented.

Microsoft Excel - Subject20-x-xx-06(29).xls

Type a question for help

L63

	A	B	C	D	E	F	G	H	I	J
1	Trial #	Knob #	Reported (Square)	Reported (Sine Env.)	Reported (SineWave)	Reported (Triangle)				
2	1	4	1st	2nd	4th	3rd				
3	2	4	1st	2nd	4th	3rd				
4	3	4	1st	2nd	4th	3rd				
5	1	5	2nd	3rd	1st	4th				
6	2	5	2nd	3rd	1st	4th				
7	3	5	2nd	3rd	1st	4th				
8	1	3	3rd	4th	2nd	1st				
9	2	3	3rd	4th	2nd	1st				
10	3	3	3rd	4th	2nd	1st				
11	1	6	4th	1st	3rd	2nd				
12	2	6	4th	1st	3rd	2nd				
13	3	6	4th	1st	3rd	2nd				
14	1	2	1st	2nd	4th	3rd				
15	2	2	1st	2nd	4th	3rd				
16	3	2	1st	2nd	4th	3rd				
17	1	7	2nd	3rd	1st	4th				
18	2	7	2nd	3rd	1st	4th				
19	3	7	2nd	3rd	1st	4th				
20	1	1	3rd	4th	2nd	1st				
21	2	1	3rd	4th	2nd	1st				
22	3	1	3rd	4th	2nd	1st				
23	1	8	4th	1st	3rd	2nd				
24	2	8	4th	1st	3rd	2nd				
25	3	8	4th	1st	3rd	2nd				
26										
27	Trial #	Knob #	% Accuracy (Square)	% Accuracy (Sine)	% Accuracy(SineWave)	% Accuracy (Triangle)				
28	1	4	1st 0.000	2nd 0.000	4th 0.000	3rd 0.000				
29	2	4	1st 0.000	2nd 0.000	4th 0.000	3rd 0.000				
30	3	4	1st 0.000	2nd 0.000	4th 0.000	3rd 0.000				
31	1	5	2nd 0.000	3rd 0.000	1st 0.000	4th 0.000				
32	2	5	2nd 0.000	3rd 0.000	1st 0.000	4th 0.000				
33	3	5	2nd 0.000	3rd 0.000	1st 0.000	4th 0.000				
34	1	3	3rd 0.000	4th 0.000	2nd 0.000	1st 0.000				
35	2	3	3rd 0.000	4th 0.000	2nd 0.000	1st 0.000				
36	3	3	3rd 0.000	4th 0.000	2nd 0.000	1st 0.000				
37	1	6	4th 0.000	1st 0.000	3rd 0.000	2nd 0.000				
38	2	6	4th 0.000	1st 0.000	3rd 0.000	2nd 0.000				
39	3	6	4th 0.000	1st 0.000	3rd 0.000	2nd 0.000				
40	1	2	1st 0.000	2nd 0.000	4th 0.000	3rd 0.000				
52										
53	Knob #	Avg Acc'y (Square)	Avg Acc'y (Sine)	Avg Acc'y(SineWave)	Avg Acc'y (Triangle)					
54	4	0.000	0.000	0.000	0.000					
55	5	0.000	0.000	0.000	0.000					
56	3	0.000	0.000	0.000	0.000					
57	6	0.000	0.000	0.000	0.000					
58	2	0.000	0.000	0.000	0.000					
59	7	0.000	0.000	0.000	0.000					
60	1	0.000	0.000	0.000	0.000					
61	8	0.000	0.000	0.000	0.000					

Ready

NUM

Figure 13-5: Data Collection Sheet

The top pane of the data collection sheet is where the data was entered during testing. The central pane (cut off in the picture) automatically calculates the accuracy of the response. And the lower pane collects and averages the accuracies for each knob/detent combination in order to afford a quick, but admittedly incomplete, analysis of the subject's performance.

The accuracy was determined by comparing the number of detents reported by the subject to the known number of detents that were presented by the Knob system. The subject's detent count was analyzed for undershoot or overshoot of the correct number and the error was calculated to determine the percent accuracy of the response. The calculation that was performed to calculate the accuracy was:

$$Accuracy = 1 - \frac{|reported\ #-\ 29|}{29} \quad (17)$$

### 13.3 Detent Test Setup

For the purposes of the experiment, the detent profile that was presented was for 29 detents for a single rotation. This number was determined to be large enough to be a challenge to test the accuracy of the knob while not being too large to unfairly test the subject's abilities.

The number 29 was chosen so as to not be a round number. I decided that a round number such as 30 would be more "expected" and that if the subject was attempting to guess the "correct" answer he or she would be more tempted to assume it was a round number. In addition I hinted to the test subject that the number of detents would be changing for each run of the experiment in order to try to thwart the subject's ability to learn what the correct number would be due to repeating the same test a number of times.

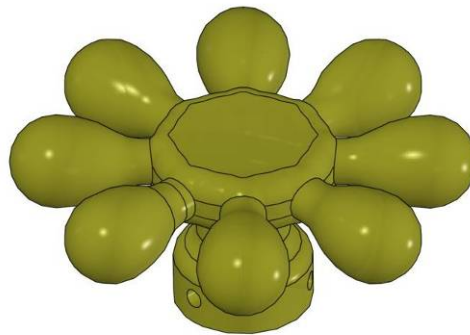


In addition, I pretended to change the detent parameters by miming typing on the keyboard and moving the mouse in order to further misdirect the subject into believing that the detent number was changing for each test run.

Each knob/style combination test was performed three times, in order to be able to take an average of the responses. After each set of three tests, the detent style was changed and the next set of three tests began. The order in which the four detent styles were presented was randomized, as described above, and the subjects were not informed as to which detent style was being performed at any given time.

The test subjects were asked at the beginning of the experiment to keep in mind their “feelings” about the different knob types. This subjective data was informally collected at the end of the complete round of testing. As each knob was used it was put on the side, but not hidden from view, in order to assist the subjects in “keeping in mind” the knobs they liked or disliked.

In order to allow the subject to learn the system before beginning the experiment, the first task that was done was for the subject to interact with the Haptic Knob using a non-experimental knob handle, shown in Figure 13-6.



**Figure 13-6:** Non-Experimental Knob Used for Preliminary Practice

The subject was allowed to interact with the Knob to get a feel for it. The procedure that was followed to introduce the subject to the Knob system was as follows:

1. Allow subject to interact with the non-test knob for a moment
2. Present a simple 5-detent profile and explain that the subject should use the knob and determine the “feel” for counting the 5 detents.
3. Present and explain a 10-detent profile, to challenge the subject a bit more.
4. Present each of the four detent styles using a profile randomly selected between 15 and 35 detents. Make the subject count and report the number of detents. Don’t explain which styles are being used just that there are different styles they will be encountering

**Table 13-1:** Pre-Experimental Practice Procedure

This procedure allowed the subject to gain some familiarity with the system while not biasing the results for any of the experimental knobs in the process. A learning curve would still be experienced once the experimentation began, but would hopefully be lessened due to the above procedure.

### **13.4 Experimental Procedure**

The specific procedure I used in performing the experiment and recording the results was as follows.

1. Greeted subject as they entered the lab and directed them to sit at a table to talk
2. Described project (ERF based Haptic interfaces) and explained the purpose for the experiment (explore knob shape, texture and detent style)
3. Introduced subject to knob test area, and offered for them to sit, stand or stand on a stool, in order to be comfortable.
4. Introduced subject briefly to the four knob shapes and two knob textures. Explained, in general, the need for testing different detent styles.

5. Resized the Ball-Grip knob for the subjects hand size, with the subject's help to determine the comfortable setting.
6. Introduced them to the non-test knob and performed pre-experimental practice procedure as describe above.
7. Gave instruction that the subject should not try to guess the correct answer but must give an accurate account of the number of detents that they *feel*. Explained that this is specifically the information needed for the study.
8. Gave instruction that the subject would determine the full range of motion by him/herself. Pointed out protrusions or etchings on each knob that would help in determining the full rotation.
9. Gave false-instruction that the number of detents will change between each test run and that the researcher would need a moment to adjust the settings.
10. Gave instruction that each test run would start when the researcher told the subject to "go", and that they should wait for the signal.
11. Setup knob and detent style per the randomized order in the subject's test file.
12. Gave "go" signal for subject to begin test run
13. Recorded the number of detents reported by the subject
14. Repeated steps 11-13 three times per knob/detent pair
15. Repeated 11-14 four times, for each of the detent styles for the given knob
16. Repeated 11-15 eight times for each of the test knobs
17. Asked about and recorded subject's subjective opinions about the knobs and detents
18. Offered to demonstrate and explain each detent style to satisfy the subject's curiosity
19. Offered to discuss the accuracy results if desired

**Table 13-2:** Experimental Procedure

### **13.5 Assembly of Data**

After performing the steps outlined in the experimental plan, the resultant data was compiled in the form of separate Excel spreadsheets. The data needed to be collated

in order to perform the statistical calculations that would analyze the data to determine the efficacy of the different design options.

The statistical package I used for this analysis was SPSS for Windows [SPSS Inc., website]. As such, the data needed to be assembled into a single spreadsheet file. To do this, I extracted the averaged accuracy of the experimental tests from the lower pane of the data collection sheet shown above in Figure 13-5. I sorted the data, once removed, into the following spreadsheet format for use in the SPSS package.

Subject	s1t1d1	s1t1d2	s1t1d3	s1t1d4	s1t2d1	s1t2d2	s1t2d3	s1t2d4	s2t1d1	s2t1d2	s2t1d3	s2t1d4
1 Subject 05	.989	.989	1.000	.956	.400	.733	.978	.889	.989	.978	.989	.967
2 Subject 06	.977	.943	1.000	.989	.989	.989	1.000	.989	.966	.989	1.000	.977
3 Subject 07	.437	.540	.920	.529	.448	.575	.977	.724	.483	.563	.874	.506
4 Subject 08	.931	.701	.966	.563	.966	1.000	1.000	.782	.839	.874	.977	.805
5 Subject 09	.506	.598	.908	.563	.678	.655	.931	.598	.920	.989	.989	.966
6 Subject 10	.632	.644	.908	.529	.931	.920	.989	.816	.552	.770	.966	.724
7 Subject 11	.782	.885	.977	.644	.805	.816	.966	.736	.931	.954	.989	.931
8 Subject 12	.690	.632	.862	.529	.667	.782	.966	.747	.782	.782	.885	.770
9 Subject 13	.701	.724	.816	.598	.667	.713	.862	.563	.782	.931	.908	.897
10 Subject 14	.667	.655	.897	.575	.460	.517	.621	.483	.977	.931	.977	.977
11 Subject 15	.793	.598	.874	.552	.655	.747	.862	.713	.644	.598	.816	.517
12 Subject 16	.908	.931	.966	.805	.759	.920	.954	.839	.954	1.000	.989	.931
13 Subject 17	.816	.943	.989	.954	.862	.931	.977	.851	.828	.920	.966	.782
14 Subject 18	.885	.885	.977	.943	.885	.954	.977	.931	.782	.931	.977	.839
15 Subject 19	.713	.816	.908	.701	.782	.690	.908	.793	.966	.931	.977	.954

**Figure 13-7: Collated Data from Experiment**

Each column was assigned a single test type, and the data was filled in for all of the test subjects. Each subject was assigned to a single row of the spreadsheet. For example s1t1d1 refers to Shape #1 (Knob #1), Texture #1 (Textured) and Detent Style #1 (Square Detents) and rows 1 through 15 refer to Subjects 05 to 19. (Subjects 01-04 were discounted because of errors in the testing procedure that were corrected for subject 05 and beyond.)

The statistical analysis that was performed on this data set will be presented in the following chapter.

## 14 HUMAN FACTORS, EXPERIMENTAL RESULTS

In order to develop an understanding of the effect that the Knob Shape, Knob Texture and Detent Style have on the usefulness of the Haptic Knob system a statistical analysis needed to be performed on the collected data. A simple averaging of the accuracy would not suffice to clarify whether the averaged high scores are significant enough to draw a decisive conclusion. It was also important to determine if the interactions between the factors also had a bearing on the efficacy of the haptic interface.

### 14.1 Introduction to Statistical Analysis

The statistical analysis I performed on the collected dataset was presented in the previous chapter. The test subjects were scored based on the accuracy of their count of the number of detents existent in a full rotation of the Haptic Knob.

I performed the data analysis using the SPSS statistical software package. I loaded the data into SPSS and performed a Repeated Measures ANOVA (Analysis of Variance) to assess the statistical significance of the experimental results.

Much of the following explanation of analysis of variance is taken from [Urdan, 2005]. The following explanation is simply an overview of the statistical analysis and should not be considered a comprehensive review of the topic. More in depth descriptions can be found in various statistical textbooks.

#### 14.1.1 Variance

The term *variance* was introduced by Ronald Fisher in 1918 in his paper *The Correlation Between Relatives on the Supposition of Mendelian Inheritance*. The first step to analyze the variance of a dataset is to calculate the average or mean value.

The *mean* of a set of sample data is the averaged or expected value of the data found by calculating:

$$\overline{X} = \frac{\sum X}{n} \quad (18)$$

Where  $\overline{X}$  is the mean of the sample dataset,  $X$  is a point in the dataset and  $n$  is the number of points in that set.

The variance is then the average of the square of the difference of the data points from that mean value. This is given by:

$$s^2 = \frac{\sum (X - \overline{X})^2}{n - 1} \quad (19)$$

The *standard deviation*,  $s$ , the measure of the typical or average deviation of the points in the dataset from the set's mean, is taken from the variance calculation by:

$$s = \sqrt{\frac{\sum (X - \overline{X})^2}{n - 1}} \quad (20)$$

These two pieces of data allow for a characterization of the distribution of the dataset by assessing how well the data “clusters” around the average data. And with further analysis, how significant that mean value is at characterizing the full set of data in a global sense.

This information allows an experiment to be performed on a subset or sample of the general population, and after analysis, determine how accurate the experimental results are at describing the results in terms of the whole population.

### 14.1.2 Analysis of Variance (ANOVA)

The purpose of the analysis of variance (ANOVA) is to compare the means of different groups for a dependent variable to see if the group means are significantly different from each other. By structuring a factorial experiment to isolate the results for different groups of data – for example, the tests with four different knob shapes would yield four different means of the accuracy measurements – the ANOVA test would provide a way of determining if the difference in the means were statistically significant. If the differences are found to be significant, that could lead to a conclusion about the most accurate knob shape in terms of the overall population.

The ANOVA is calculated by the process of dividing up the variance in the dependent variable into two components: the variance attributable to between-group differences, and the variance attributable to within-group differences, also known as error. The calculation for the  $F$  value, which will lead to an understanding of the statistical significance of the results is found by:

$$F = \frac{\text{mean\_square\_between}}{\text{mean\_square\_error}}, \left( F = \frac{MS_b}{MS_e} \right) \quad (21)$$

The Mean Square Error,  $MSe$ , is calculated by first using the following process to calculate the sum of squares error ( $SSe$ ):

1. Subtract the group mean from each individual score in each group:  $(X - \bar{X})$ .
2. Square each of these deviation scores:  $(X - \bar{X})^2$
3. Add them all up for each group:  $\Sigma(X - \bar{X})^2$ .
4. Then add up all of the sums of squares for all of the groups:

$$\Sigma(X_1 - \bar{X}_1)^2 + \Sigma(X_2 - \bar{X}_2)^2 + \dots + \Sigma(X_k - \bar{X}_k)^2$$

Where the subscripts indicate the individual groups, 1 through k.:

The Mean Square Error is then calculated by:

$$MS_e = \frac{SS_e}{N - K} \quad (22)$$

Where  $SS_e$  is the Sum of Square error,  $K$  is the number of groups and  $N$  is the number of cases combined across all groups.

The Mean Squares Between Groups is calculated first by calculating the Sum of Squares Between Groups using the following steps:

To find the  $SS_b$  we

1. Subtract the grand mean from the group mean:  $(\bar{X} - \bar{X}_T)$ ;  $T$  indicates total, or the mean for the total group.
2. Square each of these deviation scores:  $(\bar{X} - \bar{X}_T)^2$ .
3. Multiply each squared deviation by the number of cases,  $n$ , in the group:  $n(\bar{X} - \bar{X}_T)^2$
4. Add these squared deviations from each group together:  $\sum n(\bar{X} - \bar{X}_T)^2$

The Mean Square Between Groups is then calculated by:

$$MS_b = \frac{SS_b}{K - 1} \quad (23)$$

The  $F$  value is then calculated by:  $F = \frac{MS_b}{MS_e}$

The  $F$  value is then used to determine if there is a statistical significance within the calculated means. One method is to use a table similar to Table 14-1, below, which determines if the  $F$  value is above a critical threshold that indicates statistical significance. In order to use the table, the degrees of freedom first need to be identified. For the  $MS_e$  value the degrees of freedom  $df$  are simply the number of cases in the samples. The degrees of freedom for  $MS_b$  are the number of groups being compared.



The degrees of freedom allow for the effects of the sample size and sample range to have a bearing on the statistical significance of the results.

$\alpha$ levels of .05 (lightface) and .01 (boldface) for the distribution of $F$																												
Degrees of Freedom (for the numerator of $F$ ratio)																												
		1	2	3	4	5	6	7	8	9	10	11	12	14	16	20	24	30	40	50	75	100	200	500	$\infty$			
Degrees of freedom (for the denominator of the $F$ ratio)	1	161	200	216	225	230	234	237	239	241	242	243	244	245	246	248	249	250	251	252	253	253	254	254	254	1		
	2	4,052	4,999	5,403	5,625	5,764	5,859	5,928	5,981	6,022	6,056	6,082	6,106	6,142	6,169	6,208	6,234	6,258	6,286	6,302	6,323	6,334	6,352	6,361	6,366	2		
	3	18.51	19.00	19.16	19.25	19.30	19.33	19.36	19.37	19.38	19.39	19.40	19.41	19.42	19.43	19.44	19.45	19.46	19.47	19.47	19.48	19.49	19.49	19.50	19.50	3		
	4	98.49	99.00	99.17	99.25	99.30	99.33	99.34	99.36	99.39	99.40	99.41	99.42	99.43	99.44	99.45	99.46	99.47	99.48	99.49	99.49	99.49	99.49	99.50	99.50	4		
	5	10.13	9.55	9.28	9.12	9.01	8.94	8.88	8.84	8.81	8.78	8.76	8.74	8.71	8.69	8.66	8.64	8.62	8.60	8.58	8.57	8.56	8.54	8.54	8.53	5		
	6	34.12	30.82	29.46	28.71	28.24	27.91	27.67	27.49	27.34	27.23	27.13	27.05	26.92	26.83	26.69	26.60	26.50	26.41	26.35	26.27	26.23	26.18	26.14	26.12	6		
	7	7.71	6.94	6.59	6.39	6.26	6.16	6.09	6.04	6.00	5.96	5.93	5.91	5.87	5.84	5.80	5.77	5.74	5.71	5.70	5.68	5.66	5.65	5.64	5.63	7		
	8	21.20	18.00	16.69	15.98	15.52	15.21	14.98	14.80	14.66	14.54	14.45	14.37	14.24	14.15	14.02	13.93	13.83	13.74	13.69	13.61	13.57	13.52	13.48	13.46	8		
	9	6.61	5.79	5.41	5.19	5.05	4.95	4.88	4.82	4.78	4.74	4.70	4.68	4.64	4.60	4.56	4.53	4.50	4.46	4.44	4.42	4.40	4.38	4.37	4.36	9		
	10	16.26	13.27	12.06	11.39	10.97	10.67	10.45	10.27	10.15	10.05	9.96	9.89	9.77	9.68	9.55	9.47	9.38	9.29	9.24	9.17	9.13	9.07	9.04	9.02	10		
	11	5.99	5.14	4.76	4.53	4.39	4.28	4.21	4.15	4.10	4.06	4.03	4.00	3.96	3.92	3.87	3.84	3.81	3.77	3.75	3.72	3.71	3.69	3.68	3.67	11		
	12	13.74	10.92	9.78	9.15	8.75	8.47	8.26	8.10	7.98	7.87	7.79	7.72	7.60	7.52	7.39	7.31	7.23	7.14	7.09	7.02	6.99	6.94	6.90	6.88	12		
	13	5.59	4.74	4.35	4.12	3.97	3.87	3.79	3.73	3.68	3.63	3.60	3.57	3.52	3.49	3.44	3.41	3.38	3.34	3.32	3.29	3.28	3.25	3.24	3.23	13		
	14	12.25	9.55	8.45	7.85	7.46	7.19	7.00	6.84	6.71	6.62	6.54	6.47	6.35	6.27	6.15	6.07	5.98	5.90	5.85	5.78	5.75	5.70	5.67	5.65			
	15	5.32	4.46	4.07	3.84	3.69	3.58	3.50	3.44	3.39	3.34	3.31	3.28	3.23	3.20	3.15	3.12	3.08	3.05	3.03	3.00	2.98	2.96	2.94	2.93	14		
	16	11.26	8.65	7.59	7.01	6.63	6.37	6.19	6.03	5.91	5.82	5.74	5.67	5.56	5.48	5.36	5.28	5.20	5.11	5.06	5.00	4.96	4.91	4.88	4.86			
	17	5.12	4.26	3.86	3.63	3.48	3.37	3.29	3.23	3.18	3.13	3.10	3.07	3.02	2.98	2.93	2.90	2.86	2.82	2.80	2.77	2.76	2.73	2.72	2.71	15		
	18	10.56	8.02	6.99	6.42	6.06	5.80	5.62	5.47	5.35	5.26	5.18	5.11	5.00	4.92	4.80	4.73	4.64	4.56	4.51	4.45	4.41	4.36	4.33	4.31			
	19	4.96	4.10	3.71	3.48	3.33	3.22	3.14	3.07	3.02	2.97	2.94	2.91	2.86	2.82	2.77	2.74	2.70	2.67	2.64	2.61	2.59	2.56	2.55	2.54	16		
	20	10.04	7.56	6.55	5.99	5.64	5.39	5.21	5.06	4.95	4.85	4.78	4.71	4.60	4.52	4.41	4.33	4.25	4.17	4.12	4.05	4.01	3.96	3.93	3.91			
	21	4.84	3.98	3.59	3.36	3.20	3.09	3.01	2.95	2.90	2.86	2.82	2.79	2.74	2.70	2.65	2.61	2.57	2.53	2.50	2.47	2.45	2.42	2.41	2.40	17		
	22	9.65	7.20	6.22	5.67	5.32	5.07	4.88	4.74	4.63	4.54	4.46	4.40	4.29	4.21	4.10	4.02	3.94	3.86	3.80	3.74	3.70	3.66	3.62	3.60			
	23	4.75	3.88	3.49	3.26	3.11	3.00	2.92	2.85	2.80	2.76	2.72	2.69	2.64	2.60	2.54	2.50	2.46	2.42	2.40	2.36	2.35	2.32	2.31	2.30	18		
	24	9.33	6.93	5.95	5.41	5.06	4.82	4.65	4.50	4.39	4.30	4.22	4.16	4.05	3.98	3.86	3.78	3.70	3.61	3.56	3.49	3.46	3.41	3.38	3.36			
	25	4.67	3.80	3.41	3.18	3.02	2.92	2.84	2.77	2.72	2.67	2.63	2.60	2.55	2.51	2.46	2.42	2.38	2.34	2.32	2.28	2.26	2.24	2.22	2.21	19		
	26	9.07	6.70	5.74	5.20	4.86	4.62	4.44	4.30	4.19	4.10	4.02	3.96	3.85	3.78	3.67	3.59	3.51	3.42	3.37	3.30	3.27	3.24	3.22	3.21	20		

To be statistically significant the  $F$  obtained from the data must be equal to or greater than the value shown in the table.

SOURCE: From *Statistical Methods*, by G. W. Snedecor and W. W. Cochran, (7th ed.). Copyright © 1980 Iowa State University Press. Reprinted with permission.

*continued*

To be statistically significant the  $F$  obtained from the data must be equal to or greater than the value shown in the table.

SOURCE: From *Statistical Methods*, by G. W. Snedecor and W. W. Cochran, (7th ed.). Copyright © 1980 Iowa State University Press. Reprinted with permission.

continued

**Table 14-1: F Value Table from [Urdan, 2005]**

Other methods calculate a  $p$ -value based on the Mean Squares data. The  $p$ -value, known as “statistical significance” indicates the probability that the observed relationship is “true”. The higher the  $p$ -value the less significant the difference between the calculated means is, meaning the higher the  $p$ -value, the less we can believe that the observed relation between variables in the sample is a reliable indicator of the relation between the respective variables in the general population.

The  $\alpha$  value indicated in Table 14-1 is a chosen  $p$ -value level that below which the result is deemed significant. Often in research tasks a  $p$ -value of .05 (i.e., 1/20) – indicating a 5% probability that the relation between the variables found in our sample is a “fluke” – is chosen as the threshold value. A  $p$ -value *below* .05 is therefore considered an indicator of a statistically significant difference in the observed data.

The SPSS software package calculates a  $p$ -value directly from the dataset and skips the lookup table for the calculated  $F$  ratio. Going forward this  $p$ -value, calculated by the SPSS software, will be used as the indicator for statistical significance.

### 14.1.3 Repeated Measures Analysis of Variance

A *Repeated Measures Analysis of Variance* test is performed when a sample population is subject to more than one test configuration that addresses the same measured variable. For example, if a statistical study is performed to measure the test scores of a class at the beginning of the school year versus the end of the school year, the same sample population (the students) would be subject to two different tests (beginning of year and end of year exams) that measure the same variable (test scores). The repeated measures ANOVA allows for an analysis of the difference between various configurations. In the example, whether the students' scores changed in a statistically significant fashion, from the beginning of the year to the end.

Repeated-measures ANOVA divides up the variance in the measured data into the error variance as well as into how much of the total variance is attributable to differences within individuals across the different times they were measured. Calculations that are added to the analysis for the Repeated Measures ANOVA are:

**Within-subject Variance:** The differences between the different Time 1, Time 2 etc. scores for a given subject.

**Mean square for the differences between the trials ( $MS_T$ ):** The average squared deviation between the participants' average across all trials and their scores on each trial.

**Mean square for the subject by trial interaction ( $MS_s \times T$ ):** The average squared deviation between each individual's change in scores across trials and the average change in scores across trials.

I performed all of the above analyses within the SPSS statistical package. The analysis resulted in *p*-values, indicating the significance of the means calculated from the gathered data. In addition, interactions between the different factors – shape, texture and detent style – were explored. The analysis results are presented below.

## 14.2 Data Analysis

I processed the data collected from the Human Factors experiment, showing the accuracy of the Detent Counting task, through the SPSS program to perform a Repeated Measures Analysis of Variance test. The results of the SPSS processing of the data are a listing of the statistical significance of the averaged scores of the accuracy test in the form of a *p*-value. In general a *p*-value of less than .05 is considered to indicate statistical significance – that the mean value of the block of data can be seen to represent the mean value for the general population – while greater than .05 indicates that the data cannot be considered representative in that fashion.

The output of the SPSS processing is a series of tables indicating my analysis results for each of the individual Factors – Knob Shape, Knob Texture and Detent Style – and my analysis of correlations among the Factors as well. Each table will be presented individually and discussed below.





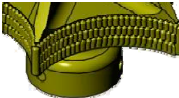

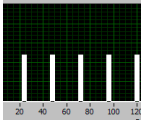
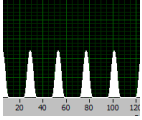
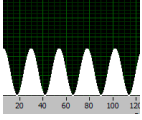
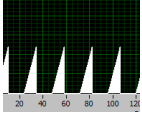
### 14.2.1 Data Organization

I entered the data, as discussed previously, into SPSS using a numerical system to denote the different designs.

Within-Subjects Factors				Descriptive Statistics			
Measure: Accuracy					Mean	Std. Deviation	N
KnobShape	Texture	DetentStyle	Dependent Variable				
1	1	1	s1t1d1	s1t1d1	.76180	.163757	15
		2	s1t1d2	s1t1d2	.76560	.153322	15
		3	s1t1d3	s1t1d3	.93120	.055848	15
		4	s1t1d4	s1t1d4	.69533	.181197	15
	2	1	s1t2d1	s1t2d1	.73027	.187347	15
		2	s1t2d2	s1t2d2	.79613	.152236	15
		3	s1t2d3	s1t2d3	.93120	.096574	15
		4	s1t2d4	s1t2d4	.76360	.137163	15
2	1	1	s2t1d1	s2t1d1	.82633	.159607	15
		2	s2t1d2	s2t1d2	.87607	.138039	15
		3	s2t1d3	s2t1d3	.95193	.054561	15
		4	s2t1d4	s2t1d4	.83620	.156060	15
	2	1	s2t2d1	s2t2d1	.76967	.148545	15
		2	s2t2d2	s2t2d2	.84313	.123986	15
		3	s2t2d3	s2t2d3	.93987	.059840	15
		4	s2t2d4	s2t2d4	.79873	.174773	15
3	1	1	s3t1d1	s3t1d1	.75347	.159325	15
		2	s3t1d2	s3t1d2	.78873	.172937	15
		3	s3t1d3	s3t1d3	.90587	.108368	15
		4	s3t1d4	s3t1d4	.72433	.187560	15
	2	1	s3t2d1	s3t2d1	.72507	.174473	15
		2	s3t2d2	s3t2d2	.76027	.176797	15
		3	s3t2d3	s3t2d3	.90447	.067303	15
		4	s3t2d4	s3t2d4	.68453	.189812	15
4	1	1	s4t1d1	s4t1d1	.56287	.133316	15
		2	s4t1d2	s4t1d2	.61040	.126218	15
		3	s4t1d3	s4t1d3	.77120	.128594	15
		4	s4t1d4	s4t1d4	.55400	.113347	15
	2	1	s4t2d1	s4t2d1	.52907	.141514	15
		2	s4t2d2	s4t2d2	.54733	.149124	15
		3	s4t2d3	s4t2d3	.70700	.128802	15
		4	s4t2d4	s4t2d4	.50067	.153069	15

**Table 14-2:** Data Organization within SPSS

I converted the Knob Shape, Texture and Detent Style options to numerical indications rather than textual. The following chart, Table 14-3, indicates the correspondence between the numerical designation and the actual Knob or Detent.

Numerical Designation	Description	
<b>Knob Shape</b>		
s1	Disc Knob	
s2	Ball Grip Knob	
s3	Enclosed Disk Knob	
s4	Hand Wheel Knob	
<b>Knob Texture</b>		
t1	Knurled	
t2	Smooth	
<b>Detent Style</b>		
d1	Square Detents	
d2	Sine Envelope Detents	
d3	Sine Waves	
d4	Triangle Detents	

**Table 14-3:** Correlation of Numerical Indicators to Actual Designs

## 14.3 Analysis Results

### 14.3.1 Individual Factor – Knob Shape

I began the analysis of the individual factors with the Knob Shape factor. I analyzed the collected data by the SPSS software by an Analysis of Variance test. The following data tables are the result of that analysis.

Measure: Accuracy

KnobShape	Mean	Std. Error	95% Confidence Interval	
			Lower Bound	Upper Bound
1	.797	.029	.735	.859
2	.855	.030	.790	.920
3	.781	.035	.706	.855
4	.598	.028	.538	.658

**Table 14-4:** Mean Values for Knob Shape Factor

Table 14-4 shows the averaged/mean values for each of the knob types. It is clear that that Knob 2, the Ball Grip Knob, has the highest averaged accuracy. The next step was to assess whether those mean values have a statistical significance relative to each other. Table 14-5 gives the pairwise comparisons between the different knob shapes.

Measure: Accuracy

(I) KnobShape	(J) KnobShape	Mean Difference (I-J)	Std. Error	Sig. <sup>a</sup>
1	2	-.058	.033	.101
	3	.016	.029	.589
	4	.199*	.034	.000
2	1	.058	.033	.101
	3	.074*	.018	.001
	4	.257*	.030	.000
3	1	-.016	.029	.589
	2	-.074*	.018	.001
	4	.183*	.034	.000
4	1	-.199*	.034	.000
	2	-.257*	.030	.000
	3	-.183*	.034	.000

Based on estimated marginal means

**Table 14-5:** Pairwise Comparisons for Knob Shape Factor

The statistical significance is indicated in the column labeled “Sig.” in the above table. The sig. value indicates statistical significance when that value is at or below .05.

In the above table, it can be seen that for Knob Shape 1 (Disk Grip Knob), the significance of the accuracy measurement relative to Knobs 2 and 3 is above .05 and therefore non-significant, while Knob 4 is below .05 and is significant.

The accuracy of Knob 2 (Ball Grip Knob) is non-significant relative to Knob 1 but is significant relative to Knobs 3 and 4. The accuracy of Knobs 3 and 4 show that the Knob 1-3 correlation is non-significant, while the rest of the comparisons are significant.

Therefore, Knob 2’s accuracy, with the highest mean value, is a better representation of the general population’s accuracy while using Knob 2 relative to Knobs 3 and 4. However, that significance does not hold relative to Knob 1.

Knob 4, with the lowest mean value for accuracy, has significance relative to all of the other knobs. Therefore Knob 4’s poor performance can be seen as being representative to the population’s use of Knob 4.

Conclusion about the data will be presented in a later section. The accuracy assessments for the Knob Texture and Detent Style are presented below.

### **14.3.2 Individual Factor – Texture**

The analysis of the accuracy measurements for the Knob Texture follows a similar route as for the Knob Shape. Table 14-6 shows the averaged/mean values for the accuracy while using the Textured or Smooth knobs.

Measure: Accuracy

Texture	Mean	Std. Error	95% Confidence Interval	
			Lower Bound	Upper Bound
1	.770	.027	.712	.827
2	.746	.023	.697	.794

**Table 14-6:** Mean Values for Knob Texture Factor

Measure: Accuracy

(I) Texture	(J) Texture	Mean Difference (I-J)	Std. Error	Sig. <sup>a</sup>
1	2	.024*	.011	.041
2	1	-.024*	.011	.041

Based on estimated marginal means

**Table 14-7:** Pairwise Comparisons for Knob Texture Factor

Table 14-6 shows the mean value for Texture 1 – the Knurled Knobs – as being higher than the mean for Texture 2 – the Smooth Knobs. Table 14-7 shows that the difference in means has a significance of .041, and is therefore statistically significant.

So, the result, that the Textured knobs result in higher accuracy, can be seen as being representative of the results that would be obtained for the general population.

### 14.3.3 Individual Factor – Detent Style

The last factor to examine individually was the Detent Style Factor. I performed the analysis to assess the accuracy measurement for the four different Detent Styles.

Measure: Accuracy

DetentStyle	Mean	Std. Error	95% Confidence Interval	
			Lower Bound	Upper Bound
1	.707	.028	.648	.766
2	.748	.029	.685	.811
3	.880	.015	.849	.912
4	.695	.031	.629	.761

**Table 14-8:** Mean Values for Detent Style Factor

Table 14-8 shows that the Detent Style with the highest mean value is Style 3 – the continuous Sine Wave.



Table 14-9 confirms that in relation to the other styles, this result is statistically significant.

Measure: Accuracy

(I) DetentStyle	(J) DetentStyle	Mean Difference (I-J)	Std. Error	Sig. <sup>a</sup>
1	2	-.041*	.011	.002
	3	-.173*	.022	.000
	4	.013	.011	.290
2	1	.041*	.011	.002
	3	-.132*	.020	.000
	4	.054*	.010	.000
3	1	.173*	.022	.000
	2	.132*	.020	.000
	4	.186*	.021	.000
4	1	-.013	.011	.290
	2	-.054*	.010	.000
	3	-.186*	.021	.000

Based on estimated marginal means

**Table 14-9:** Pairwise Comparisons for Detent Style Factor

Although Style 2 – Sine Envelope Detents – has the next highest mean value and is also statistically significant in relation to the other styles, Style 3 still yields higher overall accuracy in the tests.

#### 14.3.4 Two Factors

In addition to the above analyses, SPSS also performed an analysis of the data which took into account the interrelationship between the different factors. The mean values were calculated for the accuracy based on a pairing of the Knob Shape and Texture, the Knob Shape and Detent Style, and the Texture and Detent Style. The results of this analysis can be seen below in Tables 14-10 through 14-12.

Measure: Accuracy

KnobShape	Texture	Mean	Std. Error	95% Confidence Interval	
				Lower Bound	Upper Bound
1	1	.788	.033	.718	.859
	2	.805	.032	.736	.874
2	1	.873	.031	.805	.940
	2	.838	.030	.773	.903
3	1	.793	.037	.713	.873
	2	.769	.037	.689	.848
4	1	.625	.030	.560	.689
	2	.571	.032	.502	.640

**Table 14-10:** Mean Values for Paired Factors, Knob Shape - Texture

The highest Mean value for the pairing of Knob Shape and Texture was for the Knob Shape 2 – Texture 1, the Ball Grip Knob – Knurled pair.

Measure: Accuracy

KnobShape	DetentStyle	Mean	Std. Error	95% Confidence Interval	
				Lower Bound	Upper Bound
1	1	.746	.038	.665	.827
	2	.781	.034	.707	.855
	3	.931	.017	.894	.968
	4	.729	.038	.647	.812
2	1	.798	.038	.717	.879
	2	.860	.033	.790	.930
	3	.946	.014	.916	.976
	4	.817	.041	.729	.906
3	1	.739	.040	.654	.825
	2	.775	.042	.683	.866
	3	.905	.021	.861	.950
	4	.704	.044	.610	.799
4	1	.546	.033	.475	.616
	2	.579	.033	.508	.650
	3	.739	.026	.683	.796
	4	.527	.029	.466	.589

**Table 14-11:** Mean Values for Paired Factors, Knob Shape – Detent Style

The highest mean for the Knob Shape – Detent Style pair was for Knob 2 – Detent Style 3 – the Ball Grip Knob and continuous Sine Wave detents.

Measure: Accuracy

Texture	DetentStyle	Mean	Std. Error	95% Confidence Interval	
				Lower Bound	Upper Bound
1	1	.726	.032	.658	.794
	2	.760	.031	.693	.827
	3	.890	.018	.851	.929
	4	.702	.031	.635	.770
2	1	.689	.025	.634	.743
	2	.737	.028	.676	.797
	3	.871	.014	.840	.901
	4	.687	.032	.619	.755

**Table 14-12:** Mean Values for Paired Factors, Texture – Detent Style

The highest mean value for the Texture – Detent Style pairing was for the Texture 1 – Detent Style 3, the Knurled Knob – continuous Sine Wave detent pair.

### 14.3.5 Three Factors

Measure: Accuracy

KnobShape	Texture	DetentStyle	Mean	Std. Error	95% Confidence Interval	
					Lower Bound	Upper Bound
1	1	1	.762	.042	.671	.852
		2	.766	.040	.681	.851
		3	.931	.014	.900	.962
		4	.695	.047	.595	.796
	2	1	.730	.048	.627	.834
		2	.796	.039	.712	.880
		3	.931	.025	.878	.985
		4	.764	.035	.688	.840
2	1	1	.826	.041	.738	.915
		2	.876	.036	.800	.953
		3	.952	.014	.922	.982
		4	.836	.040	.750	.923
	2	1	.770	.038	.687	.852
		2	.843	.032	.774	.912
		3	.940	.015	.907	.973
		4	.799	.045	.702	.896
3	1	1	.753	.041	.665	.842
		2	.789	.045	.693	.885
		3	.906	.028	.846	.966
		4	.724	.048	.620	.828
	2	1	.725	.045	.628	.822
		2	.760	.046	.662	.858
		3	.904	.017	.867	.942
		4	.685	.049	.579	.790
4	1	1	.563	.034	.489	.637
		2	.610	.033	.541	.680
		3	.771	.033	.700	.842
		4	.554	.029	.491	.617
	2	1	.529	.037	.451	.607
		2	.547	.039	.465	.630
		3	.707	.033	.636	.778
		4	.501	.040	.416	.585

**Table 14-13:** Mean Values for Triple Factors, Knob Shape – Texture – Detent Style

Table 14-13 shows the means calculated for all three factors together. The highest mean accuracy was .952 for the combination of Knob Shape 2 – Texture 1 – Detent Style 3. Therefore, based on the mean of the accuracy measurement alone, the best design combination is Ball Grip Knob – Knurled Texture – continuous Sine Wave detents. Although, other combinations were not much less accurate and could be seen as decent alternatives to that design combination.

#### **14.4 Data Analysis Conclusions**

A number of conclusions can be drawn for the affect of the three different factors on the accuracy of the Haptic Knob interface. In addition, information has been gathered to understand the effects of combinations of the different factors on the accuracy of the interface.

The results of the analysis for the individual factors is as follows:

##### *Knob Shape*

The knob shape that has the highest average values for the accuracy test was the Ball Grip Knob. The statistical analysis of this value shows that Ball-Grip Knob provides better accuracy for the Knob interface than the Enclosed Disk Knob or the Hand Wheel Knob. However, although the accuracy measurement was higher than that for the Disk Knob, the result was not statistically significant enough to draw a final conclusion about whether the Ball Grip Knob is better than the Disk Knob. Assessing the analysis for the Disk Knob reveals that the only statistically significant comparison is to only one of the other knobs – the Hand Wheel Knob.

It is therefore *probable*, although not certain based on the statistical analysis, that the Ball Grip Knob is the best of the four Knob Shape options at maximizing the accuracy of the Haptic Knob interface. Testing with a larger sample of subjects might provide the statistical significance to bear out this conclusion.

#### *Knob Texture*

The analysis shows that the Knurled Texture provides a greater accuracy than the Smooth Texture. The conclusion is statistically significant and can be seen as representing the form that would maximize the Haptic Interface's efficacy for the population at large.

Therefore, the Knurled Knobs provide better accuracy when used in the Haptic Knob system.

#### *Detent Style*

The Detent Style analysis showed that the continuous Sine Wave detents provided better accuracy than the other three Detent Styles. The statistical analysis shows that this conclusion is also statistically significant.

Therefore, the Continuous Sine Wave Detents provide better accuracy when used in the Haptic Knob Interface system.

#### *Multiple Factors*

Analyses of the interactions between factors revealed that the combinations of the three highest performers listed here resulted in the highest average accuracy for the experimental tests. Although no examination of the statistical significance was available,

the analysis of the mean values seems to bear out the conclusions about the “best” design options stated here.

## **14.5 Discussion of Results**

The analysis shows that the Ball-Grip Knob with the Knurled Texture is (probably) the best Knob design for providing accurate information through the ERF-based Haptic Knob Interface device.

When the Ball-Grip Knob is used, the user tends to move his or her wrist to provide the power to rotate the knob. In addition, the knurled texture provides a better gripping surface so that the knob does not have to be grasped firmly to rotate it in a controlled manner. These two factors allow the finger tips, the sensing pads for the human sense of touch, to focus on feeling the haptic cues rather than providing the rotating force for the device. In addition, the Knurled texture provides a more detailed surface for the finger tips to interact with and may provide better transmission of the force cues than possible with the smooth surface.

The analysis also showed that the Continuous Sine Wave detents provide better accuracy than the other detent styles. When using ERF based systems, as shown previously, the ERF effect occurs differently when the system is in static or dynamic mode. By providing a continuous voltage, and keeping the ERF system active throughout the full Haptic profile for the knob, the jump between static and dynamic modes may be minimized. This allows the force cues to be presented more smoothly to the user, and minimizes the “jumping” between detents that was reported by the test subjects that sometimes characterized the other detent Styles. Many of the test subjects stated that they felt that they had skipped detents, by having to provide different force

levels for the other Detent Styles. This appears to have been mitigated by using the Continuous Sine Wave Detents to provide more consistent force sensations. It is possible that the result can be duplicated by providing a minimum amount of force between detents for the other detent styles, and future testing may bear this out.

Therefore, the best design for providing accurate Haptic Sensations within the parameters of the ERF-based system is: Ball-Grip Knob with Knurled Texture, using the Continuous Sine Wave Detents to provide force cues.

## **15 HAPTIC INTERFACE USED WITH PHYSICAL INJURY**

### **15.1 Motivation for Testing Physically Limited Subject**

While recruiting test subjects for the Human Factors experiment presented above, I discovered that one of the volunteers had been diagnosed with Carpal Tunnel Syndrome and had had surgery to address the issue approximately one year earlier. I decided that the data collected for that subject would likely be skewed by the limitations in the sensory capabilities of the subject's hand due to the Syndrome and treatment, and could therefore not be used for the overall Human Factors experiment.

However, I decided to run the test subject through the experiment anyway in order to discover whether sufferers of medical conditions of the hand would be able to use the Haptic Knob system, or if design changes would need to be made in order to allow them to make full use of the system.

I understood that any results obtained through this type of exploration would not be statistically significant enough to draw any substantial conclusions. However, it could lead to interest in pursuing the investigation in a more expanded manner.

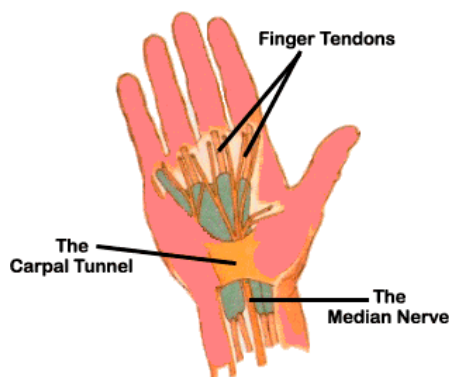
### **15.2 Carpal Tunnel Syndrome**

Much of this description of Carpal Tunnel Syndrome (CTS) is taken from [Ropper, 2005]

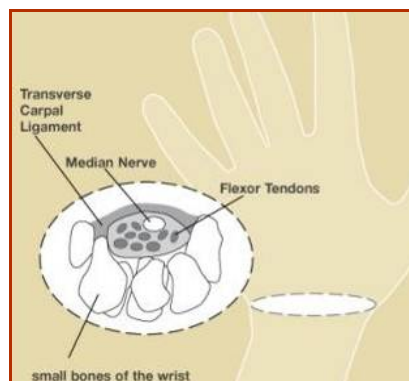
CTS is a compression of the median nerves due to swelling in the wrist that can lead to pain and numbness in the hand and arm. The swelling can occur for various reasons such as strain on the wrist from repetitive motions such as typing, swelling due to pregnancy, thickening of tissues due to rheumatoid arthritis, and other causes.



The Carpal Tunnel is an anatomical passage in the wrist through which various tendons and nerves pass. When swelling occurs at this location, it can affect the proper functioning of those nerves. Figures 15-1 and 15-2 illustrate the anatomical location of the Carpal Tunnel and the affected nerves and tendons.

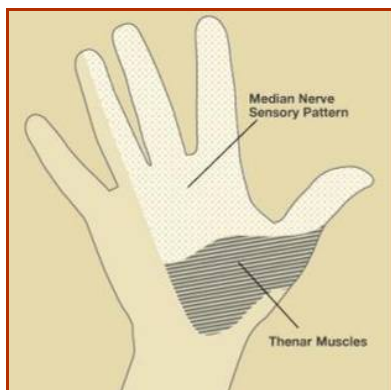


**Figure 15-1:** Location of Carpal Tunnel  
(Image from [carpal-tunnel-syndrome.net])



**Figure 15-2:** Closeup of Affected Nerves and Tendons  
(Image from [American Society for Surgery of the Hand])

The syndrome is essentially a sensory one; the loss or impairment of sensation affects the palmar aspect of the thumb, the middle finger, and especially the index finger and may or may not split the ring finger. Sensations such as tingling can occur and are often worse during the night. The pain in Carpal Tunnel Syndrome may radiate into the forearm, into the region of the biceps and rarely to the shoulder. Figure 15-3 illustrates the affected areas of the hand in which numbness, tingling or pain can occur.



**Figure 15-3:** Location of Sensation Loss or Alteration  
(Image from [American Society for Surgery of the Hand])

Treatments that can be performed include changing the pattern of wrist usage to relieve the irritation that causes the symptoms, splinting the arm to prevent compression of the nerve or surgery to divide the carpal ligament to decompress the nerve. Even after treatment numbness and weakness can linger and may never fully dissipate.

The numbness and weakness associated with Carpal Tunnel Syndrome can affect the user's functioning of the Haptic Knob Interface and may also affect the ability of the user to feel and interpret force cues. It is therefore necessary to assess the Carpal Tunnel Syndrome sufferer's capabilities in relation to the accuracy test for the Haptic Knob.

### **15.3 Data Collection and Analysis**

I collected data for the Carpal Tunnel Syndrome subject in the same manner as for the subjects of the general experiment as discussed in previous chapters, by performing the detent counting task for the four Knob Shapes, two Knob Textures and four Detent Styles. I assembled the data in a Microsoft Excel spreadsheet and then analyzed it to calculate the mean values of the subject's accuracy. Individual mean values were taken for the Knob Shapes, Knob Textures and Detent Styles by manually averaging the data for each of the tested factors individually.

By comparing the averaged data of the Carpal Tunnel Syndrome subject to the mean values for the overall study, I could form an impression about the performance of the test subject. Since this analysis is limited to a single test subject, it can be seen as an exploratory analysis of the issue of using Haptic Interfaces for sufferers of hand injuries, but not an in depth evaluation of the issues surrounding that topic.

The following Tables tabulate the averaged values of the test subject's accuracy in the detent counting task. The calculated mean values from the original experiment are included in the tables for purposes of comparison.

<b>Knob Shape</b>	<b>Mean Accuracy</b>	<b>General Mean</b>	<b>Difference</b>
1 – Disc Grip	<b>0.718</b>	0.797	-0.079
2 – Ball Grip	<b>0.878</b>	0.855	+0.023
3 – Captured Disk Grip	<b>0.817</b>	0.781	+0.036
4 – Hand Wheel	<b>0.381</b>	0.598	-0.217

**Table 15-1:** Accuracy for Knob Shape Factor

<b>Knob Texture</b>	<b>Mean Accuracy</b>	<b>General Mean</b>	<b>Difference</b>
1 – Knurled	<b>0.719</b>	0.770	-0.051
2 – Smooth	<b>0.678</b>	0.746	-0.068

**Table 15-2:** Accuracy for Knob Texture Factor

<b>Detent Style</b>	<b>Mean Accuracy</b>	<b>General Mean</b>	<b>Difference</b>
1 – Square Detents	<b>0.586</b>	0.707	-0.121
2 – Sine Envelope Detents	<b>0.714</b>	0.748	-0.034
3 – Sine Wave, continuous	<b>0.808</b>	0.880	-0.072
4 – Triangle Detents	<b>0.685</b>	0.695	-0.010

**Table 15-3:** Accuracy for Detent Style Factor

## 15.4 Physically Limited Subject Conclusions

The test subject's results were similar, in form, to the general study's result. The test subject's averages indicate that the knobs 2 (Ball Grip) was the most accurate. However, unlike the general results, knob 1 (Disk Grip) was second in accuracy. As before, the knurled texture was more accurate than the smooth. As well, the Continuous Sine Wave detents were the most accurate compared to the other detent styles. The subject's data differed from the norm in that the accuracy varied from the general means from about +2% to -21%, as shown in the tables above.

In discussion with the subject, I learned that the Carpal Tunnel surgery had been performed two years earlier and that extensive rehabilitation had occurred since then. Much improvement had been made over that time and her grip strength and sensory abilities had returned to acceptable levels. I was assured that if the examination had taken place about a year earlier the results would have been much different and would probably have indicated lower accuracy on the measurements, and possibly different preferences on all of the tested factors.

Additionally, the subject reported that although she was able to complete the experiment, she experienced much pain in her injured hand by the end and would not have cared to continue using the system. Specifically the Ball-Grip knob – curiously the most accurate knob – caused the most amount of pain in her hand and arm, possibly due to the wrist motion necessary to operate that particular knob. In addition, the subject reported that since the surgery and rehabilitation, she still experienced tingling in the hand. Although this was not the case during the testing procedures, I might presume that

if the tingling occurred during testing it would interfere with the subject's ability to accurately perform the detent counting task.

## **15.5 Future Study**

Although qualitatively the CTS subject's results were similar to the general results, the data and discussion indicate a need to explore the issue further. Testing of people with more active Carpal Tunnel Syndrome or those with more recent surgical intervention would indicate whether those subjects could use the current Haptic Knob system in an acceptably accurate manner.

A haptic interface should be designed to be useable by almost anyone who accesses it, including those with hand injuries. Being able to document the abilities of people with hand injuries, whether current, post surgery or post rehabilitation, would allow for the development of haptic interfaces that can present useful information to those individuals. In order to collect this information, it would be necessary to conduct a full-scale experiment that would result in statistically significant conclusions about the ability of sufferers of Carpal Tunnel Syndrome, and possibly other hand injuries, to make use of the ERF-based Haptic Knob interface.

## **16 FUTURE WORK / CONCLUSIONS**

### **16.1 Future Work**

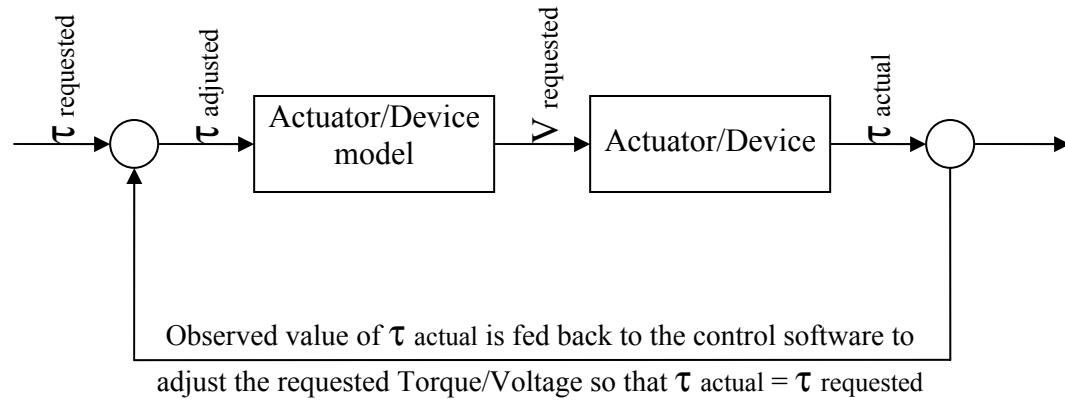
I have done much work to develop and test the three ERF-based actuators as well as the haptic devices, as has been presented above. There is more work to be done to refine the knowledge that has already been accumulated about these devices, as well as to continue the process to develop believable and useful haptic interfaces. The following section contains some of the ideas and plans for future work that can be done to continue this research project.

#### **16.1.1 Open/Closed Loop Control**

The experiments and demonstrations that I have conducted in the course of this research have used an Open-Loop control method to control the ERF actuators and to present sensations via the haptic devices. This method uses the mathematical models as a basis for determining the strength of the electric field necessary to generate a given torque output.

While this method is viable for an extremely accurate model as well as very accurate and controllable hardware, it can fall short when the model and hardware are not as precise. As can be seen in the Response Time tests presented above, the torque output for a given voltage level can vary wildly (refer to the “variability” in the presented graphs). This characteristic can be addressed using a better control scheme.

Closed Loop control methods use a feedback loop to sense the output of a system and to then adjust the input to “fix” the output to the desired levels. Figure 16-1 shows a simple control schematic that may be used to control the ERF actuators and, by extension, the Haptic devices in the future.



**Figure 16-1:** Closed-Loop Control Scheme for ERF actuator Torque output.

Since the Feedback loop of the Closed-Loop control scheme will send information about the actual torque outputs, the controlling software will be able to adjust the voltage values to more accurately reach the proper torque levels. This type of scheme should alleviate many of the inaccuracies seen in the Response tests. Work must be done to create these control algorithms and tune them so that the torque outputs of the actuators and devices will be accurate and reliably reproducible. Both characteristics are necessary for a haptic device to be used in any mission critical application.

### 16.1.2 Dynamic Response Improvement and Testing

The response times seen in the tests presented above show a frequency of 20 Hz for the FP actuator within that actuator's hardware setup. While this may be acceptable for certain haptic interfaces, it leaves room for improvement when applied to applications requiring higher speeds and accuracy. More work can be done to speed up this response time.

Some approaches, as presented above, may be to develop better hardware solutions to the power generation as well as the input/output and computer processing

systems. These types of improvements should speed up the response times of the ERF actuator systems.

Once the response times have been improved, new experimentation can be done to classify the capabilities of the actuator and devices. Dynamic response times, as well as hysteresis and other information about the actuator capabilities, will be useful when designing new devices using the ERF actuators.

### **16.1.3 Haptic Interface Software Development**

Now that the hardware and software have been developed, the next step will be to increase the capabilities of the software that control the actuators within the framework of the Haptic Interface devices.

Software can be developed to generate different force and torque output profiles than have been presented here. In addition, the ability to create a freeform force profile would improve the abilities of the system. As well, the extension of the Joystick software to allow more flexibility in the Virtual Channels beyond the horizontal and vertical channels available with the current software, would allow the Channels to be used in new and more unique ways. By developing this interface in a flexible way, using graphical tools when applicable, robust software can be created that will be able to control the actuator and the haptic devices in a variety of applications without the need for long development cycles.

This software will need to be designed based on the information developed from the human factors experiments performed so far. The data obtained leads to some software designs that would increase the force capabilities of the system.



### **16.1.4 Human-Factors, Additional Factors**

Although a number of Factors were already tested, other Factors may play a role in the understandability of the Haptic Interface system. Some additional Factors to explore are – Level of Forces that can be felt, the Angular Size of the Detents that can be detected, the use of additional Multimodal Cues such as auditory cues to improve performance, Additional Knob Shapes, Additional Knob Textures, and many others.

The exploration of different Factors may lead to an even better design of the Haptic Interface system.

### **16.1.5 Human Factors Testing for Haptic Joystick**

Now that the Haptic Knob design has been explored using the Human Factors experiment, the next step would be to extend the test to include the Haptic Joystick. Questions that can be addressed are;

- Do the results for the Knob experiment apply to the Joystick as well? Does the Ball-Grip – Textured surface – Continuous Sine Wave combination also yield the most effective interface for the Haptic Joystick?
- Are there Handle-Grasp configurations that would be even more effective for a joystick interface?
- Are there additional factors that can be studied in reference to the Joystick? Such as – channel width, number of channel, Zone sizes, etc.

Exploration of these and other design factors would allow the Joystick design to be improved in the same way that the Knob's design was improved through the results obtained from the experimental testing.

### **16.1.6 Human Trials for Users with Hand Injury**

The exploration of the test subject suffering from Carpal Tunnel Syndrome, suggested that additional testing would be useful. In order for a Haptic Interface to be viable it must be able to work well for almost any user. This includes people with less-than-perfect sensory capabilities in their hands.

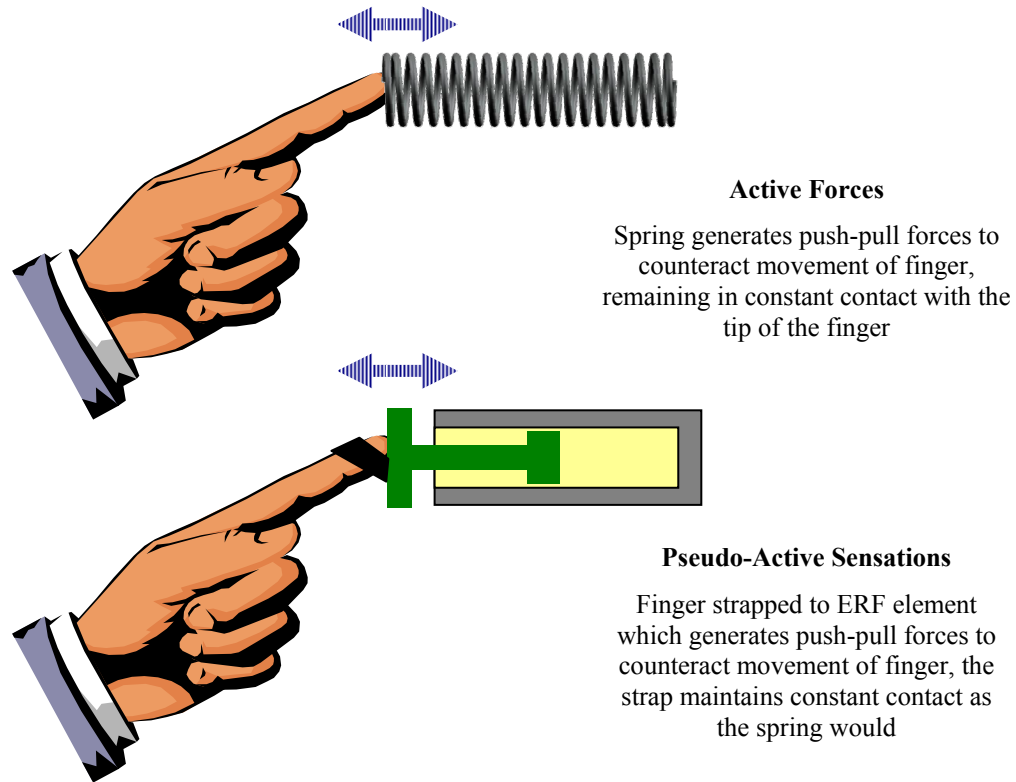
Formal experiments to explore this question would help to improve the device for use with non-ideal subjects.

### **16.1.7 Simulated Active Forces**

During the course of the research, I wrote a simple program for the Haptic Knob to present detents based not on positional data, but rather timing data alone. This allowed for troubleshooting the system, without needing the encoder to be operational.

This program generated detents on a timed schedule rather than one based on position. When the system was used it was shocking to discover how much the detents felt like actual vibrations when the Knob was used. Due to the timing-based detents, the bumps were felt on a regular schedule, and felt to me and additional observers as if the system were vibrating.

Sine the ERF actuator only provides passive forces it is impossible for the system to actually vibrate. However, since the *sensation* of vibration did exist, it suggests that with the right design method, additional pseudo-active sensations can be generated. For example, Figure 16-2 shows a concept for simulating a spring within the limits of the passive actuation system.



**Figure 16-2:** Possible Method to Generate Pseudo-Active Sensations with ERF Actuator

Pressing a spring with a finger provides resistance when pushing and maintains contact between the spring and the finger when the finger is pulled back, and provides a resistive sensation when pulled far enough. By physically attaching the finger to a passive ERF device it may be possible to fool the senses into thinking that the same sequence of forces is being felt.

Additional schemes are possible, and future research may answer whether it is possible to generate pseudo-active sensations using devices that can only generate passive forces. If pseudo-active sensations are possible it would open up a new realm of possibilities for the use of the Haptic Interfaces designed in the course of this project.

## 16.2 Conclusions

In almost any industry, as well as the automotive industry, the increase in controls has created a desire to simplify and enhance the human-machine interface by using innovative technological solutions. I have proposed that the use of haptic feedback devices, that can present information to a user in the form of tactile and force sensations, can improve that interface by employing additional methods of presenting information, beyond the visual and auditory methods in effect today.

I have proposed that the use of Electro-Rheological Fluid (ERF) -based actuators to create these haptic interfaces will result in small, energy-efficient, and lightweight, yet powerful, interfaces. By controlling the viscous properties of ERFs, through the simple application of an electric field, it is possible to generate a large range of force sensations to convey large and varied amounts of data. By being able to simulate the “feel” of many existing control devices, and changing these feelings “on-the-fly” using computer controlled devices, it will be possible to combine many of the interfaces encountered today into simpler more intuitive devices. In addition, newer and more innovative interfaces can be developed.

I presented the design of two ERF-based actuators . I reviewed the analytical models and performed parametric analyses. I also described experimental systems and data. My results indicate that it is possible to control the ERF-actuators and that more robust control methods may be useful for future refinements.

The actuators are able to produce different resistive torque values based on the applied voltage, and the mode of operation (static or dynamic). The torque produced can be controlled electronically to simulate different effects such as detents, limit stops,

friction, etc. This type of haptic feedback interface system enhances the human-machine interface by increasing the amount of information transmitted to the operator while using a simpler interface to do so.

I presented concepts for applying the haptic devices for the Haptic Knob and the Haptic Joystick. I developed and created different force sensation concepts using software models.

I developed a second generation actuator based on one of the original actuator designs. It increased the force capabilities while decreasing the power consumption of the system. I then incorporated this actuator into newer Haptic Knob and Haptic Joystick systems. I wrote updated software to control those systems and allow for more robust force simulations.

I used the Haptic Knob to explore three different design factors through a Human Factors experiment that asked the test subjects to use the knob for an intricate counting task to determine the accuracy possible with the Knob system. The three factors tested were Knob Shape, Knob Texture and Detent Style. The experimental results showed that the most effective knob shapes were those that generate wrist motion in the user, freeing up the fingers to sense the force cues being presented. The textured knobs performed better than the smooth and the detents which maintained a continuous force level performed the best. These conclusions allow for the development of a more accurate and capable Haptic Knob interface based on the better performing design choices.

I have also presented some ideas for future steps to be taken. A number of avenues of exploration exist to further develop and refine the haptic interfaces using ERF actuators.

This research project has shown that ERF-based Haptic Interface systems are viable and can present understandable and useful force information. These results have been promising and there is the potential for much excitement to continue this research to further enhance the human-machine interface.

## 17 REFERENCES

- Arai F., Akiko K., Fukuda T., Matsuura H. and Ota H., "Safety Oriented Mechanism and Control Using ER Fluid in the Joint," *Proceedings of the 1998 IEEE International Conference on Robotics and Automation*, Leuven, Belgium, May 1998, pp. 2482-2487.
- Bar-Cohen Y., Pfeiffer C., Mavroidis C. and Dolgin B., "MEMICA: a Concept for Reflecting Remote-Manipulator Forces", *NASA Tech Briefs*, Vol. 24, No. 2, pp. 7a-7b, 2000a.
- Bar-Cohen Y., Mavroidis C., Bouzit M., Dolgin B., Harm D., Kopchok G., White R., "Virtual Reality Robotic Operation Simulations Using MEMICA Haptic System," *SmartSystems 2000: The International Conference for Smart Systems and Robotics for Medicine and Space Applications*, September 6 to 8, 2000b, Houston, Texas.
- Bar-Cohen Y., Mavroidis C., Pfeiffer C., Culbert C. and Magruder D., "Haptic Interfaces", Chapter in *Automation, Miniature Robotics and Sensors for Non-Destructive Testing and Evaluation*, Y. Bar-Cohen Editor, The American Society for Nondestructive Testing, Inc. (ASNT), pp. 461-468, 2000c.
- Bar-Cohen Y., Mavroidis C., Bouzit M., Pfeiffer C. and Dolgin B., "Remote Mechanical Mirroring using Controlled Stiffness and Actuators (MEMICA)", NTR, January 18, 1999, Item No. 0237b, Docket 20642, January 27, 1999. Rutgers U. Docket #99-0056, A US and International PCT patent application has been filed by Rutgers University in September 2000d.
- Bar-Cohen, Y. and Breazeal, C., *Biologically Inspired Intelligent Robots*, Y. Bar-Cohen (Ed.), ISBN 0-8194-4872-9, SPIE Press Monograph Series, May 2003
- Biorobotics Laboratory, Harvard University, <http://biorobotics.harvard.edu>.
- Block, H. and Kelly, J. P., "Electro-Rheology", *Journal of Physics, D: Applied Physics*, Vol. 21, 1988, pp. 1661.
- Böse H., Berkemeier J. and Trendler A., "Haptic System Based on Electrorheological Fluid," *Proceedings of the ACTUATOR 2000 Conference*, 19-21 June 2000, Bremen GERMANY.
- Bouzit M., Popescu G., Burdea G., and Boian R., "The Rutgers Master II-ND Force Feedback Glove", *Proceedings of IEEE VR 2002 Haptics Symposium*, pp. 145-152, Orlando FL, March 2002.
- Bridgestone-Firestone Inc., <http://www.bridgestone-firestone.com>
- Bullough W. A., Johnson A. R., Hosseini-Sianaki A., Makin J. and Firoozian R., "Electro-Rheological Clutch: Design, Performance Characteristics and Operation," *Proceedings of the Institution of Mechanical Engineers. Part I, Journal of Systems and Control Engineering*, Vol. 207, No. 2, 1993, pp. 87-95.
- Burdea, G., *Force and Touch Feedback for Virtual Reality*, New York, John Wiley and Sons, 1996.

- Caldwell D., Medrano-Cerda G. and Bowler C.J., 1997, "Investigation of Bipedal Robot Locomotion Using Pneumatic Muscle Actuators", *International Conference on Robotics and Automation*, Albuquerque, NM, pp. 799-804.
- Carpal-Tunnel-Syndrome.net, <http://carpal-tunnel-syndrome.net>
- Choi, S. B., "Vibration Control of a Flexible Structure Using ER Dampers," *Transactions of the ASME, Journal of Dynamic Systems, Measurement and Control*, Vol. 121, 1999, pp. 134-138.
- Conrad H., "Properties and Design of Electrorheological Suspensions," *MRS Bulletin*, Vol. 23, No. 8, August 1998, pp. 35-42.
- Coulter J. P., Weiss K. D. and Carlson D. J., "Engineering Applications of Electrorheological Materials," in *Advances in Intelligent Material Systems and Structures-Volume 2: Advances in Electrorheological Fluids*, Kohudic M. A. (Editor), Technomic Publishing Company, Inc., Lancaster, PA, 1994, pp. 64-75.
- Division of Research Integrity, Northeastern University, Boston, MA, [http://www.research.neu.edu/research\\_integrity/human\\_subjects/review\\_board/](http://www.research.neu.edu/research_integrity/human_subjects/review_board/)
- Duclos, T., Carlson, J., Chrzan, M. and Coulter, J. P., "Electrorheological Fluids – Materials and Applications," in *Intelligent Structural Systems*, Tzou and Anderson (Editors), Kluwer Academic Publishers, Netherlands, 1992, pp. 213-241.
- ER Fluids Developments Ltd, "Electro-Rheological Fluid LID 3354," *Technical Information Sheet*, United Kingdom, 1998.
- Furusho J., Zhang G. and Sakaguchi M., "Vibration Suppression Control of Robot Arms Using a Homogeneous-Type Electrorheological Fluid," *Proceedings of the 1997 IEEE International Conference on Robotics and Automation*, Albuquerque, NM, 1997, pp. 3441-3448.
- Furusho J., Sakaguchi M., Takesue N. and Koyanagi K., "Development of ER Brake and its Application to Passive Force Display", *Proceedings of the 8th International Conference on ER Fluids and MR Suspensions*, Nice, France, 2001, pp.57-62
- Gast, A. P., and Zukoski, C. F., "Electrorheological Suspensions as Colloidal Suspensions," *Advances in Colloid and Interface Science*, Vol. 30, 1989, pp. 153.
- Ghandhi M. V., Thompson B. S. and Shakir S., "Electro-Rheological Fluid Based Articulating Robotic Systems," in *Advances in Design Automation: Vol. 2; Robotics, Mechanisms and Machine Systems*, ASME DE Vol. 10-2, 1987, pp. 1-10.
- Health Physics Society, <http://www.hps.org/publicinformation/ate/q1433.html>, 2001a
- Health Physics Society, <http://www.hps.org/hpspublications/articles/microwaveoven.html>, 2001b
- Human Machine Interface Laboratory, Center for Advanced Information Processing, Rutgers University, <http://www.caip.rutgers.edu/vrlab/>.
- Human-Machine Interaction Subarea, Real World Active Intelligence Area, Department of Computer-Controlled Mechanical Systems, Osaka University, Japan <http://www-dyna.mech.eng.osaka-u.ac.jp/welcome-e.html>



- Hurmuzlu Y., Ephanov A., and Stoianovici D. (1998) "Effect of a Pneumatically Driven Haptic Interface on the Perceptual Capabilities of Human Operators ", *Presence*, MIT Press, Vol. 7, No. 3 pp. 290-307.
- Immersion Corporation, *Cyberglove II*,  
[http://www.immersion.com/3d/products/cyber\\_glove.php](http://www.immersion.com/3d/products/cyber_glove.php)
- Immersion Corporation, *Cyberforce*,  
[http://www.immersion.com/3d/products/cyber\\_force.php](http://www.immersion.com/3d/products/cyber_force.php)
- Immersion Corporation, *Cybergrasp*,  
[http://www.immersion.com/3d/products/cyber\\_grasp.php](http://www.immersion.com/3d/products/cyber_grasp.php)
- Institut für Mikrotechnik Mainz,  
[http://www.imm-mainz.de/seiten/en/u\\_050204040411\\_2358.php](http://www.imm-mainz.de/seiten/en/u_050204040411_2358.php)
- Intelligent Mechanical and Manufacturing Systems Research, Department of Mechanical, Materials and Manufacturing, Engineering, University of Newcastle upon Tyne  
<http://www.ncl.ac.uk/mmmeng/research/pmt/tactile.html>.
- JHU Haptics Lab, <http://www.haptics.me.jhu.edu/research/>
- Kenaley G. L. and Cutkosky M. R., "Electrorheological Fluid-Based Robotic Fingers With Tactile Sensing," *Proceedings of the 1989 IEEE International Conference on Robotics and Automation*, Scottsdale AR, pp. 132-136 (1989).
- Kroemer, K, Kroemer, H. and Kroemer-Elbert, K., *Ergonomics: How to Design for Ease and Efficiency*, Upper Saddle River, NJ, Prentice Hall, 2<sup>nd</sup> ed., 2003a, pp. 369
- Kroemer, K, Kroemer, H. and Kroemer-Elbert, K., *Ergonomics: How to Design for Ease and Efficiency*, Upper Saddle River, NJ, Prentice Hall, 2<sup>nd</sup> ed., 2003b, pp. 370
- Kroemer, K, Kroemer, H. and Kroemer-Elbert, K., *Ergonomics: How to Design for Ease and Efficiency*, Upper Saddle River, NJ, Prentice Hall, 2<sup>nd</sup> ed., 2003c, pp. 372-373
- Lampe D., *Materials Database on Commercially Available Electro- and Magnetorheological Fluids (ERF and MRF)*, <http://www.tu-dresden.de/mwlr/lampe/HAUENG.HTM>, updated on 01/30/1997.
- Logitech Inc., <http://www.logitech.com>.
- Luecke, G.R., and Chai, Y.H., "Contact Sensation in the Synthetic Environment Using the ISU Force Reflecting Exoskeleton," *IEEE Virtual Reality Annual Symposium (VRAS'97)*, pg. 192-198, March 3-5, 1997, Albuquerque, NM.
- Mahvash M. and Okamura A. M., "A Fracture Mechanics Approach to Haptic Synthesis of Tissue Cutting with Scissors," *First Joint Eurohaptics Conference and Symposium on Haptic Interfaces for Virtual Environment and Teleoperator Systems*, 2005, pp. 356-362
- Mavroidis C., Pfeiffer C. and Bar-Cohen Y., "Controlled Compliance Haptic Interface Using Electro-Rheological Fluids," *Proceedings of the 2000 SPIE Conference on Electro-Active Polymer Actuators and Devices (EAPAD 2000)*, Newport Beach, CA, March 5-9, 2000a, Vol. 3987, pp. 300-310.

- Mavroidis C., Pfeiffer C., Celestino J. and Bar-Cohen Y., "Design and Modeling of an Electro-Rheological Fluid Based Haptic Interface," *Proceedings of the 2000 ASME Mechanisms and Robotics Conference*, Baltimore MD, September 10-13, 2000b, Paper DETC2000/MECH-14121.
- Mavroidis C., Pfeiffer C., Lennon J., Paljic A., Celestino J., and Bar-Cohen Y., "Modeling and Design of an Electro-Rheological Fluid Based Haptic System for Tele-Operation of Space Robots," *Proceedings of the ROBOTICS 2000 Conference: The 4<sup>th</sup> International Conference and Exposition/Demonstration on Robotics for Challenging Situations and Environments*, February 27-March 2, 2000c, Albuquerque, NM, pp. 174-180.
- Mavroidis C., Bar-Cohen Y. and Bouzit M., "Haptic Interfacing Using Electrorheological Fluids," Topic 7, Chapter 19, *Electroactive Polymer (EAP) Actuators as Artificial Muscles - Reality, Potential and Challenges*, Y. Bar-Cohen (Ed.), ISBN 0-8194-4054-X, SPIE Press, February 2001, pp. 567-594.
- McMaster-Carr, <http://www.mcmaster.com>
- Merriam-Webster's Online Dictionary, <http://www.m-w.com>
- Microsoft Corp., <http://www.microsoft.com/hardware/sidewinder/devices/default.asp>.
- Monkman G. J., "Electrorheological Tactile Display", *Presence*, MIT Press, Vol. 1, No. 2, 1992.
- NASA Space Johnson Center, Robot Systems Technology Branch, Robonaut Project, <http://robonaut.jsc.nasa.gov>.
- National Instruments, <http://www.ni.com>
- Nikitzuk, J., "Rehabilitative Knee Orthosis Driven By Electro-Rheological Fluid Based Actuators", Masters of Science Thesis, Department of Mechanical and Aerospace Engineering, Rutgers University, 2004.
- NIST Tactile Visual Display, [http://www.nist.gov/public\\_affairs/factsheet/visualdisplay.htm](http://www.nist.gov/public_affairs/factsheet/visualdisplay.htm).
- PERCRO, L-Exos <http://www.percro.org/index.php?pageId=L-Exos>
- Ropper, A., Brown, R., Adams, R. and Victor, M., *Adams and Victor's Principles of Neurology*, Eighth Edition, McGraw-Hill Companies, New York, 2005.
- Sakaguchi M. and Furusho J., "Development of ER Actuators and Their Applications to Force Display Systems," *Proceedings of the 1998 IEEE Virtual Reality Annual International Symposium (VRAIS)*, Atlanta, GA, 1998, pp. 66-70.
- Sarcos Inc., <http://www.sarcos.com/humanintfc.html>
- Seed M., Hobson G. S., Tozer R. C. and Simmonds A. J., "Voltage-Controlled Electrorheological Brake," *Proceedings of the IASTED International Symposium on Measurements, Processes and Controls*, Sicily, September 1986, pp. 280-284.
- Sensable Technologies, *The Phantom*, <http://www.sensable.com/haptics/products/phantom.html>.

- Sherman KP, Ward JW, Sherman VY, Mohsen AMMA "Surgical Trainee Assessment using a VE Knee Arthroscopy Training System (VE-KATS): Experimental Results", *Proceedings of Medicine Meets Virtual Reality 2001*, pages 465-470. IOS Press, 2001
- Simulation and Visualisation Research Group, Department of Computer Science, The University of Hull, UK, <http://www2.dcs.hull.ac.uk/simmod/index.htm>.
- Smart Technology Ltd, "Technical Information Sheet – Electro-Rheological Fluid LID 3354S", 2001
- Sproston J. L., Stanway R., Williams E. W. and Rigby S., "The Electrorheological Automotive Engine Mount," *Journal of Electrostatics*, Vol. 32, 1994, pp. 253-259.
- SPSS Inc., <http://www.spss.com/spss/>
- Stanway, R., Sproston, J. L., and El-Wahed, A. K., "Applications of Electro-Rheological Fluids in Vibration Control: A Survey," *Smart Materials and Structures*, Vol. 5, No. 4, 1996, pp. 464-482.
- Stramler, James H., *The Dictionary for Human Factors/Ergonomics*, Boca Raton, LA: CRC Press, 1993
- Systems Laboratory, Southern Methodist University, <http://cyborg.seas.smu.edu/syslab/PHI/MasterArm.html>.
- Taylor P. M., Hosseini-Sianaki A. and Varley C. J., "An Electrorheological Fluid-based Tactile Array for Virtual Environments," *Proceedings of the 1996 IEEE International Conference on Robotics and Automation*, Minneapolis, MN, April 1996a, pp. 18-23.
- Taylor P. M., Hosseini-Sianaki A. and Varley C. J., "Surface Feedback for Virtual Environment Systems Using Electrorheological Fluids," *International Journal of Modern Physics B*, Vol. 10, No. 23 & 24, 1996b, pp. 3011-3018.
- Trek Inc., <http://www.trekinc.com>
- Urdan, Timothy C., *Statistics in Plain English, Second Edition*, Mahwah, NJ: Lawrence Erlbaum Associates, 2005
- VRAC – Virtual Reality Applications Center, Iowa State University, <http://www.vrac.iastate.edu/research/robotics/magnetic/index.html>.
- Virtual Reality Laboratory, University of Tsukuba, Japan, [http://intron.kz.tsukuba.ac.jp/vrlab\\_web/wearablemaster/wearablemaster\\_e.html](http://intron.kz.tsukuba.ac.jp/vrlab_web/wearablemaster/wearablemaster_e.html).
- Virtual Space Devices, Inc., <http://www.vsd.bz/present.htm>
- Virtual Technologies, <http://www.virtex.com/> 1999.
- Wagner, C.R., Lederman, S.L., Howe, R.D. "Design and Performance of a Tactile Shape Display Using RC Servomotors", *Haptics-e: The Electronic Journal Of Haptics Research*, Vol. 3, No. 4, Aug 6, 2004 (www.haptics-e.org)
- Weiss K. D., Carlson D. J. and Coulter J. P., "Material Aspects of Electrorheological Systems," in *Advances in Intelligent Material Systems and Structures-Volume 2: Advances in Electrorheological Fluids*, Kohudic M. A. (Editor), Technomic Publishing Company, Inc., Lancaster, PA, 1994, pp. 30-52.

Winslow W. M., "Induced Fibrillation of Suspensions," *Journal of Applied Physics*, Vol. 20, 1949, pp. 1137.

Wood D., "Editorial: Tactile Displays: Present and Future," *Displays-Technology and Applications*, Vol. 18, No. 3, 1998, pp. 125-128.

## 18 APPENDIX

### 18.1 Datasheet and Wiring Diagram for Encoder Interface (4 Pages)



#### QUADRATURE CLOCK CONVERTER

July 2005

##### FEATURES:

- x1, x2 and x4 resolution
- Programmable output pulse width (200ns to 140µs)
- Excellent regulation of output pulse width
- TTL and low voltage CMOS compatible I/Os
- +3V to +5.5V operation (VDD - VSS)
- LS7183, LS7184 (DIP);
- LS7183-S, LS7184-S (SOIC) - See Figure 1

##### DESCRIPTION:

The LS7183 and LS7184 are CMOS quadrature clock converters. Quadrature clocks derived from optical or magnetic encoders, when applied to the A and B inputs of the LS7183/LS7184, are converted to strings of Up Clocks and Down Clocks (LS7183) or to a Clock and an Up/Down direction control (LS7184). These outputs can be interfaced directly with standard Up/Down counters for direction and position sensing of the encoder.

##### INPUT/OUTPUT DESCRIPTION:

###### RBIAS (Pin 1)

Input for external component connection. A resistor connected between this input and Vss adjusts the output clock pulse width (Tow).

###### VDD (Pin 2)

Supply Voltage positive terminal.

###### VSS (Pin 3)

Supply Voltage negative terminal.

###### A, B (Pin 4, Pin 5)

Quadrature Clock inputs A and B. Directional output pulses are generated from the A and B clocks according to Fig. 2. A and B inputs have built-in immunity for noise signals less than 50ns duration (Validation delay, T<sub>VD</sub>). The A and B inputs are inhibited during the occurrence of a directional output clock (UPCK or DNCK), so that spurious clocks resulting from encoder dither are rejected.

###### MODE (Pin 6)

MODE is a 3-state input to select resolution x1, x2 or x4. The input quadrature clock rate is multiplied by factors of 1, 2 and 4 in x1, x2 and x4 mode respectively in producing the output UP/DN clocks (See Fig. 2). x1, x2 and x4 modes selected by the MODE input logic levels are as follows:

Mode = 0 : x1 selected  
 Mode = 1 : x2 selected  
 Mode = Float : x4 selected

##### PIN ASSIGNMENT - TOP VIEW

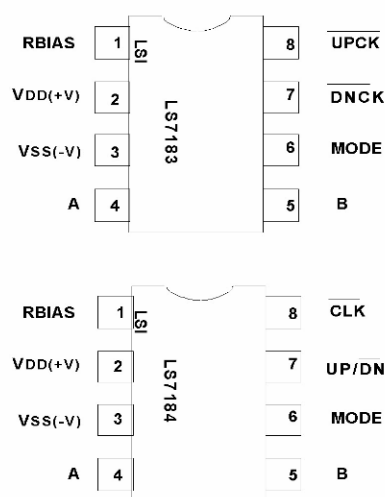


FIGURE 1

###### LS7183 - DNCK (Pin 7)

In LS7183, this is the DOWN Clock Output. This output consists of low-going pulses generated when A input lags the B input.

###### LS7184 - UP/DN (Pin 7)

In LS7184, this is the count direction indication output. When A input leads the B input, the UP/DN output goes high indicating that the count direction is UP. When A input lags the B input, UP/DN output goes low, indicating that the count direction is DOWN.

###### LS7183 - UPCK (Pin 8)

In LS7183, this is the UP Clock output. This output consists of low-going pulses generated when A input leads the B input.

###### LS7184 - CLK (Pin 8)

In LS7184, this is the combined UP Clock and DOWN Clock output. The count direction at any instant is indicated by the UP/DN output (Pin 7).

**NOTE:** For the LS7184, the timing of CLK and UP/DN requires that the counter interfacing with LS7184 counts on the rising edge of the CLK pulses.

**ABSOLUTE MAXIMUM RATINGS:**

PARAMETER	SYMBOL	VALUE	UNITS
DC Supply Voltage	$V_{DD} - V_{SS}$	7.0	V
Voltage at any input	$V_{IN}$	$V_{SS} - 0.3$ to $V_{DD} + 0.3$	V
Operating temperature	$T_A$	-20 to +85	°C
Storage temperature	$T_{STG}$	-55 to +150	°C

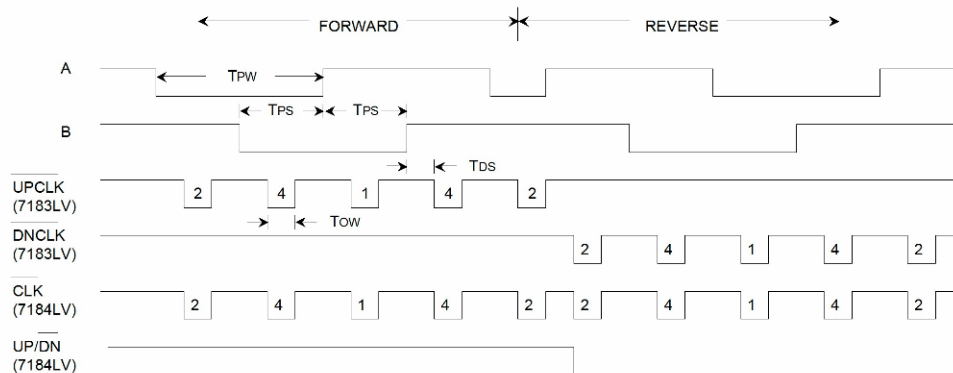
**DC ELECTRICAL CHARACTERISTICS:**(Unless otherwise specified  $V_{DD} = 3V$  to  $5V$  and  $T_A = -20^{\circ}C$  to  $+85^{\circ}C$ )

PARAMETER	SYMBOL	MIN	TYPE	MAX	UNITS	CONDITON
Supply Voltage	$V_{DD}$	3.0	-	5.5	V	-
Supply current	$I_{DD}$	-	30	45	$\mu A$	$V_{DD} = 3V$
	$I_{DD}$	-	110	150	$\mu A$	$V_{DD} = 5V$
MODE input:						
Logic 0	$V_{ml}$	-	-	0.6	V	-
Logic 1	$V_{mh}$	$V_{DD} - 0.6$	-	-	V	-
Logic float	$V_{mf}$	$(V_{DD}/2) - 0.5$	$V_{DD}/2$	$(V_{DD}/2) + 0.5$	V	-
Logic 0 input current	$I_{ml}$	-	3.0	5.0	$\mu A$	$V_{DD} = 3V$
	$I_{ml}$	-	12.0	16.0	$\mu A$	$V_{DD} = 5V$
Logic 1 input current	$I_{mh}$	-	-3.0	-5.0	$\mu A$	$V_{DD} = 3V$
	$I_{mh}$	-	-12.0	-16.0	$\mu A$	$V_{DD} = 5V$
A,B inputs:						
Logic 0	$V_{ABl}$	-	-	$0.3V_{DD}$	V	-
Logic 1	$V_{ABh}$	$0.7V_{DD}$	-	-	V	-
Input current	$I_{ABik}$	-	0	10	nA	-
RBIAS input:						
External resistor	$R_B$	5k	-	10M	ohm	-
All outputs:						
Sink current	$I_{ol}$	-1.2	-1.8	-	mA	$V_O = 0.5V, V_{DD} = 3V$
	$I_{ol}$	-2.5	-3.5	-	mA	$V_O = 0.5V, V_{DD} = 5V$
Source current	$I_{oh}$	1.2	1.8	-	mA	$V_O = 2.5V, V_{DD} = 3V$
	$I_{oh}$	2.5	3.5	-	mA	$V_O = 4.5V, V_{DD} = 5V$

**TRANSIENT CHARACTERISTICS**

(TA = -20°C to +85°C)

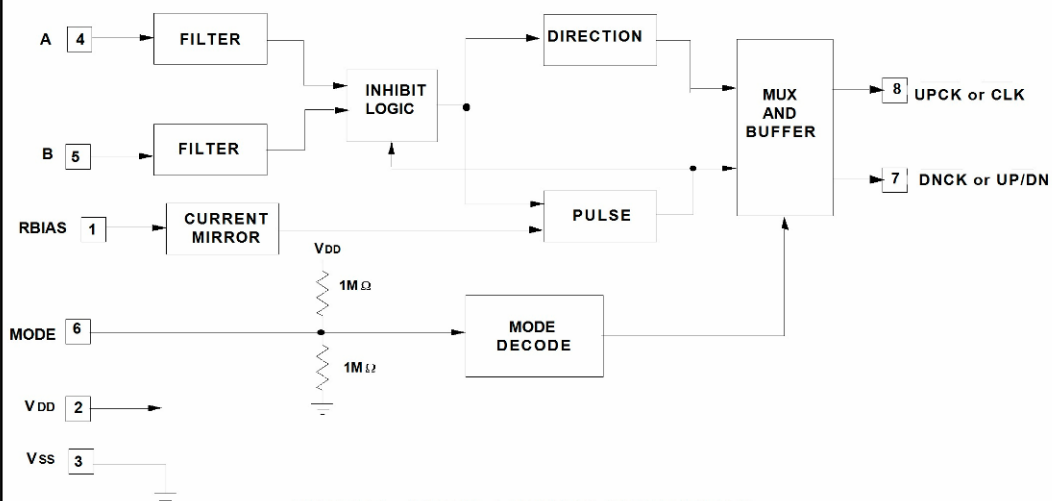
PARAMETER	SYMBOL	MIN	TYPE	MAX	UNITS	CONDITON
Output Clock Pulse Width	$T_{OW}$	190	-	-	ns	See Fig. 2
A,B inputs:						
Validation Delay	$T_{VD}$	-	25	50	ns	$V_{DD} = 5V$
	$T_{VD}$	-	50	100	ns	$V_{DD} = 3V$
Phase Delay	$T_{PS}$	$T_{VD} + T_{OW}$	-	Infinite	s	-
Pulse Width	$T_{PW}$	$2T_{PS}$	-	Infinite	s	-
Frequency	$f_{A,B}$	-	-	$1/(2T_{PW})$	Hz	-
Inupt to Output Delay	$T_{DS}$	-	200	270	ns	$V_{DD} = 3V$
	$T_{DS}$	-	110	150	ns	$V_{DD} = 5V$



**NOTE:** Output clocks labelled 1, 2 and 4 have the following interpretations.

- 1: Generated in x1, x2 and x4 modes
- 2: Generated in x2 and x4 modes only
- 4: Generated in x4 mode only

**FIGURE 2. LS7183, LS7184 INPUT/OUTPUT TIMING**



**FIGURE 3. LS7183, LS7184 BLOCK DIAGRAM**

The information included herein is believed to be accurate and reliable. However, LSI Computer Systems, Inc. assumes no responsibilities for inaccuracies, nor for any infringements of patent rights of others which may result from its use.



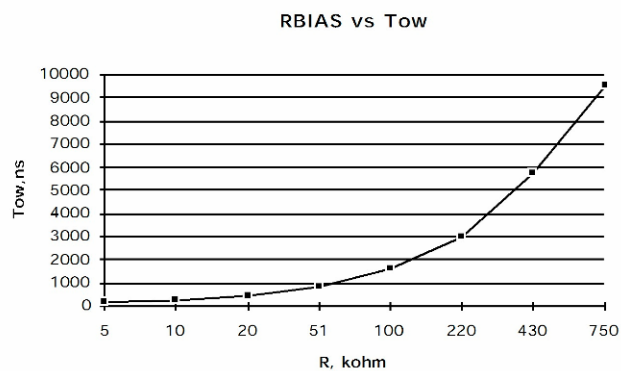
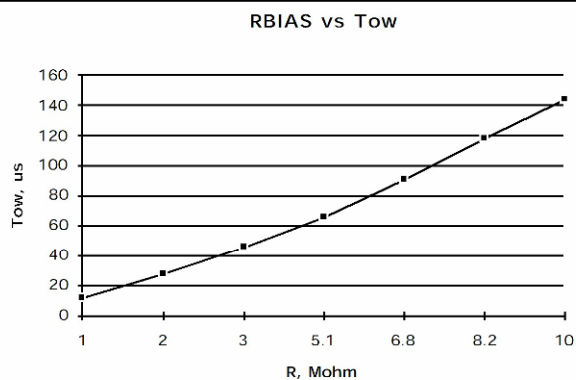
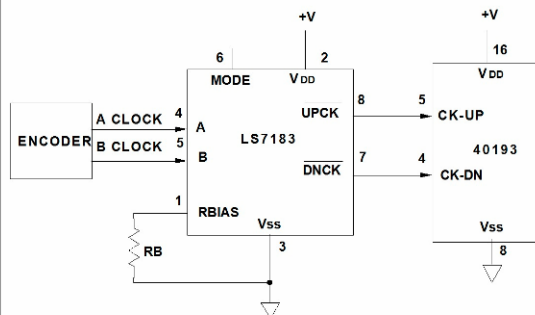
Figure 4. Bias resistance vs pulse width. R in  $k\Omega$ .Figure 5. Bias resistance vs pulse width. R in  $M\Omega$ .

FIGURE 6A. TYPICAL APPLICATION FOR LS7183 IN x4 MODE

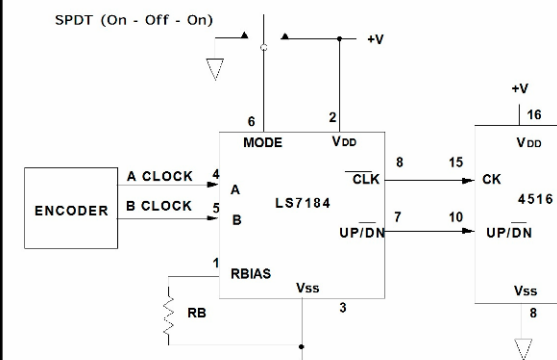
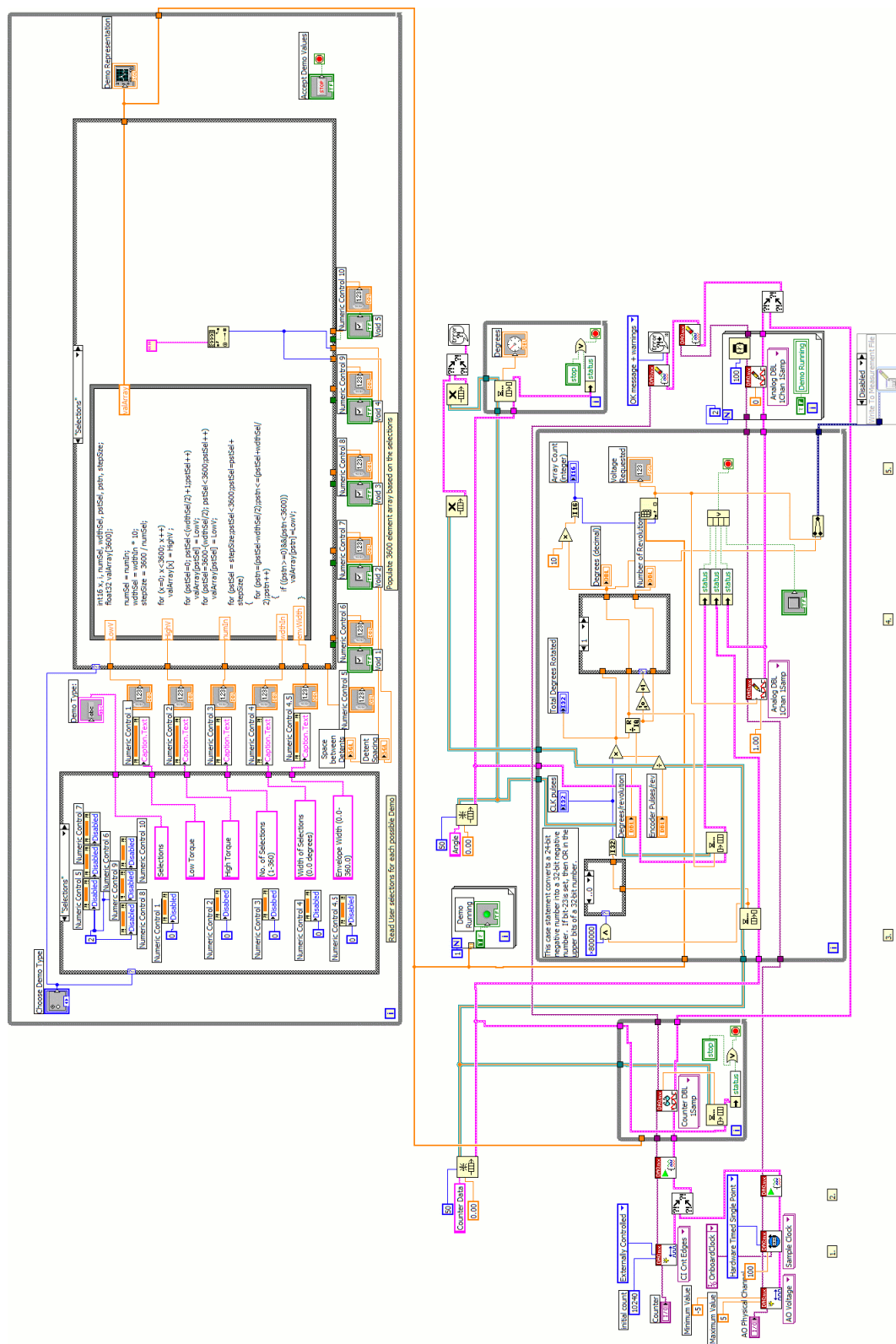


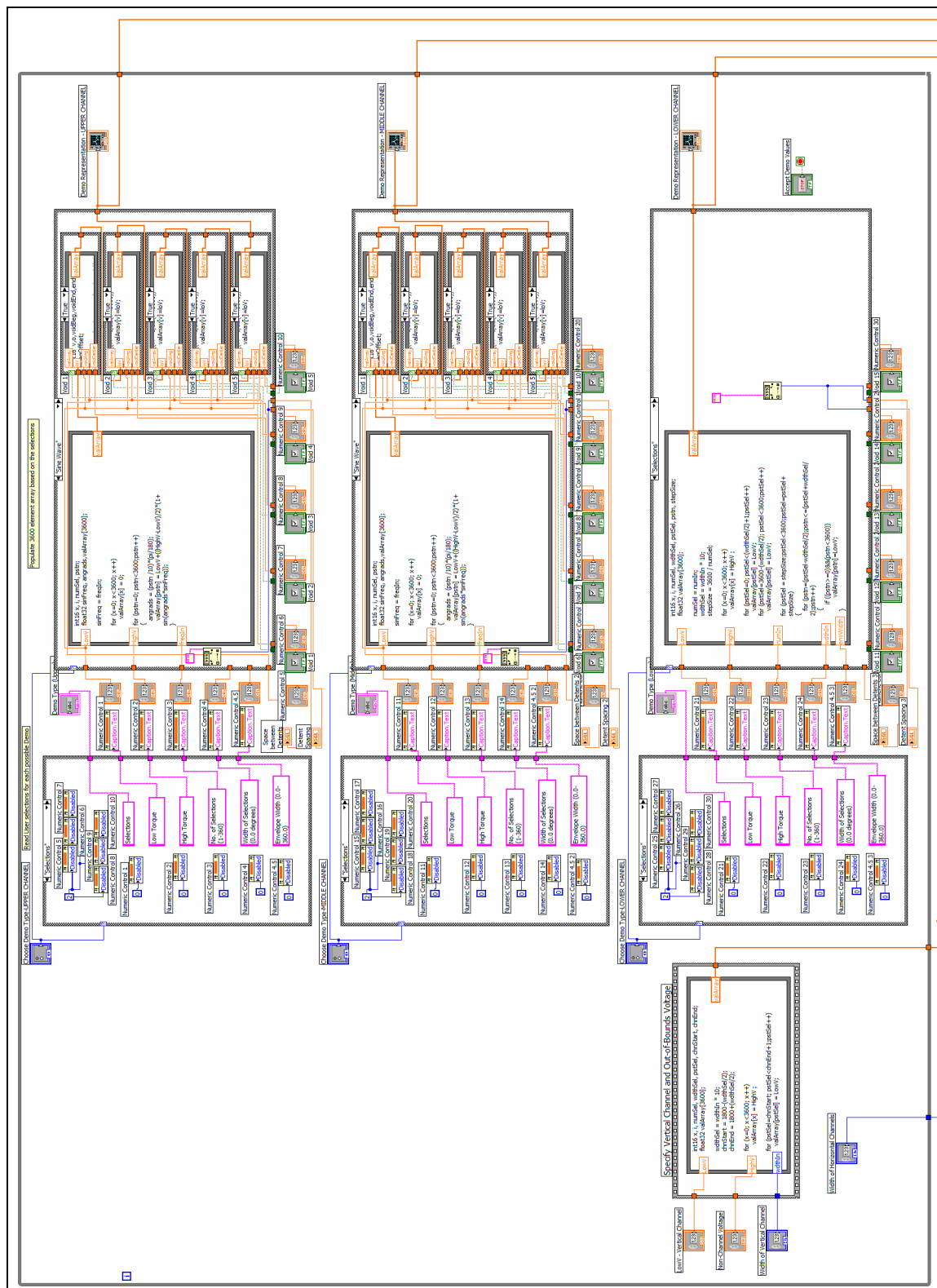
FIGURE 6B. TYPICAL APPLICATION FOR LS7184 WITH MODE SELECTION



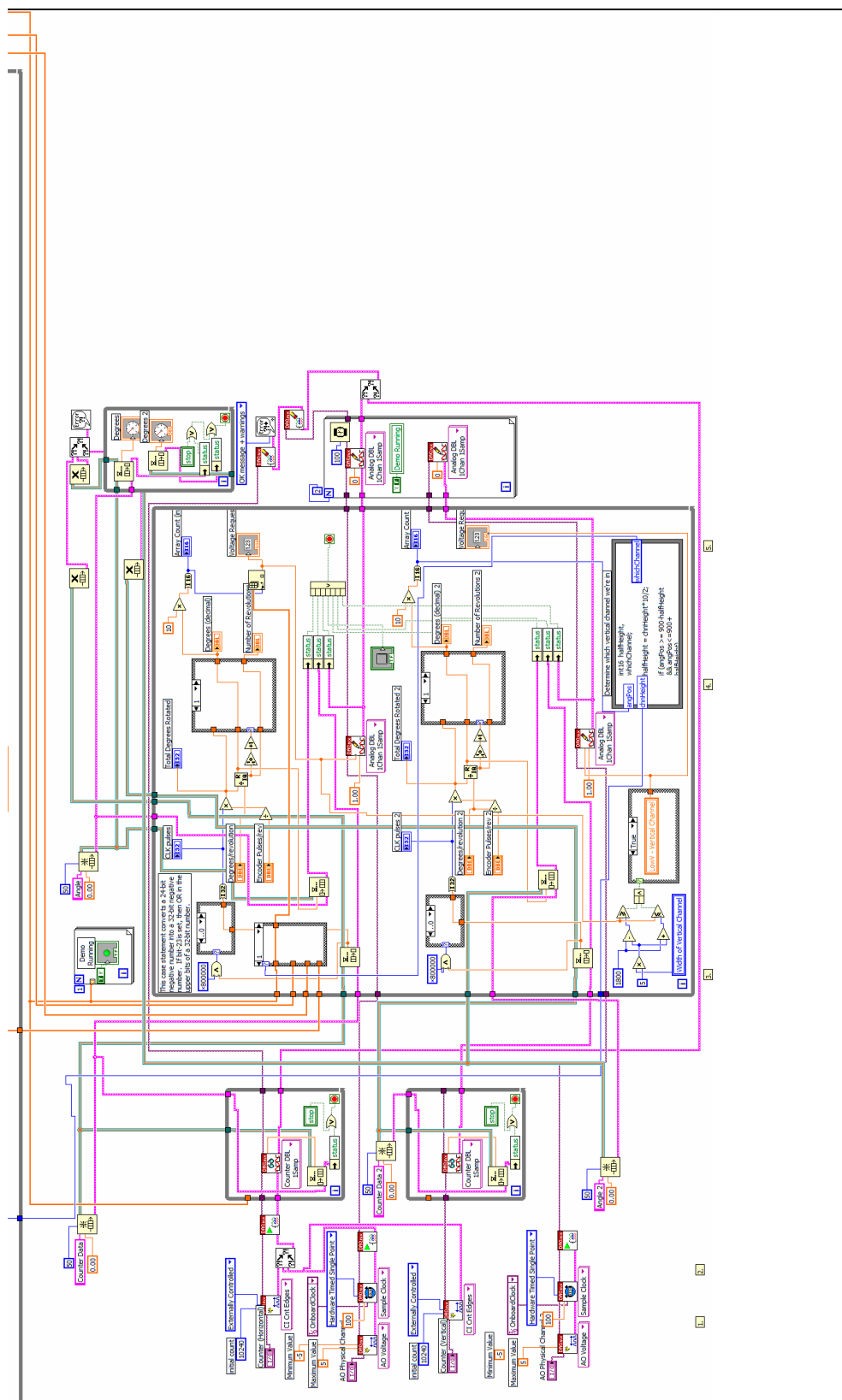
## 18.2 LabVIEW Program – Haptic Knob



## 18.3 LabView Program – Haptic Joystick (2 Pages)



(Continued, Next Page)



## 18.4 IRB Approval, Northeastern University

### 18.4.1 IRB Application (10 Pages)

#### Appendix A Application for Approval for Use of Human Participants in Research

Before completing this application, please read the *Policies and Procedures for Human Research Protections* to understand the responsibilities for which you are accountable as an investigator in conducting research with human participants. The document, *Application Instructions*, provides additional assistance in preparing this submission. ***Incomplete applications will be returned to the investigator. You may complete this application online and save it as a Word document.***

*If this research is related to a grant, contract proposal or dissertation, a copy of the full grant/contract proposal/dissertation must accompany this application.*

#### A. Investigator Information

Principal Investigator (PI cannot be a student) Constantinos Mavroidis

Investigator is (circle one) NU Faculty ~~NU Staff~~ Other \_\_\_\_\_

College Engineering

Department Mechanical Engineering

Address 334 Snell Engineering

Telephone 617-373-4121 Email Mavro@coe.neu.edu

Is this student research? YES ~~NO~~ If yes, provide the following information:

Student Name Avi (Allen) Fisch Undergrad    MA/MS    PhD X

Campus Address 334 Snell Engineering Anticipated graduation date September 06

Telephone 617-373-7733 Email FischA@aol.com

Contact Person Constantinos Mavroidis Tel: 617-373-4121

Address 334 Snell Engineering Email Mavro@coe.neu.edu

#### B. Protocol Information

Title ERF Based Force Feedback Interface

Projected # subjects 20 Begin date of project June 15, 2006 End date June 14, 2007  
month, day, year month, day, year

Anticipated funding source for project (or none) none

Has/will this proposal been/be submitted through: DSPA    Provost    Corp & Foundation

*For NU IRB use:*

Date Received: \_\_\_\_\_ NU IRB No. \_\_\_\_\_

Review Category: \_\_\_\_\_ Approval Date \_\_\_\_\_

C. Will participants be:	YES	NO	Does the project involve:	YES	NO
Children (<age 18)?	_____	<u>X</u>	Blood Removal?	_____	<u>X</u>
Northeastern U. students?	<u>X</u>	_____	Investigational <del>drug</del> <u>device</u> ?	<u>X</u>	_____
Institutionalized persons/prisoners?	_____	<u>X</u>	Audiotapes/Videotapes?	_____	<u>X</u>
Cognitively impaired persons?	_____	<u>X</u>			
Non or Limited English-speaking?	_____	<u>X</u>			
People living outside USA?	_____	<u>X</u>			
Pregnant women/fetuses?	_____	<u>X</u>			
Other? _____					

***Please answer each of the following questions using non-technical language. Missing or incomplete answers will delay your review while we request the information.***

**D. State your research question(s) and related hypotheses.**

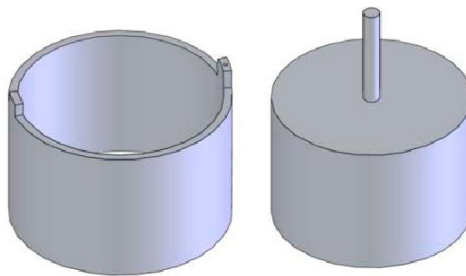
This project aims to develop force feedback (haptic) interface devices to present information to a user through his/her sense of touch. By adding the sense of touch to the senses of hearing and sight, interface devices can be made that provide more information to a user, allowing greater control over devices as well as more accurate and information-dense simulations. All this is accomplished through the implementation of Electro-Rheological fluids (ERF) based devices. Various haptic devices exist today, but most use traditional technologies such as motors or pneumatic systems to produce forces. By using ERF devices, more compact and efficient devices can be created. The interface that is being examined is a haptic knob that uses a single ERF element to generate forces. This haptic knob can generate various types of force profiles, such as a detent-knob, a selection-knob, etc., by activating the ERF elements.

The question that is being examined is whether the type of knob - the actual handle of the haptic knob that the user is grasping - will affect the effectiveness of the ERF-based system. Three general Knob types are under consideration as well as the addition of textures to the knob surface. The final goal of this project is to identify which knob type provides the user the greatest ability to receive force feedback information as well as the determination of the knob type that allows a user the greatest amount of control over a haptic interface.

**E. Provide a brief summary in non-technical language.**

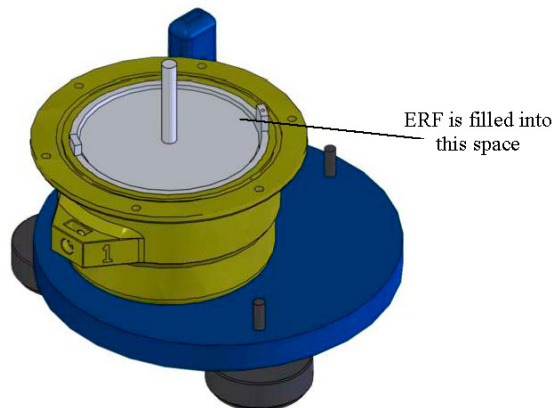
The research presented here aims to develop a force-feedback or haptic interface that will present force information to a user through his or her sense of touch. The addition of touch cues to visual and auditory cues in an interface will increase the amount of useful information that can be presented.

Forces are generated for the haptic interface through actuator elements that produce forces that resist rotation. These forces are produced by controlling the properties of a Smart Material called Electrorheological Fluids (ERFs). ERFs are fluids that change their properties (i.e. thickness) under the influence of electric fields. An electric field is generated by putting two conducting elements – electrodes - facing each other with a space in between. The image below shows the electrodes that are used in the ERF actuator.



**Electrodes used in ERF actuator. Fixed electrode on left, rotating electrode on right. Electrodes are approximately 3" in diameter and 2" in height**

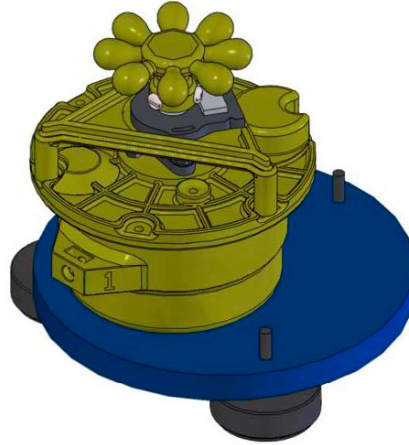
The actuator is assembled by nesting the electrodes together, and filling the gap between them with ERF, as in the image below.



**Nested electrodes are placed within a non-conducting enclosure**

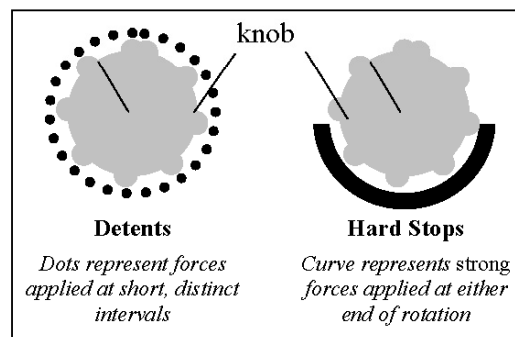
The electrodes are attached to wiring to create an electrical circuit. The outer, fixed electrode is attached to the supply Voltage, while the inner, rotating electrode is attached to the Ground wire. When voltage is applied to the circuit an electric field is generated in the gap that exists between the two electrodes. This electric field activates the ERF, changing the forces that resist rotation of the inner electrode.

Using the electrically controlled rheological properties of ERFs, compact actuators capable of supplying high resistive and controllable torques, have been developed. A Force Feedback interface in the form of a Haptic Knob has been created by attaching a handle to the rotating element of the ERF actuator. The picture below shows the assembled Haptic Knob. All exposed components are made from a non-conducting plastic or are not in contact with the electrically active components.



**Assembled Haptic Knob, including encoder to read rotation and a force sensor (hidden) to read applied forces.**

The sensors that are incorporated into the Haptic Knob system allow for the reading of the handle's position as well as the amount of force that is being applied by the user. Using these pieces of information a computer program can vary the forces generated by the ERF actuator in a manner that will change the force profile – the “feeling” – of the Haptic Knob. The following graphic demonstrates two of the many force profiles that are possible by using the controllable ERF element.



**Some of the force profiles that can be generated and changed on-the-fly with the Haptic Knob**

The study will compare six different types of knobs – the handles of the Haptic Interface – in order to determine if the shape and texture of the handle will have an effect on the accuracy and capabilities of the Haptic Knob. These Knob shapes, shown in the image below, each have an influence on the movement of the hand that is grasping it.



**Three basic knob types – Disc, Lobed, Hand Wheel**  
**Surface Texture will be added to each for a total of six knob types.**

An experiment will be performed that examines the abilities of a person to use the Haptic Knob in the six configurations. It is hoped that it will be possible to identify the knob shape that maximizes the force information that can be presented to a user, and therefore optimize the design of the Haptic Knob.

**F. Identify study personnel on this project. Include name, credentials, role, organization affiliation.**

Constantinos Mavroidis –Professor of Northeastern University, Department of Mechanical Engineering, Principle Investigator (advisor), 617-373-7733.

Avi (Allen) Fisch – Visiting Scientist of Northeastern University, will conduct recruitment, testing and data collection, 617-373-7733.

Brian Weinberg – Robotics Lab Research Engineer and PhD student of Northeastern University, assist with ERF device and lab activities, 617-373-7733.

**G. Identify other organizations or institutions that are involved. Attach current Institutional Review Board (IRB) approvals or letters of permission as necessary.**

None

**H. Recruitment Procedures**

*Describe the participants you intend to recruit. Provide all inclusion and exclusion criteria. Include age range, number of subjects, gender, ethnicity/race, socio-economic level, literacy level and health (as applicable) and reasons for exempting any groups. Describe how/when/by whom inclusion/exclusion criteria will be determined.*

The participants will be at least 18 years old males or females that exhibit a normal ability to use a knob based interface. The exclusion will be any individual with recent injury or surgery to their fingers, hands or arms.



*Describe the procedures that you will use to recruit these participants. Be specific. How will potential subjects be identified? Who will ask for participation? If you intend to recruit using letters, posters, fliers, ads, website, email etc., copies must be included as attachments for stamped approval. Include scripts for intended telephone recruitment.*

Participants will be recruited by word of mouth to fellow Robotics lab members and Mechanical Engineering graduate students. Following the approval of each participant, an informational session will be provided prior to testing to familiarize the individuals with the device, activities to be performed and a demonstration.

*What remuneration, if any, is offered?*

None

### **I. Consent Process**

*Describe the process of obtaining informed consent. Be specific. How will the project and the participants' role be presented to potential participants? By whom? When? Where? Having the participant read and sign a consent statement is done only after the researcher provides a detailed oral explanation and answers all questions. Include a copy of informed consent statements that you intend to use, if applicable. If translations are necessary, you may wish to wait until the consent statement has final approval in English.*

Prior to formal consent, the individuals will be given a detailed informational session by the investigators of the project providing all the details involved with the activities they will be performing and the objectives. A demonstration of the device and the activities to be performed will also be provided by the investigators.

*If your population includes children, prisoners, people with limited mental capacity, language barriers, problems with reading or understanding, or other issues that may make them vulnerable or limit their ability to understand and provide consent, describe special procedures that you will institute to obtain consent appropriately. If participants are potentially decisionally-impaired, how will you determine competency?*

*None involved.*

### **J. Study Procedures**

*Provide a detailed description of all activities the participant will be asked to do and what will be done to the participants. Include the location, number of sessions, time for each session, and total time period anticipated for each participant, including long term follow up.*

Each individual will participate in one session each lasting approximately one hour.

The arm and hand measurements and age of each participant will be recorded at the beginning of the session. The individual will then be given a number to distinguish their testing session.

The protocol to be used will be as follows:

1. Participants will be allowed a short, 5minute, familiarization session, allowing them to see and touch the Knob to familiarize themselves with the task. In addition they will be allowed time to arrange themselves into a comfortable position by adjusting seat heights and the like in order to perform the tasks more comfortably.  
If deemed necessary, an example of a Haptic sensation will be demoed on the Knob to further familiarize the participant with the system. A generic non-experimental knob-handle will be used for this demo.
2. An experimental Knob-handle will be placed on the device.
3. The user will perform an experimental selection task in which they will be asked to identify a particular selection point by force feedback sensations alone.
4. In addition, the user will perform a counting task in which they will determine the number of “bumps” or selection points represented in a full rotation of the Knob.
5. This task will be repeated at various force levels.
6. The user will rest for 1-2 minutes while another randomly selected knob-handle is attached.
7. Repeat steps 3-6 for all knob-handle variations.

There will be no long term follow-up unless the participants are interested in discussing the results.

*Who will conduct the experimental procedures, questionnaires, etc? Where will this be done? Include copies of all questionnaires, interview questions, tests, instruments, etc.*

The procedures will be conducted by Avi Fisch, NU Visiting Scientist.

All activities will be performed in the Robotics and Mechtronics Laboratory (161 Egan Center) where the Haptic Knob is located.

Individuals will have the option to stop testing and/or discontinue their participation at any time.

#### **K. Risks**

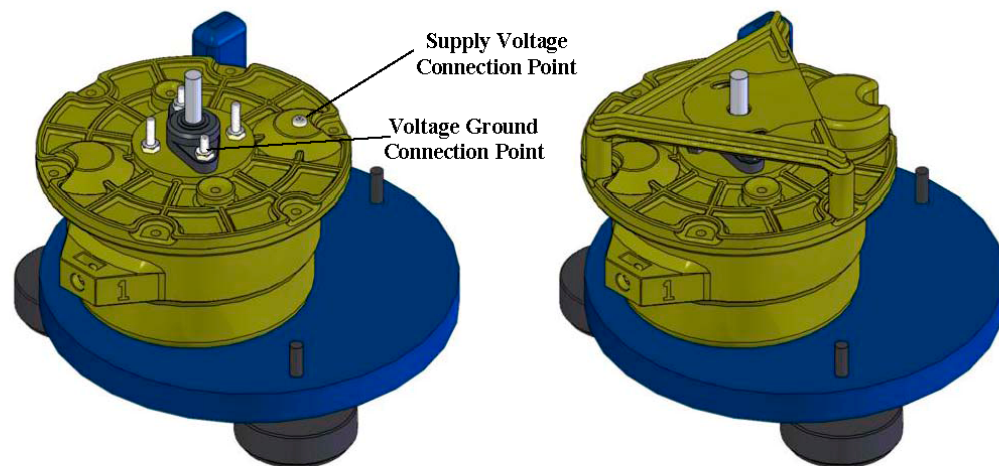
*Identify possible risks to the participant as a result of the research. Consider possible psychological harm, loss of confidentiality, financial, social, or legal damages as well as*

*physical risks. What is the seriousness of these risks and what is the likelihood that they may occur?*

Any risks associated with the use of the Haptic Knob device are equivalent to those when using any other knob based interface. There is minimal risk of finger fatigue after performing the required activities for an amount of time. It is expected that this would be a limited amount of fatigue that will fade rapidly.

The ERF device is purely passive however, meaning it does not have the ability to move on its own, therefore only resistance to motion is possible and the amount of force applied is determined by the individual effort. Therefore risk of force related injury from the device is extremely minimal.

The Haptic Knob utilizes some electrical components, some of which use high voltage, at a maximum of 4 kV. There is negligible risk of electrically related injury however due to the extremely low current that is used (the maximum output current of the power supply is 10 milliamps). This current is well within published safety limits and poses no health risks. The device being tested will only be using a maximum of 5 milliamps to operate however, thereby adding another factor of safety. In addition all electrical components of the Haptic Knob are kept isolated from the user and are not connected to the handle of the knob which will be grasped. In addition electrical wiring will have sufficient insulation and all electrical connections on the device will be covered and inaccessible to the user. The following images illustrate the location of the electrical contacts and the means by which they will be kept covered and inaccessible. In addition, the knob-handle that will be attached at the top of the device will be made from non-conducting plastic and will be attached to the rotating shaft by non-conducting set screws in order to completely isolate the user from the electrified components.



**Left picture shows Electrical Connection points. Right picture shows non-conductive covers that are placed over these points to isolate them from the user**

In addition, the Electrical equipment, such as power supply and computer, will be placed on a bench away from the user. The device used for supplying the power is a Trek 609C high voltage amplifier. It will be plugged into a GFCI throughout all the tests. In

the unlikely occurrence of some catastrophic accident the power supply used has fast acting fuses and cut off safety features that immediately shut off all power in the event of a short circuit. Likewise in the case of a fluid leak, the ERF is a non-toxic, non-corrosive, and high dielectric fluid (does not conduct electricity) and will not pose a danger if a user comes in contact with it.

*Describe in detail the safeguards that will be implemented to minimize risks. What follow-up procedures are in place if harm occurs? What special precautions will be instituted for vulnerable populations?*

The power supply is a low power device with fast acting safety features that ensure safety for its users. Although it does amplify the voltage up to 4 kV, when working with electrical devices it is the current that poses the most danger when dealing with an electrical circuit. The 10 milliamp maximum current output of the power supply is well within safety limits and is not high enough to cause any health problems. The device itself is designed to only use a maximum current of 5 milliamps.

It is not anticipated that any harm will be caused by the device.

#### **L. Confidentiality**

*Describe in detail the procedures that will be used to maintain anonymity or confidentiality during collection and entry of data. Who will have access to data? How will the data be used, now and in the future?*

Subjects will be identified only by number. No personal matter will be included with their collected data. All data will be locked in the Robotics and Mechatronics Laboratory of Northeastern University in a file cabinet. Only Professor Constantinos Mavroidis, Avi Fisch, and the lab manager, Brian Weinberg will have access to the files.

*How and where will data be stored? When will data, including audiotapes and videotapes, be destroyed? If data is to be retained, explain why. Will identifiers or links to identification be destroyed? When? Signed consent documents must be retained for 3 years following the end of the study. Where and how will they be maintained?*

All data will be stored in a locked cabinet in the Robotics Laboratory of Northeastern University. No identifiable data will be on the sheets. Informed consent sheets will be kept separate, filed and stored likewise.

**M. Benefits**

*What benefits can the participant reasonably expect from his/her involvement in the research? If none, state that. What are potential benefits to others?*

The participants will be able to help maximize the design of a device that they may eventually be able to use in future interface devices.

Potential benefits of a Haptic interface are the creating of new and more efficient interface devices for any number of interface systems.

**N. Attachments**

**Identify attachments that have been included and those that are not applicable (n/a).**

- n/a   Copy of fliers, ads, posters, emails, web pages, letters for recruitment
- n/a   Scripts of intended telephone conversations
- n/a   Copies of IRB approvals or letters of permission from other sites
- x    Informed consent statement (Approved form must be stamped by IRB before use)
- n/a   Copies of all instruments, surveys, focus group or interview questions, tests, etc.
- x    Signed assurance of principal investigator (required)

## 18.4.2 Consent Form



**Northeastern**

U N I V E R S I T Y

### Notification of IRB Action

Date: July 31, 2006

IRB #: 06-06-12

**Division of Research Integrity**

413 Lake Hall  
Northeastern University  
Boston, Massachusetts 02115-5000

Phone: 617.373.7570  
Facsimile: 617.373.4595

Principal Investigator(s): Constantinos Mavroidis  
Avi Fisch

Department: Mechanical Engineering

Address: 334 Snell Engineering  
Northeastern University

Title of Project: ERF-Based Force Feedback Interface

Participating Sites: N/A

Informed Consent: One (1) signed consent form

DHHS Review Category: Expedited #7

Monitoring Interval: 12 months

**Approval Expiration Date: July 30, 2007**

#### Investigator's Responsibilities:

3. The informed consent form bearing the IRB approval stamp must be used when recruiting participants into the study.
4. The investigator must notify IRB **immediately** of unexpected adverse reactions, or new information that may alter our perception of the benefit-risk ratio.
3. Study procedures and files are subject to audit any time.
4. Any modifications of the protocol or the informed consent as the study progresses must be reviewed and approved by this committee **prior to being instituted**.
5. Continuing Review Approval for the proposal should be requested at least one month prior to the expiration date above.
6. This approval applies to the protection of human subjects only. It does not apply to any other university approvals that may be necessary.

Matthew O. Hunt, PhD, Chair  
Northeastern University Institutional Review Board

Nan C. Regina  
Director, Research Integrity

Northeastern University FWA #: 4630

## 18.4.3 IRB Approval (3 Pages)

### ERF BASED FORCE FEEDBACK INTERFACE

Northeastern University, Mechanical Engineering

Investigators: Constantinos Mavroidis<sup>1</sup>, Avi Fisch<sup>2</sup>, Brian Weinberg<sup>3</sup>

<sup>1</sup> Principle Investigator and Professor, Department of Mechanical Engineering,

<sup>2</sup> Visiting Scientist, Department of Mechanical Engineering

<sup>3</sup> Robotics Lab Research Engineer and PhD Graduate Student, Department of Mechanical Engineering

### Consent to Participate in a Research Study

We are inviting you to take part in a research study. This form will tell you about the study, but the researcher will explain it to you first. You may ask this person any questions that you have. When you are ready to make a decision, you may tell the researcher if you want to participate or not. You do not have to participate if you do not want to. If you decide to participate, the researcher will ask you to sign this statement and will give you a copy to keep.

#### Description of Project:

- The research presented here aims to develop a new breed of knob-based interface device. It uses a controllable force-feedback system to change the force profiles – the actual “feel” of the knob – on-the-fly in order to present force information to a user through their sense of touch.
- The forces that are presented to the user are generated through a device based on the use of a type of Smart Fluid called Electrorheological Fluid (ERF). ERFs are fluids which changed their viscosity – their thickness – in response to an electric field. By tuning the strength of the electric field the amount of viscosity and therefore the amount of force can be tuned.
- The ERF elements, known as passive actuators, coupled with a knob-type of interface allow for a very compact, yet powerful interface system that will present data to a user in the form of force feedback cues.
- The study will compare the effect of different knob shapes and surface textures on the accuracy and understandability of the force-feedback interface.
- Participants will use the force-feedback knob to perform a task. The accuracy of how that task is performed will help determine which knob shape will be the most effective.
- A brief description of the activities you will be asked to perform are as follows:
  - Familiarize yourself with the look and feel of the system.
  - Perform simple selection and counting tasks using the Knob system. There will be two different tests with about 5 repetitions of each test at different force levels.
  - Perform the same tasks with different knob shapes and textures.

**APPROVED**

NU IRB# 06-06-12  
 VALID: 7/31/06  
 THROUGH: 7/30/07



**What are the risks and possible discomforts?**

There is minimal risk of finger fatigue from using the force feedback knob for an extended period of time. This risk is expected to be the same as for using any knob based interface. Any discomfort is expected to be minimal and dissipate quickly.

In addition, the system uses high voltage to generate the electric field that activates the ERF components of the device. The maximum Voltage that will be applied is 4 kV and the maximum Current is 10 milliamps. The device uses extremely low current, however, which is within established safety guidelines for electrical systems, and does not pose any health risks. In addition, safety features have been included in the design of the device as well as in the power supply used, in order to isolate the participants from the electrical components to minimize the risks even further.

**What are the benefits of the study?**

You will be helping to develop the next generation of interface systems.

**Where will this take place and how much time will this take?**

The testing will take place in the Robotics and Mechatronics Laboratory (161 Egan) and will take approximately one hour to complete.

**Confidentiality:**

Your participation in this study is confidential. You will receive a number prior to the study which will be used by the investigators to identify you. This information will be kept in a confidential file in the Robotics Laboratory (161 Egan, Northeastern University) which only the investigators will have access to. You will have full access to all records or information that is collected during this study. The information that we derive from your participation will be held in a confidential manner. No reports or publication will use the information gathered to identify you in any way. All information that is gathered from tests will be stored in a locked file cabinet in the Robotics Laboratory. In rare instances, authorized people may request to see research information about you and other people in the study. This is done only to be sure that the research is done properly. We would only permit people who are authorized by organizations such as Northeastern University to see this information.

**If I do not want to take part in this study, what choices do I have?**

You may terminate yourself from this study at any point. If you have any further questions before or after the study, any of the investigators will be willing to help answer them and discuss them further with you. Any additional questions can be directed to 617-373-7733.

**Termination of study:**

I have the right to stop anytime during this study. If I should decide to stop, my information to that point will be destroyed. If I should wish to stop, I should inform one of the investigators of my decision.

**Rights:**

**Who can I contact about my rights as a participant?**



If you have any questions about your rights as a participant, you may contact Human Subjects Research Protection, Division of Research Integrity, 413 Lake Hall, Northeastern University, Boston, MA 02115, Tel. 617-373-7570. You may call anonymously if you wish.

**Emergency Contact Information:**

Name: \_\_\_\_\_  
Relationship to participant: \_\_\_\_\_  
Phone Number: \_\_\_\_\_

I have read the Consent Form and all of my questions have been answered. My signature on this form indicates that I have read and understand the information above and that I **agree** to participate in this study. I have received a copy of this form for my records.

\_\_\_\_\_  
Signature of Research Participant                      Date

\_\_\_\_\_  
Printed Name of Person Above

\_\_\_\_\_  
Signature of Person Who Explained Study to                      Date  
Participant and Obtained Informed Consent

\_\_\_\_\_  
Signature                      Date

## CURRICULUM VITA

Allen Fisch

### EDUCATION

- B.S., Mechanical Engineering, May 1992, Columbia University, New York, NY
- M.S., Mechanical and Aerospace Engineering, May 2004, Rutgers University, Piscataway, NJ
- Ph.D., Mechanical and Aerospace Engineering, May 2007, Rutgers University, Piscataway, NJ,

### RESEARCH EXPERIENCE

February 2004 – May 2007: Doctoral Research with Dr. Constantinos Mavroidis, Department of Mechanical and Industrial Engineering, Northeastern University, Boston, MA

September 2000 – January 2004: Graduate Research with Dr. Constantinos Mavroidis, Department of Mechanical and Aerospace Engineering, Rutgers, The State University of New Jersey, Piscataway, NJ

### PUBLICATIONS

1. Fisch A., Nikitzuk J., Weinberg B., Melli-Huber J., Mavroidis C., Wampler C., "Development of an Electro-Rheological Fluidic Actuator and Haptic Systems for Vehicular Instrument Control" *Proceedings of IMECE2003 2003 ASME International Mechanical Engineering Congress and Exposition*, November 15 - 21, 2003 – Washington, D.C.
2. Fisch A., Mavroidis C., Melli-Huber J. and Bar-Cohen Y., "Chapter 4: Haptic Devices for Virtual Reality, Telepresence, and Human-Assistive Robotics" Invited Chapter in *Biologically-Inspired Intelligent Robots*, Editors: Yoseph Bar-Cohen and Cynthia Breazeal, SPIE Press, 2003.
3. Melli-Huber J., Weinberg B., Fisch A., Nikitzuk J., Mavroidis C., Wampler C., "Electro-Rheological Fluidic Actuators for Haptic Vehicular Instrument Controls", *Proceedings of the Eleventh Symposium on Haptic Interfaces for Virtual Environment and Teleoperator Systems*, March 22 and 23, 2003, Los Angeles, CA. Also submitted for publication in the IEEE / ASME Transaction

4. De Laurentis K., Mavroidis C., Nikitzuk J. and Fisch A., "Optimal Design, Experimentation and Comparison of Shape Memory Alloy Wire Bundle Actuators", submitted for publication in the *Journal of Dynamic Systems, Measurement and Control, Transactions of the ASME*, July 2002.
5. DeLaurentis K., Fisch A., Nikitzuk J., Mavroidis C., "Design and Experimentation of Shape Memory Alloy Wire Bundle Actuators", *Proceedings of the 14th CISM-IFTOMM Symposium on the Theory and Practice of Robots and Manipulators, RoManSy 2002*, G. Bianchi, J.C. Guinot and C. Rzymkowski (Editors), Springer-Verlag, pp. 339-350.
6. DeLaurentis K., Fisch A., Nikitzuk J., Mavroidis C., "Optimal Design of Shape Memory Alloy Wire Bundle Actuators", *Proceedings of the 2002 IEEE International Conference of Robotics and Automation*, Washington, D.C., May 11-15, 2002, pp. 2363-2368.
7. DeLaurentis K., Fisch A., Nikitzuk J., Mavroidis C., "Design of Shape Memory Alloy Wire Actuators", *Proceedings of the ACTUATOR 2002 Conference, the 8th International Conference on New Actuators*, Bremen, Germany, June 10-12, 2002, pp. 588-591.